Tesis de Doctorado

Programa de Desarrollo de las Ciencias Básicas (PEDECIBA) Área Biología
Sub-área Biología Celular y Molecular

Función mitocondrial en espermatozoides. Un marcador para la infertilidad masculina.

Ing. Pilar Irigoyen

Directora
Dra. Rossana Sapiro
Co-directora
Dra. Adriana Cassina

Departamento de Histología y Embriología.
Centro de investigaciones biomédicas (CEINBIO).
Facultad de Medicina, Universidad de la República, Uruguay.

Tribunal
Presidenta: Dra. Adriana Geisinger.
Vocales: Dres. Rodolfo Ungerfeld y Leonor Thomson.

Montevideo, diciembre del 2024.

Agradecimientos

Agradezco a todo el equipo del Departamento de Histología y Embriología y al Centro de Investigaciones Biomédicas que hicieron posible esta tesis y siempre me recibieron cálidamente, haciéndome sentir parte desde el primer día. En particular, agradezco a mis compañeros del "*sperm team*" que en todo momento están dispuestos a ayudarme, hicieron mi día a día más feliz y sin dudas, este trabajo también es de ellos.

Gracias a Celia Santi y su laboratorio, así como a Laura Castro y Santiago Mansilla, ambas colaboraciones fueron muy ricas y claves para esta tesis. Durante el trabajo compartido, siempre se mostraron listos para transmitirme sus conocimientos. Fue un lindo trabajo en equipo, que espero, sea el comienzo de muchos juntos.

Especialmente, agradezco a mis dos orientadoras que dieron dos visiones muy distintas y valiosas para el proyecto. Agradezco las oportunidades que me dieron, su compromiso, paciencia y disposición. Durante estos 7 años, no solo me transmitieron enseñanzas invaluables, sino también su pasión por la ciencia que espero llevar conmigo para inspirar a otros de igual forma.

A los miembros del tribunal por aceptar la corrección de esta tesis, y en particular a Leonor y Rodolfo, que junto a Noel Álvarez, me acompañaron desde mi pasaje a doctorado formando mi CAS desde el año 2019. Las discusiones de resultados y sus aportes han sido fundamentales para el trabajo que hoy presento.

A mis amigos y mi familia, que me apoyan en todo y son los que me hacen quien soy hoy.

A Reprovita, y todas sus integrantes, quienes nos facilitaron las muestras que sin ellas hubiese sido imposible llevar adelante el proyecto.

Al Programa de Desarrollo de Ciencias Básicas, la Agencia Nacional de Investigación e Innovación, la Comisión Académica de Posgrados y la Comisión Sectorial de Investigación Científica por su apoyo. Sus financiaciones me han permitido participar de cursos y congresos internacionales que me han enriquecido significativamente llevando mi camino en la ciencia a otro nivel.

Índice

1. Abreviaciones

$^{\bullet}$OH: radical hidroxilo.
4-HNE: 4-Hydroxynonenal.
AA: antimicina A.
ACO2: aconitasa mitocondrial.
ADP: adenosín disfosfato.
ALH: *amplitude of lateral head displacement.*
AMP: adenosín monofosfato.
ATP: adenosín trisfosfato.
BCF: *beat cross frequency*.
BSA: albúmina sero bovina.
Ca^{+2}: ión calcio.
CAP: capacitados.
CO_2: dióxido de carbono.
Curva ROC: Receiver Operating Characteristic curve.
$FADH_2$ y FAD: flavín adenín dinucleótido (forma reducida y oxidada).
FCCP: carbonyl cyanide-p-trifluoromethoxyphenylhydrazone.
Fe^{2+}: hierro.
FIV: fecundación in vitro.
H^+: catión hidrógeno, protones.
H_2O_2: peróxido de hidrógeno.
HRR: respirómetro de alta resolución.
K^+: catión potasio.
KO: *knockout.*
LIN: *linearity coefficient.*
MCU: uniportador de calcio mitocondrial.
MME: membrana mitocondrial externa.
MMI: membrana mitocondrial interna.
NADH y NAD+: nicotinamida adenina dinucleótido (forma reducida y oxidada).
NADP: nicotinamida adenina dinucleótido fosfato.
NC: no capacitados.
$O_2^{\bullet-}$: superóxido.
OMS: Organización Mundial de la Salud.
$ONOO^-$: peroxinitrito.
PMM: potencial de membrana mitocondrial.
PS: plasma seminal.
RA: reacción acrosómica.
RCR: índice de control respiratorio.
RNS: especies reactivas del nitrógeno.
ROS: especies reactivas de oxígeno.
SOD: superóxido dismutasa.
STR: *straightness of trajectory*.
TMRM: tetramethyl rhodamine methyl ester perchlorate.
TRA: tecnologías de reproducción asistida.
VAP: *average path velocity.*
VCL: *curvilinear velocity.*
VSL: *linear velocity.*
WT: *wild type*, salvaje.
ZP: zona pelúcida.

2. Resumen

La infertilidad conyugal es un problema de salud creciente a nivel mundial que afecta al 15% de las parejas en edad reproductiva. El factor masculino solo o combinado con el femenino puede ser responsable de la infertilidad conyugal hasta en un 50% de los casos. En un 30% de estos, las causas se mantienen desconocidas considerándose una enfermedad de tipo idiopática. Un factor común es la presencia de un alto número de espermatozoides defectuosos e incapaces de fecundar en el eyaculado. La causa del aumento de espermatozoides defectuosos puede ser múltiple llevando a que los mecanismos celulares y moleculares sean difíciles de dilucidar.

Para adquirir su capacidad fecundante los espermatozoides deben completar un proceso en el aparato reproductor femenino denominado capacitación. Como resultado de la capacitación, los espermatozoides adquieren una forma especial de motilidad conocida como hiperactivación y la posibilidad de sufrir una reacción acrosómica (RA) regulada. La entrada del ion calcio (Ca^{+2}) al flagelo a través de los canales CatSper es clave en este proceso. Se sabe además que las especies reactivas del oxígeno (ROS) pueden regular la capacitación espermática, sin embargo, la contribución mitocondrial en el proceso es debatida.

La hipótesis fue que durante la capacitación hay un aumento en la actividad mitocondrial mediada por la entrada de Ca^{+2} a la mitocondria, que se traduce en un incremento en la producción de ROS que cumplen un rol modulador sobre la capacidad fecundante del espermatozoide. Planteamos que el análisis de la función mitocondrial y la producción de oxidantes podría ayudar a mejorar el diagnóstico del hombre infértil.

Para comprobar nuestra hipótesis, primero estudiamos el incremento de la actividad mitocondrial en el proceso de capacitación y su rol en la fecundación. Para ello, en colaboración con el laboratorio de la Dra. Santi de la Washington University, comparamos la actividad mitocondrial en espermatozoides de ratón no capacitados (NC) con capacitados (CAP) mediante respirómetro de alta resolución (HRR) y medimos el potencial de membrana mitocondrial (PMM) por citometría de flujo. Observamos un incremento de la función mitocondrial en los espermatozoides CAP con respecto a los NC. Esto se vió acompañado de un aumento de la [Ca^{+2}] mitocondrial dependiente de la actividad de los canales CatSper y uniportador de calcio mitocondrial (MCU). Mostramos que estas modificaciones en la función mitocondrial son necesarias para la hiperactivación y por consiguiente la fecundación en ratones. Nuestros resultados apoyan que algunos de estos mecanismos son conservados en los espermatozoides humanos.

Por otro lado, analizamos el rol de la mitocondria en la producción de ROS durante la capacitación utilizando muestras de semen humanas diagnosticadas como normozoospérmicas. Comparamos entre espermatozoides NC y CAP la función mitocondrial mediante HRR donde observamos un aumento en el índice de control respiratorio (RCR) en las muestras CAP y de la respiración no mitocondrial (en presencia de antimicina A (AA), inhibidor del complejo III de la cadena respiratoria). Se determinó la concentración extracelular de peróxido de hidrógeno (H_2O_2), la cual fue tres veces mayor en espermatozoides CAP. Para confirmar si el aumento del H_2O_2 depende de la formación de superóxido ($O_2^{\bullet -}$) mitocondrial se midió la cantidad de aconitasa mitocondrial (ACO2), su actividad y papel en el flujo metabólico del ciclo de Krebs. Con esta metodología, observamos que las mitocondrias de los espermatozoides CAP producen 59 ± 22 % más de $O_2^{\bullet -}$ que los NC. No observamos cambios entre CAP y NC cuando se analizaron blancos claves de daño oxidativo como la peroxidación lipídica (mediante Western blot para hidroxinonenal) o la actividad de la succinato deshidrogenasa mediante HRR en espermatozoides permeabilizados.

Por último, observamos que en espermatozoides NC provenientes de muestras de semen que presentan alteraciones en el espermograma, disminuye el RCR medido con HRR y aumenta la producción de H_2O_2 con respecto a los espermatozoides NC de donantes normales. En ambos métodos, utilizamos por primera vez curvas ROC (Receiver Operating Characteristic) para probar su capacidad diagnóstica.

Tomados en su conjunto, estos datos demuestran que la mitocondria interviene en la regulación de la función del espermatozoide en condiciones normales durante la capacitación modulando la hiperactivación y la producción de $O_2^{\bullet -}$ en humanos. Además, el mecanismo estaría asociado a un aumento de la concentración de Ca^{+2} mitocondrial. Finalmente, nuestros datos con espermatozoides humanos provenientes de muestras alteradas sugieren que estos mecanismos podrían estar afectados en individuos con infertilidad masculina. Postulamos que el estudio del metabolismo mitocondrial podría ser una nueva herramienta para mejorar el análisis de semen de rutina.

3. Introducción

3.1. Infertilidad

3.1.1. Definición e impacto

La infertilidad conyugal, según la Organización Mundial de la Salud (OMS), consiste en la incapacidad en las parejas para lograr el embarazo tras 12 meses o más de relaciones sexuales regulares sin protección[1,2]. Aunque la infertilidad no compromete la integridad física del individuo, esta puede tener un impacto negativo sobre el desarrollo del mismo, produciendo estigmatización, dificultades económicas y frustración, debilitando su personalidad, ya que muchas personas consideran la concepción como un objetivo de vida[3,4]. Se trata de un problema creciente a nivel mundial como consecuencia del aumento de la edad de la pareja en el momento de la concepción, sumado a cambios en el estilo de vida y variaciones en factores ambientales además de otros factores aún desconocidos[5–7]. Se calcula que afecta al 15 % de las parejas en edad reproductiva[8]. En el año 2010 correspondía a 48,5 millones de parejas[9–11]. Como solución, las parejas infértiles tienen acceso a las tecnologías de reproducción asistida (TRA)[12]. Actualmente se calcula que existen en el mundo más de 8 millones de personas nacidas como resultado de las TRA (datos reportados por: International Committee Monitoring Assisted Reproductive Technologies ICMART, https://www.icmartivf.org).

En Uruguay la infertilidad adquiere un especial significado, donde según los datos publicados por el censo 2023 del Instituto Nacional de Estadística, la población uruguaya es de menos de tres millones y medio de personas y en los últimos 12 años ha crecido únicamente un 1 % (https://www.gub.uy/instituto-nacional-estadistica). Además, en solo 7 años, la tasa global de la fecundidad alcanzó lo que se denominan niveles ultra-bajos, reduciéndose de 2 a 1,27 hijos por mujer y los nacimientos descendieron aproximadamente de 47 a 33 mil (https://www.colibri.udelar.edu.uy/jspui/bitstream/20.500.12008/37645/6/DT%20UM-PP%2011.pdf)[3]. A su vez, resultados publicados anteriormente por nuestro laboratorio muestran que en los últimos 30 años la calidad del semen de la población uruguaya ha ido disminuyendo, en particular en lo que respecta a la concentración y morfología normal espermática[13].

Por todo lo anterior, se trata de un tema de interés y preocupación para el estado uruguayo, lo que se ve reflejado en políticas recientes como la ley (Nº 19.167) de reproducción humana asistida aprobada en el año 2013, por medio de la cual el Fondo Nacional de Recursos financia tratamientos de baja y alta complejidad de TRA. A su vez, en el año 2022 el Parlamento aprobó una norma para que pacientes oncológicos puedan acceder a métodos de conservación de la fertilidad. Los TRA, se tratan de procedimientos de alto costo que pueden alcanzar los 8000 USD en nuestro país (https://www.fnr.gub.uy). Actualmente, el Fondo Nacional de Recursos ha financiado 5015 solicitudes que han resultado en 1799 partos (2.099 nacidos vivos) (https://www.fnr.gub.uy). Esto quiere decir, que, a pesar del éxito de estas técnicas, más de la mitad de las parejas que buscan apoyo médico para la infertilidad no logran concebir y tener un hijo al final de su atención médica, teniendo las TRA una baja efectividad y por tanto una relación costo/beneficio baja.

Se postula que la principal razón de estos fracasos es que uno o ambos de los miembros de la pareja produce gametos que no pueden sustentar la fertilización y/o el desarrollo embrionario[14]. De hecho, la TRA no trata específicamente ni intenta esclarecer las causas subyacentes de la infertilidad de la pareja, sino que intenta superar esta condición con el objetivo de lograr el embarazo. En consecuencia, cuando los defectos en los gametos no pueden ser eludidos por las técnicas actualmente propuestas, la TRA fracasa. Para tratar realmente la infertilidad, se plantea que un primer paso sería obtener una mejor comprensión de la fisiología de los gametos para

conocer cuáles mecanismos se encuentran alterados en los pacientes que no logran el embarazo[14]. Este tipo de enfoque debería aumentar la probabilidad de adoptar la mejor estrategia para los pacientes afectados y, si es necesario, debería guiar el desarrollo de terapias innovadoras.

3.1.2. Infertilidad masculina y estudio del hombre infértil

Al evaluar los posibles orígenes de la infertilidad conyugal, se ha visto que las causas masculinas pueden superar el 50 % de los casos[15,16]. Aunque tradicionalmente no se ha enfatizado la contribución masculina a la infertilidad en las parejas, se estima que corresponde a un 30 % y en un 20 % adicional se combinan ambos factores, pudiendo el factor masculino estar involucrado en un 50 % de los casos[3,15,17,18].

Múltiples afecciones en el hombre pueden producir alteraciones en la producción y calidad del semen provocando infertilidad. Se describen: causas espermáticas congénitas o adquiridas (ej. alteraciones tubulares) y no espermáticas (ej. obstrucción de las vías espermáticas)[15]. Los determinantes no genéticos de la infertilidad incluyen: varicocele, criptorquidia, hipogonadismo hipogonadotrófico, anomalías estructurales de las vías espermáticas, infecciones genitales, cirugías pélvicas previas, varicocele, disfunción eyaculatoria/sexual, cáncer, enfermedades sistémicas, exposición a medicamentos o tóxicos, factores ambientales y causas inmunológicas[15,16,19].

El método paraclínico más utilizado y punto de partida en el diagnóstico de la infertilidad en el varón es el espermograma convencional[1,2]. En este se analizan las características físicas y químicas del semen y se determinan: características macroscópicas (volumen, olor, color, viscosidad y pH), el estudio cito-morfo-dinámico de los espermatozoides (concentración, motilidad, vitalidad y morfología), así como la presencia de otros tipos celulares en el eyaculado[1]. Los resultados obtenidos son evaluados utilizando valores de corte y recomendaciones establecidas por la OMS para catalogar a un hombre como infértil (Tabla 1)[1,2]. Aquellas muestras que todos sus valores se encuentren dentro de los límites establecidos se diagnostican como normozoospérmicas. Se considera oligozoospermia cuando la concentración de espermatozoides es menor a 15 millones/mL, astenozoospermia cuando menos de un 32 % de los espermatozoides poseen una motilidad progresiva y teratozoospermia cuando el porcentaje de espermatozoides normales es menor al 4 %. Finalmente, existen combinaciones de las distintas patologías, por ejemplo: astenoteratozoospermia[1].

Es de especial interés para esta tesis el estudio de la motilidad. La misma se clasifica en progresiva rápida (tipo a), progresiva lenta (tipo b), no progresivos (tipo c) e inmóviles (tipo d)[1]. En nuestro caso hemos utilizado sistemas computarizados para clasificar los espermatozoides según su motilidad y medir las diferentes variables cinéticas y trayectorias de cada célula por separado (Sperm Class Analyzer® system -CASA). Algunas mediciones de motilidad que el equipo permite obtener son la: VCL (Curvilinear Velocity), VSL (Linear Velocity), LIN (Linearity Coefficient), ALH (amplitude of lateral head displacement) y VAP (Average Path Velocity) (Figura 1) [1,20]. Las mismas son importantes para describir patrones característicos de motilidad como la hiperactivación [21].

TABLA 1. Límite del intervalo de referencia para la fertilidad natural según la OMS 2010 (quinta edición) y OMS 2021 (sexta edición)[1,2]. Principales parámetros. Nivel de confianza 95%.

Variables espermáticas	*Cut-off* 2010	*Cut-off* 2021
Volumen seminal (mL)	≥ 1,5	≥ 1,4
pH	7,2 - 8,2	6-10
Concentración espermática (millón/mL)	≥ 15	≥ 15
Espermatozoides con motilidad progresiva (a+b) (%)	≥ 32	≥ 30
Morfología espermática (%)	≥ 4	≥ 4
Vitalidad espermática (%)	≥ 58	≥ 54
Células redondas (millón/mL)	<1	<1

Un porcentaje significativo de pacientes poseen espermogramas normales pero infertilidad inexplicada, sugiriendo la existencia de deficiencias funcionales en el espermatozoide necesarias para la fecundación que no son detectadas por el espermograma clásico[22]. Por esta razón, la OMS propone procedimientos opcionales como por ejemplo: el estudio del daño del ADN, pruebas de estrés oxidativo, *swim up*, evaluación de RA inducida, entre otras[1,22]. En otros casos de infertilidad se detectan valores alterados en el espermograma, pero no es posible dilucidar las causas manteniéndose desconocidas[22]. Entre un 30-40% de los casos la infertilidad masculina es una enfermedad de tipo idiopática[23]. Un factor común es la presencia de un alto número de espermatozoides defectuosos e incapaces de fecundar en el eyaculado[9,15,23]. La causa del aumento de espermatozoides defectuosos puede ser múltiple llevando a que los mecanismos celulares y moleculares sean difíciles de dilucidar.

Por tanto, si bien el espermograma aporta información importante sobre el paciente (espermatogénesis, funcionalidad espermática, funcionamiento de las glándulas anexas, permeabilidad de la vía, existencia de infección o inmunidad, androgenicidad), por sí solo no es diagnóstico de fertilidad ni de infertilidad, menos aún sirve para dirigir al médico a las causas ni a un posible tratamiento de la patología[1,24,25]. Los resultados deben ser interpretados en términos de probabilidad, en conjunto con la historia clínica, datos de la pareja y demás exámenes pertinentes (exámenes físicos, evaluación hormonal, cariotípica)[1].

Esta situación limita gravemente las estrategias de tratamiento para rescatar la fertilidad, por lo que la inclusión de pruebas avanzadas de laboratorio en el análisis de semen de rutina puede ayudar a diagnosticar con precisión la infertilidad masculina. Probablemente, este problema sea reflejo de la falta de conocimiento que se tiene con respecto a las causas y a la fisiopatología de dicha afección[26].

3.2. Espermatozoides

3.2.1. Desarrollo y estructura

Se trata de una célula haploide, producida mediante un proceso de división y diferenciación denominado espermatogénesis (Figura 2)[26,27]. La producción de espermatozoides a partir de las espermatogonias ocurre en los túbulos seminíferos en el testículo[26,28]. La espermatogénesis comienza en la pubertad bajo la influencia de concentraciones cada vez mayores de gonadotrofinas hipofisarias y continúa durante toda la vida del individuo[26,27]. Puede dividirse en tres fases: mitosis y diferención de espermatogonias, meiosis de espermatocitos (reducción del número de cromosomas) y espermiogénesis, donde los espermátides redondeados se transforman en una forma más alargada[26–29]. Por tanto, el proceso implica la reducción del

contenido genético y la compactación del núcleo, así como la generación de otras estructuras importantes para cumplir su función[26,27]. Estos eventos son acompañados de una pérdida de la mayor parte del contenido citoplasmático, resultando una célula pequeña de 60 µm de longitud en el humano [3,30].

El espermatozoide humano maduro es una célula polarizada con una estructura de cabeza nuclear en un extremo y un flagelo en el otro (Figura 3.A)[26,27]. Su cabeza es aplanada y puntiaguda y mide 4,5 µm de largo por 3 µm de ancho por 1 µm de espesor[26,28]. Está ocupada casi por completo por el núcleo condensado. Interpuesto entre el núcleo y la membrana plasmática, se encuentra la vesícula acrosomal, una vesícula que contiene enzimas como la acrosina, hialuronidasa y fosfatasa ácida, que degradan proteínas y glúcidos complejos permitiendo la penetración de la membrana pelúcida del ovocito[26,31]. La misma se origina a partir del aparato de Golgi y cubre dos tercios anteriores de la cabeza, de manera que su membrana interna queda adherida a la envoltura nuclear[26]. Por detrás del acrosoma existe una fina capa densa de ultraestructura característica, interpuesta entre las membranas plasmática y nuclear[26]. Esta capa se denomina lámina densa postacrosomal[26,30,31]. El flagelo se subdivide en: cuello, pieza intermedia, principal y terminal (Figura 3.A)[26,32,33]. El cuello corto contiene los centriolos y el origen de las fibras gruesas[26,33]. En este sector también se puede observar una pequeña masa bulbosa de citoplasma residual que se llama gota citoplasmática[26,27]. La pieza intermedia es de alrededor de 7 µm de longitud y contiene un gran número de mitocondrias dispuestas en forma helicoidal alrededor de las fibras gruesas y el complejo axonémico (Figura 3.B)[26,33]. El axonema está formado por microtúbulos que emanan a partir de un centriolo localizado en la base del núcleo del espermatozoide[32,33]. La pieza principal mide alrededor de 40 µm de longitud y tiene un espesor de 0,5 µm; contiene la vaina fibrosa por fuera de las fibras gruesas y del complejo axonémico (Figura 2.B)[27]. La pieza terminal, que corresponde más o menos a los últimos 5 µm del flagelo sólo contiene el complejo axonémico (Figura 3.B)[26,27,32]. Una vez formados los espermatozoides estos son liberados a la luz del túbulo mediante el proceso denominado espermiación[26].

La correcta estructura del espermatozoide es un requisito esencial para la fecundación, ya que alteraciones en la misma pueden llevar a que el espermatozoide no alcance el ovocito debido a que se afecte su motilidad, a la fragmentación del ADN debido a una mala compactación del mismo o a la alteración de procesos claves como la capacitación[34,35]. Por lo que los defectos estructurales en el espermatozoide se asocian con la infertilidad masculina[1,33–36].

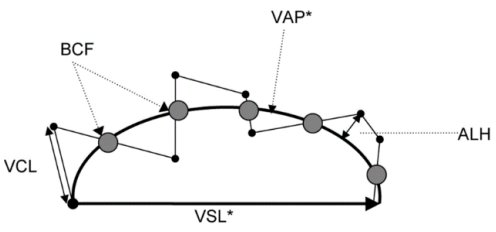

FIGURA 1: Esquema de algunos de las variables de velocidad del espermatozoide obtenidos mediante el sistema CASA. Figura extraída del siguiente artículo[20]. VCL=Curvilinear Velocity, BCF= beat cross frequency, VAP= Average Path Velocity, ALH= amplitude of lateral head displacement, VSL= linear velocity. Parámetros calculados: LIN=linearity coefficient= VSL/ VCL x100 y STR= straightness of trajectory=VSL/VAP x100[20].

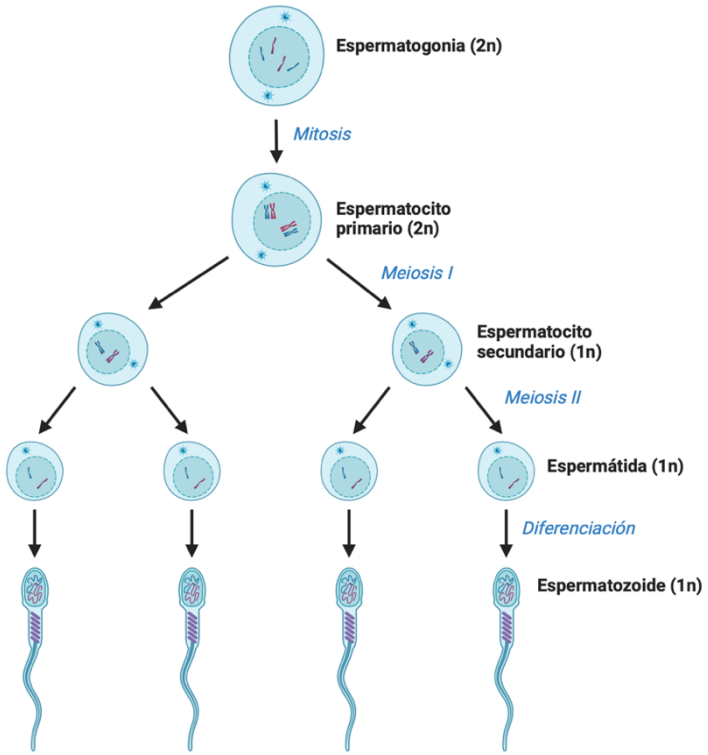

FIGURA 2: Esquema de la espermatogénesis que muestra la generación de espermatozoides a partir de la espermatogonia en el túbulo seminífero[26,28]. Se diagraman las distintas generaciones sucesivas de células espermatógenas y como se recombinan y distribuyen los cromosomas paterno-materno. n= número de cromosomas haploide[26,28]. Aunque no se representa en el esquema, durante el proceso todas las células progenitoras permanecen conectadas por puentes intercelulares a medida que experimentan las divisiones mitótica y meiótica y la diferenciación de los espermátides. Los cuerpos residuales correspondientes al exceso de citoplasma también permanecen conectados y son fagocitados por las células de Sertoli en la última etapa (no representados)[26,28]. Realizado en Biorender.

3.2.2. Función: maduración y capacitación

El espermatozoide es el gameto masculino. Su principal función es transmitir el genoma paterno a la nueva generación[37]. Esto se realiza mediante un proceso denominado fecundación, que en condiciones *in vivo* en los mamíferos implica el desplazamiento del espermatozoide hasta el oviducto para encontrarse con el ovocito[3,26]. Para que la fecundación sea exitosa los espermatozoides deben ser capaces de moverse progresivamente desde el cérvix al oviducto y poder penetrar el ovocito[26,27]. Ambas capacidades las adquieren mediante dos procesos denominados: maduración y capacitación espermática, que ocurren en momentos y sitios diferentes[26,27].

Los espermatozoides abandonan los túbulos seminíferos siendo inmóviles. Su transporte lo realizan en un líquido secretado por las células de Sertoli ayudados por las contracciones peristálticas de las células peritubulares contráctiles[26,27]. Su trayecto es hacia los túbulos rectos, que se anastomosan formando la *rete testis* y luego se conectan con las vías espermáticas extra-testiculares[26]. Durante dos semanas (en el humano) permanecen en el epidídimo donde, mediante moléculas disueltas en su luz, los espermatozoides realizan el proceso de maduración. Esto es llevado a cabo mediante la adición, eliminación o modificación de moléculas en el espermatozoide, que les otorga la capacidad de moverse de forma progresiva[12,27]. Además, la cabeza del espermatozoide se modifica por adición de colesterol y glucoconjugados (importantes para la penetración de la zona pelúcida (ZP)) y se asocia a la superficie el factor descapacitante proveniente del líquido epididimario[12,26,37]. Este proceso, denominado descapacitación, inhibe de manera reversible la capacidad fecundante del espermatozoide[26].

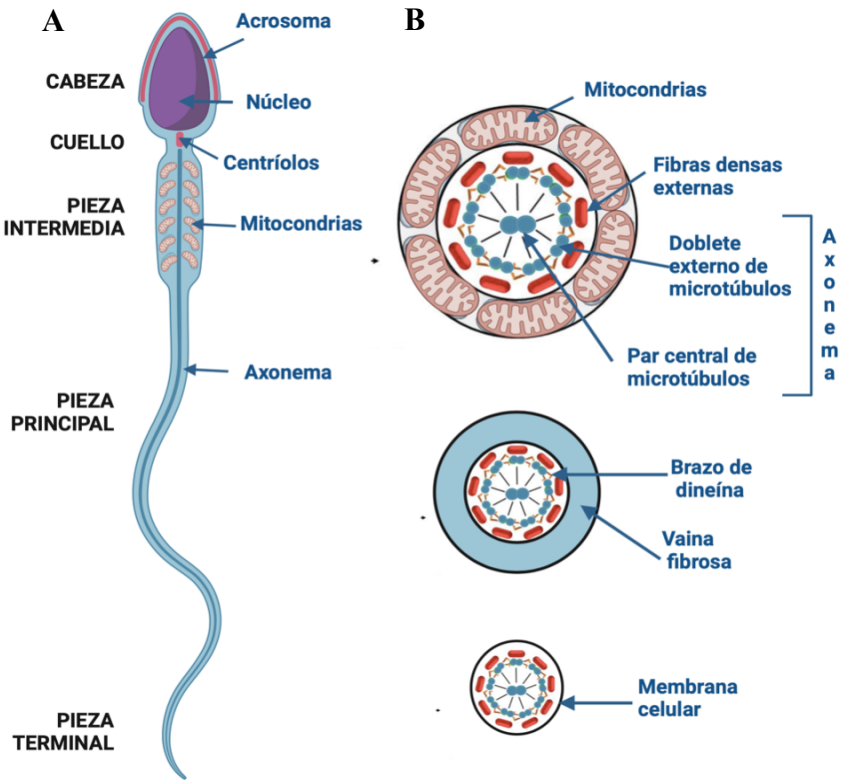

FIGURA 3: Diagrama de la estructura del espermatozoide humano. A. Regiones que componen la célula B. Cortes transversales de las distintas regiones del flagelo que varían en su composición interna. La pieza intermedia, principal y terminal (respectivamente) en su conjunto corresponden al flagelo. Realizado en Biorender.

Estos cambios evitan que la RA, es decir la fusión de la vesícula acrosomal con la membrana plasmática, se produzca antes de encontrarse en el tracto reproductor femenino[12,26,27].

El eyaculado está constituido por los espermatozoides y el plasma seminal (PS), producido por las células de las vías espermáticas y la secreción de las glándulas sexuales anexas[38]. El PS aporta nutrientes como la fructosa y moléculas importantes para cumplir su función (ej. fibrinolisina- sirve para la licuefacción del semen, prostasomas aumentan la disponibilidad de Ca^{+2}, péptido promotor de la fertilización, entre otras)[38–40]. Además, posee una gran capacidad antioxidante protectora y un pH alcalino que contribuye a neutralizar el pH ácido de la uretra y la vagina[38,40,41]. Los espermatozoides eyaculados se desplazan por el útero con una velocidad de 3-4 mm/min en dirección hacia la trompa uterina alcanzándola en más o menos 1 hora en el humano[26]. Unos 200 espermatozoides permanecen en el sitio con capacidad fecundante hasta 4 días[26]. Se propone que los espermatozoides humanos capacitados pueden realizar movimiento quimiotáctico utilizando gradientes de progesterona[37,42–44].

Sin embargo, los espermatozoides de mamíferos recién eyaculados no son aptos para fecundar. Durante su migración, estos deben sufrir ciertos cambios bioquímicos y funcionales en la cabeza y el flagelo conocidos como capacitación (Figura 4)[27,37,45,46]. Como resultado de la capacitación los espermatozoides presentan dos claras manifestaciones celulares: la hiperactivación y la exocitosis del acrosoma de forma regulada[47–49]. Sin embargo, no existe un marcador definido de la capacitación[37,45,50]. La hiperactivación consiste en un cambio de una motilidad de tipo progresiva a una con un patrón de latido flagelar asimétrico, de alta amplitud y velocidad que determina una trayectoria no progresiva que les facilita la penetración de la matriz del cúmulo

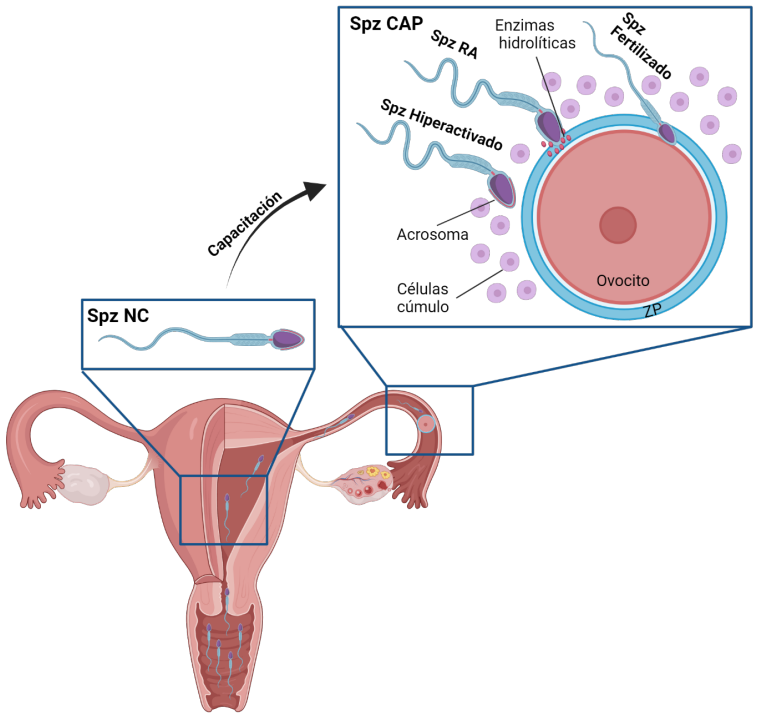

FIGURA 4: Diagrama del recorrido y las modificaciones (hiperactivación y reacción acrosómica (RA)) que sufre el espermatozoide luego de la eyaculación dentro del tracto femenino hasta lograr fertilizar al ovocito. Spz= espermatozoide. NC= no capacitado. CAP= capacitado. ZP= zona pelúcida. Realizado en Biorender.

oóforo y la ZP[51–54]. Además, existe evidencia de que la hiperactivación ayuda a los espermatozoides a nadar a través de sustancias viscoelásticas en el tracto reproductivo femenino y desempeña un papel en el desprendimiento de los espermatozoides de las células epiteliales en el oviducto[51]. Por otro lado, la RA consiste en la liberación del contenido acrosomal por exocitosis al exterior celular[31]. Este contiene enzimas que colaborarán en la penetración de la matriz extracelular que rodea al ovocito[54,55]. Tradicionalmente se aceptaba que el contacto del espermatozoide con la matriz extracelular del ovocito o la ZP desencadenaba la RA (Figura 4). Sin embargo, evidencias recientes utilizando *live imaging* en espermatozoides de ratón que expresan GFP en el acrosoma, mostraron que la unión a la ZP no es suficiente para inducir la RA[56]. Únicamente un 5 % de los espermatozoides que llegan a la ampolla de la trompa de falopio (sitio donde se da la fecundación) tienen el acrosoma intacto, por lo que sufren la RA antes de unirse a la ZP[56]. La RA resulta en una redistribución de las proteínas de membrana y en la exposición de un nuevo dominio de membrana en la superficie celular permitiendo la unión a la ZP ya sea por la ahora expuesta membrana acrosomal interna o la membrana plasmática[57,58] . Se ha observado que si alguno de estos dos indicadores de capacitación (hiperactivación y RA) falla la fecundación no se lleva a cabo[59].

Estos cambios funcionales implican varias modificaciones a nivel molecular[37,60]. Durante el transporte hasta el ovocito existen diferentes concentraciones de iones que modifican la función del espermatozoide y derivan en la capacitación[48,61,62]. Los espermatozoides son transcripcionalmente inactivos, por lo que juegan un rol importante en estas modificaciones las fosfatasas, quinasas, transportadores y canales de iones, lípidos y otras proteínas específicas del espermatozoide[37,45,46,48,63]. Durante la capacitación existe pérdida del colesterol de la membrana plasmática con aumento de la fluidez de la misma y cambios en la permeabilidad iónica, que resultan en un aumento del pH intracelular y en una hiperpolarización de la membrana plasmática[37,45,46,61,64]. El canal SLO3, sensible al pH, juega un rol clave en el cambio del potencial de la membrana bombeando potasio (K^+) al exterior de la célula[64–66]. Además, ocurre un aumento en la [Ca^{2+}] intracelular mediado por el canal CatSper (también sensible al pH), que importa Ca^{2+} extracelular al interior del flagelo[55,59,64,67]. Ambos canales son específicos del

espermatozoide y se ubican en la pieza principal del flagelo[64–67]. Estas modificaciones moleculares derivan y producen cascadas de señalización complejas donde aumenta la actividad de la adenilato ciclasa, incrementando la producción de AMP cíclico, que a su vez activa la proteína quinasa A que genera un aumento en la fosforilación en tirosina de muchas proteínas, probablemente claves en los fenómenos de la capacitación[37,45,48,54,68].

La capacitación se puede lograr *in vitro*, incubando (1-2 hs ratón o humanos 4-12 hs) a los espermatozoides en medios que remeden la composición de iones y metabolitos presentes en el tracto genital femenino[37,45,47,48]. Esencialmente necesita de Ca^{2+}, bicarbonato, una fuente de proteína y una fuente de energía (piruvato, glucosa, lactato)[69]. La fuente de proteína, en general albúmina de suero bovino (BSA), induce cambios en los niveles de colesterol de la membrana plasmática, causando cambios en su fluidez y aumentando la permeabilidad a Ca^{2+} y bicarbonato[45,63,70]. La omisión de alguna de estas moléculas en la incubación espermática disminuye su habilidad para adquirir la capacidad fecundante[47].

A pesar de la extensa investigación, los cambios metabólicos que se producen durante la capacitación son controvertidos y parecen ser especie-específicos[53]. Desde un punto de vista molecular, la mejor caracterización de la capacitación se realizó en el ratón dado las ventajas que ofrece el modelo. Posteriormente, se han explorado estos descubrimientos en otras especies pero las bases celulares y moleculares de la capacitación en el humano son aún poco conocidas[21]. Un aspecto que ha ganado atención recientemente es el rol de la mitocondria en el mismo, dado que muchas evidencias indican que se trata de un proceso de regulación redox, que necesita mayor cantidad de ATP e involucra un importante flujo de Ca^{2+}[55,59,71].

3.3. Mitocondrias

3.3.1. Estructura y funciones

Las mitocondrias son organelos de las células eucariotas compuestos por dos membranas no contiguas con funciones diferentes: la membrana mitocondrial externa (MME) y la interna (MMI) (Figura 5)[72]. La MME participa en el intercambio de pequeñas moléculas e información entre la mitocondria y el resto de la célula[72,73]. La MMI presenta invaginaciones denominadas crestas que aumentan su superficie y está enriquecida de proteínas involucradas en la fosforilación oxidativa, fusión mitocondrial y síntesis y transporte de proteínas[74]. Entre las dos membranas se encuentra el espacio intermembrana y en el interior de la MMI se encuentra la matriz mitocondrial[72–75]. Mientras que la MME es altamente permeable, la MMI tiene una permeabilidad selectiva, y separa los intermediarios y enzimas de las rutas metabolicas citosólicas de los de los procesos metabolicos que ocurren en la matriz[72,74,75]. Esta propiedad es esencial para el desarrollo de sistemas de transporte específicos que regulan el movimiento de moléculas hacia y desde las mitocondrias[72,74,75].

El transporte de electrones a lo largo de los cuatro complejos (nombrados del I al IV) ubicados en la MMl libera energía acoplada a la salida de protones desde la matriz al espacio intermembrana (Figura 6)[73,74]. Este movimiento genera un gradiente electroquímico, utilizado por la ATP sintasa (complejo V) que permite el ingreso de protones (H^+) a la matriz sintetizando moléculas de ATP[74]. Los electrones que entran en la cadena de transporte provienen de moléculas de NADH y $FADH_2$ producidos en la glucólisis, oxidación del piruvato y el ciclo de Krebs[73,74]. El aceptor final de H^+ es el oxígeno que sufre una reducción tetravalente a agua a nivel de la citocromo oxidasa[73,74]. La membrana interna mitocondrial posee transportadores específicos que permiten la entrada a la matriz del piruvato, ácidos grasos, aminoácidos o derivados alfa-ceto[73,74]. De la misma forma el ADP y el fosfato son transportados hacia el interior de la matriz al mismo tiempo que se transporta al exterior el ATP producido[73,74].

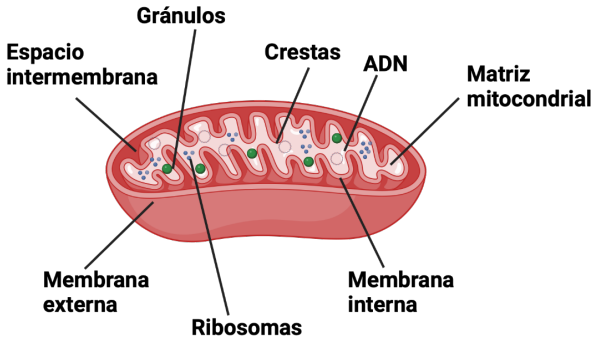

FIGURA 5: Diagrama de corte transversal de la mitocondria, se observan las diferentes estructuras y compartimentos que la componen. Realizado en Biorender.

Si bien su función fisiológica predominante es suministrar energía en forma de ATP, las mitocondrias desempeñan muchas otras funciones que son vitales para la célula. Entre estas, las mitocondrias proporcionan intermediarios metabólicos para la biosíntesis de macromoléculas, señalizan para vías la apoptosis, producen ROS que sirven como segundos mensajeros y regularla [Ca^{2+}] intracelular (matriz citoplasmática y mitocondrial)[76,77]. Por ende, se encuentran involucradas en múltiples procesos vitales para la célula. Un funcionamiento anormal de alguno de los procesos en los que actúa la mitocondria se podía catalogar como disfunción mitocondrial, pudiendo ser la causa de diversas enfermedades[75,76,78]. Por tanto, el estudio correcto de la función mitocondrial se ha convertido en una preocupación para la investigación en búsqueda de herramientas que ayuden al estudio de estas enfermedades como para el diagnóstico de enfermedades mitocondriales primarias[78].

3.3.1.1. Función de la mitocondria en la homeostasis del calcio (en células somáticas)

El Ca^{2+} juega un papel crucial en la producción de energía y en los procesos de señalización intracelular, además de influir en el destino de la célula al inducir o prevenir la apoptosis[79]. Para que estos procesos se lleven a cabo adecuadamente, es esencial regular las concentraciones de este catión tanto fuera como dentro de la célula, ya que su desregulación podría llevar a la muerte celular[77,79,80]. Existen varios sistemas que cooperan para regular la liberación de Ca^{2+} de almacenes intracelulares y/o del influjo del ión a través de la membrana plasmática permitiendo a la célula mantener concentraciones adecuadas y garantizar el correcto funcionamiento de los sistemas metabólicos intracelulares[77,79]. La concentración de Ca^{2+} en el citosol es alrededor de 100 nM, unas 10.000 veces menor que en el espacio extracelular, aunque este puede aumentar hasta 1-3 µM ante diferentes estímulos[79,80]. Esto se debe a que la concentración de Ca^{2+} está controlada por diferentes mecanismos que incluyen ATPasas, transportadores de Ca^{2+}, intercambiadores de Na^{+}/Ca^{2+} y proteínas de unión[77,79,80]. Los niveles subcelulares de Ca^{2+} varían; en los orgánulos intracelulares, conocidos como almacenes de Ca^{2+}, siendo la concentración de este ion es mayor que en el citoplasma ($1–5 \times 10^{-4}$ M)[79,80]. Si bien el principal almacén interno de Ca^{2+} se encuentra en el retículo endoplásmico y, en las células musculares, en el retículo sarcoplasmático, las mitocondrias también juegan un rol central en la homeostasis del Ca^{2+} celular [77,80].

El ciclo del Ca^{+2} a través de MMI utiliza la corriente de H^{+}, el transporte de metabolitos y otras reacciones como la NADH/NADP transhidrogenasa y la importación de proteínas[76]. Mientras que la MME es altamente permeable al Ca^{2+} gracias a la presencia del canal aniónico dependiente de voltaje, la MMI es impermeable y se requieren canales y transportadores

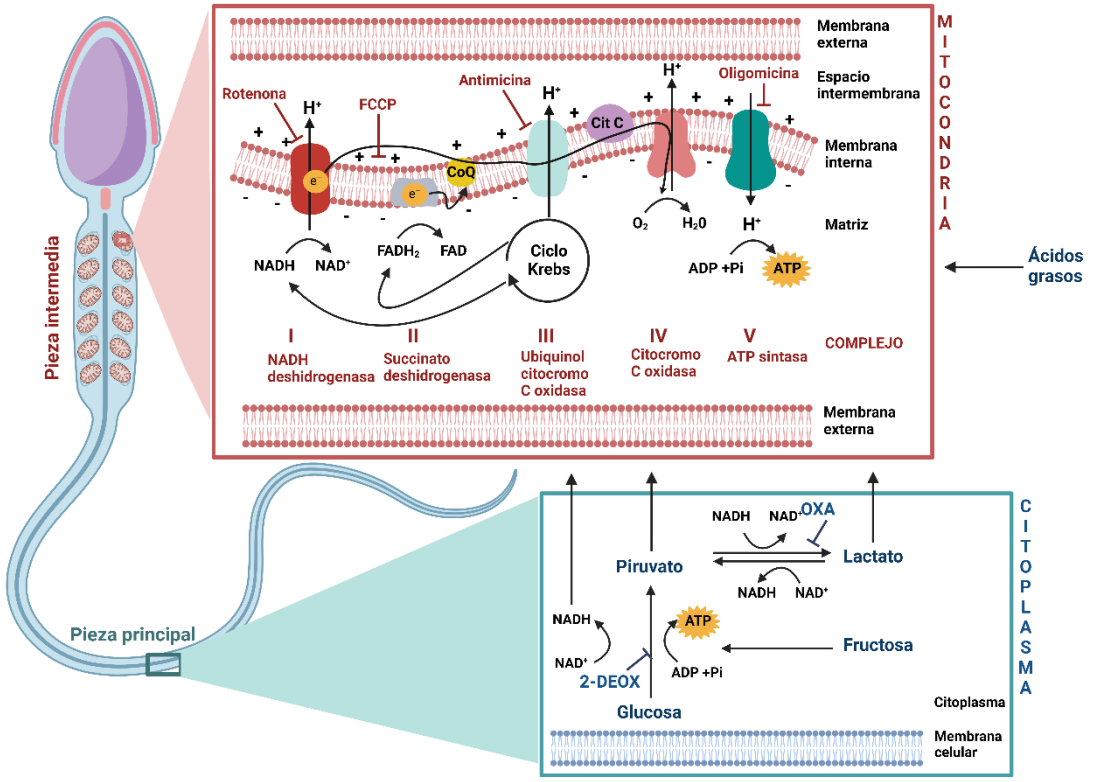

FIGURA 6: Esquema de las dos principales vías metabólicas y su ubicación en el espermatozoide. Lugar donde actúan los diferentes inhibidores y el desacoplante FCCP (carbonyl cyanide-p-trifluoromethoxyphenylhydrazone). OXA= oxamato, 2-DEOX= 2-Deoxyglucosa. Realizado en Biorender.

especializados para permitir su captación[81]. La entrada de Ca^{2+} en la matriz mitocondrial está mediada por un canal iónico, el MCU (*mitocondrial calcium uniporter*) [82]. Recientemente, se ha sugerido que las mitocondrias pueden expresar más de un MCU y se ha propuesto una vía alternativa de entrada de Ca^{2+}, un anti puerto de Ca^{2+}/H^{+}[82]. La entrada de Ca^{2+} a través de la MCU está impulsada por el PMM (dentro negativo; $\Delta\Psi m$) que existe a través de la MMI[83]. Dado que la $[Ca^{2+}]$ citosólico en estado de reposo es de alrededor de 100 nM y el PMM debido a la actividad de la cadena respiratoria es de ~−180 mV, la predicción es que, en equilibrio electroquímico, $[Ca^{2+}]$ mitocondrial podría alcanzar valores tan altos como 0,1 M[82,83].

La captación de Ca^{2+} mitocondrial se consideró como un mecanismo de reservorio que se pone en acción cuando se producen elevaciones patológicas de Ca^{2+} citosólico[81]. Sin embargo, el metabolismo oxidativo mitocondrial fisiológico depende de la $[Ca^{2+}]$ en la matriz mitocondrial ya que la actividad de enzimas mitocondrias están reguladas por el Ca^{2+}[81,83]. El Ca^{2+} actúa tanto en el espacio intermembrana mitocondrial, regulando la actividad de los transportadores de sustratos, como en la matriz, estimulando el ciclo de Krebs, la formación de NADH y, consecuentemente, la actividad de la cadena respiratoria, aumentando la producción de ATP[81]. Se describió que cuatro deshidrogenasas mitocondriales están reguladas por Ca^{2+}[81,83]. Una de ellas, es la deshidrogenasa de FAD-glicerol fosfato, que se encuentra en la membrana interna y detecta el Ca^{2+} en el espacio intermembrana, mientras que las otras tres son enzimas importantes para el ciclo de Krebs que detectan el Ca^{2+} de la matriz: la fosfatasa de la deshidrogenasa del piruvato, la enzima que modula la actividad de la piruvato deshidrogenasa; la isocitrato deshidrogenasa y la oxoglutarato deshidrogenasa[81–83]. La estimulación mediada por Ca^{2+} de estas enzimas conduce a que se regenere NAD+ a NADH y FAD a $FADH_2$, lo que resulta en una mayor actividad de la cadena respiratoria, incrementando el metabolismo mitocondrial

y la producción de ATP[81]. Recientemente se reportó que el Ca^{2+} puede actuar directamente modulando la cadena de transporte de electrones (en particular la actividad de los complejos I, II y III) y la ATP sintasa para acelerar la respiración[81]. Además de modular el metabolismo mitocondrial en la matriz, el Ca^{2+} también tiene un papel en la regulación de los transportadores de nucleótidos, metabolitos y cofactores[81].

Es importante aclarar que una captación excesiva de Ca^{2+} mitocondrial modula la muerte celular apoptótica, sensibilizando el orgánulo a los estímulos apoptóticos[80,81]. En condiciones fisiológicas, la transferencia de Ca^{2+} a las mitocondrias es adecuada y esencial para la funcionalidad mitocondrial y no induce la apertura del poro de transición de permeabilidad; este proceso, junto con la liberación de citocromo c y la activación de la cascada apoptótica, ocurre cuando las mitocondrias absorben una gran cantidad de Ca^{2+}[81]. Por esta razón, las mitocondrias también están dotadas de moléculas de extrusión de Ca^{2+}, los intercambiadores Na^{+}/Ca^{2+} (NCLX) y H^{+}/Ca^{2+}(mHCX), que exportan Ca^{2+} fuera de las mitocondrias y restringen la acumulación de Ca^{2+} dentro de la matriz, manteniendo así la homeostasis de Ca^{2+} mitocondrial[81].

3.3.1.2. Función de la mitocondria en la formación de ROS (en células somáticas)

En las células eucariotas, las mitocondrias, el sistema enzimático del citocromo P450 (CYP450), los peroxisomas, la xantina oxidasa y las NADPH oxidasas son las principales fuentes de ROS. Sin embargo, la mayor producción de estas especies ocurre en las mitocondrias que generan aproximadamente el 90% de las ROS celulares[74,84,85]. En condiciones fisiológicas, en el entorno del 0,2-0,5% del oxígeno molecular, sufre una reducción parcial por un electrón a nivel del complejo I (tanto por transporte directo como inverso de electrones), complejo III y las flavo-deshidrogenasas, formando el anión superóxido ($O_2^{\bullet-}$) (Figura 7)[84–89]. Aunque los complejos I y III son los principales sitios de producción en las mitocondrias, el Complejo II puede producir ROS en menor medida[74,84,85]. El sitio FAD del Complejo II puede producir $O_2^{\bullet-}$ hacia la matriz[90,91]. La formación del radical libre $O_2^{\bullet-}$ aumenta frente a un daño o en presencia de inhibidores de la cadena respiratoria como la AA (inhibidor del complejo III) (Figura 7)[76,91,92]. Las mitocondrias regulan la producción de ROS a través de varios mecanismos, incluyendo la modulación del PMM, el estado redox de los complejos de la cadena de transporte de electrones y la disponibilidad de oxígeno[90,92].

El $O_2^{\bullet-}$ se trata de una ROS primaria que es capaz de interactuar con otras moléculas formando ROS secundarias, ya sea directamente o en procesos catalizados por enzimas o metales[74,90,91]. La mitocondria posee enzimas antioxidantes, por un lado la superóxido dismutasa de manganeso (SOD2, MnSOD) en la matriz y de cobre y zinc (SOD1, CuZnSOD) en el espacio intermembrana que cataliza la dismutación del $O_2^{\bullet-}$ formando peróxido de hidrógeno (H_2O_2, otra especie oxidante), que difunde a través de las membranas biológicas[87,90,93–95]. SOD1 también se encuentra presente en el citoplasma[90,93,94]. El H_2O_2 formado puede ser tóxico; por lo tanto, se degrada con la intervención de enzimas específicas (dentro o fuera de la mitocondria) como la catalasa, la tiorredoxina peroxidasa y la glutatión peroxidasa. La tirorredoxina peroxidasa y la glutatión peroxidasa utilizan glutatión reducido y tiorredoxina como sustrato, respectivamente, para reducir el H_2O_2 a agua[74,90,93]. El glutatión oxidado y la tiorredoxina luego son reducidos por la glutatión reductasa y la tiorredoxina reductasa, respectivamente, utilizando NADPH como sustrato[74,90,93].

Por otro lado, cuando un ión ferroso transfiere un electrón al H_2O_2, se forma otra ROS que es el radical hidroxilo ($^{\bullet}OH$) el cual es la única especie capaz de dañar directamente la mayor parte de las biomoléculas[90,95]. El $O_2^{\bullet-}$ formado en la mitocondria también puede reaccionar con óxido

nítrico a concentraciones equimolares (k= 1010 $M^{-1}s^{-1}$) formando peroxinitrito ($ONOO^-$), una especie altamente oxidante y nitrante[96]. El $ONOO^-$ se puede formar dentro de la mitocondria ya que el óxido nítrico producido en la reacción catalizada por la óxido nítrico sintetasa (citosólica) difunde a través de las membranas y se encuentra en el sitio específico de formación de $O_2^{\bullet-}$ en la cadena respiratoria[93,94]. Otra de las enzimas antioxidantes es la peroxirredoxina 3 la cual reduce el peroxinitrito ($ONOO^-$)[81,83,86]. El $ONOO^-$ está en equilibrio con su forma protonada, el ácido peroxinitroso siendo su pKa de 6,8, por lo que, en condiciones fisiológicas, ambas formas estarán presentes[97,98]. El ácido peroxinitroso puede descomponerse por homólisis, formando el radical dióxido de nitrógeno ($^{\bullet}NO_2$) y $^{\bullet}OH$[97,98]. Las especies reactivas del nitrógeno (RNS) son las moléculas derivadas del óxido nítrico, el cual es producido en los tejidos biológicos por enzimas denominadas óxido nítrico sintasas[97]. Por último, otra de las especies oxidantes que juega un papel importante en interacción con las RNS, es el radical carbonato[89]. Su formación ocurre en presencia de $ONOO^-$ y dióxido de carbono (CO_2), por lo que podría generarse en muchas condiciones biológicamente relevantes[89].

Las ROS desempeñan un papel importante en el funcionamiento normal celular, participando en la señalización de procesos celulares (a través de la regulación redox de la fosforilación de proteínas, canales iónicos y factores de transcripción), en la eliminación de patógenos por el sistema inmune y procesos de biosíntesis pero también son conocidas por estar asociadas a múltiples enfermedades[99]. Una enfermedad asociada a ROS puede deberse a una falta de ROS (ej., enfermedad granulomatosa crónica, ciertos trastornos autoinmunes) o a un exceso de ROS (p. ej., enfermedades cardiovasculares, neurodegenerativas, cáncer, diabetes e infertilidad). [76,100–102]. El estrés nitro-oxidativo se define como la pérdida del equilibrio entre oxidantes y la capacidad de los sistemas biológicos de detoxificar los reactivos intermedios o de reparar el daño resultante[91,103] . Los radicales libres son especies químicas de vida media corta que poseen uno o más electrones desapareados. Son por lo general inestables, tienden a ser altamente reactivos. Los mismos son agentes muy oxidantes capaces de interaccionar con moléculas como aminoácidos, lípidos, proteínas, enzimas y cofactores de enzimas, afectando su función[96,103,104]. Por ejemplo, las ROS desencadenan cascadas de peroxidación lipídica que generan aldehídos de masa molecular pequeña, como la acroleína, el malondialdehído y el 4-hidroxinonenal (4-HNE)[105–107]. Estas moléculas poderosamente electrófilas se unen covalentemente a proteínas en los residuos como la histidina, lisina y cisteína en las proteínas[107]. La secuencia de eventos incluye la peroxidación lipídica, pérdida de integridad de la membrana con aumento de permeabilidad, daño estructural del ADN y, finalmente, apoptosis[74,95,106]. Un análisis de las proteínas que se unen preferentemente a estos aldehídos reveló que afectan especialmente a las proteínas mitocondriales, un blanco clave que se ve afectado por estas modificaciones es la succinato deshidrogenasa, perpetuando la producción de ROS por la cadena de transporte de electrones[108]. El delicado balance entre los efectos perjudiciales y beneficiosos de los radicales libres es un aspecto muy importante para los seres vivos y es mantenido mediante mecanismos denominados de “regulación redox”. Estos procesos protegen a los organismos y mantienen la “homeostasis redox” controlando el estado redox [85].

3.3.2. Mitocondrias espermáticas

Si bien los espermatozoides pierden la mayor parte de sus organelos y contenido citoplasmático durante la espermatogénesis, conservan un importante número de mitocondrias (varía según especies, entre 50-75 mitocondrias)[109,110]. A medida que la espermatogénesis progresa hacia etapas más avanzadas, las mitocondrias sufren una transformación para volverse más condensadas, alargadas y eficientes en la fosforilación oxidativa[111]. Su morfología es diferente a las de las células somáticas[27]. Éstas se disponen, unidas por puentes disulfuro formando una vaina helicoidal compacta por fuera de las fibras densas del flagelo (Figura 8)[112]. Se encuentran

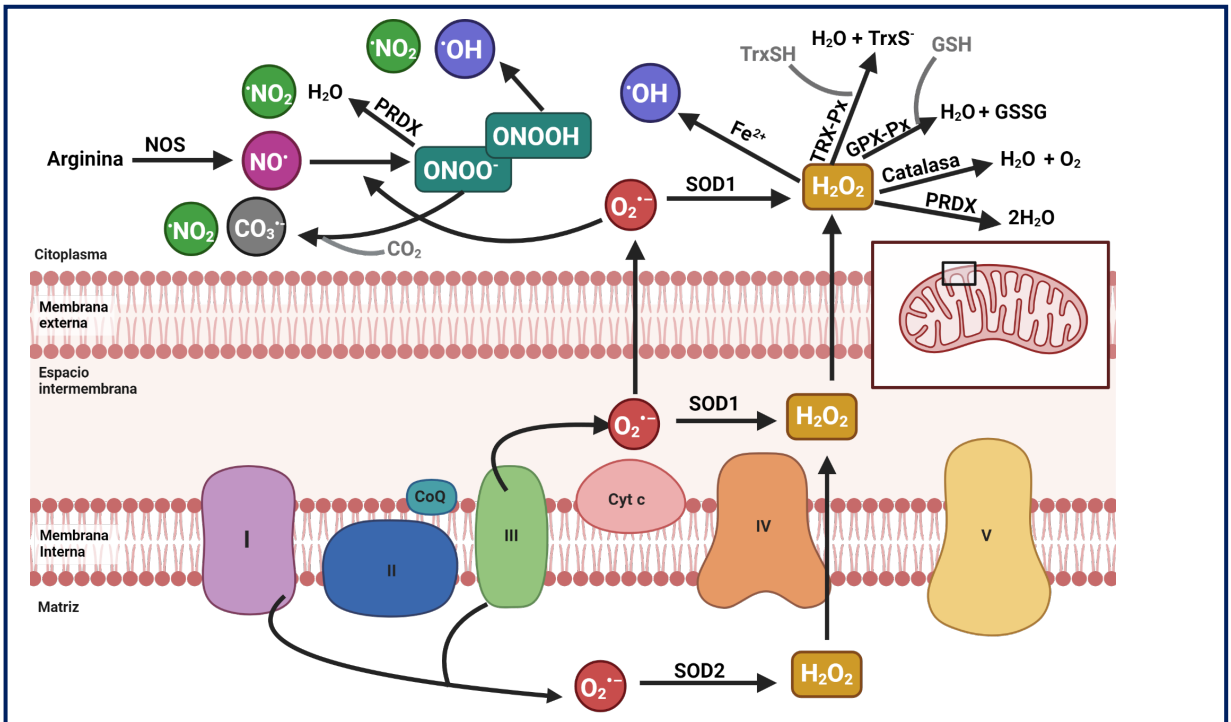

FIGURA 7: Esquema de la producción de especies reactivas del oxígeno y del nitrógeno (ROS y RNS, respectivamente) a nivel de la cadena de transporte de electrones de la mitocondria. Como resultado de la reducción parcial de oxígeno principalmente a nivel de los complejos I y III, se genera superóxido ($O_2^{\bullet-}$), una ROS primaria. El $O_2^{\bullet-}$ mediante la acción de las enzimas superóxido dismutasas (SOD), dismuta rápidamente en peróxido de hidrógeno (H_2O_2), una ROS más estable y capaz de transportarse a través de las membranas. El H_2O_2 es rápidamente removido por sistemas antioxidantes como: 1) catalasa, lo descompone en agua (H_2O) y oxígeno (O_2), 2) glutatión peroxidasa, GPX-Px, utiliza como sustrato glutatión reducido (GSH) resultando en H_2O y glutatión oxidado (GSSG), 3) tiorredoxina peroxidasa, TDX-Px, utiliza tiorredoxina (TrxSH) como sustrato, resultando H_2O y tiorredoxina oxidada (TrxS). Además, el H_2O_2 puede interaccionar con el hierro (Fe^{2+}) y formar el radical hidroxilo ($^{\bullet}OH$). Las óxido nítrico sintasas (NOS) son enzimas clave para la producción y la regulación del óxido nítrico ($NO^{\bullet}$), el cual interacciona con el $O_2^{\bullet-}$ formando el peroxinitrito ($ONOO^-$) y su forma protonada (ONOOH). Las peroxirredoxinas (PRDX) utilizan grupos tiol (-SH) para reducir H_2O_2 y $ONOO^-$ en H_2O. Si bien las enzimas antioxidantes en el esquema se representan en el citosol también hay catalasas, GPX, GSH y PRDX dentro de la mitocondria. Figura realizada en Biorender según referencia[114].

conectadas por conectores intermitocondriales y ancladas al citoesqueleto mediante disposiciones ordenadas de proteínas en la membrana mitocondrial externa[26,112,113]. Los mecanismos que generan y mantienen su disposición organizada se desconocen con exactitud[109].

Las mitocondrias espermáticas poseen proteínas específicas que modulan la función de la célula en los diferentes estadíos del proceso de fertilización[109]. Se han identificado muchas proteínas implicadas en la capacitación, en la organización de la cola, la transducción de señales, chaperonas y proteínas de canales iónicos[115]. Existen evidencias que indican que la morfología y función mitocondrial son importantes para la actividad de esta célula, lo que se relaciona consistentemente con la infertilidad masculina, mostrando en muchos casos una correlación con los parámetros del semen [116–120]. Si bien, se ha visto que la función mitocondrial espermática es necesaria para la fecundación[121], su función no se encuentra completamente dilucidada.

3.3.2.1. Rol de la mitocondria en la motilidad

Para que el espermatozoide pueda cumplir su función y transmitir el genoma paterno a la nueva generación, *in vivo*, primero debe desplazarse hasta el oviducto donde se encontrará con el ovocito[26,27]. Para ello, es necesaria una motilidad espermática de tipo progresiva, con amplitud lateral de cabeza baja y una velocidad progresiva recta suficientemente rápida[122]. El hecho de que el movimiento flagelar sea dependiente de la producción de ATP, sumado a que las mitocondrias de los espermatozoides se ubican en la región del inicio del movimiento del flagelo y que la fosforilación oxidativa produce más ATP por molécula de glucosa que la glucólisis, ha llevado a que la respiración históricamente ha sido considerada como la fuente principal de producción de ATP para la motilidad espermática[122–125].

En diferentes trabajos, se observó que en muestras humanas de pacientes infértiles con astenozoospermia sus piezas intermedias son más pequeñas, con un menor número de mitocondrias, con un ensamblaje anormal y membranas mitocondriales con defectos estructurales en comparación con muestras de espermogramas normales[117,126]. Además, datos previos de nuestro laboratorio donde se estudió por primera vez la función mitocondrial en espermatozoides humanos (células intactas) con un respirómetro de alta resolución (HRR) mostraron que la función mitocondrial (RCR) se correlaciona positivamente con la motilidad progresiva[116]. Esto apoya estudios comparativos recientes donde observaron que la velocidad del espermatozoide está correlacionada con el número de mitocondrias y la producción de ATP[111].

Sin embargo, algunos autores, sostienen que la principal vía para la obtención de energía en los espermatozoides es a partir de la glucólisis[127]. Como se muestra en la Figura 7, el espermatozoide es una célula muy compartimentalizada donde las mitocondrias están restringidas a la primera parte del flagelo y por tanto sería poco probable que el ATP se pueda distribuir lo suficientemente rápido por todo lo largo del flagelo por difusión simple para mantener la motilidad[128,129]. Además, se observó que la motilidad espermática se mantiene en presencia de inhibidores de la fosforilación oxidativa pero no en presencia de inhibidores de la glucólisis[130,131]. Por otro lado, se ha demostrado que la glucólisis es esencial para la producción de ATP en el espermatozoide mediante el uso de modificaciones genéticas en ratones. Los ratones KO para la gliceraldehido-3-fosfato deshidrogenasa (espermatogénica) son infértiles y los ratones KO de fosfoglicerato quinasa 2 son severamente subfértiles, debido a una motilidad espermática disminuida y bajos niveles de ATP[132,133]. En contraste, los ratones KO de citocromo c (testicular), una proteína esencial para la respiración mitocondrial, son fértiles[134].

No obstante, existe un amplio rango de variación entre los espermatozoides de las especies de mamíferos con respecto al principal mecanismo de producción de ATP en estas células, siendo por tanto un tema de extenso debate[110,127,135]. Esta aparente discrepancia podría ser consecuencia de que los espermatozoides (al igual de como ocurre en otros tipos celulares), podrían obtener ATP de ambas vías metabólicas: glucólisis y fosforilación oxidativa[122,136]. En el caso de los espermatozoides esto podría depender de la disponibilidad de sustratos y concentración de oxígeno presentes en el tracto femenino[122,137].

3.3.2.2. Rol de la mitocondria en la capacitación

Como fue mencionado, durante la migración desde la cervix al oviducto, los espermatozoides sufren ciertos cambios bioquímicos y funcionales correspondientes a la capacitación[37,46,48]. A pesar de llevar más de medio siglo estudiando cuáles son los mecanismos moleculares que

fundamentan estas modificaciones fisiológicas sigue siendo un conocimiento bastante incompleto. Un aspecto que ha ganado atención en este último tiempo es el rol de la mitocondria en el proceso, ya que varios autores reportaron un aumento de su actividad durante la capacitación en distintos modelos, por ejemplo en el ratón[49,53], humano[138] y jabalí[122].

Unos de los mecanismos que no son completamente comprendidos son los que se producen como consecuencia de la entrada de Ca^{2+} durante la capacitación en el cual las mitocondrias podrían participar. En el espermatozoide, el Ca^{2+} es considerado un regulador de la motilidad, participante de la capacitación y segundo mensajero esencial para la RA[139]. Los espermatozoides deficientes de CatSper no se hiperactivan y los ratones mutantes son infértiles, aunque presentan RA y fosforilación en tirosina normal[140]. Además, los espermatozoides KO para CatSper presentan un contenido de ATP bajo con respecto a los ratones salvajes[141]. En otros modelos celulares, la entrada regulada de Ca^{2+} en las mitocondrias regula el metabolismo mitocondrial pero esto no ha sido suficientemente estudiado en el espermatozoide[142–144]. Por otro lado, existen evidencias de la existencia de reservorios internos de Ca^{2+} en el espermatozoide los cuales son fundamentales para la propagación de las señales de este ion, habiéndose identificado transportadores de Ca^{2+}, por ejemplo, el MCU[82,110,145].

Por otro lado, la capacitación es un proceso de regulación redox, promovido por la generación de bajos niveles de ROS[71,95]. Bajas concentraciones de H_2O_2 inducen la capacitación[95,146]. Esta especie regula las vías de señalización en espermatozoides humanos, hamster y bovinos, teniendo una correlación positiva con la fosforilación en tirosina[95]. Además, existen otras ROS alternativas que también son capaces de estimular la CAP como el $O_2^{\bullet-}$, el óxido nítrico y $ONOO^-$[147–150]. Las ROS podrían promover la capacitación por múltiples mecanismos: inducen la oxidación del colesterol y el consiguiente flujo de salida de la membrana plasmática; estimulan la actividad de la adenil ciclasa, acompañado de la activación de la proteína quinasa A; activan proteínas extracelulares reguladas por señales de tipo quinasa; inhiben la actividad tirosina fosfatasa, induce la alcalinización citoplasmática y aumentar los niveles de Ca^{2+} intracelular[71,95]. Además, se ha demostrado que la catalasa es capaz de inhibir la fosforilación en tirosina y suprimir la hiperactivación, RA y la fusión del ovocito con el espermatozoide[71]. Si bien la capacitación se asocia con un aumento en la función mitocondrial tanto en humanos, como en ratones y equinos y por tanto parecería racional pensar que posee un rol en esta función, potencialmente las ROS pueden ser generadas por otras fuentes[49,151–153]. Por ejemplo, por enzimas oxidasas como las aminoácido oxidasas o la NADPH oxidasas tanto de espermatozoides como de leucocitos[154–156]. Por tanto, la contribución de cada fuente no está completamente aclarada y puede tener implicaciones para la comprensión del papel de las mitocondrias de los espermatozoides.

Exceso de ROS se asocia con infertilidad[157]. Se ha observado que una sobreexposición a estos metabolitos conduce a un estado de estrés oxidativo que limita el potencial de fertilización y la capacidad de estos gametos para apoyar el inicio del desarrollo embrionario normal [158,159]. Nuestro laboratorio observó que la disfunción mitocondrial se relaciona con un aumento del daño nitro-oxidativo en los espermatozoides[116]. Se ha establecido que un desequilibrio entre oxidantes y antioxidantes afecta la calidad de los espermatozoides afectando su morfología, motilidad y viabilidad[160]. Dependiendo del tipo de estudios, el estrés nitro-oxidativo se vincula con el 25% al 87% de los casos de subfertilidad masculina[102,161]. El estrés nitro-oxidativo lleva al daño de diversas estructuras, afectando proteínas claves, el ADN mitocondrial (más susceptible que el nuclear ya que se encuentra menos compactado) y los fosfolípidos de membranas[108,116]. Esto se ve exacerbado por el hecho de que los espermatozoides poseen una gran susceptibilidad al estrés oxidativo, ya que durante la espermatogénesis se pierden muchos de los componentes citoplasmáticos de los espermatozoides, entre esto sus defensas antioxidantes[26,116,162]. Se

postula que la falta de enzimas antioxidantes en los espermatozoides se compensa con una alta capacidad antioxidante del plasma seminal (PS).[163] La SOD, la catalasa, la GSH-Px, la vitamina C (ácido ascórbico), la vitamina E (tocoferol) y el zinc son las principales defensas antioxidantes del PS[164]. Esto representa la capacidad antioxidante total y es baja en hombres infértiles[164,165]. Sin embargo, en la práctica clínica, generalmente no se mide la producción de ROS ni la capacidad antioxidante del PS[166].

A pesar de la gran cantidad de datos que apuntan a la importancia de la mitocondria espermática para la fertilidad masculina, los mecanismos involucrados no se encuentran claros.

FIGURA 8: Disposición de las mitocondrias en la pieza intermedia del espermatozoide. Flechas marcan las mitocondrias. A. Espermatozoide equino, microfotografía electrónica de barrido. Fotografía extraída de la bibliografía[109]. B. Espermatozoide humano, microscopía electrónica de transmisión. Fotografía obtenida por Fernanda Skowronek. Ax= axonema.

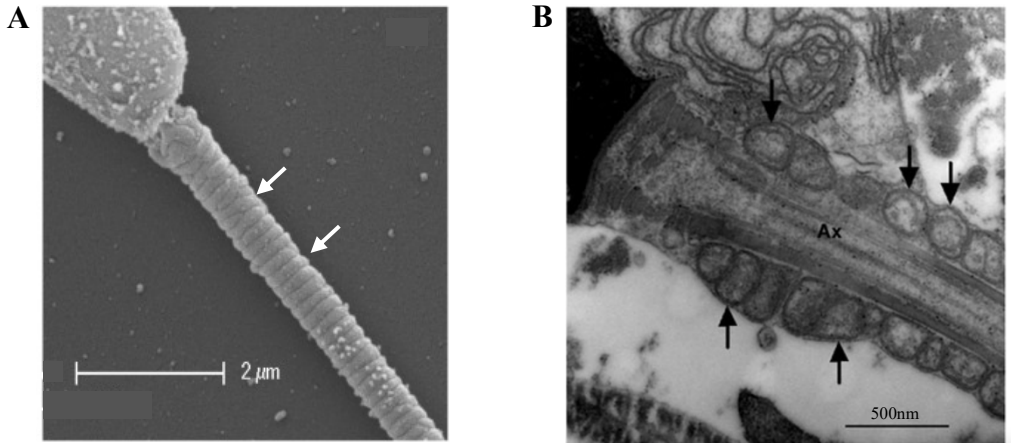

4. Hipótesis y objetivos

4.1 Hipótesis

Durante la capacitación espermática existe un incremento en la función mitocondrial que se traduce en un aumento en la concentración de Ca^{2+} mitocondrial y de la formación de ROS por el organelo los cuales cumplen un rol modulador sobre la capacidad fecundante del espermatozoide.

4.2. Objetivo General

Demostrar que la función mitocondrial aumenta durante la capacitación de los espermatozoides, dilucidando los posibles mecanismos involucrados y sus consecuencias fisiológicas. Determinar si esto puede constituir un blanco diagnóstico de la infertilidad masculina.

4.3. Objetivos específicos

1) Profundizar en los mecanismos involucrados en el incremento de la función mitocondrial y cómo esta contribuye en la habilidad del espermatozoide para fecundar.
2) Estudiar la función de la mitocondria en la producción de ROS durante la capacitación espermática.
3) Desarrollar nuevas herramientas enfocadas en el estudio de la función mitocondrial y la producción de ROS para mejorar el diagnóstico del hombre infértil.

5. Materiales, métodos y resultados

Los métodos y resultados para los tres objetivos específicos serán presentados en distintos subcapítulos, cada uno conformado por uno o más artículos publicados o en formato borrador. En cuatro de los cinco artículos incluidos en la tesis, soy la primera autora.

El primer bloque de resultados de esta tesis está formado por el artículo "*Increased mitochondrial activity upon CatSper channel activation is required for mouse sperm capacitation"* publicado en la revista Redox Biology junto con resultados del artículo titulado *"Intramitochondrial Calcium Increase: A Conserved Mechanism of Mitochondrial Activation in Human and Mouse Sperm During Capacitation"* (en formato borrador, son datos preliminares). Ambos trabajos fueron realizados en colaboración con el laboratorio de la Dra. Santi en la Washington University.

El artículo "*Mitochondrial function and reactive oxygen species production during human sperm capacitation: Unraveling key players"* publicado en FASEB corresponde al segundo bloque de resultados.

Por último, los artículos "*Mitochondrial metabolism determines the functional status of human sperm and correlates with semen parameters" y "High-resolution respirometry to assess mitochondrial function in human spermatozoa"* publicados en la revista Frontiers in Cell and Development y Journal of Visualized Experiments (JoVE), respectivamente, constituyen los últimos resultados para cumplir con el tercer objetivo.

5.1. Profundizar en los mecanismos involucrados en el incremento de la función mitocondrial y cómo esta contribuye en la habilidad del espermatozoide para fecundar

Artículo 1: Increased mitochondrial activity upon CatSper channel activation is required for mouse sperm capacitation.

Juan J. Ferreira[#], Adriana Cassina[#], Pilar Irigoyen, Mariana Ford, Santiago Pietroroia, Nikita Peramsetty, Rafael Radi, Celia M. Santi* y Rossana Sapiro*.
[#] Ambos autores comparten la primera autoría.
*Ambas autoras comparten la última autoría.
Redox Biology 46 (2021)102176 . DOI:10.1016/j.redox.2021.102176

El objetivo del trabajo fue comprender si el flujo de Ca^{2+} resultante de la activación de los canales CatSper durante la capacitación, produce un incremento en el Ca^{2+} mitocondrial que aumenta su función para que se de la fecundación. Comparamos la actividad mitocondrial en espermatozoides NC y CAP mediante HRR, el PMM por citometría de flujo y microscopía, el intercambio ATP/ADP utilizando un inhibidor específico de la translocasa y la concentración Ca^{2+} por microscopía. Esto se realizó en espermatozoides de ratón salvajes (WT) o *knockout* para CatSper. Observamos que en espermatozoides CAP de ratones WT hay un incremento en la función mitocondrial acompañado de un aumento del Ca^{2+} mitocondrial. Esto no ocurrió en los espermatozoides CAP del *knockout* para CatSper. A su vez, vimos que el aumento de la función mitocondrial en espermatozoides CAP de ratones WT dependía del canal MCU, ya que no ocurría el aumento al inhibir el canal. Utilizando inhibidores de la actividad mitocondrial, mostramos que esta función es importante para que se logre la hiperactivación y la fertilización en ratones WT. Por tanto, nuestro trabajo propuso un nuevo mecanismo de la capacitación, donde la activación de los canales CatSper produce un aumento del Ca^{2+} citoplasmático en la pieza principal que se propaga por la pieza media generando un aumento del Ca^{2+} mitocondrial mediado por el canal MCU. Esto resulta en un aumento de la función mitocondrial lo que promueve la hiperactivación y fecundación *in vitro*. Estos datos contribuyen a entender el rol de la mitocondria en la fisiología del espermatozoide, abriendo la posibilidad a un nuevo target diagnóstico.

En este trabajo, mi contribución fue realizando experimentos de respirometría y citometría de flujo en espermatozoides de ratones WT, para estudiar la función mitocondrial en la capacitación. Además, analicé los parámetros de la capacitación: RA, fosforilación en tirosina e hiperactivación en muestras capacitadas con inhibidores mitocondriales.

Artículo 2 (borrador): Intramitochondrial Calcium Increase: A Conserved Mechanism of Mitochondrial Activation in Human and Mouse Sperm During Capacitation

Pilar Irigoyen[#], Juan J. Ferreira[#], Adriana Cassina, Celia M. Santi* y Rossana Sapiro*.
[#] Ambos autores comparten la primera autoría.
*Ambas autoras comparten la última autoría.

Se trata de un trabajo preliminar que se origina a partir de mi pasantía en el laboratorio de la Dra. Santi. En el mismo buscamos demostrar si el mecanismo descrito en el artículo anterior es conservado en los espermatozoides humanos. Para ello utilizamos las mismas técnicas para

comparar espermatozoides NC versus CAP. El trabajo implicó 43 donantes normozoospérmicos. Por el momento, observamos que al igual que lo que ocurre en el ratón, durante la CAP hay un aumento en la actividad mitocondrial (tanto del RCR como PMM) acompañado de un incremento en el Ca^{2+} mitocondrial. De la misma forma, el mecanismo demostró ser necesario para la hiperactivación ya que esta disminuye al inhibir la mitocondria. Queda pendiente aumentar el N de los experimentos y demostrar que canales se encuentran involucrados en el mecanismo.

Redox Biology 48 (2021) 102176

Contents lists available at ScienceDirect

Redox Biology

journal homepage: www.elsevier.com/locate/redox

Increased mitochondrial activity upon CatSper channel activation is required for mouse sperm capacitation

Juan J. Ferreira [c,d,1], Adriana Cassina [b,1], Pilar Irigoyen [a], Mariana Ford [a], Santiago Pietroroia [a], Nikita Peramsetty [c,d], Rafael Radi [b], Celia M. Santi [c,d,**], Rossana Sapiro [a,*]

[a] Departamento de Histología y Embriología and Centro de Investigaciones Biomédicas (CEINBIO), Facultad de Medicina UDELAR, Montevideo, Uruguay
[b] Departamento de Bioquímica and Centro de Investigaciones Biomédicas (CEINBIO) Facultad de Medicina, Universidad de la República, Montevideo, Uruguay
[c] Department of Obstetrics and Gynecology, Center for Reproductive Health Sciences, Washington University in St. Louis, School of Medicine, St. Louis, MO, United States
[d] Department of Neuroscience, Washington University in St. Louis, School of Medicine, St. Louis, MO, United States

ARTICLE INFO

Keywords:
Mitochondrial activity
CatSper channels
Spermatozoa capacitation
Fertilization
Hyperactivation
Calcium

ABSTRACT

To fertilize an oocyte, sperm must undergo several biochemical and functional changes known as capacitation. A key event in capacitation is calcium influx through the cation channel of sperm (CatSper). However, the molecular mechanisms of capacitation downstream of this calcium influx are not completely understood. Capacitation is also associated with an increase in mitochondrial oxygen consumption, and several lines of evidence indicate that regulated calcium entry into mitochondria increases the efficiency of oxidative respiration. Thus, we hypothesized that calcium influx through CatSper during capacitation increases mitochondrial calcium concentration and mitochondrial efficiency and thereby contributes to sperm hyperactivation and fertilization capacity. To test this hypothesis, we used high-resolution respirometry to measure mouse sperm mitochondrial activity. We also measured mitochondrial membrane potential, ATP/ADP exchange during capacitation, and mitochondrial calcium concentration in sperm from wild-type and CatSper knockout mice. We show that the increase in mitochondrial activity in capacitated wild-type sperm parallels the increase in mitochondrial calcium concentration. This effect is blunted in sperm from CatSper knockout mice. Importantly, these mechanisms are needed for optimal hyperactivation and fertilization in wild-type mice, as confirmed by using mitochondrial inhibitors. Thus, we describe a novel mechanism of sperm capacitation. This work contributes to our understanding of the role of mitochondria in sperm physiology and opens the possibility of new molecular targets for fertility treatments and male contraception.

1. Introduction

To fertilize an oocyte, sperm must undergo several biochemical and functional changes known as capacitation. During capacitation, sperm switch from progressive to hyperactivated motility and undergo a regulated release of acrosomal content in a process called the acrosome reaction (AR) [1,2]. These processes, which normally occur in the female reproductive tract, allow sperm to free themselves from the oviduct wall, penetrate the zona pellucida, and fuse with the oocyte. An important event controlling capacitation is an increase in intracellular [Ca^{2+}] [3] mediated by the cation sperm-specific channel (CatSper) [4,5]. *CatSper* Knockout (KO) mice are infertile because their sperm fail to hyperactivate and fertilize oocytes. However, the downstream effects of CatSper-mediated Ca^{2+} increase in sperm have not been fully elucidated [6,7].

In other cell types, regulated Ca^{2+} entry into mitochondria increases the efficiency of oxidative respiration [8,9] via activation of many Ca^{2+}-dependent mitochondrial enzymes resulting in the increase of ATP production [10]. Whether Ca^{2+} plays similar roles in sperm mitochondria is unknown [11]. Complicating this picture is the unclear role of

* Corresponding author. Departamento de Histología y Embriología and Centro de Investigaciones Biomédicas (CEINBIO), Facultad de Medicina UDELAR, Montevideo, Uruguay.
** Corresponding author. Department of Obstetrics and Gynecology, Center for Reproductive Health Sciences, Washington University in St. Louis, School of Medicine, St. Louis, MO, United States.
E-mail addresses: Santic@wustl.edu (C.M. Santi), rsapiro@fmed.edu.uy (R. Sapiro).
[1] Both authors contributed equally to this work.

https://doi.org/10.1016/j.redox.2021.102176
Received 9 October 2021; Received in revised form 29 October 2021; Accepted 29 October 2021
Available online 1 November 2021

mitochondria in sperm capacitation. Although some data suggest that sperm rely on glycolysis instead of mitochondrial respiration to produce ATP for motility and fertilization [12], other studies showed that mitochondrial respiration increases during capacitation in both human [13,14] and mouse [35] sperm. However, the significance of this increase in mitochondrial activity during capacitation and its role in sperm hyperactivation, acrosome reaction (AR), and fertilization remains to be established.

Given that sperm from CatSper KO mice have reduced ATP production [15], we hypothesized that Ca^{2+} influx through CatSper channels during capacitation enhances mitochondrial activity, thereby contributing to sperm hyperactivation and fertilization. To test our hypothesis, we studied mitochondrial activity using high-resolution respirometry (HRR), measurements of mitochondrial membrane potential (MMP) and evaluation of the ATP/ADP exchange during capacitation, as well as measurements of mitochondrial Ca^{2+}, both in wild-type and CatSper KO sperm. In addition, we analyzed the effects of mitochondrial function inhibitors on hallmark parameters of capacitation: AR, hyperactivation, tyrosine phosphorylation and the ability of the sperm to fertilize the egg.

2. Material and methods

2.1. Animals and ethics statement

All experimental procedures were approved by the Comisión Honoraria de Experimentación animal-CHEA,(Uruguay), or by the Animals studies committee of Washington University (St. Louis, MO,USA); and performed following the National Institute of Health Guide for the Care and Use of Laboratory Animals.

Animals were kept under a 12/12 h dark/light cycle at a constant temperature of 22 ± 2°C with free access to food and water. Wild-type sperm cells were obtained from male mice from two different strains, CB6F1/J mice (80–120 days old) in Montevideo-Uruguay and C57BL/6 male (60–90 days old) in Saint Louis, MO, USA. CatSper1 knock-out mice (CatSper KO) 60–90 days old were used in Saint Louis, MO, USA. Both were obtained from Jackson Laboratory. Acr-eGFP + Su9-Red2 transgenic mice (60-90 day-old) expressing green fluorescent protein (GFP) in the acrosome and red fluorescent protein (RFP) in the mitochondrial were obtained from Kelle Moley's laboratory, at Washington University in Saint Louis, School of Medicine, MO, USA. Oocytes were obtained from CB6F1/J female mice (4–8 weeks old), allocated in Montevideo-Uruguay. Mice were sacrificed via cervical dislocation.

2.2. Sperm collection and motility analysis

Motility analysis was performed in parallel in two laboratories. In Montevideo-Uruguay (UdelaR), sperm was collected from cauda epididymis in TYH media buffered with HEPES (NaCl 119.3 mM, KCl 4.7 mM, $CaCl_2.2H_2O$ 1.71 mM, KH_2PO_4 1.2 mM, $MgSO_4.7H_2O$ 1.2 mM, $NaHCO_3$ 25.1 mM, Glucose 5.56 mM, Sodium pyruvate 0.51 mM, HEPES 10 mM, Phenol Red 0.0006%), supplemented with 4 mg/ml Bovine serum albumin and incubated for 60 min at 37 °C to induce capacitation. Sperm suspensions were loaded into pre-warmed sperm counting chambers (depth 20 μm) (DRM-600, Millennium Sciences, Inc. CELL-VU®, NY) and placed on a microscope stage at 37 °C. Sperm motility was examined using a Computer Assisted Semen Analysis (CASA) system (SCA6 Evolution, Microptic, Barcelona, Spain). The microscope used was Nikon (Japan) Eclipse E200 with phase contrast 100X equipped with Basler (Germany) acA780-75gc camera. The default settings included the following: frames acquired: 30; frame rate: 60 Hz; head size: 5–70 μm2. Sperm with hyperactivated motility were sorted using the following parameters: curvilinear velocity (VCL) > 182 μm/s and linearity coefficient (LIN) < 32%, Straightness (STR) > 57%. At least 500 sperm were analyzed in each experiment. In Saint Louis, MO, USA (Washington University) sperm was collected from cauda epididymis, incubated in non-Capacitated (NC) HS media buffered with HEPES (in mM: 135 NaCl, 5 KCl, 2 $CaCl_2$, 1 $MgSO_4$, 20 HEPES, 5 glucose, 10 lactic acid, 1 Na-pyruvate) at pH 7.4 for 15–20 min at 37 °C. After this time, the motile fraction of the sample was removed from the tube and split based on conditions to be tested. To achieve capacitation, sperm were incubated for 90 min at 37 °C in capacitated (CAP) HS medium with 5 mg/ml Bovine serum albumin (BSA), and 15 mM $NaHCO_3$ added. NC sperm were incubated for 90 °C at 37°C in HS without BSA and $NaHCO_3$ [55] . Drugs or inhibitors were added in NC or CAP HS media. For motility tests, 3 μl of the sample were placed into a 20 μm Leja standard count 4 chamber slide, pre-warmed at 37°C, and a minimum of 200 cells were counted. CASA analysis was performed with a Hamilton–Thorne digital image analyzer (HTR-CEROS II v.1.7; Hamilton–Thorne Research, Beverly, MA, United States). CASA settings used for the analysis were: objective Zeiss 10XNH; 30 frames were acquired at 60 Hz; camera exposure: 8 ms; camera gain: 300; integrated time: 500 ms; elongation max (%): 100; elongation min (%): 1; head brightness min 170; head size max: 50 μm^2; head size min: 5 μm^2; static tail filter: false; tail brightness min: 70; tail brightness auto offset: 8; tail brightness mode: manual; progressive STR (%): 80; progressive VAP (μm/s): 25. The criteria used to define hyperactivated sperm was: curvilinear velocity (VCL) > 150 μm/s, lateral head displacement (ALH) > 7.0 μm, and linearity coefficient (LIN) of 32%.

2.3. Acrosome reaction (AR) evaluation

AR status was evaluated both in NC and CAP sperm samples. Induced AR was obtained by incubating the cells with 10 μM of the calcium ionophore A23187 for 30 min prior the end of the capacitation process. Mitochondrial inhibitors were added to CAP media with and without A23187, and 2.5 μM Antimycin A (AA) (Sigma Aldrich, St. Louis, MO) or 2.5 μM Carbonyl cyanide-4-(trifluoromethoxy) phenylhydrazone (FCCP; Sigma-Aldrich). For all conditions 15 μl samples were placed onto glass slides, fixed in 4% paraformaldehyde for 30 min and washed twice with phosphate buffered saline (PBS). After washing, slides were incubated with 0.22% Coomassie stain (Coomassie Blue G-250; Thermo Scientific, Massachusetts), 50% methanol, 10% glacial acetic acid, 40% water for 2 min. Excess dye was removed by washing thoroughly using distilled water. Slides were air-dried and coverslips were placed on slides using mounting medium at room temperature. Stained sperm were examined under bright field microscopy at 400X (Nikon E100, Japan) to verify the percentage of sperm that had undergone AR. A minimum of 200 sperm was evaluated in each experiment.

2.4. In vitro fertilization (IVF) protocol

CB6F1/J female mice (4–8 weeks old) were super-ovulated using intraperitoneal administration of 5IU Pregnant Mare Serum Gonadotropin (PMSG) (Syntex, Argentina) followed by 5UI human Chorionic Gonadotropin (hCG) (Intervet, Netherlands) 48 h later. After 12–15 h of hCG injection, female mice were sacrificed, and the oocyte-cumulus complex was isolated in 250 ml of TYH-CO_2 buffered media (NaCl 119.3 mM, KCl 4.7 mM, $CaCl_2.2H_2O$ 1.71 mM, KH_2PO_4 1.2 mM, $MgSO_4.7H_2O$ 1.2 mM, $NaHCO_3$ 25.1 mM, Glucose 5.56 mM, Sodium pyruvate 0.51 mM, Phenol red 0.0006%). Fertilization wells containing 30–50 eggs were inseminated with sperm (final concentration of 2.5×10^6 cells/ml) that had been CAP for 1 h in TYH-CO_2 buffered media supplemented with 4 mg/ml Bovine serum albumin at 37 °C and % CO_2 to induce capacitation, with or without mitochondria inhibitors (AA or FCCP) depending on the experimental conditions, washed twice by centrifugation, and resuspended in TYH-CO_2 media. After 3 h of insemination, eggs were washed and left in fresh media. To assess fertilization, eggs were evaluated after 24 h post-insemination, and two-cell stage embryos were counted.

2.5. High-resolution respirometry and respiration control ratio

Sperm cells oxygen consumption was determined by HRR [16]. HRR integrates highly sensitive oxygraphis (Oxygraph-2 K; Oroboros Instruments GmbH, Innsbruck, Austria) with software (DatLab, version 4.2; Oroboros Instruments GmbH) that presents respiration in terms of oxygen rate (pmol $O_2/10^6$ cells/sec). Basal oxygen consumption was measured for 10 min, then 2 μg/ml Oligomycin (Sigma-Aldrich, St. Louis, MO) were added to the chamber to block mitochondrial ATP synthase. Maximal respiration was obtained by subsequent 0.5 μM stepwise of FCCP. Finally, 2.5 μM Antimycin A (Sigma-Aldrich) was added to distinguish mitochondrial from residual (non-mitochondrial respiration) oxygen consumption. A total of 15 million sperms cells/ml per condition were evaluated. Stirring speed was set to 750 rpm. For each sperm sample (Fig. 1A), we measured mitochondrial basal respiration rate. By subtracting the oligomycin-resistant respiration rate from the basal respiration rate, we calculated the oxygen consumption rate linked to ATP synthesis. We also measured maximal respiration rate in the presence of FCCP. Finally, we measured the non-mitochondrial respiration rate, which we subtracted from all the other values. From these measurements, we calculated 1) Coupling efficiency = ratio between respiration linked to ATP synthesis and basal respiration [1–2/1], 2) RCR = ratio between maximal and oligomycin-resistant respiration rates [3/2], and 3) spare respiratory capacity = ratio between the maximal and basal respiration rates) [3/1]. It is important to note that the resulting values were internally normalized in each sample, and they were independent of cell number, protein mass, and viability. It is also important to notice that the cell's respiration inhibited by oligomycin in intact cells is comparable to isolated mitochondria state 4 oligomycin (in the presence of substrate plus ADP plus oligomycin). The maximal respiration rate caused by the addition of the uncoupler FCCP to intact cells is comparable to state 3 ADP of isolated mitochondria in presence of an excess of substrate plus ADP [17].

2.6. Mitochondrial membrane potential measurements

Flow cytometry: Sperm collected from cauda epididymis was allowed to swim-out in TYH media CAP media, buffered with HEPES, for 5–10 min. Tissue was extracted and the suspended cells were split into two samples with a final concentration of 106 cells/ml. One of the samples was treated immediately for 25 min at 37°C with 300 nmol/L of lipophilic cationic dye tetramethyl rhodamine methyl ester perchlorate (TMRM) (Sigma-Aldrich Inc., St Louis, MO, USA) and was considered as our (control) NC condition. The second sample was incubated for 90 min at 37°C and 5% CO_2 to induce capacitation, and TMRM was added 25 min before finishing the incubation period. TMRM was washed from both conditions by centrifuging the samples at 400 g and resuspended in 400 ml of PBS. Half of the washed sample (500 μl) was analyzed by flow cytometry and the remaining (500 μl) was incubated with 20 μM FCCP for 15 min and analyzed. Values obtained with FCCP were used as F_{min} to normalize the sample's fluorescence. We used the Geo Mean fluorescence values of FCCP at each experiment as minimum fluorescence to normalized fluorescence of M1 and M2 and discard differences related to the loading of TMRM for each experiment.

Flow cytometry analysis was performed using a FACS Calibur flow cytometer (Becton Dickinson, San Jose, CA). Cellular size and granularity were analyzed in the forward and side scatter (FSC–H and SSC-H), respectively. For each sample, 30000 single events were recorded in the forward light scatter/side light scatter dot plot. A gate was used to separate sperm from debris. TMRM was detected using a 585/42 nm bandwidth filter (FL-2). Samples were analyzed with Cell Quest software. Two populations of cells (M1 and M2, Fig. 1-C) with different MMP were consistently obtained. We analyzed the population with higher MMP (M2) based on several factors: 1) MMP measurements after capacitation for both populations made in our laboratory, 2) previously described methodology by Uribe P. et al. [18], and 3) similar results published using TMRM in sperm by Yang Q. et al. [19] . See Supplementary Fig. 1, for analysis of M1 population.

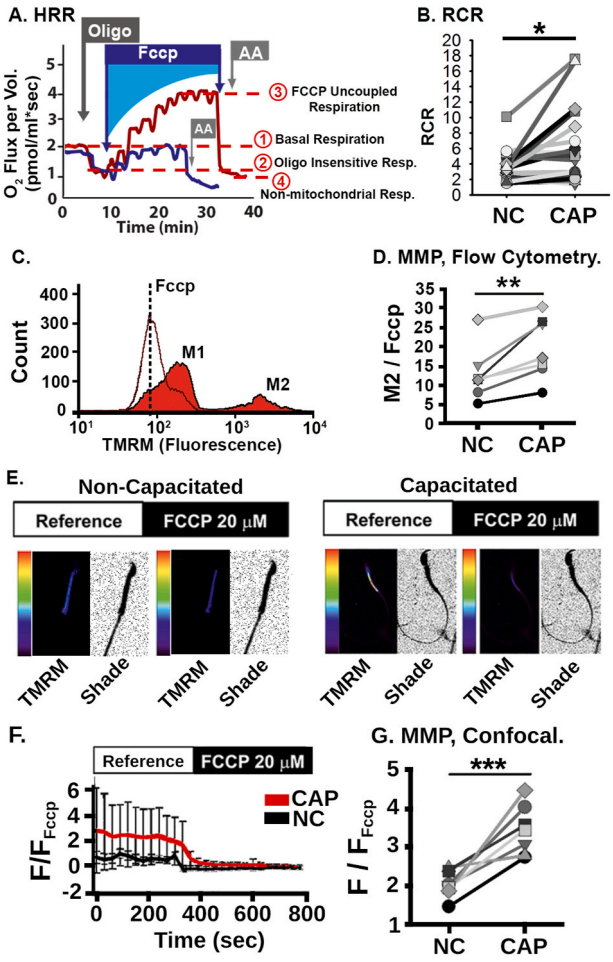

Fig. 1. Capacitated sperm exhibit increased mitochondrial function. A. Representative trace of oxygen consumption rate from CAP mouse sperm (red line) and NC (blue line). Dotted lines show representative respirometry parameters in CAP condition. Sperm cells were exposed sequentially to oligomycin (oligo), Carbonyl cyanide 4-(trifluoromethoxy) phenylhydrazone (FCCP), and Antimycin A (AA). **B.** Respiratory Control Ratio (RCR) values measured from wild-type CAP and NC sperm (n = 21). **C.** Representative histograms of TMRM fluorescence from CAP sperm, recorded with flow cytometry. **D.** Graph shows normalized TMRM fluorescence values (MMP) of M2 cell population under NC and CAP conditions (n = 7). See Supplementary Fig. 1, for analysis of M1 population. E. Representative confocal images of Wild-type sperm loaded TMRM before and after application of FCCP, under NC (left) and CAP (right). TMRM images shows the fluorescence obtained under the same technical specifications measured under NC (left) and CAP (right) conditions. Shade images represent the shape of the sperm cell used. Color bars represent color code for the gray scale from 0 to 255. Fluorescence was measured only in the sperm midpiece, and only cells responding to FCCP were included in the measurements. **F.** Representative normalized traces of TMRM fluorescence from NC and CAP sperm. Fluorescence was measured only in the sperm midpiece. Only cells responding to FCCP were included in the measurements. **G.** Graphs show normalized TMRM sperm midpiece fluorescence for NC and CAP sperm samples (n = 8). For **B** and **D**. paired *t-test* was used to determine statistical significance and an independent *t-test* was used in G. *p < 0.05 and ***p < 0.001. (n) represents the number of animals. (For interpretation of the references to color in this figure legend, the reader is referred to the Web version of this article.)

Single Cell MMP measurements by Confocal Imaging: Sperm cells were collected from cauda epididymis. Sperm were obtained by Swim-out in HS NC or CAP media for 10–15 min. NC samples were incubated in NC HS media, and CAP samples in CAP HS media, for 90 min at

37°C. At 60 min of incubation 200–300 nmol/L TMRM was added to all conditions and incubated for 30 min at 37°C. TMRM was washed from all samples by centrifugation and cells were resuspended in NC HS media and allowed to attach for 5–10 min to Poly-L-lysine (0.1%)-coated coverslips. Basal TMRM fluorescence for all the different conditions was measured before the addition of 20 μM FCCP, which was used to determine F_{min} and to normalize basal fluorescence values.

Fluorescence values from different animals and different conditions were adjusted to the same laser intensity and gain voltage. Recordings were performed with a confocal microscope (Leica SP8) and LAS X 3.5.2.18963 software equipped with an ACS APO 40x, 1.15 Numerical aperture objective, and oil-immersion objective. The parameters for the acquisition were: "xyt" images, 1024 x 1024 pixels, pixel size 0.269 μm, pinhole of 600.0 μm, 400 Hz unidirectional sampling, frames were obtained every 30 s. Excitation was performed by 543-nm laser and emitted fluorescence was measured at 556 nm–600 nm. All experiments were performed at room temperature (22–23°C). Fluorescence was measured only in regions of interest (ROI) corresponding to the sperm midpiece, using ImageJ software (version 1.48). Data was analyzed using pclamp 10 and Sigmaplot 12.

2.7. Fluo-5N and mitochondrial markers co-localization images

Sperm from wild-type mice (C57Bl6) or Acr-eGFP + Su9-Red2 transgenic mice were collected by swim-up in HS media, loaded with 2–4 μM Fluo-5N cell permeant AM-ester (Fluo-5N AM or Fluo-5N), and incubated with 200 nM MitoTracker® Red CMXRos – M7512 (Invitrogen, USA). To load Fluo-5N, cells were incubated at 37°C for 45–60 min in HS with 2 μM Fluo-5N AM and 0.05–0.1% Pluronic Acid F-127. MitoTracker was added 20–30 min before the Fluo-5N loading was finished. Sperm were then centrifuged, resuspended in HS NC media, and allowed to attach for 5–10 min to Poly-L-lysine (0.1%)- coated coverslips. Images were acquired using a confocal microscope (Leica SP8) and LAS X 3.5.2.18963 software equipped with an ACS APO 63x, 1.15 Numerical aperture objective, oil-immersion objective. Images's dimensions were 2048 x 2048 pixels. Sperm were excited at 488 nm and 543 nm and emitted fluorescence was measured at 500–530 and > 560 nm, for Fluo-5N and MitoTracker respectively. All experiments were performed at room temperature (22–23°C). ImageJ software (version 1.48) was used to analyze the images.

2.8. Mitochondrial Ca^{2+} measurements

After swim-up in HS NC or CAP media, motile cells were incubated with 2–4 μM Fluo-5N AM and 0.05% Pluronic F-127 at 37°C for 60–90 min. After loading, sperm cells were centrifuged at 1500–2000 rpm for 5–10 min and resuspended in the corresponding media. Sperm were allow to attach to Poly-L-lysine (0.1%) coated coverslips placed on the recording chamber's floor for 5 min. A local perfusion device with an estimate exchange time of 10 s was used to apply various test solutions. Calcium signals were recorded with a Leica AF 6000LX system with a Leica DMi8000 inverted microscope, equipped with a 63X objective (HC PL FluoTar L 63X/0.70 Dry) air objective and an Andor-Zyla-VCS04494 camera. An halogen lamp was used with a 488 ± 20 nm excitation filter and a 530 ± 20 nm emission filter. Data was collected with Leica LasX 2.0.014332 software. Acquisition parameters were: 20 ms exposure time, 4x4 binning, 1024 x 1024 pixels resolution. Whole images were collected every 10 s. LAS X, ImageJ, Clampfit 10 (Molecular Devices), and SigmaPlot 12 were used to analyze data.

ROI were selected in the sperm midpiece. Reference Fluo-5N fluorescence was measured at the beginning of the experiments (F_{Ref}), for all the conditions. To compare F_{Ref} levels across different animals and experimental conditions, we normalized Fluo-5N fluorescence using F_{min} and F_{max} obtained from each cell. F_{min} was obtained by perfusing cells with 0 mM Ca^{2+} + 2 mM EGTA and 2–5 μM Ionomycin. F_{max} was obtained by perfusing the cells with 2 mM Ca^{2+} + 2–5 μM Ionomycin. Experiments were performed at room temperature.

2.9. Statistical analysis

Sigmaplot version 12.0 (Systat Software Inc.), and GraphPad Prism version 6.01 for Windows (GraphPad Software, La Jolla California USA http://www.graphpad.com) were used for all statistical analysis. An unpaired Student's t-test was used to compare independent samples, and a paired *t*-test was used to compare data in studies performed in the same sample. Data are expressed as the mean ± SD. P-value < 0.05 was considered statistically significant.

3. Results

3.1. Mitochondrial respiration increases in capacitated mouse sperm

High-resolution respirometry (HRR) was performed in non-capacitated (NC) and capacitated (CAP) sperm. Fig. 1A shows a representative trace of oxygen consumption rate measured in capacitated sperm. The mean respiratory control ratios (RCR) (5.8 Mean ± 4.8 SD vs. 3.5 Mean ± 1.9 SD) and coupling efficiency (0.56 Mean ± 0.20 SD vs. 0.48 Mean ± 0.18 SD) were both significantly higher in CAP than in NC sperm (Fig. 1B and Table 1). We found no significant difference in spare respiratory capacity. We next measured MMP in NC or CAP sperm with the dye TMRM [18,20]. By flow cytometry we detected two sperm populations (M1 and M2, Fig. 1C) with different MMP in both NC and CAP sperm. Similar populations have been reported previously in human sperm [18]. We found that the normalized fluorescence of the M2 population was significantly higher in CAP sperm than in NC sperm (13.22 Mean ± 6.6 SD vs. 8.83 Mean ± 7.80 SD, n = 7, Fig. 1D). In addition, the M2 peak was completely abolished upon addition of the uncoupling agent carbonyl cyanide 4-(trifluoromethoxy) phenylhydrazone (FCCP) in both NC and CAP sperm. These data suggest that MMP in the M2 population increases during capacitation. We also used confocal imaging to measure TMRM fluorescence in the midpiece of individual NC and CAP sperm (see Fig. 1E and F for a representative example), we found that TMRM fluorescence was significantly higher in CAP than in NC sperm (3.27 Mean ± 0.50 SD vs. 2.05 Mean ± 0.36 SD, Fig. 1G). Taken together, these data reveal that mitochondrial activity is higher CAP than in NC sperm.

3.2. Mitochondrial respiration during capacitation is important for hyperactivated motility and oocyte fertilization

To address whether mitochondrial activity was required for the functional hallmarks of capacitation, we capacitated sperm for 1 h in control conditions or in the presence of FCCP or AA. A significantly higher percentage of sperm were hyperactivated in control conditions than in the presence of FCCP or AA (20.43 Mean ± 9.89 SD, n = 15, vs. 10.51 Mean ± 8.44 SD, n = 15, vs. Mean 7.58 ± 7.76 SD, n = 11, Fig. 2A). In contrast, FCCP and AA had no effect on the percentage of sperm that underwent spontaneous or induced AR (Fig. 2B). Additionally, AA had no effect on protein tyrosine phosphorylation (Supplementary Fig. 2). Sperm treated with FCCP or AA were significantly less able to fertilize oocytes than untreated sperm (Fig. 2C) Fig. 2D shows a representative in vitro fertilization control experiment (without any mitochondrial inhibitors) at 2-cell stage embryo.

Together, these data indicate that while mitochondrial activity during capacitation is not required for the AR or tyrosine phosphorylation, it significantly contributes to sperm hyperactivation and, notably, to their ability to fertilize oocytes.

3.3. Mitochondrial respiration is impaired in sperm from CatSper knockout (KO) mice

By analyzing HRR in sperm from CatSper KO mice we found that

Table 1
Oximetry values in NC and CAP sperm from wild-type and CatSper KO mice. Coupling efficiency = Oligomycin-sensitive respiration/basal respiration; RCR = Maximal respiration in the presence of FCCP/ATP turnover; spare respiratory capacity = Maximal respiration in the presence of FCCP/Basal Respiration.

Index		Wild-type				CatSper KO		
		Mean	SD	P-Value		Mean	SD	p-value
Coupling efficiency	**NC**	0.48	0.18	**0.009**	**NC**	0.37	0.06	**0.1**
	CAP	0.56	0.20		**CAP**	0.32	0.11	
RCR	**NC**	3.5	1.9	**0.012**	**NC**	2.12	0.50	**0.84**
	CAP	5.8	4.8		**CAP**	2.05	0.70	
Spare Respiration Capacity	**NC**	1.5	0.8	**0.96**	**NC**	1.34	0.36	**0.72**
	CAP	1.5	0.9		**CAP**	1.43	0.61	

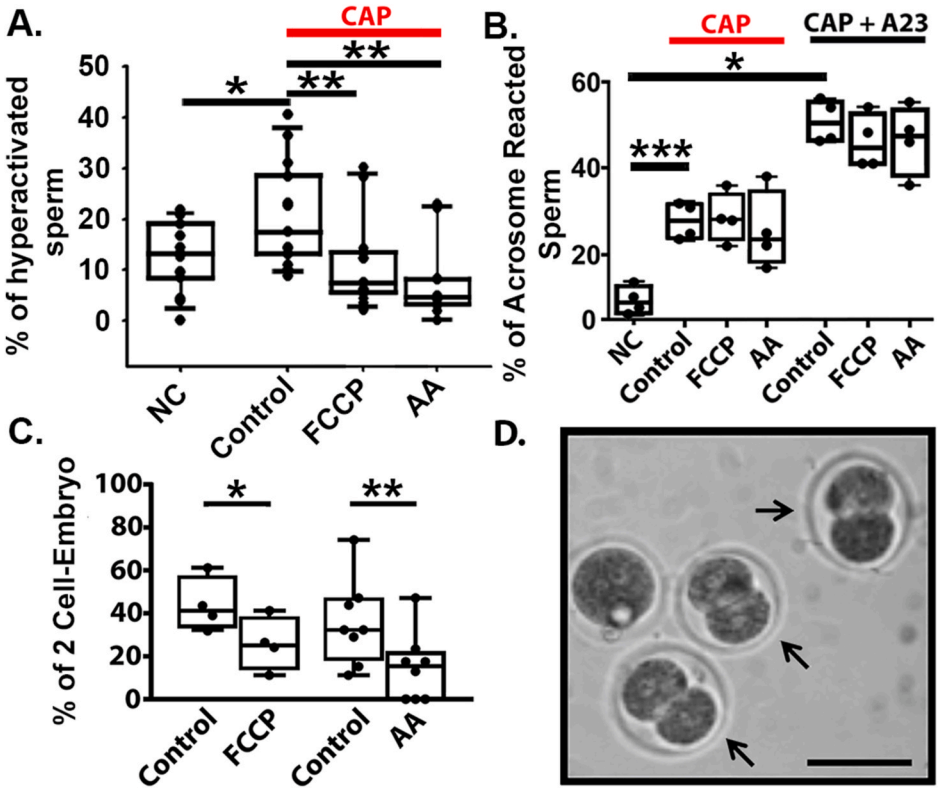

Fig. 2. Mitochondrial inhibitors impair mouse sperm capacitation and *in vitro* fertilization. A. Hyperactivation measurements obtained by CASA from CAP sperm in control conditions and in the presence of FCCP and AA. **B.** Spontaneous AR and A23187-induced AR from NC, CAP control, and CAP with FCCP or AA. **C.** Percentage of oocytes that reached the 2-cells stage embryo after 24 h of sperm addition. Graph shows mean ± SD. **D.** Representative phase contrast image of the 2-cell embryo stage (arrows) from experiment C under control conditions. Bar represents a 50 μm scale. To determine statistical significance between the groups, independent *t-test* were used on A and B, and Paired *t-test* was used in C. *p < 0.05, **p < 0.01, and ***p < 0.001 respectively. In A and C dots black represents the number of animals while in C represents each trial.

respiration values in sperm from CatSper KO mice did not differ between NC and CAP conditions (Fig. 3 A, B and Table 1). The MMP showed no statistical difference between CAP and NC in CatSper KO mice (2.90 Mean ± 0.92 SD vs. 3.10 Mean ± 0.48 SD, $P = 0.746$, Fig. 3C and D). Fig. 3E shows the variation in MMP after CAP for wild-type and CatSper KO mice; MMP increase in wild-type sperm during capacitation is statistically larger than in the KO sperm. Our results indicate that CatSper is involved in increasing sperm mitochondrial activity during capacitation.

3.4. *Mitochondrial Ca^{2+} concentration increases during capacitation in sperm from wild-type but not CatSper KO mice*

We next wanted to test whether the CatSper-dependent increase in cytoplasmic [Ca^{2+}] during capacitation (Supplementary Fig. 3) leads to an increase in mitochondrial [Ca^{2+}]. To do so, we developed a new method to measure mitochondrial [Ca^{2+}] in mouse sperm by using the fluorescent Ca^{2+}-indicator, Fluo-5N. Whereas Fluo-4 measures [Ca^{2+}] in the 100 nM–300 nM range and is suitable for measuring cytoplasmic [Ca^{2+}], Fluo-5N has a lower Ca^{2+}-binding affinity and is suitable for measuring [Ca^{2+}] in the 1 μM to 1 mM range, appropriate for measuring [Ca^{2+}] in mitochondria [21]. We first confirmed that Fluo-5N co-localized in the sperm midpiece with mitochondrial markers. In sperm from Acr-eGFP + Su9-Red2 transgenic mice, which express green fluorescent protein (GFP) in the acrosome and red fluorescent protein in mitochondria (RFP), Fluo-5N co-localized with RFP in the sperm midpiece (Supplementary Figs. 4A and E). Likewise, Fluo-5N co-localized with MitoTracker® red in the sperm midpiece (Supplementary Figs. 4B and E). In contrast, Fluo-4 distributed throughout the entire sperm (Supplementary Figs. 4C and E). Although Fluo-5N was also detected in the acrosome (Supplementary Figs. 4A and E), we excluded this in our assays by only measuring fluorescence in the sperm midpiece. Combined fluorescence profiles of the midpiece labeled with the different fluorophores are shown in Supplementary Fig. 4F. While RFP and MitoTracker® red fluorescence curves completely overlap with Fluo-5N profile in mitochondria, the overlay with Fluo- 4 is partial, which indicates that neither RFP nor Mitotracker colocalize with Fluo-4 AM in the cytoplasm (supplementary 4). To further confirm that our assay measured mitochondrial [Ca^{2+}], we loaded sperm with either Fluo-5N or Fluo-4 and continuously measured fluorescence in the midpiece before and after adding FCCP (Supplementary Fig. 5A). As expected, Fluo-5N fluorescence decreased in the midpiece upon addition of FCCP (Supplementary Fig. 5B), whereas Fluo-4 fluorescence in the midpiece increased (Supplementary Fig. 5C), suggesting that FCCP caused Ca^{2+} to be released from the mitochondria into the cytosol. Thus, we concluded

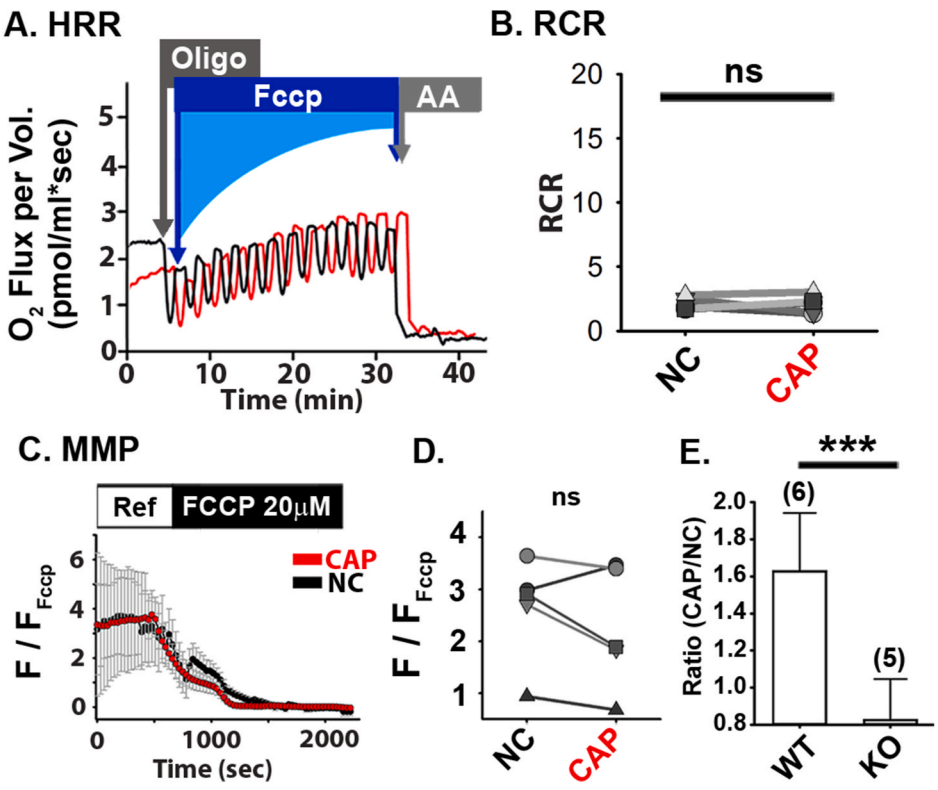

Fig. 3. CatSper KO sperm lacks capacitation-induced mitochondrial function increase. A. Representative recordings of a HRR from CAP (red line), and NC (black line) in CatSper KO sperm. Oxygen consumption was measured in control conditions and after the addition of mitochondrial inhibitors, Oligomycin, FCCP and AA. **B.** Respiratory control ratio (RCR) measurements from CAP and NC CatSper KO mouse sperm. A paired *t-test* was used to determine statistical significance (n = 5). **C.** Paired representative traces of normalized TMRM fluorescence, under CAP and NC conditions. **D.** Graph shows normalized TMRM fluorescence under NC and CAP conditions (n = 5). **E.** TMRM fluorescence ratio after CAP (normalized to NC) in wild-type and CatSper KO mice. To determine statistical significance, paired *t-test* was used. ns $p > 0.050$ and ***$p < 0.001$. Error bars represent SD. (n) represents the number of animals. (For interpretation of the references to color in this figure legend, the reader is referred to the Web version of this article.)

that our method accurately measured [Ca^{2+}] of the mitochondria in the sperm midpiece.

We then applied this method to determine if mitochondrial Ca^{2+} content was different between NC and CAP wild-type sperm. Fig. 4A shows representative images of CAP wild-type sperm loaded with Fluo-5N. At 2 mM extracellular [Ca^{2+}], we observed that mitochondrial Ca^{2+} was higher in CAP than in NC wild-type sperm (Fig. 4B and D). In contrast, when we performed the experiment at 0 mM extracellular [Ca^{2+}], we observed no difference in mitochondrial Ca^{2+} content between CAP and NC wild-type sperm (Fig. 4B and D). This is an expected result, as capacitation does not occur in the absence of extracellular calcium.

We found that mitochondrial Ca^{2+} content increased with higher extracellular [Ca^{2+}] (0, 0.5,1 and 2 mM) in both NC and CAP wild-type sperm, however, the increase was significantly larger in CAP sperm (Fig. 4D, Table 2). Whereas mitochondrial Fluo-5N fluorescence reached a plateau at 1 mM extracellular Ca^{2+} in NC sperm, the Fluo-5N fluorescence further increased at 2 mM extracellular Ca^{2+} in CAP sperm, consistently with the extracellular [Ca^{2+}] reported to achieve capacitation [22].

We conclude that mitochondrial [Ca^{2+}] depends on extracellular [Ca^{2+}]. Importantly, mitochondrial [Ca^{2+}] are significantly higher in CAP than in NC wild-type sperm. To determine whether the increase in mitochondrial [Ca^{2+}] in CAP sperm was dependent on CatSper activity; we measured changes in mitochondrial [Ca^{2+}] during capacitation in sperm from CatSper KO mice. Our results showed that in CatSper KO sperm, at 2 mM extracellular [Ca^{2+}], there is no difference in Fluo-5N fluorescence of the midpiece between NC and CAP conditions (Fig. 4C). When we plotted values of fluorescence in the midpiece of sperm from CatSper KO mice, we found that mitochondrial [Ca^{2+}] only increased when we changed extracellular [Ca^{2+}] from 0 to 0.5 mM, and then it remained constant. This increase was similar in NC and CAP sperm (Fig. 4E). The fact that Ca^{2+} increased at all in response to increased extracellular [Ca^{2+}] in sperm from CatSper KO mice suggests that Ca^{2+} can enter sperm through another pathway. Consistent with this idea, Ca^{2+} measurements obtained with the ratiometric dye Fura 2 a.m. showed that the cytosolic [Ca^{2+}] of CatSper KO sperm was 90–100 nM (Supplementary Fig. 3**).** Nonetheless, mitochondrial [Ca^{2+}] was significantly lower in CAP sperm from CatSper KO mice than in CAP sperm from wild-type mice (Fig. 4D and E and Table 2).

Another way to validate that CatSper channels were involved in the increased mitochondrial [Ca^{2+}], was to treat sperm from wild-type mice with the CatSper channel blocker Mibefradil during capacitation. Mibefradil (20 μM) significantly reduced the increase of mitochondrial [Ca^{2+}] associated with capacitation (Supplementary Fig. 6). Taken together these results confirmed that mitochondrial [Ca^{2+}] increase involved CatSper activation. This pharmacological approach confirms that the absence of CatSper conductance is uniquely responsible for the calcium defects that we have seen in the CatSper KO and rules out potential pleiotropic effects of the CatSper gene knock out (Supplementary Fig. 5).

3.5. *Increase in mitochondrial function associated with capacitation depends on the mitochondrial Ca^{2+} uniporter (MCU)*

We suspected that the increase of mitochondrial [Ca^{2+}] in CAP sperm occurred via Ca^{2+} influx through the MCU, which resides in the internal mitochondrial membrane [23]. To test this idea, we treated sperm with the specific MCU inhibitor Ru360 during capacitation [24], and then measured capacitation-associated changes in mitochondrial [Ca^{2+}], MMP, and sperm hyperactivation.

First, we found that mitochondrial [Ca^{2+}] was significantly reduced after capacitation in the presence of Ru360 when compared with those without Ru360 (Fig. 5A and B and Table 3). Second, we treated CAP sperm with vehicle or Ru360, loaded them with TMRM in the presence of 2 mM extracellular Ca^{2+}, and used our confocal microscopy assay to measure MMP. The normalized TMRM fluorescence was lower in sperm treated with Ru360 than in those without Ru360 (1.789 Mean ± 0.717 SD vs. 3.00 Mean ± 0.43 SD, P = 0.027, Fig. 5C). Moreover, whereas the MMP was 60% higher in CAP than NC sperm treated with vehicle, the

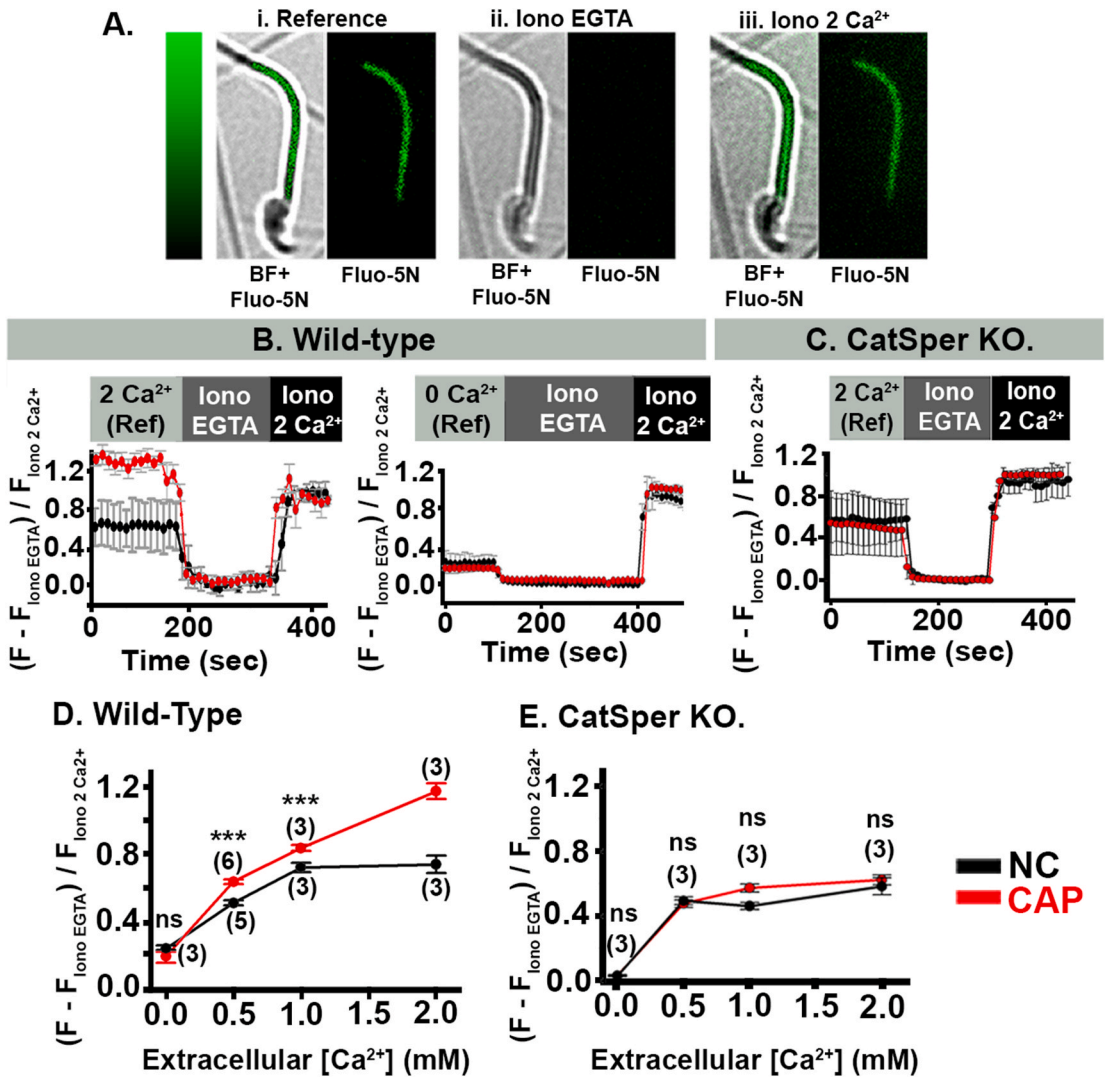

Fig. 4. Sperm mitochondrial [Ca^{2+}] increases during capacitation (CAP) in wild-type, but not in CatSper KO sperm. A. Representative images of CAP sperm loaded with Fluo-5N; and perfused with i) 2 mM Ca^{2+} (Reference), ii) 0 Ca^{2+} + 2 mM EGTA and Ionomycin (Iono EGTA), iii) Ionomycin +2 mM Ca^{2+} (Iono 2 Ca^{2+}). Images in i, ii, iii are on the left: bright field (BF) merged with Fluo-5N fluorescence (FITC). Right, Fluo-5N fluorescence. Color bars represent color code for the gray scale from 0 to 255. B and C, Representative traces of Fluo-5N fluorescence in the sperm midpiece from NC (black) and CAP (red) sperm incubated in 2 mM Ca^{2+} (B, left), and in 0 mM Ca^{2+} (B, right). C. Representative traces of Fluo-5N fluorescence from NC and CAP CatSper KO sperm. D. Normalized values of Fluo-5N fluorescence at reference (ref), in NC and CAP sperm at different extracellular [Ca^{2+}]. E. Fluo-5N fluorescence at reference in CatSper KO samples, obtained under NC and CAP conditions, at different extracellular [Ca^{2+}]. Statistical significance between CAP and NC samples at each extracellular [Ca^{2+}] were evaluated with an independent *t-test*. Fluorescence values are shown in Table 2 ns $p > 0.050$, and ***$p < 0.001$. (n) represents the number of animals. (For interpretation of the references to color in this figure legend, the reader is referred to the Web version of this article.)

Table 2
Fluo-5N fluorescent values corresponding to mitochondrial [Ca^{2+}] before and after CAP at different extracellular [Ca^{2+}]. Fluo-5N fluorescence values were normalized using Ionomycin +0 mM Ca^{2+} + EGTA (Iono EGTA) values and Ionomycin +2 mM Ca^{2+} (Iono 2 Ca^{2+}) values. To determine statistical significance between NC and CAP samples at each extracellular [Ca^{2+}], independent *t-test* were used.

Extracellular [Ca^{2+}] mM		Wild-type			P-Value		CatSper KO			p-value
		Mean	SD	n			Mean	SD	n	
0	**NC**	0.2398	0.1556	3	**0.197**	**NC**	0.0201	0.0167	3	**0.396**
	CAP	0.1935	0.1136	3		**CAP**	0.0234	0.0248	3	
0.5	**NC**	0.5122	0.2798	5	**0.035**	**NC**	0.4893	0.1984	3	**0.676**
	CAP	0.6394	0.2413	6		**CAP**	0.4717	0.1995	3	
1	**NC**	0.7242	0.2798	3	**0.01**	**NC**	0.4562	0.1649	3	**0.63**
	CAP	0.8402	0.208	3		**CAP**	0.5688	0.257	3	
2	**NC**	0.7427	0.4494	3	**0.022**	**NC**	0.579	0.3106	3	**0.155**
	CAP	1.1791	0.4635	3		**CAP**	0.6194	0.3805	3	

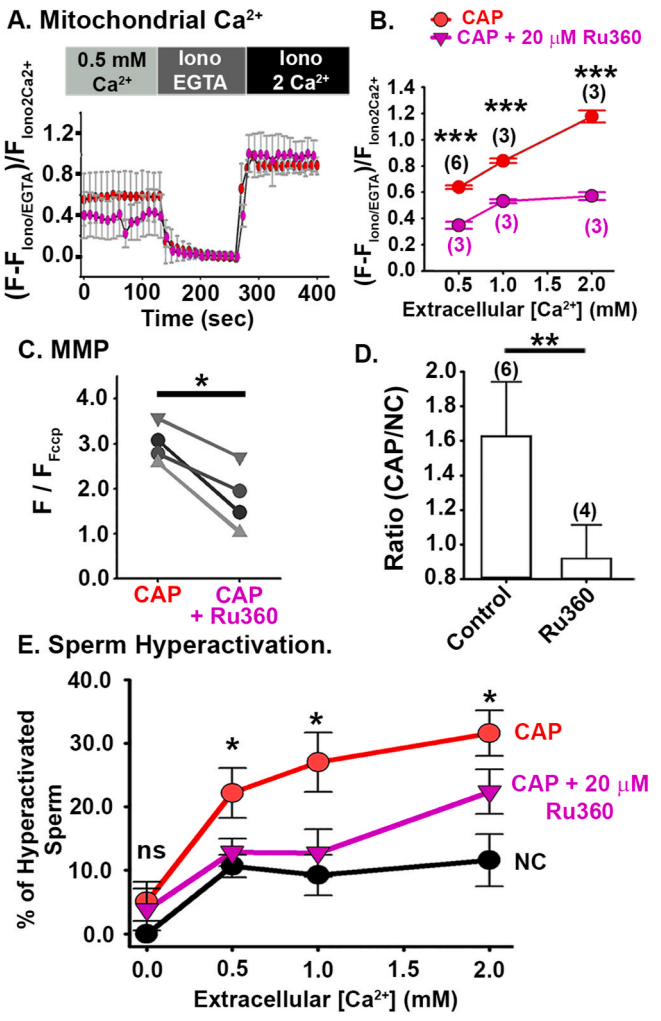

Fig. 5. Effect of the Mitochondrial Calcium Uniporter inhibitor, Ru360 on mitochondrial [Ca^{2+}], mitochondrial function, and sperm hyperactivation. A. Representative Fluo-5N fluorescence traces from CAP sperm and CAP with Ru360 at 0.5 mM extracellular Ca^{2+}. **B.** Normalized Fluo-5N fluorescence in NC and CAP conditions, at different extracellular [Ca^{2+}]. Graph shows mean values ± SD of cells responding to Iono EGTA and Iono 2Ca^{2+}. An independent *t-test* was used to determined statistical difference. **C.** Normalized TMRM fluorescence under CAP and CAP + Ru360 conditions (n = 4). To determine statistical significance, paired *t-test* were used. **D.** TMRM fluorescence ratio in wild-type sperm, under CAP (control) and CAP + Ru360. To determine statistical significance an independent *t-test* was used. **E.** Percentage of hyperactivated sperm measured by CASA from sperm samples incubated in NC, CAP or CAP +20 μM Ru360 media, at different extracellular [Ca^{2+}]. Values are also presented in Table 4. An independent *t-test* were used to evaluate statistical significance between NC, CAP and CAP + Ru360 groups at different [Ca^{2+}] (n = 5). Error Bars in figure represent SD. ns $P > 0.050$, *$p < 0.050$, **$p < 0.010$, and ***$p < 0.001$. (n) represents the number of animals.

Table 3
Fluo-5N fluorescence values corresponding to mitochondrial Ca^{2+} from wild-type sperm CAP in the presence of Ru360 at different extracellular [Ca^{2+}]. Fluo-5N values were normalized using Ionomycin +0 mM Ca^{2+} + EGTA (Iono EGTA) values and Ionomycin +2 mM Ca^{2+} (Iono 2 Ca^{2+}) values.

Extracellular [Ca^{2+}] mM		Wild-type		
		Mean	SD	n
0.5	**CAP + Ru360**	0.3483	0.027	3
1	**CAP + Ru360**	0.5324	0.015	3
2	**CAP + Ru360**	0.5725	0.0298	3

MMP was 5% lower in CAP than NC sperm treated with Ru360 (Fig. 5D). Thus, we concluded that Ru360 abolished the MMP increase observed in wild-type sperm after capacitation.

Finally, we assessed the effects of Ru360 on sperm hyperactivation by performing computer-assisted sperm analysis (CASA). In NC sperm, only 10% of sperm were hyperactive even at the highest extracellular [Ca^{2+}] tested (2 mM). In CAP samples treated with vehicle, approximately 30% of sperm were hyperactive at 2 mM extracellular [Ca^{2+}]. However, Ru360 treatment significantly diminished capacitation-induced hyperactivation (Fig. 5E and Table 4). To exclude the possibility that Ru360 impaired hyperactivation by directly inhibiting CatSper channels, we used Fluo-4 AM fluorescence to measure Ca^{2+} influx through CatSper channels in the absence and presence of Ru360. We found that membrane depolarization with KCl still triggers an increase of cytoplasmic [Ca^{2+}] even in the presence of Ru360, confirming that this compound did not inhibit Ca^{2+} influx through CatSper channels (Supplementary Fig. 7A). Together, these results suggest that the increase in mitochondrial [Ca^{2+}] contributes to sperm hyperactivation, and that this increase depends on extracellular [Ca^{2+}].

3.6. Hyperactivation relies on ADP/ATP translocase activity

In Fig. 1B, we showed that the RCR was higher in CAP sperm than in NC sperm, suggesting that mitochondria in CAP sperm produce more ATP, which could be required for sperm hyperactivation. To test this idea, we inhibited ATP/ADP exchange between the mitochondria and the cytosol by capacitating sperm in the presence of Atractyloside (ATR) (an inhibitor of the adenine nucleotide translocase residing in the inner mitochondrial membrane). Measurements with CASA, showed that the percentage of hyperactivated sperm was significantly lower in sperm treated with ATR than in those treated with vehicle (26.57 Mean ± 5.95 SD, n = 10, vs. 34.02 Mean ± 8.77 SD, n = 9, $P < 0.01$, Fig. 6A). To exclude the possibility that ATR impaired hyperactivation by directly inhibiting CatSper, we used Fluo-4 AM fluorescence to measure Ca^{2+} influx through CatSper in the absence and presence of ATR. This experiment confirmed that ATR did not inhibit Ca^{2+} influx through CatSper channels (Supplementary Fig. 7B). It is noteworthy that the percentages of hyperactivity inhibition were very similar when sperm were incubated in the presence of Ru360 or ATR, (35.77 Mean ± 26.85 SD, n = 6, vs. 26.42 Mean ± 10.41 SD, n = 6; Fig. 6B). This result suggests that Ca^{2+} entry into mitochondria during capacitation is important for the ATP production involved in sperm hyperactivation.

Table 4
Percentage of hyperactivation from Fig. 5E. Hyperactivated motility was measured with CASA in NC, CAP (Control), and CAP+20 μM Ru360 samples at different [Ca^{2+}]. Independent *t-test* was used to evaluate statistical significance between NC, CAP and CAP + Ru360 groups at the same [Ca^{2+}].

Extracellular [Ca^{2+}] mM		Wild-type			p-value	
		Mean	SD	n		
0	NC	0	2.50E-03	4	0.197	
	CAP	5.0865	6.1481	4		**0.91**
	CAP + Ru360	3.8123	7.3331	5		
0.5	**NC**	10.6899	4.3254	6	**0.035**	
	CAP	22.1885	9.6493	6		**0.04**
	CAP + Ru360	12.85	5.283	6		
1	**NC**	9.2572	7.7815	6	**0.01**	
	CAP	25.8553	10.9269	7		**0.03**
	CAP + Ru360	17.4244	7.8503	7		
2	**NC**	11.5959	9.2466	5	**0.022**	
	CAP	28.3665	10.678	6		**0.03**
	CAP + Ru360	17.7953	10.2253	6		

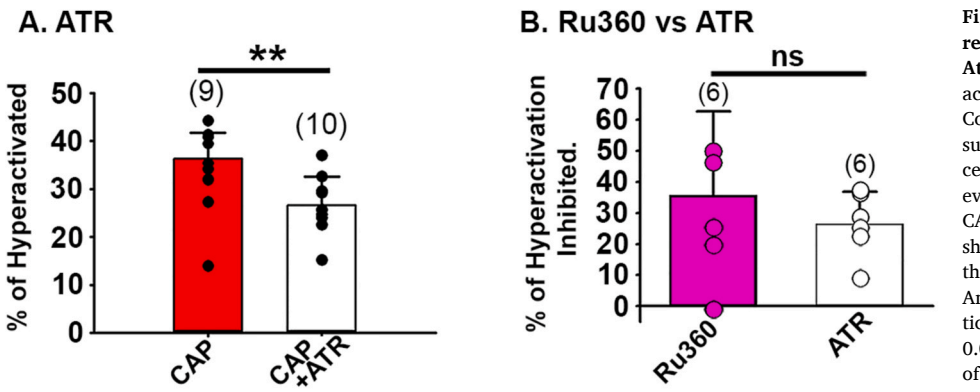

Fig. 6. Mouse sperm hyperactivation is reduced by ADP/ATP translocase inhibitor Atractyloside (ATR). A. Percentage of hyperactivated sperm measured by CASA from CAP Control and CAP +5 μM ATR conditions. Measurements were done in media with 2 mM extracellular Ca^{2+}. Independent *t-test* was used to evaluate statistical significance between CAP and CAP + ATR. Error Bars represent SD. **B.** Graph shows percentage of hyperactivation inhibited by the presence of Ru360 or ATR during capacitation. An independent *t-test* was used to evaluate statistical significance. Error Bars represent SD. ns $p > 0.050$, and $^{**}p < 0.010$. (n) represents the number of animals.

4. Discussion

Together, our data support the following model (Fig. 7): CatSper channel activation during sperm capacitation induces Ca^{2+} influx and an increase in cytoplasmic [Ca^{2+}]. This increase in intracellular [Ca^{2+}] starts in the principal piece, propagates through the midpiece, and reaches the head in a few seconds [15]. The MCU then transports Ca^{2+} into the mitochondria, leading to increased mitochondrial efficiency, which promotes sperm hyperactivation and sperm's ability to fertilize an oocyte.

The role of mitochondria in mammalian sperm function, quality, and fertilization ability has been intensely debated for several years [12,14,25,26,35]. The contribution of mitochondria to sperm bioenergetics is unclear, and the source of the ATP used for sperm motility and hyperactivation has been long debated. The studies carried out in several species have provided different or conflicting results. In mouse sperm, glycolysis-produced ATP is sufficient to sustain progressive motility [12,27]. Conversely, in human sperm, a strong correlation has been noted between mitochondrial functionality and sperm motility or overall quality [28,29]. Therefore, one idea is that sperm have versatile metabolism, allowing them to use species or environment dependent mechanisms for energy production [29,30].

Here, we measured mitochondrial activity in NC and CAP mouse sperm by two independent methods. First, we used HRR to measure mitochondrial oxygen consumption in intact and motile sperm cells [16,31,32]. During capacitation, mitochondrial coupling efficiency increased, indicating that mitochondrial electron transport chain is more closely coupled to ADP phosphorylation in CAP sperm than in NC sperm. Additionally, we noted an increase in RCR in CAP sperm, suggesting that mitochondrial function improved to increase ATP production, or to maintain the elevated MMP. However, the reserve respiratory capacity, which reflects the capacity of sperm to respond to energy demands, was not modified in CAP sperm, suggesting that sperm operate close to their bioenergetic limit [17]. As a second method to study mitochondrial function, we used the voltage-sensitive dye TMRM to measure sperm MMP both at the sperm population, and single cell level, observing an increase in MMP and mitochondria function [33]. Therefore, we conclude that sperm mitochondrial function increases during capacitation.

Our work has a significant advantage over previous findings

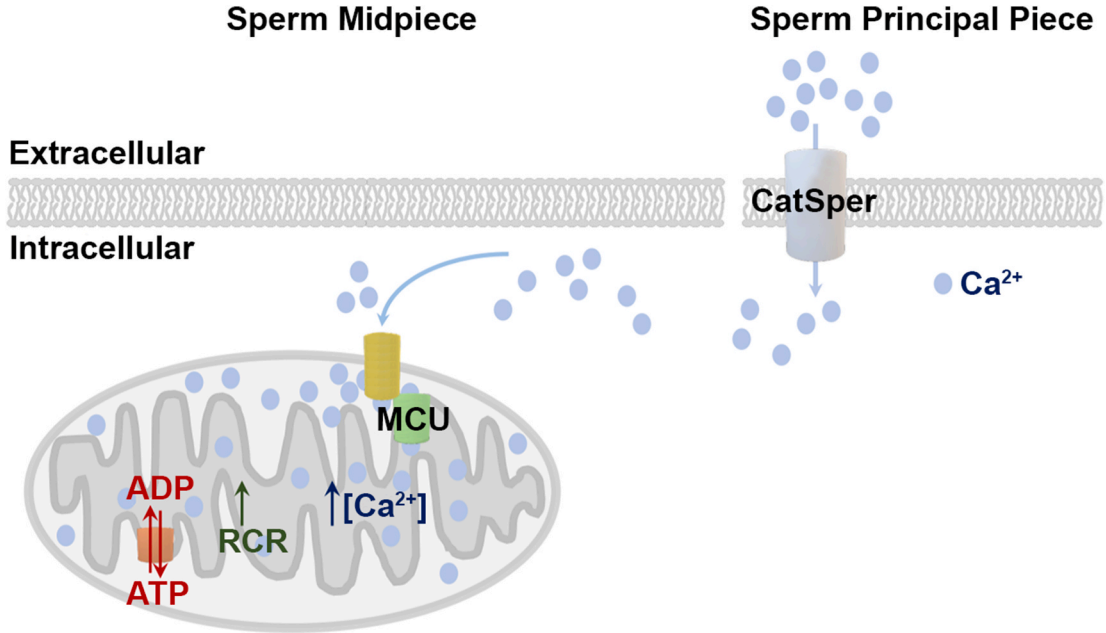

Fig. 7. Proposed model for a role of sperm mitochondria in capacitation/hyperactivation processes. CatSper activation during capacitation determines Ca^{2+} influx and the increase in cytoplasmic [Ca^{2+}], that starts in the sperm principal piece, propagates through the midpiece, and reaches the head in a few seconds (20). Our data shows that the Ca^{2+} propagation through the midpiece leads to an increase in mitochondrial Ca^{2+} mediated by MCU. The increase in mitochondrial Ca^{2+} translates into an increase in mitochondrial efficiency that in turn promotes hyperactivation and *in-vitro* fertilization. Other molecular mechanisms involved in this pathway (e. g. possible role of the redundant nuclear envelop) need to be elucidated.

regarding a role of mitochondria in sperm capacitation. Our study was conducted in intact and motile sperm, while earlier studies have used non-physiological conditions (permeabilized and/or non-motile sperm) [13,14,34–36] .

Our experiments done in the presence of mitochondrial function inhibitors indicated that mitochondrial activity is not necessary for two features of capacitation –AR and tyrosine phosphorylation– but is contributing significantly to sperm hyperactivation and fertilization ability. These findings are consistent with observations that sperm from CatSper KO mice fail to hyperactivate and fertilize, but the AR and tyrosine phosphorylation are unaffected [37]. Additionally, these findings are consistent with our observation that sperm from CatSper KO mice did not have an increase in RCR or MMP in capacitating conditions. Although the downstream targets of the CatSper-mediated cytoplasmic [Ca^{2+}] increase have not been fully characterized [6,7], sperm from CatSper KO have decreased NADH levels in the midpiece and a deficit in ATP production [5,37]. It is possible that the tail-to-head propagation of Ca^{2+} initiated by CatSper activation triggers an increase in [NAD] and may regulate ATP homeostasis [15]. Moreover, our finding that CatSper channels are required for increased mitochondrial [Ca^{2+}] in CAP sperm adds a new role for the sperm-specific Ca^{2+} channel.

Several lines of evidence suggest that, at least in somatic cells, regulated Ca^{2+} entry into mitochondria increases the efficiency of oxidative respiration [38,39]. Mitochondrial [Ca^{2+}] is considered a central regulator of oxidative phosphorylation by mediating NADH production and controlling activity of pyruvate dehydrogenase, isocitrate dehydrogenase, and α-ketoglutarate dehydrogenase [8,40]. Mitochondrial [Ca^{2+}] also plays an important role in regulating ATP synthase [8,39,41] and can trigger the release of pro-apoptotic agents by the mitochondria [42]. However, the precise role of Ca^{2+} in sperm mitochondria is still under debate [11]. Some evidence suggests that maintenance of mitochondrial Ca^{2+} homoeostasis is essential for motility regulation in human sperm [43] and bovine sperm [44,45]. Whereas in contrast, other studies reported that sperm mitochondrial [Ca^{2+}] is unaltered by mitochondrial uncoupling [46] and in bulls, mitochondrial activity in hyperactivated sperm appears not to be regulated by [Ca^{2+}] [47]. Thus, the role of Ca^{2+} in sperm mitochondrial Ca^{2+} homoeostasis may be species-specific.

Our data showing that mitochondrial Ca^{2+} uptake in mouse sperm occurs through the MCU are consistent with similar findings in somatic cells where MCU is known to control intracellular Ca^{2+} signals, cell metabolism, and cell survival [9,48]. Specifically, we found that the MCU inhibitor Ru360 decreased mitochondrial [Ca^{2+}] in mouse sperm during capacitation and inhibited sperm hyperactivation. These results agree with previous results showing that mitochondrial Ca^{2+} contributes to motility regulation in human sperm [43] and capacitation in bovine sperm [45]. Proteomic studies have confirmed that human sperm possess both MCU and MCU regulator 1 [11,49], so this protein may be required for mitochondrial Ca^{2+} uptake in human sperm as well. MCU has a low affinity for Ca^{2+} uptake [9,54], leading some to speculate that Ca^{2+} transfer into mitochondria occurs at highly specialized regions of close contact between mitochondria and endoplasmic reticulum called mitochondria-associated membranes [9]. Some of the molecular components of mitochondria-associated membranes are present in sperm, distributed in the acrosome and at the sperm neck and anterior midpiece. Endoplasmic reticulum in this location is referred to as the redundant nuclear envelope [47,51]. Further studies are needed to determine whether these sites of contact between the redundant nuclear envelope and mitochondria participate in the increase of mitochondrial [Ca^{2+}] during capacitation.

In conclusion, our results show that mitochondrial activity (i.e., oxygen consumption, generation of the electrochemical gradient, ATP/ADP exchange) increases during sperm capacitation and this increase in activity contributes to sperm hyperactivation and sperm fertilization. The increase in mitochondrial coupling efficiency is consistent with Ca^{2+} influx through CatSper channels and Ca^{2+} entry into the mitochondria through the MCU. This increase in mitochondrial Ca^{2+} could translate either into an increase in ATP production due to the Ca^{2+} dependency of many of the mitochondrial enzymes, or play a role in shaping intracellular calcium signals. Both mechanisms, acting independently or together, would be relevant to achieve sperm hyperactivation. Our discovery of new mechanisms that explain sperm function may lead to the use of new molecules for fertility treatments and male contraception.

Declaration of competing interest

The authors declare no conflict of Interest.

Acknowledgements

We thank Dr. Deborah Frank for the critical review of the manuscript, as well as Dr. Emily Hunter and Nathan Pomper for the editing assistance provided through InPrint: A Scientific Editing Network at Washington University in St. Louis. We thank Dr. Lis Puga Molina for her assistance with the CASA experiments. We also thank Dr. Valeria Valez, from CEINBIO-UdelaR, for assistance with figures design.

Appendix A. Supplementary data

Supplementary data to this article can be found online at https://doi.org/10.1016/j.redox.2021.102176.

Funding and financial

RR and AC are supported by grants from Universidad de la República (CSIC_2018 , Espacio Interdisciplinario_2019). Additional funding was obtained from the Programa de Desarrollo de Ciencias Básicas (PEDECIBA, Uruguay). PI, SP, MF and RS are supported from Universidad de la República (I + D, CSIC 2014, (I + D, CSIC 2016 and FMV_1_2017_1_136490 ANII- Uruguay).

CMS funding from NIH grant RO1 HD069631 and LEAP grant Award, Washington University in Saint Louis.

References

[1] C.R. Austin, The "capacitation" of the mammalian sperm, Nature 170 (1952) 326.
[2] M.C. Chang, Fertilizing capacity of spermatozoa deposited into the fallopian tubes, Nature 168 (4277) (1951) 697–698.
[3] J. Correia, F. Michelangeli, S. Publicover, Regulation and roles of Ca2+ stores in human sperm, Reproduction 150 (2) (2015) R65–R76.
[4] P.V. Lishko, N. Mannowetz, CatSper: a unique calcium channel of the sperm flagellum, Current Opinion in Physiology 2 (2018) 109–113.
[5] D. Ren, B. Navarro, G. Perez, A.C. Jackson, S. Hsu, Q. Shi, J.L. Tilly, D.E. Clapham, A sperm ion channel required for sperm motility and male fertility, Nature 413 (6856) (2001) 603–609.
[6] R. Rahban, S. Nef, CatSper: the complex main gate of calcium entry in mammalian spermatozoa, Mol. Cell. Endocrinol. (2020) 110951.
[7] L. Vyklicka, P.V. Lishko, Dissecting the signaling pathways involved in the function of sperm flagellum, Curr. Opin. Cell Biol. 63 (2020) 154–161.
[8] J.G. McCormack, A.P. Halestrap, R.M. Denton, Role of calcium ions in regulation of mammalian intramitochondrial metabolism, Physiol. Rev. 70 (2) (1990) 391–425.
[9] R. Rizzuto, D. De Stefani, A. Raffaello, C. Mammucari, Mitochondria as sensors and regulators of calcium signalling, Nat. Rev. Mol. Cell Biol. 13 (9) (2012) 566–578.
[10] R. Bravo-Sagua, V. Parra, C. López-Crisosto, P. Díaz, A.F.G. Quest, S. Lavandero, Calcium transport and signaling in mitochondria, Comprehensive Physiology 7 (2) (2017) 623–634.
[11] A. Amaral, B. Lourenço, M. Marques, J. Ramalho-Santos, Mitochondria functionality and sperm quality, Reproduction 146 (5) (2013) R163–R174.
[12] K. Miki, W. Qu, E.H. Goulding, W.D. Willis, D.O. Bunch, L.F. Strader, S. D. Perreault, E.M. Eddy, D.A. O'Brien, Glyceraldehyde 3-phosphate dehydrogenase-S, a sperm-specific glycolytic enzyme, is required for sperm motility and male fertility, Proc. Natl. Acad. Sci. U.S.A. 101 (47) (2004) 16501–16506.
[13] A. Ferramosca, V. Zara, Bioenergetics of mammalian sperm capacitation, BioMed Res. Int. 2014 (2014) 902953.
[14] A. Stendardi, R. Focarelli, P. Piomboni, D. Palumberi, F. Serafini, A. Ferramosca, V. Zara, Evaluation of mitochondrial respiratory efficiency during in vitro capacitation of human spermatozoa, Int. J. Androl. 34 (3) (2011) 247–255.

[15] J. Xia, D. Reigada, C.H. Mitchell, D. Ren, CATSPER channel-mediated Ca2+ entry into mouse sperm triggers a tail-to-head propagation, Biol. Reprod. 77 (3) (2007) 551–559.

[16] A. Cassina, P. Silveira, L. Cantu, J.M. Montes, R. Radi, R. Sapiro, Defective human sperm cells are associated with mitochondrial dysfunction and oxidant production, Biol. Reprod. 93 (5) (2015) 119.

[17] M.D. Brand, D.G. Nicholls, Assessing mitochondrial dysfunction in cells, Biochem. J. 435 (2) (2011) 297–312.

[18] P. Uribe, J.V. Villegas, R. Boguen, F. Treulen, R. Sánchez, P. Mallmann, V. Isachenko, G. Rahimi, E. Isachenko, Use of the fluorescent dye tetramethylrhodamine methyl ester perchlorate for mitochondrial membrane potential assessment in human spermatozoa, Andrologia 49 (9) (2017).

[19] Q. Yang, Y. Wen, L. Wang, Z. Peng, R. Yeerken, L. Zhen, P. Li, X. Li, Ca2+ ionophore A23187 inhibits ATP generation reducing mouse sperm motility and PKA-dependent phosphorylation, Tissue Cell 66 (2020) 101381.

[20] S. Creed, M. McKenzie, in: M. Haznadar (Ed.), Measurement of Mitochondrial Membrane Potential with the Fluorescent Dye Tetramethylrhodamine Methyl Ester (TMRM) BT - Cancer Metabolism: Methods and Protocols, Springer, New York, 2019, pp. 69–76.

[21] A.A. Kabbara, D.G. Allen, The use of the indicator flou-5N to measure sarcoplasmic reticulum calcium in single muscle fibres of the cane toad, J. Physiol. (2001).

[22] P.E. Visconti, J.L. Bailey, G.D. Moore, D. Pan, P. Olds-Clarke, G.S. Kopf, 47. Capacitation of mouse spermatozoa. I. Correlation between the capacitation state and protein tyrosine phosphorylation, Development 121 (4) (1995) 1129–1137.

[23] T. Pathak, M. Trebak, Mitochondrial Ca2+ signaling, in: Pharmacology and Therapeutics, 2018.

[24] Y. Kirichok, G. Krapivinsky, D.E. Clapham, The mitochondrial calcium uniporter is a highly selective ion channel, Nature 427 (6972) (2004) 360–364.

[25] S.G. Goodson, Y. Qiu, K.A. Sutton, G. Xie, W. Jia, D.A. O'Brien, Metabolic substrates exhibit differential effects on functional parameters of mouse sperm capacitation, Biol. Reprod. 87 (3) (2012) 75.

[26] J.M. Nascimento, L.Z. Shi, J. Tam, C. Chandsawangbhuwana, B. Durrant, E. L. Botvinick, M.W. Berns, Comparison of glycolysis and oxidative phosphorylation as energy sources for mammalian sperm motility, using the combination of fluorescence imaging, laser tweezers, and real-time automated tracking and trapping, J. Cell. Physiol. 217 (3) (2008) 745–751.

[27] C. Mukai, M. Okuno, Glycolysis plays a major role for adenosine triphosphate supplementation in mouse sperm flagellar movement, Biol. Reprod. 71 (2) (2004) 540–547.

[28] F. Gallon, C. Marchetti, N. Jouy, P. Marchetti, The functionality of mitochondria differentiates human spermatozoa with high and low fertilizing capability, Fertil. Steril. 86 (5) (2006) 1526–1530.

[29] E. Ruiz-Pesini, C. Diez, A.C. Lapeña, A. Pérez-Martos, J. Montoya, E. Alvarez, J. Arenas, M.J. López-Pérez, Correlation of sperm motility with mitochondrial enzymatic activities, Clin. Chem. 44 (8 Pt 1) (1998) 1616–1620.

[30] B.T. Storey, Mammalian sperm metabolism: oxygen and sugar, friend and foe, Int. J. Dev. Biol. 52 (5–6) (2008) 427–437.

[31] C.R. Darr, G.A. Cortopassi, S. Datta, D.D. Varner, S.A. Meyers, Mitochondrial oxygen consumption is a unique indicator of stallion spermatozoal health and varies with cryopreservation media, Theriogenology (2016).

[32] C.R. Moraes, S. Meyers, The sperm mitochondrion: organelle of many functions, in: Animal Reproduction Science, 2018.

[33] N. Moscatelli, B. Spagnolo, M. Pisanello, E.D. Lemma, M. De Vittorio, V. Zara, F. Pisanello, A. Ferramosca, Single-cell-based evaluation of sperm progressive motility via fluorescent assessment of mitochondria membrane potential, Sci. Rep. 7 (1) (2017) 17931.

[34] M. Balbach, J. Buck, L.R. Levin, Using an extracellular flux analyzer to measure changes in glycolysis and oxidative phosphorylation during mouse sperm capacitation, JoVE (2020).

[35] M. Balbach, M.G. Gervasi, D.M. Hidalgo, P.E. Visconti, L.R. Levin, J. Buck, Metabolic changes in mouse sperm during capacitation, Biol. Reprod. 103 (4) (2020) 791–801.

[36] A. Ferramosca, R. Focarelli, P. Piomboni, L. Coppola, V. Zara, Oxygen uptake by mitochondria in demembranated human spermatozoa: a reliable tool for the evaluation of sperm respiratory efficiency, Int. J. Androl. 31 (3) (2008) 337–345.

[37] T.A. Quill, S.A. Sugden, K.L. Rossi, L.K. Doolittle, R.E. Hammer, D.L. Garbers, Hyperactivated sperm motility driven by CatSper2 is required for fertilization, Proc. Natl. Acad. Sci. U.S.A. 100 (25) (2003) 14869–14874.

[38] S. Cortassa, M.A. Aon, E. Marbán, R.L. Winslow, B. O'Rourke, An integrated model of cardiac mitochondrial energy metabolism and calcium dynamics, Biophys. J. 84 (4) (2003) 2734–2755.

[39] J.G. McCormack, R.M. Denton, The role of intramitochondrial Ca2+ in the regulation of oxidative phosphorylation in mammalian tissues, Biochem. Soc. Trans. 21 (Pt 3) (1993) 793–799, 3.

[40] J.G. McCormack, R.M. Denton, Mitochondrial Ca2+ transport and the role of intramitochondrial Ca2+ in the regulation of energy metabolism, Dev. Neurosci. 15 (3–5) (1993) 165–173.

[41] P.R. Territo, S.A. French, M.C. Dunleavy, F.J. Evans, Calcium activation of heart mitochondrial oxidative phosphorylation: RAPID kinetics OFmV O2, NADH, and light scattering, J. Biol. (Bronx N Y) (2001). https://www.jbc.org/article/S0021-9258(18)46605-7/abstract.

[42] G. Szalai, R. Krishnamurthy, G. Hajnóczky, Apoptosis driven by IP(3)-linked mitochondrial calcium signals, EMBO J. 18 (22) (1999) 6349–6361.

[43] A. Bravo, F. Treulen, P. Uribe, R. Boguen, R. Felmer, J.V. Villegas, Effect of mitochondrial calcium uniporter blocking on human spermatozoa, Andrologia 47 (6) (2015) 662–668.

[44] S. Meyers, E. Bulkeley, A. Foutouhi, Sperm mitochondrial regulation in motility and fertility in horses, Reproduction in Domestic Animals = Zuchthygiene 54 (Suppl 3) (2019) 22–28.

[45] P.C. Rodriguez, M.M. Satorre, M.T. Beconi, Effect of two intracellular calcium modulators on sperm motility and heparin-induced capacitation in cryopreserved bovine spermatozoa, Anim. Reprod. Sci. 131 (3–4) (2012) 135–142.

[46] G. Machado-Oliveira, L. Lefièvre, C. Ford, M.B. Herrero, C. Barratt, T.J. Connolly, K. Nash, A. Morales-Garcia, J. Kirkman-Brown, S. Publicover, Mobilisation of Ca2+ stores and flagellar regulation in human sperm by S-nitrosylation: a role for NO synthesised in the female reproductive tract, Development 135 (22) (2008) 3677–3686.

[47] H.-C. Ho, S.S. Suarez, Characterization of the intracellular calcium store at the base of the sperm flagellum that regulates hyperactivated motility, Biol. Reprod. 68 (5) (2003) 1590–1596.

[48] M. Patron, A. Raffaello, V. Granatiero, A. Tosatto, G. Merli, D. De Stefani, L. Wright, G. Pallafacchina, A. Terrin, C. Mammucari, R. Rizzuto, The mitochondrial calcium uniporter (MCU): molecular identity and physiological roles, J. Biol. Chem. 288 (15) (2013) 10750–10758.

[49] H. Wang, X. Cheng, J. Tian, Y. Xiao, T. Tian, F. Xu, X. Hong, M.X. Zhu, TRPC channels: structure, function, regulation and recent advances in small molecular probes, Pharmacol. Therapeut. 209 (2020) 107497.

[51] K. Ho, C.A. Wolff, S.S. Suarez, CatSper-null mutant spermatozoa are unable to ascend beyond the oviductal reservoir, Reprod. Fertil. Dev. 21 (2) (2009) 345–350.

[52] M.M. Bradford, A rapid and sensitive method for the quantitation of microgram quantities of protein utilizing the principle of protein-dye binding, Anal. Biochem. 72 (1) (1976) 248–254. https://doi.org/10.1016/0003-2697(76)90527-3.

[54] P. Wang, C. Fernandez-Sanz, W. Wang, S.-S. Sheu, Why don't mice lacking the mitochondrial Ca2+ uniporter experience an energy crisis? J. Physiol. 598 (7) (2020) 1307–1326.

[55] Julio Chavez Cesar, et al., SLO3 K+ channels control calcium entry through CATSPER channels in sperm, J.Biol Chem 289 (46) (2014).

Supplementary Figures.

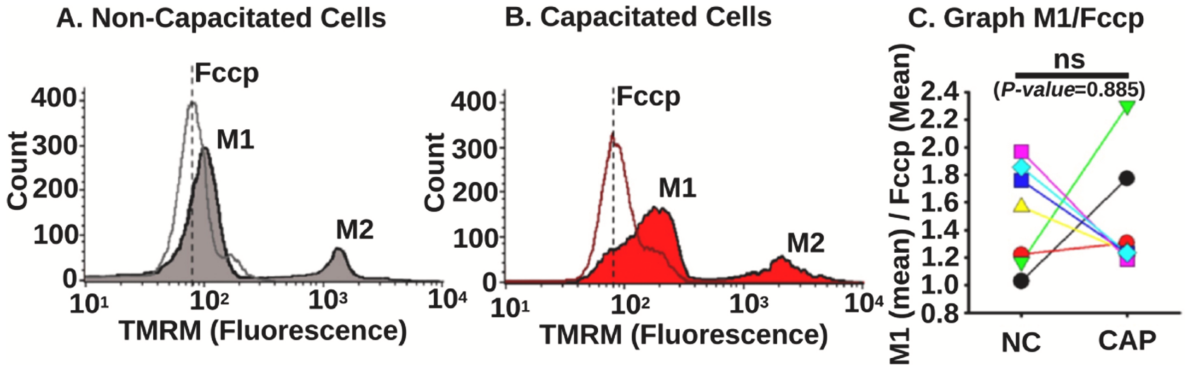

Supplementary Fig. 1
Population (M1) measurements of sperm mitochondrial membrane potential (MMP) with TMRM under NC and CAP conditions. A. and **B.** show representative histograms of the 3 populations of cells recorded with the flow cytometer (M1, M2, and FCCP) under NC and CAP conditions respectively (also shown on Fig. 1). Fluorescence values of FCCP population at each experiment were used as Fmin for normalization of M1 and M2 values. **C.** Graph showing normalized values of M1 under NC and CAP conditions. Graph shows mean, n = 8. paired *t*-test was used to determine statistical significance. ns > 0.050.

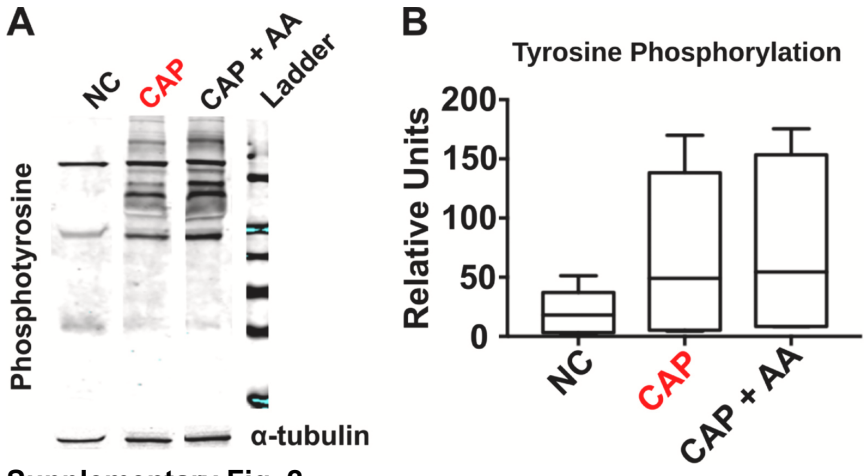

Supplementary Fig. 2
Tyrosine phosphorylation increases during capacitation and is not impaired by the mitochondrial inhibitor Antimycin A. A. Representative western blots for tyrosine phosphorylated proteins**. B.** Protein levels in independent western blots were quantified by densitometry and normalized using tubulin as loading control. Quantification of bands is expressed as mean ± SEM in units of density (n = 6). Semen samples were centrifuged at 500 g and the pellet was resuspended in lysis buffer supplemented with protease and phosphatase inhibitors. Suspensions were sonicated for 5 s and then centrifuged at 14000 g for 10 min at 4°C. Protein concentration was determined by the Bradford method [52]. Unedited images used to create Supplementary Fig. 2A and B are available.

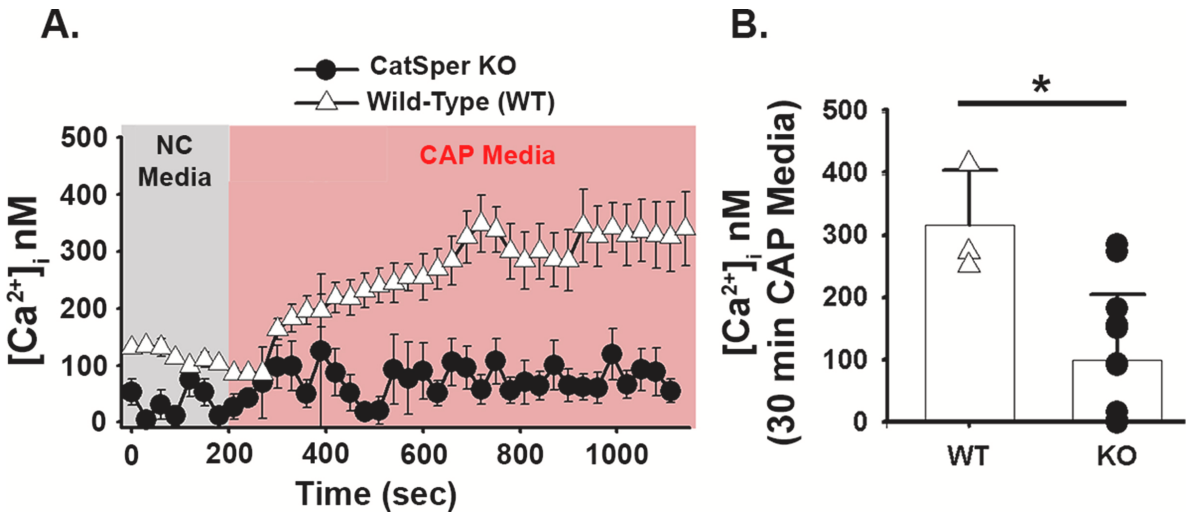

Supplementary Fig. 3

Intracellular Ca^{2+} increases during capacitation in wild-type but not in CatSper KO, mouse sperm. Ratiometric measurements with Fura-2 AM were used to calculate intracellular free [Ca^{2+}] in wild-type and CatSper KO mice sperm. Free swimming epididymal (Cauda) sperm cells were obtained using the swim-up technique in NC Media. Cells were loaded for 45 min with Fura-2 AM at a concentration of 4 μM. Before recordings start, sperm were centrifuged and resuspended in the NC HS media. **A.** Average traces of calculated intracellular [Ca^{2+}] for wild-type and CatSper KO mice. Recordings were started in HS NC and switched after 3–4 min to CAP HS Media. Bars are SEM. **B.** Average of intracellular [Ca^{2+}] in nM for wild-type and CatSper KO mice after 20–30 min of incubation in CAP HS Media.

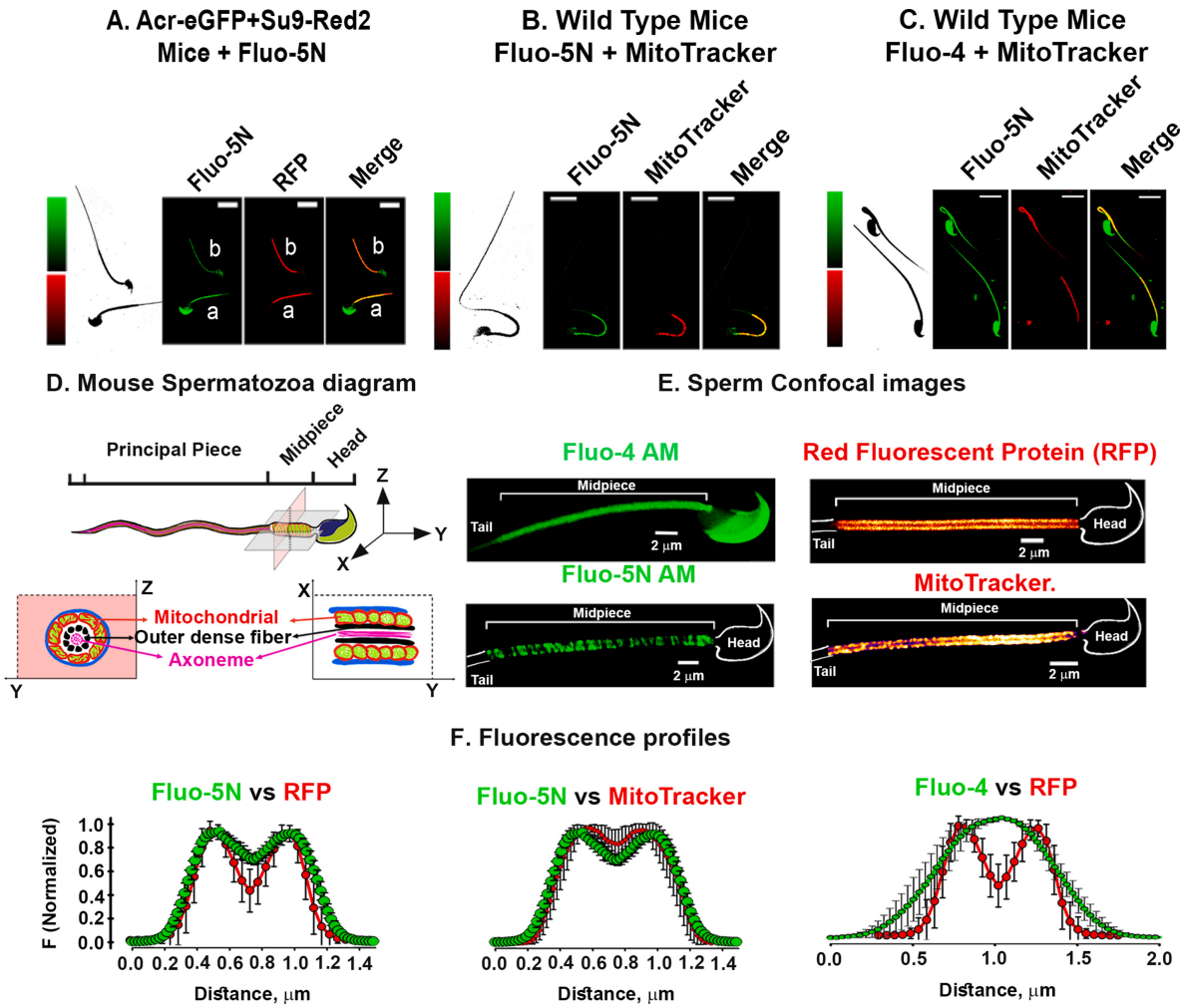

Supplementary Fig. 4

Fluo-5N fluorescence colocalizes with mitochondria markers in mouse sperm. A. Acr-eGFP + Su9-Red2 transgenic mice expressing GFP in sperm acrosome and RFP in sperm mitochondria loaded with Fluo-5N AM. Acr-eGFP + Su9-Red2 loaded with Fluo-5N AM. Localization of RFP in the midpiece of the sperm. Merge of RFP and Fluo-5N showing co-localization in yellow. **B.** Wild-type C57BL6 mice sperm loaded with Fluo-5N AM and MitoTracker AM. Merged image of Fluo-5N and MitoTracker. Colocalization showed in yellow. Middle and right panel show sperm cells without and with acrosome respectively. **C.** Wild-type mice sperm loaded with Fluo-4 AM and MitoTracker AM. Merge of Fluo-4 and MitoTracker, bars=10μm. **D:** Diagram of mitochondrial localization in the mid-piece of mouse sperm. E. Representative images of sperms labeled with Fluo-4 AM and Fluo-5N (left) and merged images of Fluo-5N and RFP or Mitotracker (right). F. Combined fluorescence profiles of the midpiece labeled with RFP, Mitotracker and Fluo-5N or Fluo-4 (n= 7–10).

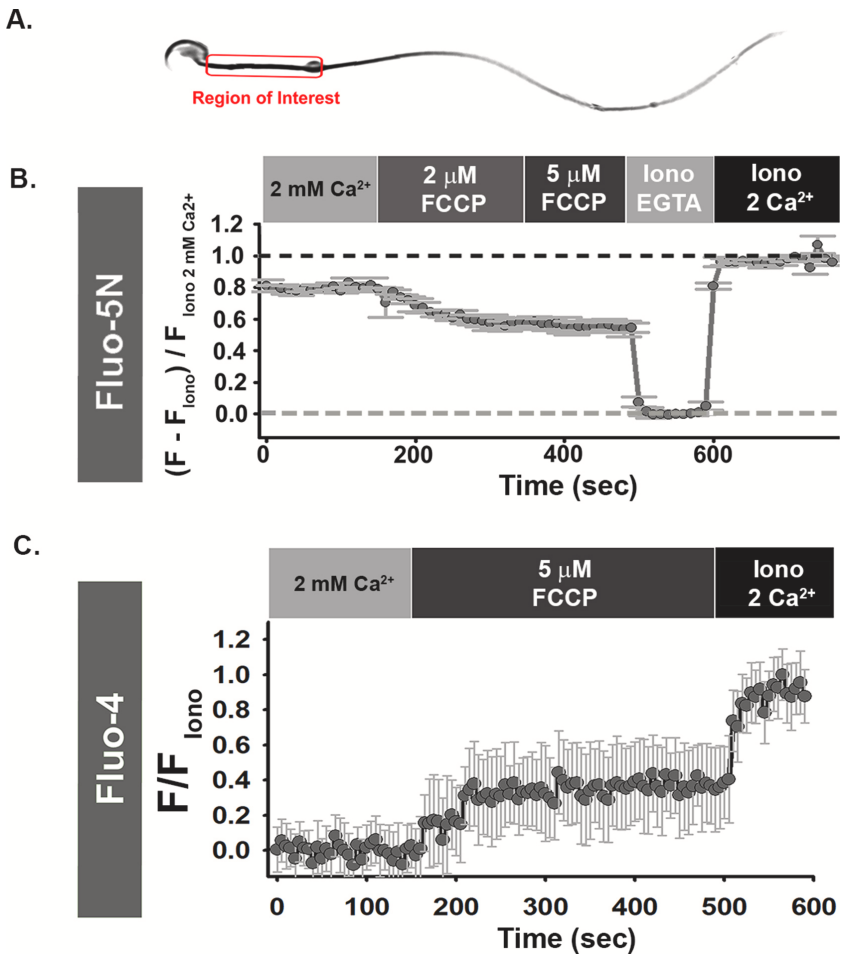

Supplementary Fig. 5

Effect of FCCP on sperm cells loaded with Fluo-5N AM or with Fluo-4 AM. A. Scheme indicating that fluorescence was measured only in the sperm midpiece. **B.** Representative recording of Fluo-5N fluorescence under conditions indicated in figure. **C.** Representative recording of Fluo-4 fluorescence under conditions indicated in the figure. Error bars represent SD. Fluo-5N fluorescence ratios were calculated as = $F_{Initial}$ - (F_{Iono} EGTA)/ F_{Iono} $2Ca^{2+}$. For Fluo-4 AM loading protocol, see Supplementary Fig. 7.

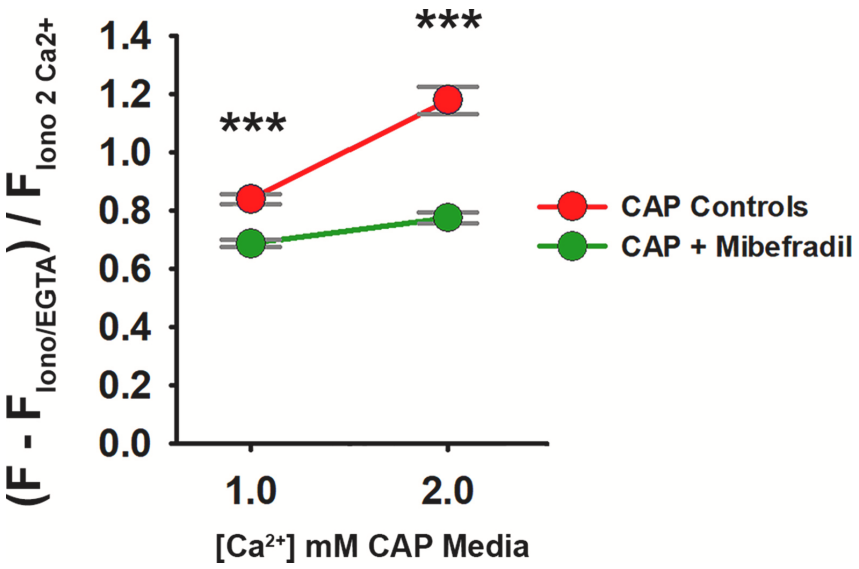

Supplementary Fig. 6
Mitochondrial [Ca^{2+}] increase during capacitation is reduced by the CatSper channel inhibitor Mibefradil. Graph shows initial fluorescence values normalized to FIono EGTA (0 mM Ca^{2+} + Ionomycin + EGTA) / $F_{Iono}2Ca^{2+}$ (Ionomycin +2 mM Ca^{2+}). Recordings were obtained at 1 and 2 mM extracellular Ca^{2+} for both conditions (CAP Control and CAP with 20 µM Mibefradil). Independent *t*-test were used to evaluate statistical significance between groups at the same extracellular [Ca^{2+}]. ***P < 0.001. Error Bars represent SD. n = 42–138 cells from 3 mice for each condition.

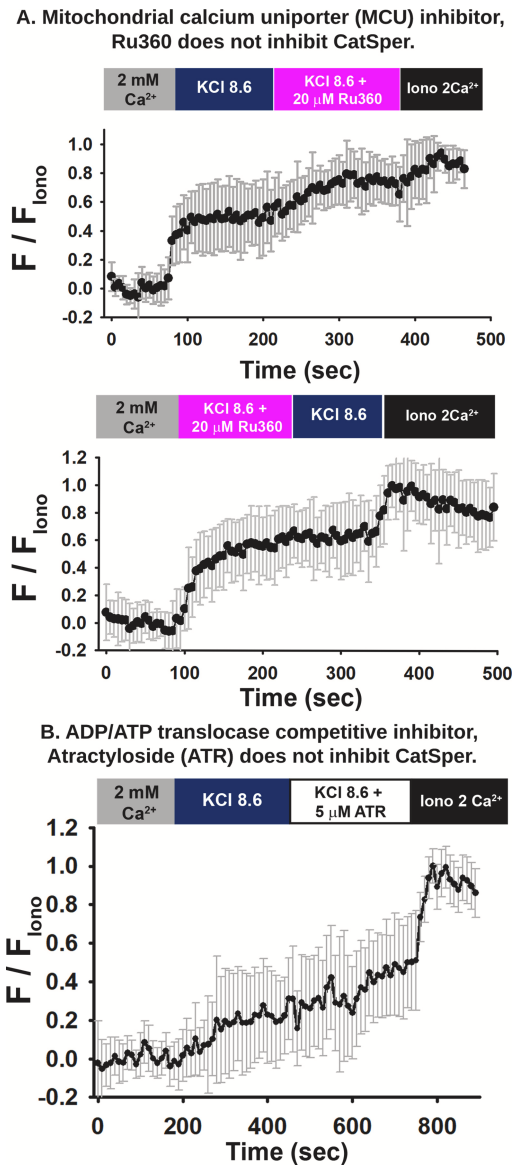

Supplementary Fig. 7

Ru360 and ATR have no effect on CatSper channels in CAP mouse sperm. Sperm cells were loaded with Fluo-4 AM and CatSper activation was triggered by alkaline depolarization (50 mM KCl, pH 8.6). **A** Top: average traces + SD of Fluo-4 fluorescence recorded under conditions indicated in fig, 20 μM Ru360 was added after stimulation of CatSper channels with alkaline depolarization. Bottom: 20 μM R360 was added simultaneously with 50 mM KCl pH 8.6. **B.** Average traces of Fluo-4 fluorescence recorded in the conditions indicated in fig, 5 μM ATR was added after stimulation of CatSper channels with alkaline depolarization. Errors bars are SD. Protocol: After swim-up, motile cells were incubated with 2–4 μM Fluo-4 AM and 0.05% Pluronic F-127 in HS media at 37 °C for 90 min. Then, cells were centrifuge at 1500 rpm for 10 min and re-suspended in the HS media. Sperm were allowed to attach to laminin (1 mg/ml), Poly-l-lysine (0.1%) or cell-tak coated coverslips placed at the bottom of the recording chamber for 5 min. Ionomycin (5 μM) and HS 2 mM Ca^{2+} were added at the end of the recordings as references of maximum fluorescence.

Intramitochondrial Calcium Increase: A Conserved Mechanism of Mitochondrial Activation in Human and Mouse Sperm During Capacitation

Pilar Irigoyen [a, b,1], Juan Ferreira [c, d,1], Adriana Cassina [b,e], Celia Santi [c, d,2] and Rossana Sapiro [a,b,2].

a. Departamento de Histología y Embriología, Facultad de Medicina, Universidad de la República, Montevideo, Uruguay

b. Centro de Investigaciones Biomédicas (CEINBIO), Facultad de Medicina, Universidad de la República, Montevideo, Uruguay

c. Department of Obstetrics and Gynecology, Center for Reproductive Health Sciences, Washington University in St. Louis, School of Medicine, St. Louis, MO, United States

d. Department of Neuroscience, Washington University in St. Louis, School of Medicine, St. Louis, MO, United States

e. Departamento de Bioquímica, Facultad de Medicina, Universidad de la República, Montevideo, Uruguay

[1] Both authors contributed equally to this work.

[2] Celia Santi and Rossana Sapiro should be considered joint senior author and corresponding author.

Celia Santi santic@wustl.edu phone:+1 3147473306

Rossana Sapiro rsapiro@fmed.edu.uy phone: +59829243414 ext 3481

1. Abstract

Capacitation is a physiological process in which sperm must undergo post-ejaculation to gain the ability to fertilize an egg. This process occurs in the female reproductive tract and involves a series of biochemical and physiological changes. A critical component of sperm capacitation is the influx of calcium ions (Ca^{2+}) through the cation channel of sperm (CatSper), which plays a pivotal role in regulating fertilization. In previous research, we found that during mouse sperm capacitation, Ca^{2+} influx leads to increased mitochondrial activity and elevated intramitochondrial Ca^{2+} concentration, which are essential for sperm hyperactivation and successful fertilization. However, studies in other species suggest that this mechanism may be species-specific.

Recently, we observed that mitochondrial activity also increases during human sperm capacitation. To determine whether this increase is associated with Ca^{2+} influx, we measured mitochondrial function in human sperm using high-resolution respirometry, assessed mitochondrial membrane potential, and quantified sperm mitochondrial Ca^{2+} concentration. Our results show that mitochondrial Ca^{2+} levels rise during capacitation, correlating with enhanced mitochondrial function. Notably, mitochondrial activation during capacitation is crucial for human sperm hyperactivation. These findings indicate that the mechanism previously identified in mice is conserved in human sperm.

Key Words

Sperm capacitation, Mitochondria activity, Hyperactivation, Calcium, Male fertility.

2. Introduction

Sperm capacitation is a crucial physiological process that enables sperm to gain the ability to fertilize an egg. This process takes place in the female reproductive tract and involves a series of biochemical and physiological changes. During capacitation, the sperm membrane undergoes modifications that increase its fluidity, while intracellular ion concentrations, particularly calcium (Ca^{2+}) and bicarbonate, are tightly regulated. These changes activate protein kinase A (PKA)-dependent signaling pathways, leading to protein phosphorylation. This results in an increase in intracellular pH and hyperpolarization of the membrane potential, which enhances sperm motility (hyperactivation) and triggers the acrosome reaction (AR) [1–4].

Intracellular Ca^{2+} flux plays a central role in capacitation, with sperm relying on rapid ion exchanges within the flagellum, facilitated by specialized ion channels[2]. Among these, the CatSper (cation channel of sperm) is the primary channel responsible for importing extracellular Ca^{2+} into the sperm tail [5–7]. Mouse sperm lacking CatSper fail to undergo hyperactivation and become infertile, despite having normal AR and tyrosine phosphorylation. Additionally, CatSper knockout sperm exhibit reduced ATP levels compared to wild-type sperm [8,9].

In previous studies on mouse sperm, we observed that Ca^{2+} influx via CatSper during capacitation increases mitochondrial Ca^{2+} levels through the mitochondrial calcium uniporter (MCU), enhancing mitochondrial efficiency. This boost in mitochondrial function contributes to sperm hyperactivation

and fertilization potential [10]. Similar to other cell types, this process likely occurs because Ca^{2+} entry into mitochondria activates Ca^{2+}-dependent mitochondrial enzymes, leading to increased ATP production necessary for motility [11–13]. Furthermore, Ca^{2+} may shape intracellular signaling cascades, although the downstream effects of CatSper-mediated Ca^{2+} influx remain incompletely understood [8,9].

In contrast, other studies have found in bulls that mitochondrial activity in hyperactivated sperm seems to be independent of Ca^{2+} regulation[14]. This indicates that the role of Ca^{2+} in sperm mitochondrial homeostasis may vary across species. Also, there are reports of inter-species differences based on the source of the sperm [15].

In one of our recent studies, we observed that mitochondrial function increases during capacitation in sperm from normozoospermic donors[16]. It is well established that different concentrations of Ca^{2+} are required for the progression of capacitation-related events in human sperm[17]. It has also been shown that patients requiring *in vitro* fertilization (IVF) or intracytoplasmic sperm injection (ICSI) often exhibit defects in Ca^{2+} reservoirs[18]. While the connection between Ca^{2+} and fertility in human sperm is evident, the precise mechanisms involved, and the potential role of mitochondria as a Ca^{2+} reservoir, remain unclear.

In this study, we aimed to investigate the relationship between mitochondrial activity and Ca^{2+} flux in sperm, focusing on their roles in sperm function. Specifically, we assessed whether the mechanism described by Ferreira and Cassina et al., 2021[10], is conserved in human sperm. Using high-resolution respirometry (HRR) to evaluate mitochondrial function in capacitated and non-capacitated sperm from normozoospermic donors, as well as measuring mitochondrial Ca^{2+} concentrations, our results revealed that, like findings in mouse sperm, mitochondrial function and Ca^{2+} uptake increase during capacitation. This process is essential for hyperactivation. Therefore, we are faced with a mechanism that may be conserved between both species.

3. Materials and Methods

3.1. Reagents

All chemicals, unless otherwise specified, were obtained from Sigma-Aldrich Chemical Co. (St. Louis, MO, United States).

3.2. Subjects selection and Ethical Guidelines

In accordance with the World Health Organization's Laboratory Manual for the Examination and Processing of Human Semen (WHO, 2021)[19], freshly ejaculated human semen samples were collected via masturbation following an abstinence period of 3 to 7 days. The samples were gathered in sterile plastic containers and promptly transported to the laboratory. This study included men who visited the Fertilab-Reprovita andrology clinics (Montevideo, Uruguay) for routine semen analysis between March 2022 and June 2024. Additionally, samples from volunteer donors from Saint Louis Fertility Clinic between September 2022 and March 2023 were also included.

The semen samples used in the study were classified as normozoospermic, based on WHO (2021) criteria[19], regardless of the participants' fertility status. Clinical examinations and diagnostic semen analyses were conducted at Reprovita or Fertilab laboratory. Samples were excluded from the study if the white blood cell count exceeded 0.5 x 10^6/mL or if leukocytospermia was present. Men with genital tract infections, varicocele, or a history of vasectomy were also excluded.

Participants who met the inclusion criteria were randomly assigned to various experimental groups (n= 5 to 14 depending on the experimental procedure). All the experiments were performed paired.

The study was approved by the Ethics Committee of the Facultad de Medicina at the Universidad de la República, Montevideo, Uruguay. Written informed consent was obtained from all participants prior to sample collection, and participant anonymity was maintained by laboratory personnel, with no involvement from the researchers.

3.3. Semen Evaluation

Fresh semen samples were allowed to liquefy at room temperature for 30 minutes. After liquefaction, semen volume, pH, biochemical composition of seminal plasma, sperm viability, and morphology were evaluated according to WHO guidelines[19].

Sperm concentration and motility parameters were analyzed using an SCA-Microoptics automated analyzer (CASA) (Barcelona, Spain) with default settings in line with WHO criteria[19]. Semen aliquots were placed in two pre-warmed CELL-VU® sperm counting chambers (Millennium Sciences, Inc., New York, USA), and ten fields per chamber were randomly examined using a Nikon microscope at 37°C. The kinetic characteristics of hyperactivation (in 5 samples) were specifically analyzed for motile sperm, defined by CASA parameters as curvilinear velocity (VCL) >150 µm/s[10,16].

3.4. Sample preparation and capacitation

Liquefied samples were centrifuged at 500 x g for 10 minutes at room temperature to separate the sperm from the seminal plasma. The sperm pellet was then resuspended in Biggers Whitten Whittingham (BWW) medium, containing 95 mM NaCl, 4.6 mM KCl, 1.7 mM $CaCl_2$, 1.2 mM KH_2PO_4, 1.2 mM $MgSO_4$, 5.6 mM glucose, 0.27 mM sodium pyruvate, 20 mM HEPES (acid-free), 44 mM sodium lactate, and 0.3% BSA at pH 7.4[20].

The sperm suspension in BWW was divided into two portions: one aliquot was designated as non-capacitated sperm (NC), while the other was treated with 25 mM $NaHCO_3$ to induce capacitation (CAP). Both aliquots were incubated for 4 hours at 37°C before further analysis.

3.4. Acrosome reaction evaluation

The AR status was assessed in both NC and CAP sperm from 5 samples using Pisum sativum agglutinin conjugated with fluorescein isothiocyanate (PSA-FITC)[16]. To induce AR, sperm cells were incubated at 37°C for 30 minutes with 10 µM progesterone at the end of the capacitation process. Additionally, the mitochondrial inhibitor antimycin A (AA) (Sigma Aldrich, St. Louis, MO) was added to CAP sperm, either with or without progesterone.

For the assay, 10 x 10^6 cells from each condition were smeared onto slides, air-dried, and fixed in 100% ethanol for 30 minutes. The slides were then incubated with 50 µg/mL PSA-FITC for 30 minutes, followed by 0.4 µg/mL DAPI for 15 minutes. After staining, the slides were air-dried and mounted with coverslips using a Tris 4:1 glycerol mounting medium. Between each step, the slides were washed twice with phosphate-buffered saline (PBS) for 10 minutes.

The stained spermatozoa were examined under a Nikon E100 microscope (Japan) at 400x magnification, with at least 200 sperm evaluated per experiment.

3.5. Mitochondrial function by high-resolution respirometry

The oxygen consumption rate (OCR) of 24 x 10^6 sperm from 14 men, in both NC and CAP states, was measured using high-resolution respirometry (HRR) with the Oxygraph-2K (Oroboros Instruments GmbH, Innsbruck, Austria), following the protocol of Irigoyen et al. (2023)[21]. Mitochondrial function was assessed in intact cells using BWW medium. Briefly, OCR was recorded before and after the sequential addition of 2 µg/mL oligomycin (an ATP synthase inhibitor), the uncoupling agent carbonyl cyanide-p-trifluoromethoxyphenylhydrazone (FCCP) at concentrations ranging from 0.1 to 1 µM, and 2.5 µM AA (a complex III inhibitor). Residual oxygen consumption was distinguished from mitochondrial respiration by subtracting the AA slope from all other values prior to parameter calculation. We compared the adjusted slopes (normalized per million cells) and calculated indices including the respiratory control ratio (RCR), defined as the ratio of maximal to oligomycin-resistant respiration rates[21,22].

3.6. Flow cytometry for membrane potential and Ca^{2+} concentration in mitochondria

Suspended cells were divided into two samples, each with a final concentration of 10^6 cells/mL. The samples (13 for TMRM and 7 for Fluo5-N) were immediately incubated at 37°C with either 300 nmol/L of the lipophilic cationic dye tetramethyl rhodamine methyl ester perchlorate (TMRM)[10] (Sigma-Aldrich Inc., St. Louis, MO, USA) for 25 minutes, or with 2–4 µM Fluo-5N AM (Invitrogen, USA) and 0.05% Pluronic F-127 for 60–90 minutes. TMRM was used to measure mitochondrial membrane potential (MMP), while Fluo-5N AM was used to measure Ca^{2+} concentration in mitochondria. After staining, the probes were removed by centrifugation at 400 g, and the samples were resuspended in 1000 µL of PBS. Half of the washed sample (500 µL) was analyzed by flow cytometry, while the other half was incubated with 20 µM FCCP or 2–5 µM ionomycin in 0 Ca^{2+} and 2 mM EGTA for 15 minutes prior to analysis. These treated samples provided Fmin values for normalizing fluorescence data. Geometric mean fluorescence values from treated samples served as the baseline for normalizing fluorescence, accounting for variations in probe loading across experiments.

Flow cytometry was conducted using a FACSCalibur flow cytometer (Becton Dickinson, San Jose, CA). Cellular size and granularity were assessed using forward scatter (FSC-H) and side scatter (SSC-H) parameters. For each sample, 30,000 single events were recorded in the forward/side scatter dot plot, with gating applied to distinguish sperm from debris. TMRM and Fluo-5N AM fluorescence

were detected using FL-2 and FL-1 filters, respectively. Data was analyzed with CellQuest software. Two distinct cell populations (M1 and M2) with varying mitochondrial membrane potentials (MMP) were consistently identified. The population with higher MMP (M2) was analyzed based on the criteria of Ferreira and Cassina et.al (2021)[10].

3.7. Statical analysis

All statistical analyses were performed using GraphPad Prism version 8.0.1 for Windows (GraphPad Software, San Diego, CA, USA). Data are presented as means with standard deviations (SD) and standard errors of the mean (SEM). The Wilcoxon signed-rank test was used to compare central tendencies, with a p-value of < 0.05 considered statistically significant. Due to limitations in biological material, sample sizes may vary between experiments.

4. Results

4.1. Subject selection

Descriptive statistics for age and semen parameters, including medians, means, standard errors (SE), standard deviations (SD), and ranges (minimum and maximum values), are detailed in Supplementary Table 1. These parameters, derived from semen sample analysis, include semen volume, sperm concentration, sperm vitality, percentage of normal sperm, sperm motility, and round cell concentration. The study population, comprising 43 men aged 23 to 40 years, was evaluated according to the 2021 WHO criteria[19] .

4.2. Mitochondrial function increase during human sperm capacitation

To investigate mitochondrial function during human sperm capacitation, oxygen consumption rates (OCR) were measured in NC and CAP sperm cells from 13 samples using high-resolution respirometry (HRR). The procedure generally follows the methods described by Irigoyen et al., 2024, with the following modifications. Key mitochondrial activity parameters and indices were calculated using equations previously described (Table 1) [21,22]. Significant differences in basal respiration were observed between NC and CAP spermatozoa, with CAP sperm showing an increase (Table 1). Also, we observed an increase in ATP turnover in CAP sperm (Table 1). Additionally, CAP sperm exhibited a significantly higher RCR compared to NC sperm, indicating enhanced mitochondrial function (Table S1, Figure 1A). CAP sperm also demonstrated improved coupling efficiency (Table 1, Figure 1B). No significant differences were found in other parameters or indices between the two groups (Table 1).

Table 1. provides detailed parameters and key respiratory indices derived from HRR traces for both non-capacitated (NC) and capacitated (CAP) human sperm. The measurement and calculation of these respiration parameters were conducted as outlined in the "Materials and Methods" section. Basal respiration reflects oxygen consumption in the presence of exogenous substrates, while proton leak corresponds to respiration that is resistant to oligomycin. ATP turnover corresponds to the difference between the previous two (basal respiration - proton leak). The maximum respiratory rate was recorded after the dissipation of the proton gradient using FCCP. Non-mitochondrial respiration was defined by oxygen consumption following the addition of AA. Several calculated indices were derived from these parameters, including the RCR, which is defined as the ratio of maximum respiratory rate to proton leak, coupling efficiency, calculated as (ATP turnover) / basal respiration, and spare respiratory capacity, defined as the ratio of maximum respiratory rate to basal respiration[21]. The table also provides data for the number of donors (N), maximum (Max) and minimum (Min) values, as well as standard deviation (SD). Statistical significance is indicated by *p < 0.05, **p < 0.01, and ***p < 0.001.

	N	Mean		Min		Max		SD		p-value
Parameters (pmol O_2 * sec^{-1} *mL^{-1} * 10^{-6} cells)		**NC**	**CAP**	**NC**	**CAP**	**NC**	**CAP**	**NC**	**CAP**	
Basal respiration	13	0.55	0.83	0.06	0.13	1.79	2.56	0.54	0.82	0.0100 *
Proton leak		0.36	0.43	0.04	0.07	1.32	1.28	0.40	0.41	0.0535
ATP turnover		0.17	0.37	0.02	0.06	0.47	1.50	0.16	0.42	< 0.0001 ***
Maximum respiratory rate		0.97	1.24	0.06	0.13	3.23	3.70	1.12	1.10	0.0803
Non-mitochondrial respiration		0.44	0.56	0.03	0.04	2.07	2.50	0.55	0.72	0.1294
Indices										
RCR		2.57	3.15	1.29	1.61	2.57	3.16	0.96	1.56	0.0254 *
Coupling efficiency		0.37	0.46	0.22	0.21	0.66	0.63	0.14	0.11	0.0068 **
Spare respiratory capacity		1.58	1.57	0.83	0.94	2.56	2.69	0.57	0.50	0.4434

Next, MMP was measured by flow cytometry in NC and CAP sperm using the TMRM dye. As reported in Ferreira et.al.[10], two distinct sperm populations (M1 and M2), representing different MMP levels, were identified in both NC and CAP sperm (Figure 1C). The one with the highest fluorescence corresponded to the M2 population. The M2 population showed significantly higher normalized fluorescence in CAP sperm compared to NC sperm.

Collectively, these findings indicate that mitochondrial activity is higher in CAP sperm than in NC sperm, suggesting a shift in bioenergetic demands during capacitation.

4.3. Mitochondrial function is necessary for hyperactivated motility

To examine the role of mitochondrial activity in human sperm capacitation-associated events, sperm were incubated for 4 hours under control conditions or in the presence of AA or FCCP. Progesterone was added during the final 30 minutes to induce the AR in select fractions. AR and VCL, a marker of hyperactivation, were assessed. The results showed a decrease in VCL with AA treatment compared to the control group (Fig. 2A). Although FCCP also reduced VCL, this reduction

was not statistically significant. Neither AA nor FCCP affected the percentage of sperm undergoing spontaneous or induced AR (Fig. 2B).

Collectively, these findings suggest that while mitochondrial activity during capacitation is not crucial for the AR, it plays a pivotal role in promoting sperm hyperactivation and is likely important for successful oocyte fertilization.

4.4. Mitochondrial Ca^{2+} concentration increases during capacitation

To investigate whether the CatSper-dependent increase in cytoplasmic Ca^{2+} during capacitation also leads to an increase in mitochondrial Ca^{2+}, similar to the events shown in mouse sperm (Ferreira and Cassina et. al. 2021[10]), we measure mitochondrial Ca^{2+} concentration using the fluorescent Ca^{2+} indicator, Fluo-5N. Fluo-5N has a lower Ca^{2+} -binding affinity, making it suitable for detecting the higher Ca^{2+} concentrations present in mitochondria. Using this method, we measured mitochondrial Ca^{2+} levels in both NC and CAP sperm by flow cytometry. Our results showed that mitochondrial Ca^{2+} levels were significantly higher in CAP sperm compared to NC sperm when extracellular Ca^{2+} was present (Figure 3). This data supports the conclusion that CatSper-dependent increases in cytoplasmic Ca^{2+} during capacitation also elevate mitochondrial Ca^{2+} levels in human sperm.

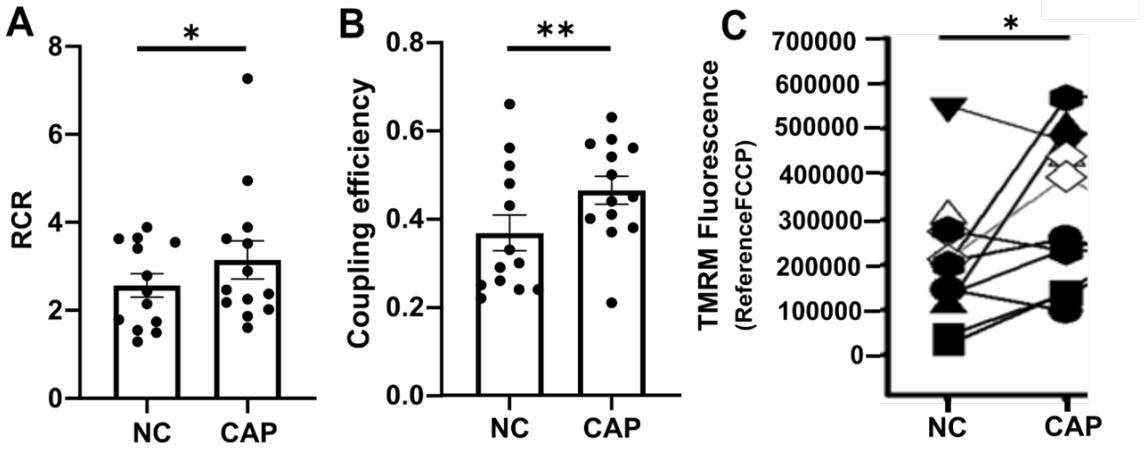

Figure 1. Mitochondrial activity increases during capacitation. A comparison between non-capacitated (NC) and capacitated (CAP) sperm: (A) RCR, calculated as the ratio of maximum respiration rate to proton leak (N=13), (B) Coupling efficiency, calculated as ATP turnover relative to basal respiration (N=13), both obtained using HRR[21], and (C) normalized TMRM fluorescence values of the M2 cell population, recorded by flow cytometry (N=12). Results are presented as mean ± SEM. *p<0.05, **p<0.01.

5. Discussion

Sperm capacitation is a critical process which involves functional changes for successful fertilization. One of the first events in capacitation is the elevation of intracellular Ca^{2+}, which activates cell signal cascades to produce the functional change in the cell[2,23]. Capacitation is historically associated with

increased energy demands[10,24–26]. Mitochondria is reported as a Ca^{2+} storage site in other cells[11,27,28], as well as having a role in buffering Ca^{2+}[28–30]. In this study, we investigated mitochondrial activity in capacitated human sperm to understand the connection between Ca^{2+} uptake and enhanced mitochondrial function. Our key contribution lies in demonstrating that human sperm capacitation is accompanied by an increase in mitochondrial activity linked with an increase in intramitochondrial Ca^{2+}, which proved to be necessary for the hyperactivation.

We compared mitochondrial function between NC and CAP human sperm using two distinct methods. First, we employed HRR to measure OCR[10,16,21,31]. Consistent with findings from other studies using extracellular flux analysis in mouse sperm[26], CAP sperm exhibited higher basal oxygen consumption, likely due to increased mitochondrial activity. In line with our previous results[16], the slope corresponding to non-mitochondrial respiration (OCR following the addition of AA) was higher in CAP sperm, suggesting increased reactive oxygen species (ROS) production. However, in the current study, this difference was not statistically significant, potentially due to the limited number of assays performed (preliminary results). We also observed increased coupling efficiency in CAP

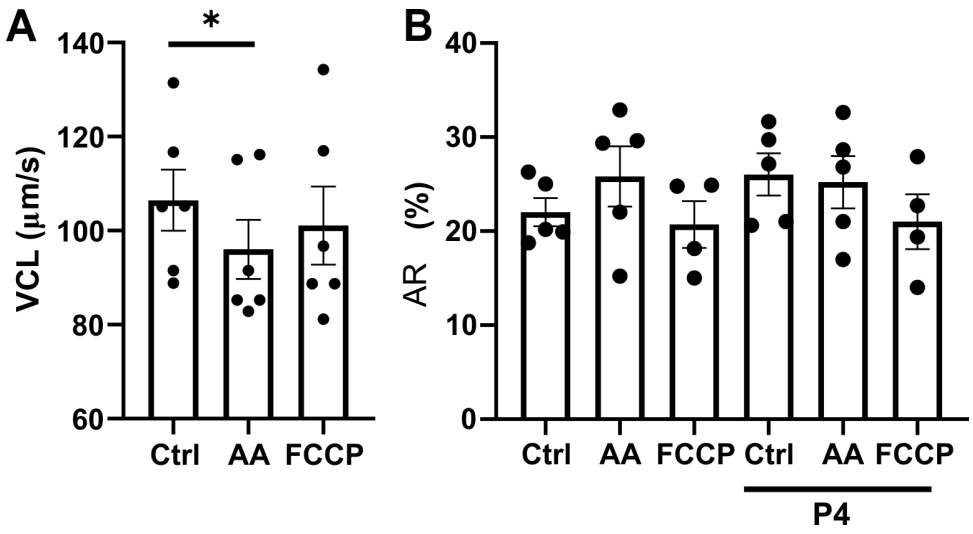

Figure 2. Mitochondrial inhibitors significantly impair mouse sperm capacitation. (A) presents measurements of curvilinear velocity (VCL) obtained by CASA from capacitated (CAP) sperm under control conditions (Ctrl) and in the presence of AA or FCCP (N=6); (B) shows both spontaneous AR and progesterone-induced (P4) AR in CAP sperm under control conditions and with AA or FCCP (N=5). The graph depicts mean ± SEM, with statistical significance determined using independent t-tests. *$p < 0.05$.

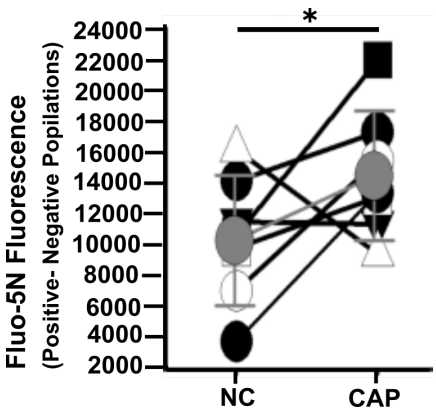

Figure 3. Mitochondrial Ca^{2+} levels increase during capacitation in Human Sperm. Mitochondrial Ca^{2+} levels were compared between non-capacitated (NC) and capacitated (CAP) sperm using the Fluo-5N probe and analyzed by flow cytometry (N=7). Data are presented as mean ± SEM, shown by the gray circles. Statistical significance was assessed with independent t-tests. *$p < 0.05$.

sperm, indicating that the mitochondrial electron transport chain is more effectively coupled to ADP phosphorylation. Finally, we detected an increase in the RCR, which reflects critical aspects of mitochondrial function, including MMP, respiratory chain activity, and oxygen consumption for ATP production [10,21,22]. While we have previously reported that mitochondrial function increases during capacitation in human sperm using HRR[16], the capacitation model in this study was different. Both NC and CAP sperm were incubated for 4 hours without or with bicarbonate, respectively. In contrast, our previous publication involved incubating both NC and CAP sperm in a complete capacitation medium, with NC samples measured at time 0[16]. We can conclude that the results obtained from both capacitation protocols are comparable, showing no significant differences. These results align with previous observations in mice[10], suggesting increased mitochondrial activity during sperm capacitation. Additionally, using the voltage-sensitive dye TMRM to measure MMP via flow cytometry[32,33], we observed an increase in MMP in CAP sperm. Thus, our results are consistent with existing literature[26,34,35], reinforcing the role of mitochondrial function in the capacitation process. It is important to note that our methods offer a distinct advantage, as they allow for the measurement of mitochondrial function within a cellular context, using intact and motile cells. This contrasts with extracellular flux measurements or those conducted on permeabilized cells, where the cellular integrity and/or motility are not preserved[21].

Experiments using mitochondrial function inhibitors revealed that while mitochondrial activity is not required for the AR, it plays a significant role in supporting sperm hyperactivation. These findings align with observations in mouse sperm, where mitochondrial inhibition leads to reduced hyperactivation and decreased *in vitro* fertilization rates[10]. However, due to ethical constraints, assessing the impact of mitochondrial inhibition on fertilization in human sperm is not feasible.

It is well established that mitochondrial Ca^{2+} uptake in somatic cells plays a crucial role in regulating mitochondrial function, metabolism, and energy production[11,27,28]. The increase in intramitochondrial Ca^{2+} entry enhances the efficiency of oxidative phosphorylation by serving as a central regulator of key enzymes, including α-ketoglutarate dehydrogenase, pyruvate dehydrogenase, isocitrate dehydrogenase, and ATP synthase[11]. For sperm cells to achieve capacitation, they must be incubated in a medium containing Ca^{2+}[25]. Previously, we demonstrated that the activation of CatSper channels, essential for Ca^{2+} influx during capacitation, is closely

associated with increased mitochondrial activity in mouse sperm[10]. In this study on human sperm, we observed a parallel increase in both mitochondrial function and intra-mitochondrial Ca^{2+} levels in CAP sperm. Based on these findings, we hypothesized that Ca^{2+} may regulate oxidative phosphorylation and be responsible for triggering the observed increase in mitochondrial activity in human CAP sperm necessary for the hyperactivation. Supporting our findings, other studies have observed that maintaining mitochondrial Ca^{2+} homeostasis is crucial for motility regulation in human sperm [36]. Recently, in pig sperm, the regulation of Ca^{2+} flux through Na^{+}/Ca^{2+} exchangers was identified as critical for the functional changes that occur during capacitation, including hyperactivation and the AR. Disruption of Ca^{2+} homeostasis during capacitation was found to prevent the expected increase in MMP and ROS, highlighting the interconnected nature of these processes[37]. The role of Ca^{2+} in regulating mitochondrial homeostasis in sperm appears to be a conserved mechanism in both human and mouse sperm. Supporting the conservation of the mechanism between both species, recent studies have revealed that human sperm with normal semen parameters but deficient in CatSper channel are unable to undergo hyperactive motility and, as a result, cannot penetrate the egg's outer layer. These patients can only achieve pregnancy through intracytoplasmic sperm injection (ICSI)[38].

In conclusion, mitochondrial activity in human sperm increases during capacitation, accompanied by enhanced mitochondrial Ca^{2+} uptake mediated by the CatSper channel. Without sufficient mitochondrial activity, hyperactivation is reduced. This study underscores the critical role of the interplay between Ca^{2+} signaling and mitochondrial function in achieving capacitation in human sperm. We propose that this mechanism is conserved between mice and humans. Further investigation is needed to understand the downstream processes.

6. Data Availability Statement

The data that support the findings of this study are available on request from the corresponding author.

7. Conflict of Interest Statement

The authors declare no conflicts of interest

8. Author Contributions

The first two authors performed and analyzed the experiments including sperm capacitation standardization and measurement of MPP. P. Irigoyen carried out respirometry studies, AR and hyperactivation experiments. J. Ferreira performed the measurement of mitochondrial calcium P. Irigoyen and J. Ferreira prepared figures. P. Irigoyen, J. Ferreira, A. Cassina, C. Santi and R. Sapiro designed the experiments, interpreted the results, and wrote the manuscript. All the authors edited, revised, and approved the final version of the manuscript. C. Santi and R. Sapiro should be considered joint senior authors.

9. Acknowledgments

Financial support for this work was received from:

Comisión Sectorial de Investigación Científica (CSIC I+D 2020, ID23), Universidad de la República (UdelaR), CSIC grupos (883455), UdelaR Espacio Interdisciplinario, Centros 2015, UdelaR, Programa de Desarrollo de las Ciencias Básicas (PEDECIBA) to, Rossana Sapiro y Adriana Cassina.

P. Irigoyen and R. Sapiro are supported by UdelaR (I+D, CSIC 2014; I+D, CSIC 2016, Iniciación a la Investigación, CSIC 2019 and FMV_1_2017_1_136490 ANII- Uruguay). P. Irigoyen is supported by PEDECIBA, POS_FMV_2018_1_1007814, and CAP-UdelaR 2020 and 2023. A. Cassina is supported by grants from UdelaR (CSIC_2018, Espacio Interdisciplinario_2021).

C.Santi funding from NIH grant and LEAP grant Award, Washington University in Saint Louis.

Finally, we would like to thank the Reprovita and Fertilab Andrology clinics, especially Andrea Torrents and Paola Carlos for allowing us access to sperm donors.

10. References

1. Visconti, P. E. *et al.* Capacitation of mouse spermatozoa. *Development* 121, 1129–1137 (1995).
2. Molina, L. C. P. *et al.* Molecular basis of human sperm capacitation. *Frontiers in Cell and Developmental Biology* vol. 6 Preprint at https://doi.org/10.3389/fcell.2018.00072 (2018).
3. Austin, C. R. The 'Capacitation' of the Mammalian Sperm. *Nature* 170, 326 (1952).
4. Chang M.C. Fertilizing Capacity of Spermatozoa deposited into the Fallopian Tubes. *Nature* 168, 697–698 (1951).
5. Lishko, P. V. & Mannowetz, N. CatSper: a unique calcium channel of the sperm flagellum. *Curr Opin Physiol* 2, 109–113 (2018).
6. Rahban, R. & Nef, S. CatSper: The complex main gate of calcium entry in mammalian spermatozoa. *Molecular and Cellular Endocrinology* vol. 518 Preprint at https://doi.org/10.1016/j.mce.2020.110951 (2020).
7. Ren, D. *et al.* A sperm ion channel required for sperm motility and male fertility. *Nature* 413, 603–609 (2001).
8. Rahban, R. & Nef, S. CatSper: The complex main gate of calcium entry in mammalian spermatozoa. *Molecular and Cellular Endocrinology* vol. 518 Preprint at https://doi.org/10.1016/j.mce.2020.110951 (2020).
9. Vyklicka, L. & Lishko, P. V. Dissecting the signaling pathways involved in the function of sperm flagellum. *Current Opinion in Cell Biology* vol. 63 154–161 Preprint at https://doi.org/10.1016/j.ceb.2020.01.015 (2020).
10. Ferreira, J. J. *et al.* Increased mitochondrial activity upon CatSper channel activation is required for mouse sperm capacitation. *Redox Biol* 48, (2021).
11. Rossi, A., Pizzo, P. & Filadi, R. Calcium, mitochondria and cell metabolism: A functional triangle in bioenergetics. *Biochimica et Biophysica Acta - Molecular Cell Research* vol. 1866 1068–1078 Preprint at https://doi.org/10.1016/j.bbamcr.2018.10.016 (2019).

12. Bravo-Sagua, R. *et al.* Calcium Transport and Signaling in Mitochondria. *Compr Physiol* 623–634 (2017).
13. Tourmente, M., Sansegundo, E., Rial, E. & Roldan, E. R. S. Capacitation promotes a shift in energy metabolism in murine sperm. *Front Cell Dev Biol* 10, (2022).
14. Ho, H.-C. & Suarez, S. S. Characterization of the Intracellular Calcium Sotre at the Base of the Sperm Flagellum That Regulates Hyperactivated Motility. *Biol Reprod* 68, 1590–1596 (2003).
15. Vicente-Carrillo, A., Álvarez-Rodríguez, M. & Rodriguez-Martinez, H. The Cation/Calcium Channel of Sperm (CatSper): A Common Role Played Despite Inter-Species Variation? *International Journal of Molecular Sciences* vol. 24 Preprint at https://doi.org/10.3390/ijms241813750 (2023).
16. Irigoyen, P., Mansilla, S., Castro, L., Cassina, A. & Sapiro, R. Mitochondrial function and reactive oxygen species production during human sperm capacitation: Unraveling key players. *FASEB Journal* 38, (2024).
17. Marín-Briggiler, C. I. *et al.* Calcium requirements for human sperm function in vitro. *Reproductive Biology Fertility and Sterility* 79, (2003).
18. Alasmari, W. *et al.* The clinical significance of calcium-signalling pathways mediating human sperm hyperactivation. *Human Reproduction* 28, 866–876 (2013).
19. WHO laboratory manual for the Examination and processing of human semen. (2021).
20. Koppers, A. J., De Iuliis, G. N., Finnie, J. M., McLaughlin, E. A. & Aitken, R. J. Significance of mitochondrial reactive oxygen species in the generation of oxidative stress in spermatozoa. *Journal of Clinical Endocrinology and Metabolism* 93, 3199–3207 (2008).
21. Irigoyen, P., Sapiro, R. & Cassina, A. High-Resolution Respirometry to Assess Mitochondrial Function in Human Spermatozoa. *Journal of Visualized Experiments* 2023, (2023).
22. Brand, M. D. & Nicholls, D. G. Assessing mitochondrial dysfunction in cells. *Biochemical Journal* 435, 297–312 (2011).
23. Breitbart, H. Intracellular calcium regulation in sperm capacitation and acrosomal reaction. *Mol Cell Endocrinol* 187, 139–144 (2002).
24. Rogers, B. J. & Morton, B. ATP Levels in Hamster Spermatozoa During Capacitation in Vitro. *Biol Reprod* 9, 361–369 (1973).
25. Hidalgo, D. M. *et al.* Capacitation increases glucose consumption in murine sperm. *Mol Reprod Dev* 87, 1037–1047 (2020).
26. Balbach, M. *et al.* Metabolic changes in mouse sperm during capacitation. *Biol Reprod* 103, 791–801 (2020).
27. Matuz-Mares, D., González-Andrade, M., Araiza-Villanueva, M. G., Vilchis-Landeros, M. M. & Vázquez-Meza, H. Mitochondrial Calcium: Effects of Its Imbalance in Disease. *Antioxidants* vol. 11 Preprint at https://doi.org/10.3390/antiox11050801 (2022).
28. Contreras, L., Drago, I., Zampese, E. & Pozzan, T. Mitochondria: The calcium connection. *Biochimica et Biophysica Acta - Bioenergetics* vol. 1797 607–618 Preprint at https://doi.org/10.1016/j.bbabio.2010.05.005 (2010).
29. Hacker, K. & Medler, K. F. Mitochondrial Calcium Buffering Contributes to the Maintenance of Basal Calcium Levels in Mouse Taste Cells. *J Neurophysiol.* 100, 2177–2191 (2008).
30. Drago, I., De Stefani, D., Rizzuto, R. & Pozzan, T. Mitochondrial Ca2+ uptake contributes to buffering cytoplasmic Ca2+ peaks in cardiomyocytes. *Proc Natl Acad Sci U S A* 109, 12986–12991 (2012).
31. Cassina, A. *et al.* Defective Human Sperm Cells Are Associated with Mitochondrial Dysfunction and Oxidant Production. *Biol Reprod* 93, 119 (2015).

32. Uribe, P. *et al.* Use of the fluorescent dye tetramethylrhodamine methyl ester perchlorate for mitochondrial membrane potential assessment in human spermatozoa. *Andrologia* 49, (2017).
33. Moscatelli, N. *et al.* Single-cell-based evaluation of sperm progressive motility via fluorescent assessment of mitochondria membrane potential. *Sci Rep* 7, (2017).
34. Carrageta, D. F. *et al.* Mitochondrial activation and reactive oxygen-species overproduction during sperm capacitation are independent of glucose stimuli. *Antioxidants* 9, 1–17 (2020).
35. Giaccagli, M. M. *et al.* Capacitation-Induced Mitochondrial Activity Is Required for Sperm Fertilizing Ability in Mice by Modulating Hyperactivation. *Front Cell Dev Biol* 9, (2021).
36. Bravo, A. *et al.* Effect of mitochondrial calcium uniporter blocking on human spermatozoa. Andrologia, 47(6). *Andrologia* 47, 662–668 (2014).
37. Yeste, M. *et al.* Inhibition of forward and reverse transport of Ca2+ via Na+/Ca2+ exchangers (NCX) prevents sperm capacitation. *Biol Res* 57, (2024).
38. Young, S. *et al.* Human fertilization in vivo and in vitro requires the CatSper channel to initiate sperm hyperactivation. *J Clin Invest* 134, (2024).

11. Supplementary Figures

Supplementary Table 1. Descriptive characteristics of semen parameters from 43 normozoospermic participants. Data were collected from the first spermiogram of individuals who attended the andrology clinic or Santi's lab. Max = maximum value; Min = minimum value. *WHO 2021 reference values[19].

Parameter	Mean	SD	Median	Max	Min	Reference limit (> or <)
Patient age (yr)	30.9	5.4	30.0	40.0	23.0	-
Volume (mL)	2.8	0.6	3.0	4.0	2.0	1.4
Sperm concentration (million/mL)	114.5	100.2	93.2	25.2	435.0	15.0
Sperm vitality (%)	88.5	2.9	89.0	93.0	84.0	54.0
Normal sperm morphology (%)	7.4	2.1	7.0	12.0	4.0	4.0
Progressive motility (a+b) (%)	58.4	7.3	59.5	71.0	44.0	30.0
Round cells (million/mL)	0.4	0.3	0.3	1.0	0.2	1.0

5.2. Estudiar la función de la mitocondria en la producción de ROS durante la capacitación espermática

Artículo 1: Mitochondrial function and reactive oxygen species production during human sperm capacitation: Unraveling key players.

Pilar Irigoyen, Santiago Mansilla, Laura Castro, Adriana Cassina* y Rossana Sapiro*.
*Ambas autoras comparten la última autoría.
FASEB Journal 2024;38:e23486. DOI:10.1096/fj.202301957RR

El objetivo del trabajo fue estudiar si el aumento en la función mitocondrial durante la capacitación se asociaba a un incremento en la producción de ROS mitocondrial. La investigación involucró 112 donantes normozoospérmicos. Analizamos la función mitocondrial mediante HRR y la producción de H_2O_2 extracelular en espermatozoides humanos CAP y NC. Observamos que, durante la capacitación, el RCR aumentó en un 36%, acompañado de un incremento en la tasa de consumo de oxígeno en presencia de AA. La oxidación de Amplex Red reveló que la detección extracelular de H_2O_2 es tres veces mayor en espermatozoides CAP que en los NC. Para confirmar que la producción de H_2O_2 depende de la formación mitocondrial de $O_2^{\bullet-}$, evaluamos la cantidad y actividad de la ACO2, así como el papel de ACO2 en el flujo metabólico del ciclo de Krebs. Estimamos que las células CAP producen, en promedio por individuo, un 59 ± 22% más de $O_2^{\bullet-}$ en estado estacionario en comparación con las células NC. Finalmente, estudiamos dos objetivos del estrés oxidativo: la peroxidación lipídica mediante western blot contra 4-HNE y la actividad de la succinato deshidrogenasa mediante HRR. No observamos modificaciones en la lipoperoxidación ni en la actividad de la succinato deshidrogenasa, lo que sugiere que, durante la capacitación, el aumento en la producción de H_2O_2 mitocondrial no es suficiente para dañar las células. Por tanto, nuestros resultados muestran la importancia de las mitocondrias para una producción controlada de ROS durante la CAP. Esta función sería necesaria para que la CAP ocurra con normalidad llevando a una fecundación exitosa.

Received: 26 September 2023 | Revised: 22 January 2024 | Accepted: 30 January 2024

DOI: 10.1096/fj.202301957RR

RESEARCH ARTICLE

The FASEB Journal

Mitochondrial function and reactive oxygen species production during human sperm capacitation: Unraveling key players

Pilar Irigoyen[1,2] | **Santiago Mansilla**[2,3] | **Laura Castro**[2,4] | **Adriana Cassina**[2,4] | **Rossana Sapiro**[1,2]

[1]Unidad Académica Departamento de Histología y Embriología, Facultad de Medicina, Universidad de la República, Montevideo, Uruguay

[2]Centro de Investigaciones Biomédicas (CEINBIO), Facultad de Medicina, Universidad de la República, Montevideo, Uruguay

[3]Departamento de Métodos Cuantitativos, Facultad de Medicina, Universidad de la República, Montevideo, Uruguay

[4]Departamento de Bioquímica, Facultad de Medicina, Universidad de la República, Montevideo, Uruguay

Correspondence
Adriana Cassina and Rossana Sapiro, Centro de Investigaciones Biomédicas (CEINBIO), Facultad de Medicina, Universidad de la República, Montevideo, Uruguay.
Email: acassina@fmed.edu.uy and rsapiro@fmed.edu.uy

Funding information
Programa de Desarrollo de las Ciencias Básicas (PEDECIBA); Agencia Nacional de Investigación e Innovación (ANII), Grant/Award Number: FMV_1_2017_1_136490 and POS_FMV_2018_1_1007814; Universidad de la República Uruguay (UdelaR), Grant/Award Number: CAP-UdelaR 2020 and 2023 and UdelaR Espacio Interdisciplinario, Centros 2015; Comisión Sectorial de Investigación Científica (CSIC)-UdelaR grupos, Grant/Award Number: 883455; CSIC I+D 2020, Grant/Award Number: ID23

Abstract

Sperm capacitation is a critical process for male fertility. It involves a series of biochemical and physiological changes that occur in the female reproductive tract, rendering the sperm competent for successful fertilization. The precise mechanisms and, specifically, the role of mitochondria, in sperm capacitation remain incompletely understood. Previously, we revealed that in mouse sperm mitochondrial activity (e.g., oxygen consumption, membrane potential, ATP/ADP exchange, and mitochondrial Ca^{2+}) increases during capacitation. Herein, we studied mitochondrial function by high-resolution respirometry (HRR) and reactive oxygen species production in capacitated (CAP) and non-capacitated (NC) human spermatozoa. We found that in capacitated sperm from normozoospermic donors, the respiratory control ratio increased by 36%, accompanied by a double oxygen consumption rate (OCR) in the presence of antimycin A. Extracellular hydrogen peroxide (H_2O_2) detection was three times higher in CAP than in NC sperm cells. To confirm that H_2O_2 production depends on mitochondrial superoxide ($O_2^{\cdot-}$) formation, we evaluated mitochondrial aconitase (ACO2) amount, activity, and role in the metabolic flux from the sperm tricarboxylic acid cycle. We estimated that CAP cells produce,

Abbreviations: AA, antimycin A; ACO2, aconitase; ADP, adenosine diphosphate; ALH, amplitude lateral head; ATP, adenosine triphosphate; BWW, Biggers Whitten Whittingham; cAMP, cyclic adenosine monophosphate; CAP, capacitated; CASA, computer aided sperm analysis; DTT, dithiothreitol; ETC, electron transport chain; FAD, flavin adenine dinucleotide; FCCP, carbonyl cyanide-P-trifluoromethoxy-phenylhydrazone; FITH, fluorescein isothiocyanate; HNE, 4-hydroxynonenal; HRP, horseradish peroxidase; HRR, high-resolution respirometry; LIN, linearity; MCU, mitochondrial calcium uniporter; NAD, Nicotinamide adenine dinucleotide; NADPH, nicotinamide adenine dinucleotide phosphate; NC, non-capacitated; NOS, nitric oxide synthase; NOX5, NADPH oxidase 5; OCR, oxygen consumption rate; OXPHOS, oxidative phosphorylation; PSA, Pisum sativum agglutinin; pY, tyrosine phosphorylation; RCR, respiratory control ratio; SD, standard deviation; SDH, succinate dehydrogenase; SOD, superoxide dismutases; VCL, linear curvilinear velocity; WHO, World Health Organization.

Adriana Cassina and Rossana Sapiro should be considered joint senior author.

on average by individual, (59 ± 22)% more $O_2^{\cdot-}$ in the steady-state compared to NC cells. Finally, we analyzed two targets of oxidative stress: lipid peroxidation by western blot against 4-hydroxynonenal and succinate dehydrogenase (SDH) activity by HRR. We did not observe modifications in lipoperoxidation nor the activity of SDH, suggesting that during capacitation, the increase in mitochondrial H_2O_2 production does not damage sperm and it is necessary for the normal CAP process.

KEYWORDS

aconitase 2, male fertility, mitochondrial activity, reactive oxygen species, respirometry assay, sperm capacitation

1 | INTRODUCTION

Mammalian sperm capacitation is a critical process that enables spermatozoa to acquire the ability to fertilize an oocyte. It involves a series of biochemical and physiological changes that occur in the female reproductive tract, ultimately rendering the sperm competent for successful fertilization. During capacitation, the sperm acquires the ability to undergo acrosome reaction and modifies their motility pattern (known as hyperactivation), permitting the spermatozoa to reach the zona pellucida and penetrate the oocyte.[1–4] Despite extensive research, there are still no definite conclusions about the biochemical mechanisms of the sperm capacitation process.

One aspect that has garnered attention in recent years is the role of mitochondria in this process.[5–9] Sperm capacitation includes several cell modifications that are accompanied by an increase in energy requirements. Ion active transport, acrosome reaction, sperm hyperactivation, and subsequent increased motility have high-ATP demands.[8] Despite the high efficiency of mitochondrial oxidative phosphorylation (OXPHOS), glycolysis is considered the preferential energy pathway for human sperm capacitation and hyperactivation.[10–12] Consequently, the source of ATP in this process is under constant debate. In this regard, our group revealed that in mice, sperm mitochondrial activity (i.e., oxygen consumption, membrane potential, and ATP/ADP exchange) increases during sperm capacitation.[6] In addition, we have shown that the increase in mitochondrial function is accompanied by Ca^{2+} influx through CatSper channels and Ca^{2+} entrance into the mitochondria through the mitochondrial calcium uniporter (MCU), and this increase in activity contributes to sperm hyperactivation and sperm fertilization.[6]

Mitochondria are known for their crucial role in energy production and calcium metabolism and serve as the principal source of reactive oxygen species (ROS) in somatic cells. In mitochondria, the electron transport chain is one of the main intracellular sites of superoxide ($O_2^{\cdot-}$) formation. Complex I (both by forward and reverse electron transport) and complex III are now recognized as the major sites of mitochondrial $O_2^{\cdot-}$ production. Superoxide renders hydrogen peroxide (H_2O_2) by spontaneous or catalyzed dismutation achieved by superoxide dismutases (SOD), manganese containing SOD (MnSOD) in the matrix and copper-zinc containing SOD (CuZnSOD) in the intermembrane space.[13–15]

ROS in small quantities drive various elements of sperm function, including capacitation, but when generated in excess, they can overwhelm the small antioxidant defenses of the spermatozoa and produce cell damage.[16–19] Oxidative stress is one of the main causes of the presence of defective sperm cells in human ejaculate,[16,20–23] and it is sustained that ROS-mediated damage to spermatozoa contributes to male infertility in 30%–80% of the cases.[23]

The source of ROS in sperm has been challenged. They can potentially be generated by sperm mitochondria[24] but also by other sources,[16,25–27] e.g., oxidase enzymes like amino acid oxidases or NADPH oxidase (NOX5)[28–30] from both spermatozoa or leucocytes. The contribution of each source in normal and pathological conditions is not completely elucidated and may have implications for understanding the role of sperm mitochondria in capacitation.

Herein, we explored the role of mitochondrial respiration using high-resolution respirometry (HRR) in both capacitated and non-capacitated sperm from normozoospermic donors, as well as their ability to produce $O_2^{\cdot-}$ during the process. Our results showed that mitochondrial function, as well as ROS production, increases in human normozoospermic cells during capacitation. These data support a functional link of $O_2^{\cdot-}$

mitochondrial in the process of sperm capacitation. Interestingly, the increase of mitochondrial $O_2^{\cdot-}$ production observed during capacitation did not produce detrimental effects on sperm.

2 | MATERIALS AND METHODS

2.1 | Reagents

Chemicals (unless otherwise indicated) were purchased from Sigma-Aldrich Chemical Co. (St. Louis, MO, United States).

2.2 | Selection of subjects and ethical guidelines

Freshly ejaculated human semen was obtained through masturbation following a recommended 3-day period of abstinence. The semen was collected into a sterile plastic container and immediately transported to the laboratory. The study involved a total of 112 men who presented to the Fertilab and Reprovita andrology clinics (Montevideo, Uruguay) for routine semen analysis between March 2018 and April 2023.

All the samples used in the study were categorized as normozoospermic based on the criteria established by the World Health Organization (WHO) criteria.[31,32] This categorization of samples was independent of fertility status. Any samples with a white blood cell count exceeding 0.5×10^6/mL or leukocytospermia were discarded.[31] Men who had genital tract infections, varicocele, or had undergone vasectomy were excluded from the study.

Men who met the inclusion criteria were finally enrolled in this work. They were randomly assigned to different experimental groups as follows: 41 men were included in respirometry studies (20 intact cells, 17 permeabilized cells for complex II analysis, and five fluorocitrate studies), 14 samples were selected for H_2O_2 measurement, 19 for 4-hydroxynonenal western blot and 16 for aconitase activity studies. In addition, 22 men were included in capacitation studies, and certain parameters were measured in samples that had been used for other experiments.

The project received approval from the Ethics Committee of the Facultad de Medicina de la Universidad de la República Montevideo, Uruguay. Before sample collection, informed written consent was obtained from all participants. The laboratory personnel ensured the anonymity of the participants without involving the researchers.

2.3 | Semen evaluation and motility analysis

Semen samples were left at room temperature for 30 min to complete liquefaction. Semen volume, pH, biochemistry analysis of seminal plasma and sperm viability, and morphology were analyzed according to WHO.[31,32]

Two sperm counting chambers CELL-VU® (Millennium Sciences, Inc., New York, USA) pre-warmed were loaded, and ten different fields per chamber were randomly examined using a Nikon microscope at 37°C. Concentration and motility parameters were analyzed using an SCA-Microoptics automated analyzer (CASA) (Barcelona, Spain) with default settings as per the WHO criteria.[31] The analysis of kinetic characteristics for hyperactivation was examined only for motile sperm and they were sorted using the reported CASA parameters: linear curvilinear velocity VCL > 150 μm/s, linearity LIN < 50%, and the amplitude lateral head ALH > 3.5 μm.[33]

2.4 | Preparation of the samples and capacitation

Samples were centrifuged at room temperature at 500*g* for 10 min to separate sperm from seminal plasma. Sperm cells were suspended in Biggers Whitten Whittingham medium (BWW: 95 mM NaCl, 4.6 mM KCl, 1.7 mM $CaCl_2$, 1.2 mM KH_2PO_4, 1.2 mM $MgSO_4$, 5.6 mM glucose, 0.27 mM sodium pyruvate, 20 mM acid-free HEPES, 25 mM $NaHCO_3$, 44 mM sodium lactate and 0.3% BSA, pH 7.4).[34] The sperm suspension in BWW was split into two different parts. An aliquot was immediately processed to avoid letting it trigger the capacitation process (non-capacitated, NC), and the other one was incubated for 4 h at 37°C (capacitated, CAP). If a subsequent washing step was included is described below.

2.5 | Acrosomal reaction

The percentage of capacitated spermatozoa was determined both in NC and CAP by Pisum sativum agglutinin (PSA) labeled with fluorescein isothiocyanate (FITC) (PSA–FITC) according to the WHO criteria.[31] To induce the acrosome reaction sperm cells were incubated for 30 min at 37°C with 10 μM of progesterone or calcium ionophore A23187. Briefly, an aliquot of 10×10^6 cells was smeared onto slides, air dried, and fixed in Ethanol 100% for 30 min. Following this, slides were incubated for 30 min with 50 μg/mL of PSA–FITC. Slides were then incubated for 15 min with 0.4 μg/mL DAPI. Finally, slides were air-dried and sealed with a cover slip using a mounting

medium (Tris 4:1 Glycerol). Between the different steps, slides were washed twice with phosphate-buffered saline (PBS) for 10 min. Stained sperm were examined under a microscope at 400× (Nikon E100, Japan) to analyze the acrosome reaction status.

2.6 | Western blot

Sperm suspensions of both conditions were washed with PBS and centrifuged for 10 min at 500*g*. The remaining pellet was resuspended in chilled lysis buffer (20 mM Tris–HCl, 150 mM NaCl, 0.1% Triton X-100, 1 mM EGTA, 25 mM sodium pyrophosphate, 0.1% SDS, and protease inhibitors (Mini Tablets Thermo Fisher, USA)) and incubated on ice. Later, samples were sonicated for 5 s at 4°C, centrifuged for 10 min at 14 000*g*, and stored at −80°C. Protein concentration was measured by the Bradford method.[35]

Proteins (30 µg) were loaded on 10%–12% SDS–polyacrylamide gel and were transferred to nitrocellulose membrane (GE Healthcare, Piscataway, NJ) overnight at 20 V and 4°C. Membranes were blocked for 1 h at room temperature in Tris Buffered Saline 0.1% vol/vol Tween-20 (TBS-T) and 5% wt/vol BSA. The membranes were washed twice with TBS-T for 5 min and incubated overnight shaking at 4°C with one of these primary antibodies: mouse monoclonal anti-phosphotyrosine (03-7700, pY20, Invitrogen), goat anti-4-HNE (ab46544, Abcam), rabbit anti-aconitase 2 (ab71440, Abcam), or rabbit anti-alpha tubulin (Cell Signaling, it was the loading control for normalized protein levels). After three washes with TBS-T, membranes were incubated at room temperature for 1 h with the corresponding secondary antibody: anti-mouse IRDye® 800CW/680CW, anti-goat IRDye® 800CW, anti-rabbit IRDye® 800CW (926-32210, 926-68070, 926-32214, 926-32211, Li-COR, Lincoln, NE). Membranes were washed three times for 10 min with TBS-T and immunoreactive proteins were detected using an infrared fluorescence detection system (Odyssey CLx, Li-COR, Biosciences). Bands were quantified by densitometry using Image Studio software (Li-COR Bioscience, version 2.0).

2.7 | Evaluation of mitochondrial function by high-resolution respirometry

Oxygen consumption rate (OCR) of 24 $\times 10^6$ sperm NC and CAP was measured by HRR (Oxygraph-2K; Oroboros Instruments GmbH, Innsbruck, Austria) following the protocol described in Irigoyen et al.[36] Briefly, the two protocols used are described below.

2.7.1 | Intact cells

The mitochondrial function of sperm cells was measured in BWW media as previously described.[6,36] Briefly, basal respiration was measured for 10 min before adding 2 µg/mL oligomycin (ATP synthetase inhibitor). Maximum respiration was obtained by subsequent stepwise addition of the uncoupling agent 0.1–1 µM carbonyl cyanide-P-trifluoromethoxy-phenylhydrazone (FCCP). Finally, a complex III inhibitor, 2.5 µM antimycin A (AA) was added to distinguish mitochondrial from residual oxygen consumption (non-mitochondrial respiration). The non-mitochondrial oxygen consumption was subtracted from all other values before calculating parameters. We compared the different slopes (values were adjusted per million cells), calculated ATP turnover (basal respiration-proton leak), and the indices as the ratio between different parameters as follows: respiratory control ratio (RCR) = maximal/proton leak, spare respiratory capacity = maximum respiratory rate/basal respiration and coupling efficiency = (basal respiration − proton leak)/basal respiration.[24,36,37]

2.7.2 | Permeabilized cells

NC and CAP cells were centrifuged for 10 min at 500*g*. The supernatant was discarded and replaced with mitochondrial respiration medium (MRM: 0.1% BSA, 5 mM KH_2PO_4, 1 mM EGTA, 5 mM MOPS, and 300 mM sucrose, pH 7.4). Mitochondrial basal respiration was measured for 5 min and then the sperm cells were permeabilized by the addition of 22.5 µM digitonin. Oxygen consumption measurements for complex II were obtained before and after the sequential addition of substrates and inhibitors of the respiratory chain: 10 mM succinate, 1.2 mM adenosine diphosphate (ADP), 2 µg/mL oligomycin, and subsequent stepwise addition of 0,1–1 µM FCCP. Finally, respiration was inhibited with 2.5 µM AA, these values were subtracted before calculating the index. The RCR for permeabilized cells was calculated as the ratio between state 3 (after ADP addition) and state 4 respiration (after addition of glutamate/malate) rates.

The role of ACO2 inhibition afforded in mitochondrial OCR was determined after the addition of 10 mM citrate, 2 mM malate, and 1 mM ADP and the subsequent addition of the ACO2 inhibitor fluorocitrate. Fluorocitrate titration consisted of three steps adding 1.5 µL of 10 mM stock (final concentrations: 7.5, 15, and 22.5 µM). Aconitase-driven respiration was confirmed by recovered respiration after the addition of 5 mM isocitrate[38]

2.8 | Evaluation of hydrogen peroxide production in sperm cells

Extracellular H_2O_2 production of sperm cells was measured by 10-acetyl-3,7-dihydroxyphenoxazine dye (Amplex™Red) in the presence of horseradish peroxidase (HRP) as previously described in Irigoyen et al.[39] Previously, NC and CAP cells were centrifuged for 10 min at 500*g* and resuspended in HAM-F10 medium (126 mM NaCl, 3.8 mM KCl, 1.08 mM NaH_2PO_4, 0.6 mM $MgSO_4.7H_2O$, 0.3 mM $CaCl_2$, 6 mM glucose, 20 mM HEPES and 6 mM NaHCO, pH 7.4). Briefly, between 2 and 6×10^6 spermatozoa were placed in 96-well Nunc F plates in a final volume of 100 µL and exposed to 8 µg/mL HRP and 50 µM Amplex Red (Invitrogen, Waltham, Massachusetts, USA). The H_2O_2 present in the sample was determined from a calibration curve obtained with H_2O_2 (final concentration 0.03–8 µM). Measurement was performed after 30 min at 37°C in a Flash Spectral Scanning Multimode Reader (Varioskan, Thermo Fisher Scientific, MA USA) at λex = 530 nm and λem = 590 nm. Duplicates were performed in samples and triplicates in the standard curve.

2.9 | Aconitase activity

NC and CAP sperm suspensions were centrifuged for 10 min at 500*g* and resuspended in a chilled lysis buffer (10 mM Tris, 0.25 M sucrose, 2 mM citrate, 1 mM succinate, pH 7.4). Later, samples were sonicated for 30 s at 4°C and incubated on ice for 20 min with Triton 0.5%. Finally, samples were centrifuged for 10 min at 15 000*g* and supernatants were immediately measured or stored at −80°C for a maximum of ten days. Under these conditions, no significant decay in ACO2 activity was detected (not shown). NC and CAP paired samples were evaluated simultaneously. Protein concentration was quantified by Bradford method.[35]

Aconitase activity was measured by coupled assay to isocitrate dehydrogenase,[40] following the production of NADPH at 340 nm ($\varepsilon_{340} = 6.22\,mM^{-1}\,cm^{-1}$) in a Shimadzu UV-2450 spectrophotometer. The reaction was performed in a final volume of 1 mL and the reaction mixture contained 50 mM Tris/HCl pH 7.8, 0.2 mM $NADP^+$, 0.6 mM $MgCl_2$, 0.5–1 U isocitrate dehydrogenase, and 5 mM sodium citrate. In some experiments, increasing concentrations of the aconitase competitive inhibitor fluorocitrate (5–40 µM), were added.

Aconitase activity was normalized to the protein concentration or the ACO2/tubulin ratio obtained by western blot densitometry. For ACO2 reactivation, the lysate was incubated with 10 mM dithiothreitol (DTT) and 100 µM $Fe(NH_4)_2(SO_4)_2$ under argon for 30 min in an anaerobic vial.

2.10 | Statistics

Statistical analysis was performed based on the GraphPad Prism statistical package version 8.0.1 for Windows, GraphPad Software, San Diego, California USA, www.graphpad.com. Data were expressed by arithmetic means and the corresponding standard deviation (SD) and standard error of the mean (SEM) in graphs. Comparison between central tendencies was performed using the Wilcoxon signed-rank test. A *p*-value of less than .05 was considered statistically significant. As biological material was limited in most of the assays, the sample size between experiments can differ.

3 | RESULTS

3.1 | Subject selection

The means, standard deviation (SD), median, maximum, and minimum values for age and semen parameters obtained from classic spermiogram analysis are presented in Table S1. These parameters include semen volume, sperm concentration, sperm vitality, percentage of normal sperm, progressive motility, and round cell concentration. The study involved 112 men, between the ages of 20 and 55 years old, who were diagnosed as normozoospermic based on the 2021 WHO criteria.[31]

3.2 | Capacitation-associated events are shown after incubation in BWW medium

Sperm capacitation is characterized by several events, namely, a change in the motility pattern known as hyperactivation (characterized by asymmetrical flagellar beating), a time-dependent increase in tyrosine phosphorylation (pY), and the acquisition of the ability to undergo the acrosome reaction.[2] We assessed these capacitation-related events immediately (referred to as NC) and after a 4-h incubation in a BWW medium[34] supplemented with BSA and bicarbonate (referred to as CAP) (Figure S1). Sperm incubated under CAP conditions exhibited a higher percentage of hyperactivated cells (Figure S1A) (NC: 0.93 ± 2.18 vs CAP: 2.67 ± 2.13, $N = 14$), an increase in pY (Figure S1B,C) (NC: 5.23 ± 4.98, CAP: 11.32 ± 12.89, $N = 8$), and a

greater number of sperm without an acrosome cap compared to NC cells (Figure S1D) (NC: 17.29 ± 6.4, CAP: 34.29 ± 18.16, CAPi: 45.25 ± 7.45, $N = 7$). Based on these findings, we can conclude that the CAP fraction represents a capacitated state.

3.3 | Mitochondrial function increases in human sperm capacitation

To investigate the role of OXPHOS in human sperm capacitation, we compared the OCR of NC and CAP sperm cells from 19 samples using HRR. Various parameters and three indices representing mitochondrial function, described by Brand et al. and Irigoyen et al.,[36,37] were obtained (Table S2). The indices are ratios of oxygen consumption and are therefore internally normalized to cell number. We observed significant differences in non-mitochondrial consumption, RCR, and spare respiratory capacity indices.

CAP spermatozoa exhibited a higher RCR than NC, indicating improved mitochondrial function under these conditions (Table S2, Figure 1A) (NC: 2.63 ± 0.75, CAP: 3.65 ± 1.40, $N = 20$). Furthermore, CAP sperm showed an increase in spare respiratory capacity (Table S2, Figure 1B) (NC: 1.38 ± 0.26, CAP: 1.86 ± 0.68, $N = 20$), suggesting that they operate far to their bioenergetic limit.

Conversely, CAP sperm demonstrated a higher OCR in the presence of AA compared to NC (Table S2, Figure 1C) (NC: 0.14 ± 0.13, CAP: 0.29 ± 0.28, $N = 20$). The addition of AA inhibits electron flow at complex III specifically at the coenzyme-Q cycle, favoring the formation of $O_2^{\cdot-}$. Therefore, the higher slope of mitochondrial oxygen consumption in CAP sperm could indicate a greater mitochondrial ROS generation.

3.4 | Increased H_2O_2 production during capacitation

To investigate whether this condition is associated with an increase in ROS, we compared the extracellular H_2O_2 production between NC and CAP sperm obtained from 23 samples. To achieve this objective, we measured the reaction between Amplex™ red and H_2O_2 in the presence of HRP.[39] As illustrated in Figure 2A, CAP sperm exhibited H_2O_2 production that was three times higher than NC sperm. This finding aligns with previous studies that have demonstrated the essential role of ROS species at low concentrations in the capacitation processes.[9,41–43]

The lipid aldehyde 4-hydroxynonenal (4-HNE) is the most abundant and reactive aldehyde, resulting from the peroxidation of polyunsaturated fatty acids (PUFAs). It induces protein damage and subsequent alteration in cell function.[44] Mammalian spermatozoa, in particular, are characterized by a high proportion of PUFA. To further investigate potential indications of oxidative stress damage in CAP samples, specifically about the observed increase in H_2O_2 levels, we examined the presence of 4-HNE in proteins from NC and CAP sperm by Western blot (Figure 2B,C). As shown in Figure 2C, there were no significant differences in 4-HNE between the two states (NC: 3.70 ± 2.74, CAP: 3.77 ± 3.28, $N = 19$).

Aldehydes have been found to bind to succinate dehydrogenase affecting its activity in sperm cells.[20] As shown in Figure 2D,E, the RCR of complex II, which

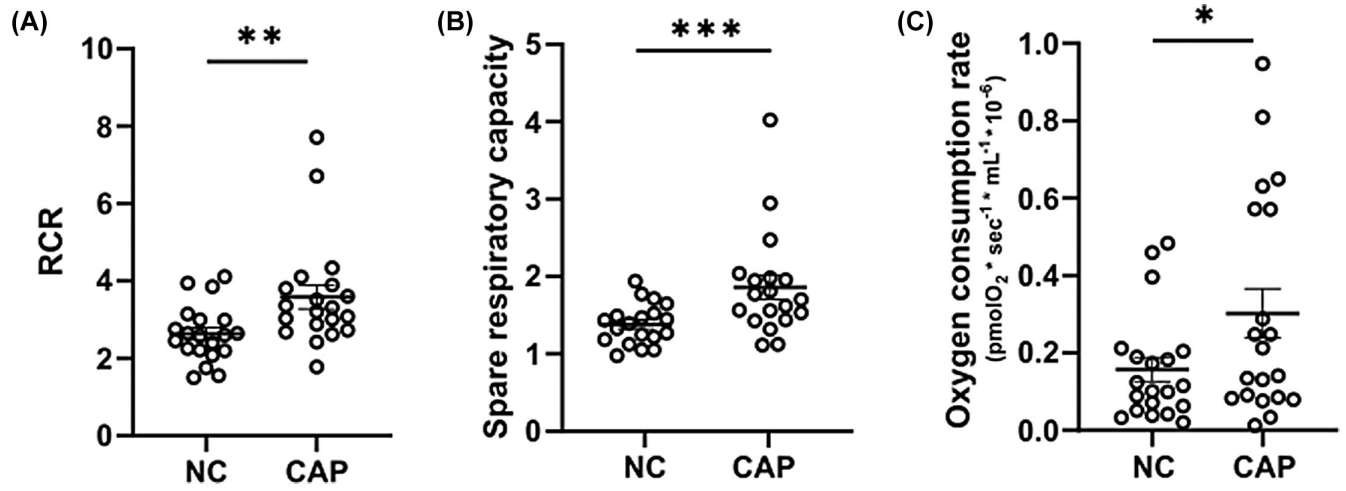

FIGURE 1 Mitochondrial activity is higher during capacitation. (A) Respiratory Control Ratio (RCR) values are calculated as maximum respiratory rate/proton leak. (B) Spare respiratory capacity values are calculated as maximal respiratory rate/basal respiration. (C) Non-mitochondrial respiration consumption (Antimycin A-resistant respiration rates) per million of sperm cells. CAP, capacitated sperm cells; NC, non-capacitated sperm cells; Results are expressed as mean ± SEM. *$p < .05$, **$p < .01$ ($N = 20$).

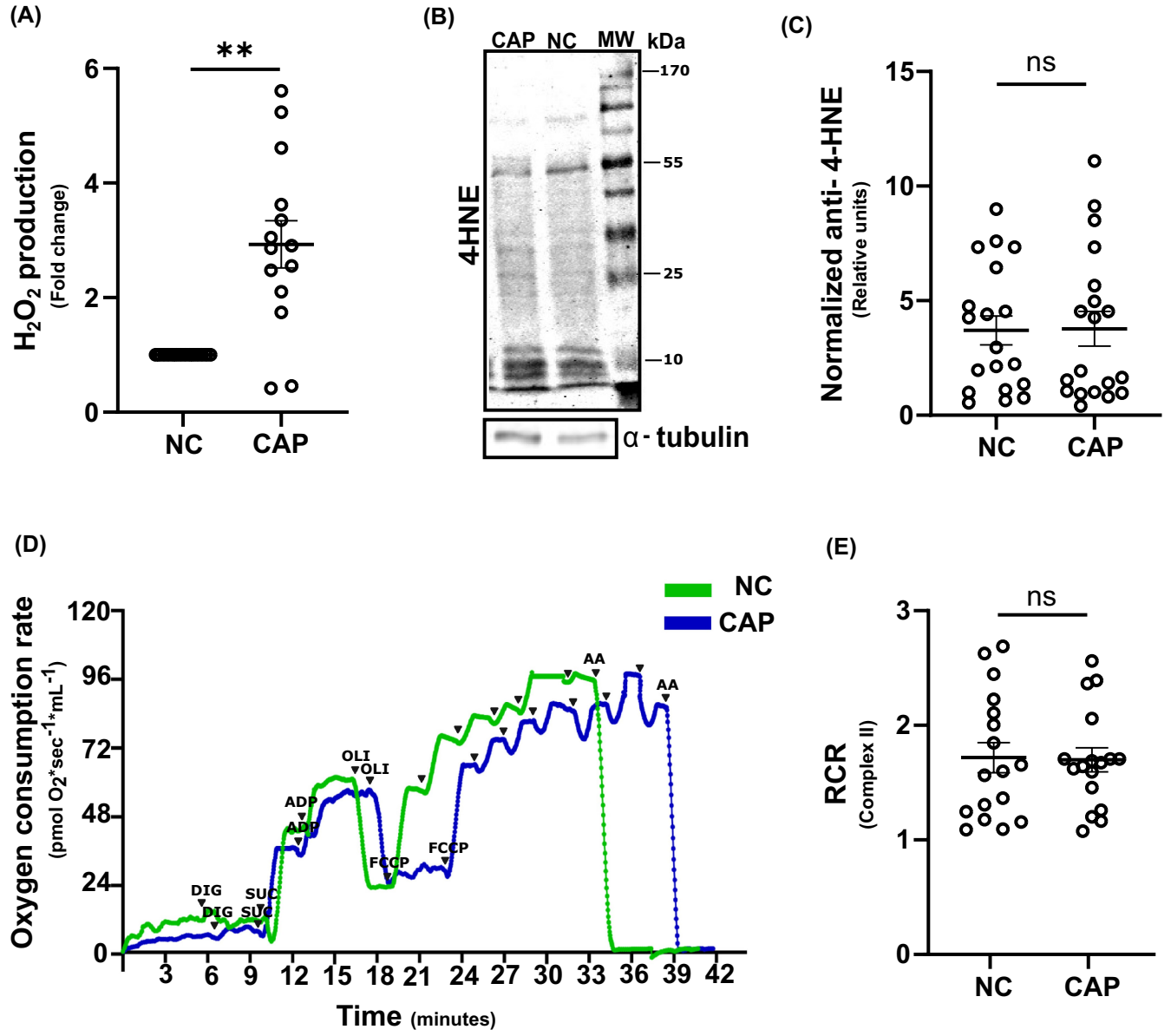

FIGURE 2 H_2O_2 production is increased in capacitated human sperm (CAP) without substantial evidence of oxidative stress damage. (A) Production of extracellular H_2O_2 by 10^6 sperm cells using the Amplex red™ system ($N = 13$). (B) Representative western blot with antibody against 4-Hydroxynonenal (4-HNE). (C) Protein levels of anti-4-HNE normalized to tubulin (loading control) detected in independent western blot ($N = 19$). (D) Representative respiratory traces for 30×10^6 sperm cells NC (green line) and CAP (blue line). AA, antimycin A; ADP, adenosine diphosphate; DIG, digitonin; FCCP, carbonyl cyanide *p*-trifluoro methoxyphenylhydrazone; OLI, oligomycin; SUC, succinate. (E) Respiratory control ratio (RCR) calculated as state 3 (after addition of 1.2 mM ADP)/state 4 (after addition of −10 mM succinate) ($N = 17$). Results are expressed as mean ± SEM. n.s = $p > .050$, ** $p < .01$.

reflects its function, was the same between NC and CAP sperm (NC: 1.72 ± 0.54, CAP: 1.70 ± 0.43, $N = 17$). This suggests that the observed increase in H_2O_2 production in CAP sperm does not significantly impact the activity of the complex.

Therefore, under CAP conditions, there was an increase in the production of extracellular H_2O_2 without causing significant oxidative damage.

3.5 | Mitochondrial aconitase revealed that superoxide production increased during sperm capacitation

ACO2 is a tricarboxylic-acid enzyme that catalyzes the reversible isomerization of citrate to isocitrate via *cis*-aconitate. Active ACO2 contains a non-redox $[4Fe\text{-}4S]^{2+}$ prosthetic group in which one of the iron ions, Fe_α is not

ligated to a protein residue, and thus can bind to hydroxyl groups of substrates or water; hence, the integrity of the Fe-S cluster is essential for the catalytic activity. Due to Fe_{α} accessibility to the solvent, ACO2 is an extremely oxidant-sensitive tricarboxylic-acid enzyme. Oxidized inactive $[3Fe\text{-}4S]^{+}$-ACO2 can be reactivated in vitro by reincorporation of Fe^{2+}; which is favored by reductants, or in vivo favored by Fe-chaperons partners such as Frataxin. The ratio $[3Fe\text{-}4S]^{+}$-ACO2 to $[4Fe\text{-}4S]^{+}$-ACO2 has been used to determine the steady-state concentration of $O_2^{\cdot-}$ in cells even in the presence of other oxidants that also react with ACO2.[45,46]

Analysis of samples from 12 independent donors revealed that ACO2 levels in sperm cells decreased on average 65% after undergoing capacitation, while the ACO2-specific activity was only reduced by 24%. Surprisingly, ACO2 activity normalized by the ACO2/TUB ratio revealed no significant differences in ACO2 activity (Figure 3B–E).

Upon reactivation of NC and CAP cells, an increase of 71% and 140%, respectively, was observed (Figure 3F,G). From this data, active and inactive ACO2 proportions can be calculated for NC and CAP cells, as shown in Figure 3H. In CAP cells, total ACO2 is decreased, and the reactivable proportion of ACO2 is higher than in NC cells. It is important to point out that our biochemical analysis of ACO2 activity allows us to calculate the amount of ACO2 that is active concerning total ACO2, which is impossible when commercial activity kits are used as DTT and Fe^{2+} are included in the reaction mixture.

As ACO2 is sensitive to $O_2^{\cdot-}$ and is one of its few specific targets, the ratio between inactive and active ACO2 in cells can be used as a proxy of the mitochondrial $O_2^{\cdot-}$ levels in steady-state.[45] The ratio of $O_2^{\cdot-}$ levels in steady-state between CAP and NC cells can be calculated by the next equation:

$$\frac{\left[O_2^{\bullet-}\right]_{CAP}}{\left[O_2^{\bullet-}\right]_{NC}} = \frac{\left(\frac{[3Fe-4S]^{+}ACO2}{[4Fe-4S]^{2+}ACO2}\right)_{CAP}}{\left(\frac{[3Fe-4S]^{+}ACO2}{[4Fe-4S]^{2+}ACO2}\right)_{NC}}$$

By applying this equation to samples shown in Figure 3, we estimated that CAP cells produce, on average by individual, (59 ± 22)% more $O_2^{\bullet-}$ in steady-state in comparison to NC cells. As the second-order rate constant for the reaction between the mammalian ACO2 and $O_2^{\bullet-}$ has been reported to be in the range of 0.8×10^7 to $2.3 \times 10^8\,M^{-1}s^{-1}$[45], it is possible to calculate the absolute $O_2^{\bullet-}$ steady-state concentration by applying the following equation:

$$k_2\left[O_2^{\bullet-}\right]\left[[4Fe-4S]^{2+}ACO2\right] = k\left[[3Fe-4S]^{2+}ACO2\right]$$

where k represents the pseudo-first-order rate constant for reactivation. Considering the data reported for A549 lung carcinoma human cells ($k = 0.8 \times 10^7\,M^{-1}s^{-1}$ and $k_2 = 0.0014\,s^{-1}$), we can calculate that in NC sperm cells, $O_2^{\cdot-}$ steady-state concentrations would be 200 ± 40 pM and in CAP cells 260 ± 30 – pM (pooled data).

As the RCR during sperm capacitation is increased and ACO2 is decreased, we aim to explore the role of ACO2 in the metabolic flux from the tricarboxylic acid cycle and the respiratory chain. Fluorocitrate, a suicide aconitase inhibitor, was used to perform aconitase activity and aconitase-dependent respiration titrations to asses the control exerted by ACO2 in a metabolic step or network following cell respiration. The aconitase-driven respiration was assessed by the addition of citrate and ADP as substrates (Figure 4A), and fluorocitrate was sequentially added until inhibition was observed. The specificity of the inhibition was confirmed as the respiration was recovered by isocitrate (Figure 4A,B). Due to sample limitations, we could not perform a complete fluorocitrate titration to obtain an exact threshold for inhibition and the control coefficients exerted by ACO2 in sperm cells as we did before for rat mitochondria.[47] However, Figure 4C reveals that the IC_{50} for fluorocitrate inhibition of ACO2 could be determined in NC lysates and is 5.3 μM similar to that reported for different rat tissues ACO2.[47] As shown in Figure 4, the OCR of NC cells decreases only on average by an individual 42 ± 2% when ACO2 is inactivated by 90% at the same fluorocitrate concentration (22.5 μM). In total, these experiments dismiss the essential role of ACO2 exerting flux control over respiration in spermatic human cells.

4 | DISCUSSION

As mentioned earlier, sperm capacitation is a critical process required for successful fertilization in mammals. Capacitation is accompanied by an increase in energy demand.[1,4,48] This concept has been challenged by the fact that glycolysis is considered the preferred energy metabolism pathway for capacitation and hyperactivation of human spermatozoa,[10–12] suggesting that the role of mitochondria in sperm drives other functions beyond ATP synthesis.

The importance of mitochondria in sperm biology is underlined by several studies, improper mitochondrial function can impair sperm quality, reviewed in Refs. [22,49]. In humans, mitochondrial metabolism correlates positively with human parameters in NC sperm.[24,39] In addition, mitochondrial membrane potential (MMP), which serves as an indicator of mitochondrial energy and functional status, is related to sperm viability,[5] fertilization,[50] and the

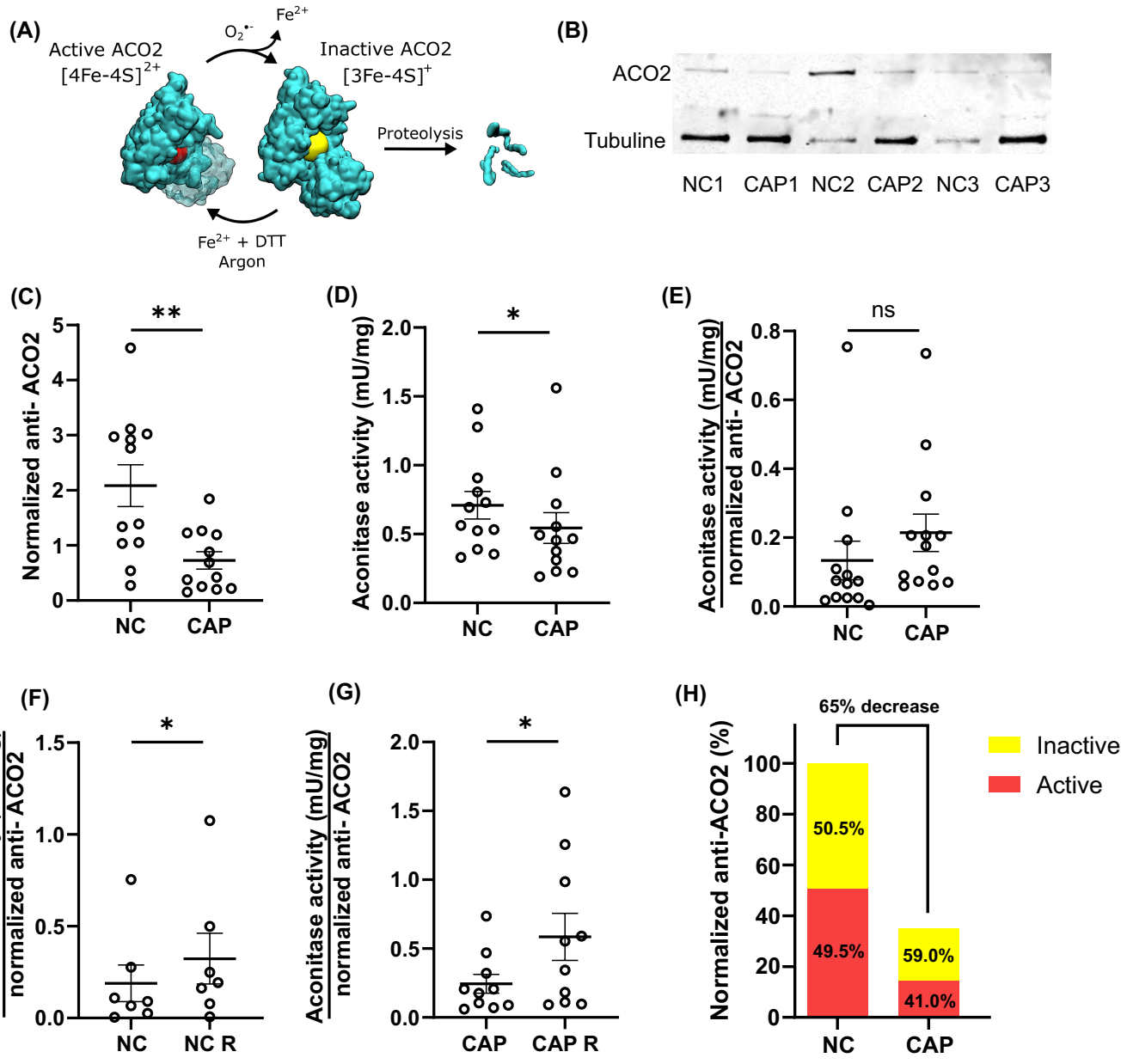

FIGURE 3 Analysis of ACO2 activity revealed increased mitochondrial superoxide production during sperm capacitation. (A) $[4Fe\text{-}4S]^{2+}$-ACO2 reacts fast with superoxide leading to an inactive $[3Fe\text{-}4S]^{+}$-ACO2 form. In the presence of Fe^{2+} and DTT under Argon, full activity can be recovered. Oxidized ACO2 (among other modifications) is a target of mitochondrial Lon protease. (B, C) Expression and quantification of ACO2 in sperm cells determined by immunoblotting assay. Tubulin was used as a loading control. (D) Aconitase activity in sperm sample lysates was measured by the coupled assay using isocitrate dehydrogenase. (E) Aconitase activity normalized to ACO2 expression. (F, G) Normalized aconitase activity of NC and CAP sperm cells before and after incubation with 100 µM Fe^{2+} and 10 mM DTT under argon flow for 30 min. R: Reactivated. (H) Active and inactive ACO2 proportions relative to ACO2 protein levels. n.s = $p > .050$, *$p < .05$, **$p < .01$.

ability to carry out the acrosome reaction.[51] Other authors have also shown that capacitation induces mouse sperm mitochondria to form better-defined cristae confirming the important role of mitochondria during capacitation.[52]

In the present work, we demonstrated an increase in RCR and the spare mitochondrial capacity in human sperm, confirming similar behavior in mitochondrial mice and human sperm[6]. Notably, the respiratory control ratio reflects the most crucial points of mitochondrial function, e.g., the respiratory chain, mitochondrial membrane potential, and the amount of oxygen consumed dedicated to the production of ATP,[36,37,39] suggesting that an overall increase in sperm mitochondrial activity occurs during capacitation. In human sperm, a 34% increase in the

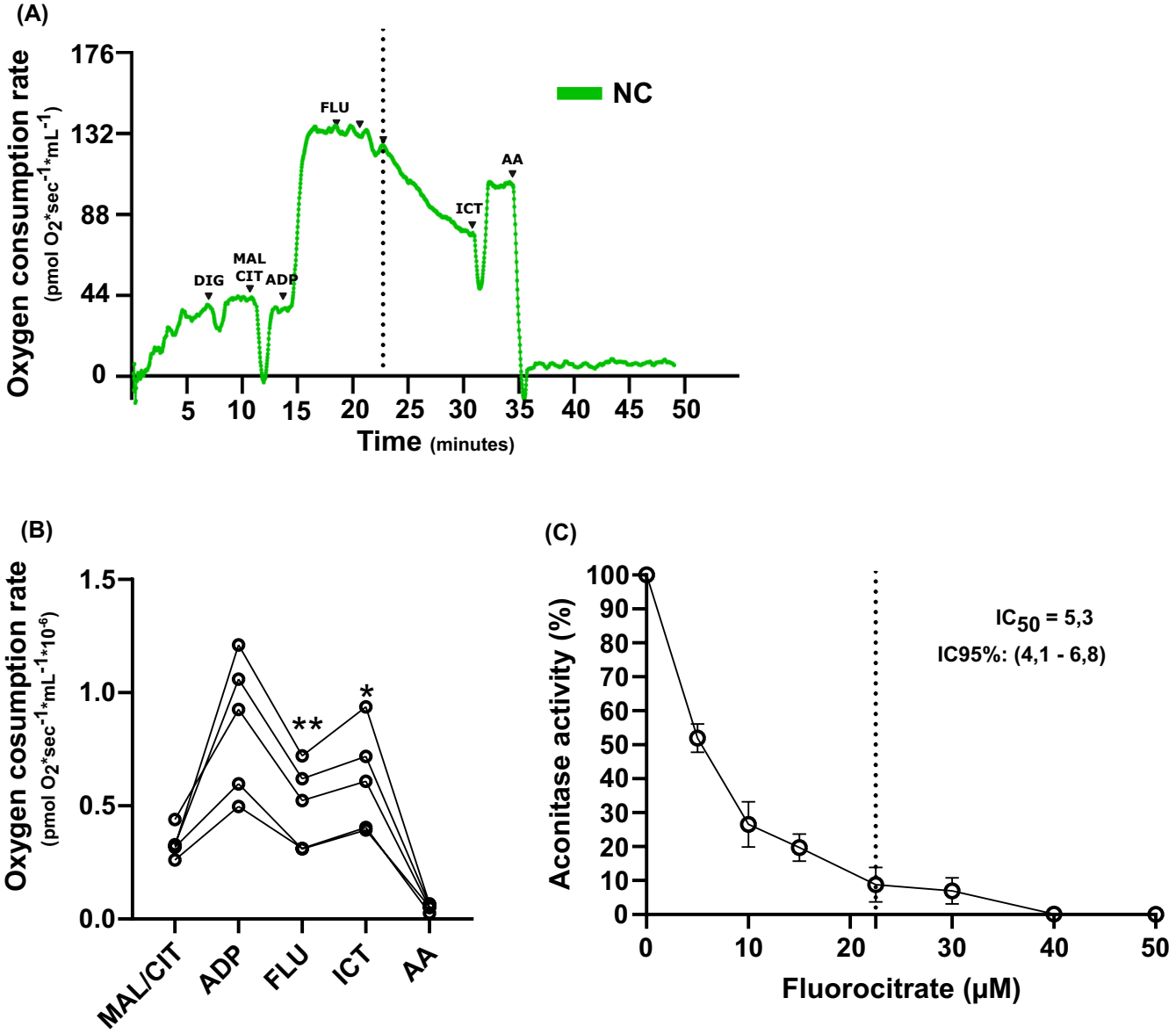

FIGURE 4 Mitochondrial oxygen consumption elicited by aconitase in non-capacitated human sperm. (A) Representative respiratory traces in digitonin-permeabilized cells in the presence of increasing concentrations of fluorocitrate (final concentrations: 7.5, 15, and 22.5 μM). Blue line: O_2 concentration. Red line: O_2 flux per volume correlated. DIG = Digitonin (22.5 μM), MAL/CIT = Malate/Citrate (2 mM/10 mM), ADP = Adenosine diphosphate (1.25 mM), FLU = Fluorocitrate (7.5, 15 and 22.5 μM), ICT = Isocitrate (5 mM) and AA = Antimycin A (2.5 μM). (B) Decrease in oxygen consumption in the presence of 22.5 μM of fluorocitrate ($N = 5$). (C) Aconitase activity in sperm cells as a percentage of control at different concentrations of fluorocitrate. IC_{50} = concentration of fluorocitrate needed to reduce aconitase activity by 50% ($N = 3$). Results are expressed as mean ± SEM. A paired Mann–Whitney test was used to evaluate the statistical significance between ADP vs. FLU and FLU vs. ICT. *$p < .05$, **$p < .01$.

spare mitochondria capacity was also observed (Table S2), suggesting that during capacitation either recruitment of more active mitochondria occurs or more mitochondrial respiratory chain complexes are activated than in non-capacitated conditions.[37] In agreement with these data, other authors observed an increase in mitochondrial membrane potential during mouse capacitation.[7] Importantly, sperm mitochondria form a helicoidal sheath stabilized by sulfur bridges that do not permit phenomena like fusion, fission, or mitochondrial biogenesis.[53,54] As a consequence, the number of mitochondria in the mature sperm is considered to be constant. In addition, as all the experiments were performed as paired. Therefore, the increase in spare respiratory capacity observed in CAP sperms reflects that more mitochondrial complexes are being recruited instead of changes in mitochondrial mass.

In parallel with the increase in mitochondrial function, capacitated human sperm showed increased oxygen

consumption after the addition of AA compared with NC sperm. In the presence of mitochondrial substrates, AA inhibits the Coenzyme Q cycle, leading to an increase in semiquinone formation and thus $O_2^{\cdot-}$ formation by Complex III. Since we did not use rotenone to inhibit Complex I, we cannot exclude the role of this mitochondrial complex as an $O_2^{\cdot-}$ generator through reverse electron transport in this model.[13]

An important question in the field is which is the main trigger of the observed increase in mitochondrial activity, and consequently, the production of superoxide during capacitation. To achieve capacitation, sperm must be incubated in a medium with Ca^{2+}. We have previously shown that Ca^{2+} influx through CatSper channels during capacitation enhances mitochondrial activity.[6] Other cell types present enhanced oxidative phosphorylation efficiency promoted by Ca^{2+} in the presence of the complex I substrates pyruvate plus malate and in the presence of α-ketoglutarate.[55] In the matrix, Ca^{2+} stimulates pyruvate-, α-ketoglutarate–, and isocitrate dehydrogenases (to regenerate oxidized NAD+ to NADH and FAD to FADH2) but also complex III of the ETC and the F1/Fo-ATP synthase to accelerate respiration.[56] Therefore, we hypothesized that Ca^{2+} may regulate the increase in mitochondrial function that should be partly directed to ROS production. We can propose that the augmented supply of NADH and FADH are responsible for maintaining a reduced pool of forms of flavin mononucleotide or ubiquinone to pass an electron to O_2 to form $O_2^{\cdot-}$.[13,57]

Spermatozoa have been considered highly susceptible to oxidative stress since as early as 1943. At that time, catalase was shown to protect human sperm from the reduction in motility that occurs when they are incubated under aerobic conditions.[58] In addition, high levels of spontaneous ROS generation have been linked to the defective sperm function that occurs in cases of human infertility.[59] Since then, several ROS sources have been described in sperm cells, including mitochondria, nitric oxide synthase, and oxidases (nicotinamide adenine dinucleotide phosphate [NADPH] oxidase 5 [NOX5] and L-amino acid oxidase).[30]

Mitochondrial ROS formation can be sensed using several approaches that include fluorescent probes and the detection of intra-mitochondrial oxidized targets. In addition, the differential diffusibility of the reactive species makes them detectable inside the mitochondria, outside the organelle, or even outside the cells. To measure sperm ROS production we used a previously published assay[39,60–62] based on the detection of extracellular H_2O_2. The measured H_2O_2 represents the ROS generated by the sperm, but could not reflect the mitochondrial origin. We have overcome this issue by measuring ACO2 as a surrogate of mitochondrial $O_2^{\cdot-}$ production. Through ACO2 we were able to analyze the subcellular source of ROS but also determine the relative amount of $O_2^{\cdot-}$ production by capacitated sperm. Due to the selectivity of $O_2^{\cdot-}$ reactivity toward the Fe-S cluster of aconitase, its activity has become a sensitive assay for measuring the variation in $O_2^{\cdot-}$ levels inside cells and mitochondria in a wide variety of cell types and conditions. Aconitase is also present in the cytosol (ACO1) and functions as the iron-responsive protein-1. Herein we evaluated total aconitase activity but considering that in somatic cells mitochondrial aconitase activity represents approximately 80% of the activity,[63] and spermatic cells lose most of the cytoplasmic proteins, we avoided mitochondrial isolation and following cell lysis and mitochondrial membrane permeabilization, activity was measured and considered as ACO2. Data provided in Figure 3, allowed us to estimate that mitochondria from CAP cells produce almost 60% more $O_2^{\cdot-}$ in steady-state in comparison to NC cells. In addition, western blot analysis revealed that ACO2 is rapidly degraded during capacitation. In somatic cells, the half-life of ACO2 was reported to range from 60 to 500 hours,[64] however, during capacitation, it was significantly shortened to 3.1 ± 4.3 hours ($N = 12$), as shown in Figure 3. We did not explore the mechanisms for the rapid ACO2 degradation but based on what it was reported we speculated that Lon protease is contributing to oxidized-ACO2 proteolysis.[65,66] Nevertheless, other post-translational modifications could not be ruled out. In this regard, decreased ACO2 activity and an increase in sialylation of Asp612 of ACO2 were reported during sperm mouse capacitation.[67] In this report, ACO2 sialylation was postulated as responsible for the metabolic switch from oxidative metabolism to glycolysis during sperm capacitation in mice. Nevertheless, ACO2 activity was only reduced by 20% in that report, and although we could not determine the precise threshold for sperm human ACO2 due to sample limitations, our data support that ACO2 activity should be highly compromised to impact mitochondrial respiration. In addition, other post-translational ACO2 modifications were reported in somatic cells that remained to be explored in sperm cells such as acetylation,[68] tyrosine nitration,[46,69] serine,[70] and tyrosine phosphorylation[71] that might be responsible for changes in activity or half-life of ACO2.

Depending on the formation rate and equilibrium state levels, ROS contributes to signaling events or may mediate mitochondrial dysfunction and pathology through oxidative modifications of mitochondrial or extra-mitochondrial macromolecules. Accordingly, sperm ROS production has been reported to play a dual role in function or dysfunction.[72] When generated in moderate amounts, ROS promotes sperm capacitation by facilitating cholesterol efflux from the plasma

membrane,[73] enhancing cAMP generation,[74] inducing cytoplasmic alkalinization,[75] increasing intracellular calcium levels, and stimulating the protein phosphorylation[61,76] events that drive the attainment of capacitated state.[16,77,78] However, when ROS generation is excessive and/or the antioxidant defenses of the reproductive system are compromised, a state of oxidative stress may be induced that disrupts the fertilizing capacity of the spermatozoa and the structural integrity of their DNA, (reviewed by Aitken et al.[16]). Here, we showed an increase of ROS during capacitation that does not produce sperm damage (there is no change neither in lipid peroxidation nor the complex II activity), suggesting that ROS production is part of a regulated process. Moreover, we have been able to determine and quantify the contribution of mitochondrial $O_2^{\cdot-}$ to capacitated vs. non-capacitated sperm. In this context, we can speculate that the measured increase of $O_2^{\cdot-}$ (nearly 60% more in CAP than NC) is driving the process of capacitation, and it could be considered a threshold that, when exceeded, may produce sperm damage. Still, some potential pitfalls need to be resolved, for instance, which would be the primary signaling targets of mitochondrial $O_2^{\cdot-}$ or H_2O_2 that mediated capacitation events in our conditions. In addition, the question if increasing mitochondrial ROS production that leads to oxidative damage is still capable of acquiring capacitation remains unresolved.

We also must take into account that these experiments have been performed in a population of normozoospermic men and that sperm from men with altered spermiograms may have different behaviors. However, our data have the strength to shed light on quantitative data of mitochondrial ROS linked to capacitation and mitochondrial sperm activity.

In conclusion, the activity of mitochondrial human sperm increases during capacitation, accompanied by an enhancement of mitochondrial $O_2^{\cdot-}$ formation. Moreover, we determined that this increase in mitochondrial ROS production did not lead to oxidative damage, suggesting a role in sperm signaling. Our data underlies the importance of mitochondrial ROS as molecules that control the functional steps of sperm capacitation.

AUTHOR CONTRIBUTIONS

P. Irigoyen performed and analyzed the experiments, including sperm capacitation standardization, respirometry studies, measurement of ROS production, and oxidative stress damage analysis. P. Irigoyen, S. Mansilla, and L. Castro performed and analyzed aconitase experiments. P. Irigoyen and S. Mansilla prepared figures. P. Irigoyen, S. Mansilla, L. Castro, A. Cassina, and R. Sapiro designed the experiments, interpreted the results, and wrote the manuscript. All the authors edited, revised, and approved the final version of the manuscript. A. Cassina and R. Sapiro should be considered joint senior authors.

ACKNOWLEDGMENTS

Financial support for this work was received from Comisión Sectorial de Investigación Científica (CSIC I+D 2020, ID23), Universidad de la República (UdelaR), CSIC grupos (883455), UdelaR Espacio Interdisciplinario, Centros 2015, UdelaR, Programa de Desarrollo de las Ciencias Básicas (PEDECIBA) to L. Castro, S. Mansilla, Rossana Sapiro and Adriana Cassina. P. Irigoyen and R. Sapiro are supported by UdelaR (I+D, CSIC 2014; I+D, CSIC 2016, Iniciación a la Investigación, CSIC 2019 and FMV_1_2017_1_136490 ANII- Uruguay). P. Irigoyen is supported by PEDECIBA, POS_FMV_2018_1_1007814, and CAP-UdelaR 2020 and 2023. A. Cassina is supported by grants from UdelaR (CSIC_2018, Espacio Interdisciplinario_2021). The figures were illustrated using Biorender.com. Finally, we would like to thank the Reprovita and Fertilab Andrology clinics, especially Andrea Torrents and Paola Carlos, for allowing us access to sperm donors and Paola Rosemberg for technical assistance.

DISCLOSURES

The authors declare no conflicts of interest.

DATA AVAILABILITY STATEMENT

The data that support the findings of this study are available on request from the corresponding author.

ORCID

Pilar Irigoyen https://orcid.org/0000-0002-8400-8274
Santiago Mansilla https://orcid.org/0000-0002-3208-9981
Laura Castro https://orcid.org/0000-0002-5771-7630
Adriana Cassina https://orcid.org/0000-0002-3409-9235
Rossana Sapiro https://orcid.org/0000-0002-9755-9016

REFERENCES

1. Puga Molina LC, Luque GM, Balestrini PA, Marín-Briggiler CI, Romarowski A, Buffone MG. Molecular basis of human sperm capacitation. *Front Cell Dev Biol*. 2018;6:72.
2. Stival C, Puga Molina L d C, Paudel B, Buffone MG, Visconti PE, Krapf D. Sperm capacitation and acrosome reaction in mammalian sperm. *Adv Anat Embryol Cell Biol*. 2016;220:93-106.
3. Austin CR. Observations on the penetration of the sperm in the mammalian egg. *Aust J Sci Res B*. 1951;4(4):581-596.
4. Chang MC. Fertilizing capacity of spermatozoa deposited into the fallopian tubes. *Nature*. 1951;168(4277):697-698.
5. Barbagallo F, La Vignera S, Cannarella R, Aversa A, Calogero AE, Condorelli RA. Evaluation of sperm mitochondrial function: a key organelle for sperm motility. *J Clin Med Res*. 2020;9(2):363.

6. Ferreira JJ, Cassina A, Irigoyen P, et al. Increased mitochondrial activity upon CatSper channel activation is required for mouse sperm capacitation. *Redox Biol*. 2021;48:102176.
7. Giaccagli MM, Gómez-Elías MD, Herzfeld JD, et al. Capacitation-induced mitochondrial activity is required for sperm fertilizing ability in mice by modulating hyperactivation. *Front Cell Dev Biol*. 2021;9:767161.
8. Ferramosca A, Zara V. Bioenergetics of mammalian sperm capacitation. *Biomed Res Int*. 2014;2014:902953.
9. Carrageta DF, Guerra-Carvalho B, Sousa M, et al. Mitochondrial activation and reactive oxygen-species overproduction during sperm capacitation are independent of glucose stimuli. *Antioxidants (Basel)*. 2020;9(8):750.
10. Williams AC, Ford WC. The role of glucose in supporting motility and capacitation in human spermatozoa. *J Androl*. 2001;22(4):680-695.
11. Goodson SG, Qiu Y, Sutton KA, Xie G, Jia W, O'Brien DA. Metabolic substrates exhibit differential effects on functional parameters of mouse sperm capacitation. *Biol Reprod*. 2012;87(3):75.
12. Tourmente M, Sansegundo E, Rial E, Roldan ERS. Capacitation promotes a shift in energy metabolism in murine sperm. *Front Cell Dev Biol*. 2022;10:950979.
13. Murphy MP. How mitochondria produce reactive oxygen species. *Biochem J*. 2009;417(1):1-13.
14. Kuznetsov AV, Margreiter R, Ausserlechner MJ, Hagenbuchner J. The complex interplay between mitochondria, ROS, and entire cellular metabolism. *Antioxidants (Basel)*. 2022;11(10):1995.
15. Quijano C, Trujillo M, Castro L, Trostchansky A. Interplay between oxidant species and energy metabolism. *Redox Biol*. 2016;8:28-42.
16. Aitken RJ, Drevet JR, Moazamian A, Gharagozloo P. Male infertility and oxidative stress: a focus on the underlying mechanisms. *Antioxidants (Basel)*. 2022;11(2):306.
17. Agarwal A, Mulgund A, Sharma R, Sabanegh E. Mechanisms of Oligozoospermia: an oxidative stress perspective. *Syst Biol Reprod Med*. 2014;60(4):206-216.
18. Aitken RJ, Lewis SEM. DNA damage in testicular germ cells and spermatozoa. When and how is it induced? How should we measure it? What does it mean? *Andrology*. 2023;11(8):1545-1557.
19. Aitken RJ. Reactive oxygen species as mediators of sperm capacitation and pathological damage. *Mol Reprod Dev*. 2017;84(10):1039-1052.
20. Aitken RJ, Smith TB, Jobling MS, Baker MA, De Iuliis GN. Oxidative stress and male reproductive health. *Asian J Androl*. 2014;16(1):31-38.
21. Castellini C, D'Andrea S, Cordeschi G, et al. Pathophysiology of mitochondrial dysfunction in human spermatozoa: focus on energetic metabolism, oxidative stress and apoptosis. *Antioxidants (Basel)*. 2021;10(5):695.
22. Costa J, Braga PC, Rebelo I, Oliveira PF, Alves MG. Mitochondria quality control and male fertility. *Biology*. 2023;12(6): 827.
23. Bisht S, Faiq M, Tolahunase M, Dada R. Oxidative stress and male infertility. *Nat Rev Urol*. 2017;14(8):470-485.
24. Cassina A, Silveira P, Cantu L, Montes JM, Radi R, Sapiro R. Defective human sperm cells are associated with mitochondrial dysfunction and oxidant production. *Biol Reprod*. 2015;93(5):119.
25. Henkel R, Kierspel E, Stalf T, et al. Effect of reactive oxygen species produced by spermatozoa and leukocytes on sperm functions in non-Leukocytospermic patients. *Fertil Steril*. 2005;83(3):635-642.
26. Baumber J, Vo A, Sabeur K, Ball BA. Generation of reactive oxygen species by equine neutrophils and their effect on motility of equine spermatozoa. *Theriogenology*. 2002;57(3):1025-1033.
27. Aziz N, Agarwal A, Lewis-Jones I, Sharma RK, Thomas AJ. Novel associations between specific sperm morphological defects and Leukocytospermia. *Fertil Steril*. 2004;82(3):621-627.
28. Bánfi B, Molnár G, Maturana A, et al. A Ca^{2+}-activated NADPH oxidase in testis, spleen, and lymph nodes. *J Biol Chem*. 2001;276(40):37594-37601.
29. Miguel-Jiménez S, Pina-Beltrán B, Gimeno-Martos S, Carvajal-Serna M, Casao A, Pérez-Pe R. NADPH oxidase 5 and melatonin: involvement in ram sperm capacitation. *Front Cell Dev Biol*. 2021;9:655794.
30. Musset B, Clark RA, DeCoursey TE, et al. NOX5 in human spermatozoa: expression, function, and regulation. *J Biol Chem*. 2012;287(12):9376-9388.
31. World Health Organization. *WHO Laboratory Manual for the Examination and Processing of Human Semen*. World Health Organization; 2021.
32. World Health Organization. *WHO Laboratory Manual for the Examination and Processing of Human Semen*. World Health Organization; 2010.
33. Marín-Briggiler CI, Luque GM, Gervasi MG, et al. Human sperm remain motile after a temporary energy restriction but do not undergo capacitation-related events. *Front Cell Dev Biol*. 2021;9:777086.
34. Koppers AJ, De Iuliis GN, Finnie JM, McLaughlin EA, Aitken RJ. Significance of mitochondrial reactive oxygen species in the generation of oxidative stress in spermatozoa. *J Clin Endocrinol Metab*. 2008;93(8):3199-3207.
35. Bradford MM. A rapid and sensitive method for the quantitation of microgram quantities of protein utilizing the principle of protein-dye binding. *Anal Biochem*. 1976;72:248-254.
36. Irigoyen P, Sapiro R, Cassina A. High-resolution respirometry to assess mitochondrial function in human spermatozoa. *J Vis Exp*. 2023;(196). doi:10.3791/65493
37. Brand MD, Nicholls DG. Assessing mitochondrial dysfunction in cells. *Biochem J*. 2011;435(2):297-312.
38. Scandroglio F, Tórtora V, Radi R, Castro L. Metabolic control analysis of mitochondrial aconitase: influence over respiration and mitochondrial superoxide and hydrogen peroxide production. *Free Radic Res*. 2014;48(6):684-693.
39. Irigoyen P, Pintos-Polasky P, Rosa-Villagran L, Skowronek MF, Cassina A, Sapiro R. Mitochondrial metabolism determines the functional status of human sperm and correlates with semen parameters. *Front Cell Dev Biol*. 2022;10:926684.
40. Hausladen A, Fridovich I. Measuring nitric oxide and superoxide: rate constants for aconitase reactivity. *Methods Enzymol*. 1996;269:37-41.
41. Rivlin J, Mendel J, Rubinstein S, Etkovitz N, Breitbart H. Role of hydrogen peroxide in sperm capacitation and acrosome reaction. *Biol Reprod*. 2004;70(2):518-522.
42. Griveau JF, Renard P, Le Lannou D. An in vitro promoting role for hydrogen peroxide in human sperm capacitation. *Int J Androl*. 1994;17(6):300-307.

43. O'Flaherty C. Redox regulation of mammalian sperm capacitation. *Asian J Androl*. 2015;17(4):583-590.
44. Walters JLH, De Iuliis GN, Nixon B, Bromfield EG. Oxidative stress in the male germline: a review of novel strategies to reduce 4-Hydroxynonenal production. *Antioxidants (Basel)*. 2018;7(10):132.
45. Gardner PR. Aconitase: sensitive target and measure of superoxide. *Methods Enzymol*. 2002;349:9-23.
46. Tórtora V, Quijano C, Freeman B, Radi R, Castro L. Mitochondrial aconitase reaction with nitric oxide, S-nitrosoglutathione, and peroxynitrite: mechanisms and relative contributions to aconitase inactivation. *Free Radic Biol Med*. 2007;42(7):1075-1088.
47. Castro L, Demicheli V, Tórtora V, Radi R. Mitochondrial protein tyrosine nitration. *Free Radic Res*. 2011;45(1):37-52.
48. Austin CR. The 'capacitation' of the mammalian sperm. *Nature*. 1952;170:326.
49. Boguenet M, Bouet P-E, Spiers A, Reynier P, May-Panloup P. Mitochondria: their role in spermatozoa and in male infertility. *Hum Reprod Update*. 2021;27(4):697-719.
50. Marchetti P, Ballot C, Jouy N, Thomas P, Marchetti C. Influence of mitochondrial membrane potential of spermatozoa on in vitro fertilisation outcome. *Andrologia*. 2012;44(2):136-141.
51. Gallon F, Marchetti C, Jouy N, Marchetti P. The functionality of mitochondria differentiates human spermatozoa with high and low fertilizing capability. *Fertil Steril*. 2006;86(5):1526-1530.
52. Wang H, Dou Q, Jeong KJ, Choi J, Gladyshev VN, Chung J-J. Redox regulation by TXNRD3 during epididymal maturation underlies capacitation-associated mitochondrial activity and sperm motility in mice. *J Biol Chem*. 2022;298(7):102077.
53. Leung MR, Chiozzi RZ, Roelofs MC, et al. In-cell structures of conserved supramolecular protein arrays at the mitochondria–cytoskeleton Interface in mammalian sperm. *Proc Natl Acad Sci*. 2021;118(45):e2110996118.
54. Otani H, Tanaka O, Kasai K, Yoshioka T. Development of mitochondrial helical sheath in the middle piece of the mouse spermatid tail: regular dispositions and synchronized changes. *Anat Rec*. 1988;222(1):26-33.
55. Vilas-Boas EA, Cabral-Costa JV, Ramos VM, Caldeira da Silva CC, Kowaltowski AJ. Goldilocks calcium concentrations and the regulation of oxidative phosphorylation: too much, too little, or just right. *J Biol Chem*. 2023;299(3):102904.
56. Glancy B, Balaban RS. Role of mitochondrial Ca^{2+} in the regulation of cellular energetics. *Biochemistry*. 2012;51(14):2959-2973.
57. Wong H-S, Dighe PA, Mezera V, Monternier P-A, Brand MD. Production of superoxide and hydrogen peroxide from specific mitochondrial sites under different bioenergetic conditions. *J Biol Chem*. 2017;292(41):16804-16809.
58. MacLeod J. The Rôle of oxygen in the metabolism and motility of human spermatozoa. *Am J Phys*. 1943;138(3):512-518.
59. Aitken RJ, Clarkson JS. Cellular basis of defective sperm function and its association with the genesis of reactive oxygen species by human spermatozoa. *J Reprod Fertil*. 1987;81(2):459-469.
60. Richer SC, Ford WC. A critical investigation of NADPH oxidase activity in human spermatozoa. *Mol Hum Reprod*. 2001;7(3):237-244.
61. Baumber J, Sabeur K, Vo A, Ball BA. Reactive oxygen species promote tyrosine phosphorylation and capacitation in equine spermatozoa. *Theriogenology*. 2003;60(7):1239-1247.
62. Yánez-Ortiz I, Catalán J, Mateo-Otero Y, et al. Extracellular reactive oxygen species (ROS) production in fresh donkey sperm exposed to reductive stress, oxidative stress and NETosis. *Antioxidants (Basel)*. 2021;10(9):1367.
63. Condò I, Malisan F, Guccini I, Serio D, Rufini A, Testi R. Molecular control of the cytosolic aconitase/IRP1 switch by extramitochondrial frataxin. *Hum Mol Genet*. 2010;19(7):1221-1229.
64. Mathieson T, Franken H, Kosinski J, et al. Systematic analysis of protein turnover in primary cells. *Nat Commun*. 2018;9(1):689.
65. Delaval E, Perichon M, Friguet B. Age-related impairment of mitochondrial matrix aconitase and ATP-stimulated protease in rat liver and heart. *Eur J Biochem*. 2004;271(22):4559-4564.
66. Bota DA, Davies KJA. Lon protease preferentially degrades oxidized mitochondrial aconitase by an ATP-stimulated mechanism. *Nat Cell Biol*. 2002;4(9):674-680.
67. Silva Balbin Villaverde AI, Ogle RA, Lewis P, et al. Sialylation of asparagine 612 inhibits aconitase activity during mouse sperm capacitation; a possible mechanism for the switch from oxidative phosphorylation to glycolysis. *Mol Cell Proteomics*. 2020;19(11):1860-1875.
68. Kosanam H, Thai K, Zhang Y, et al. Diabetes induces lysine acetylation of intermediary metabolism enzymes in the kidney. *Diabetes*. 2014;63(7):2432-2439.
69. Han D, Canali R, Garcia J, Aguilera R, Gallaher TK, Cadenas E. Sites and mechanisms of aconitase inactivation by peroxynitrite: modulation by citrate and glutathione. *Biochemistry*. 2005;44(36):11986-11996.
70. Lin G, Brownsey RW, MacLeod KM. Regulation of mitochondrial aconitase by phosphorylation in diabetic rat heart. *Cell Mol Life Sci*. 2009;66(5):919-932.
71. Taddei ML, Pardella E, Pranzini E, Raugei G, Paoli P. Role of tyrosine phosphorylation in modulating cancer cell metabolism. *Biochim Biophys Acta Rev Cancer*. 2020;1874(2):188442.
72. Aitken RJ, Drevet JR. The importance of oxidative stress in determining the functionality of mammalian spermatozoa: a two-edged sword. *Antioxidants (Basel)*. 2020;9(2):111.
73. Boerke A, Brouwers JF, Olkkonen VM, et al. Involvement of bicarbonate-induced radical signaling in oxysterol formation and sterol depletion of capacitating mammalian sperm during in vitro fertilization. *Biol Reprod*. 2013;88(1):21.
74. Aitken RJ, Harkiss D, Knox W, Paterson M, Irvine DS. A novel signal transduction cascade in capacitating human spermatozoa characterised by a redox-regulated, cAMP-mediated induction of tyrosine phosphorylation. *J Cell Sci*. 1998;111(Pt 5):645-656.
75. Ecroyd HW, Jones RC, Aitken RJ. Endogenous redox activity in mouse spermatozoa and its role in regulating the tyrosine phosphorylation events associated with sperm capacitation. *Biol Reprod*. 2003;69(1):347-354.
76. Aitken RJ, Paterson M, Fisher H, Buckingham DW, van Duin M. Redox regulation of tyrosine phosphorylation in human spermatozoa and its role in the control of human sperm function. *J Cell Sci*. 1995;108(Pt 5):2017-2025.

77. de Lamirande E, Jiang H, Zini A, Kodama H, Gagnon C. Reactive oxygen species and sperm physiology. *Rev Reprod*. 1997;2(1):48-54.
78. Ford WCL. Regulation of sperm function by reactive oxygen species. *Hum Reprod Update*. 2004;10(5):387-399.

SUPPORTING INFORMATION

Additional supporting information can be found online in the Supporting Information section at the end of this article.

How to cite this article: Irigoyen P, Mansilla S, Castro L, Cassina A, Sapiro R. Mitochondrial function and reactive oxygen species production during human sperm capacitation: Unraveling key players. *The FASEB Journal*. 2024;38:e23486. doi:10.1096/fj.202301957RR

Supplementary Table 1. Characteristics of normozoospermic participants' age and sperm parameters. Data were from the first spermiogram of 112 individuals who attended the andrology clinic. Max = maximum value. Min = minimum value. ǂ WHO 2021 reference values.

Parameter	Mean	SD	Median	Max	Min	ǂ Reference limit
Age (yr)	35	7	35	55	20	-
Volume (mL)	3.7	1.3	3.5	9.0	1.5	> 1.4
Sperm concentration (million/mL)	74	52	62	416	15	> 15
Sperm vitality (%)	90	6	92	99	66	> 54
Normal sperm morphology (%)	9	3	9	15	4	> 4
Progressive motility (a+b) (%)	62	11	64	93	32	> 30
Round cells (million/mL)	0.3	0.3	0.2	1	0.1	< 1

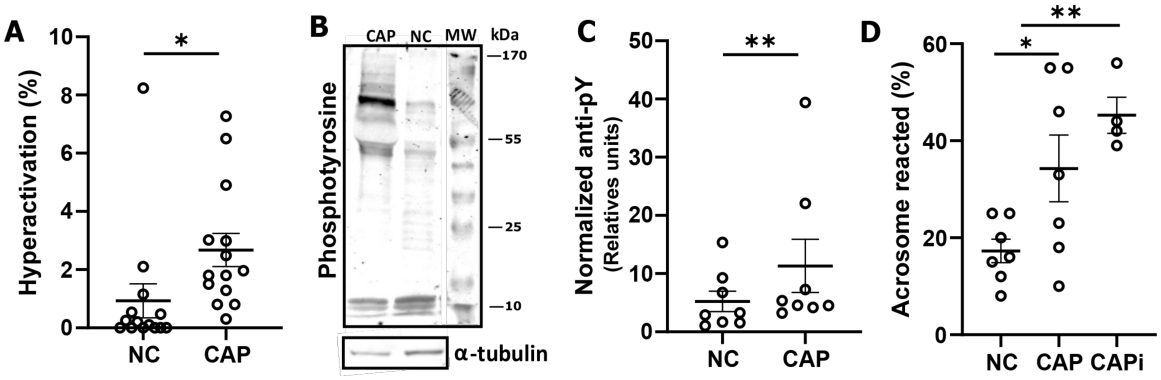

Supplementary Figure 1. Incubation for 240 min in BWW medium supplemented with 25 mM HCO_3^- and 3 mg/mL BSA capacitates human sperm. Comparison of capacitation-related events between incubation for 0 min (NC) and 240 min (CAP). **A.** Hyperactivated sperm (N = 14) measured by CASA system. **B.** Representative western blot for tyrosine phosphorylated proteins. **C.** Protein levels of anti-phosphotyrosine (pY) normalized to tubulin (loading control) detected in independent western blot (N = 8). **D**. Acrosome reaction spontaneous or induced by 10 µM progesterone (CAPi) by PSA-FITC in microscopy (N = 7). Results are expressed as mean ± SEM. *$p < 0.05$ and **$p < 0.01$.

Supplementary Table 2. Parameters and main respiratory indices obtained by HRR traces from non-capacitated (NC) and capacitated (CAP) human sperm. Respiration parameters were measured and calculated as indicated under the "Material and Methods" section. Basal respiration corresponded to oxygen consumption in the presence of exogenous substrates. Proton leak corresponded to oligomycin-resistant respiration. ATP turnover is the subtraction between basal and proton leak respiration Maximum respiratory rate was obtained after dissipation of the proton gradient by FCCP. Non-mitochondrial respiration was defined as the oxygen consumption after the addition of AA. The calculated indices were calculated from parameters: RCR = maximum respiratory rate/proton leak, coupling efficiency = (basal respiration - proton leak) / basal respiration, and spare respiratory capacity = maximum respiratory rate / basal respiration. N = number of donors. Max = maximum value. Min = minimum value. SD = standard deviation. *p < 0.05, **p < 0.01 and ***p < 0.001.

	N	Mean		Min		Max		SD		p-value
Parameters (pmol O_2 * sec^{-1} *mL^{-1} * 10^{-6} cells)		**NC**	**CAP**	**NC**	**CAP**	**NC**	**CAP**	**NC**	**CAP**	
Basal respiration	19	0.46	0.34	0.12	0.15	1.12	0.69	0.29	0.14	0.1042
Proton leak		0.27	0.18	0.06	0.04	0.93	0.36	0.21	0.09	0.1819
ATP turnover		0.21	0.16	0.04	0.03	0.59	0.37	0.16	0.08	0.1688
Maximum respiratory rate		0.63	0.62	0.17	0.20	1.64	1.25	0.42	0.27	> 0.9999
Non-mitochondrial respiration		0.14	0.29	0.02	0.01	0.48	0.95	0.13	0.28	0.0297 *
Indices										
RCR		2.63	3.65	1.50	1.78	4.11	7.71	0.75	1.40	0.0020 **
Coupling efficiency		0.45	0.46	0.16	0.11	0.61	0.77	0.14	0.16	0.5949
Spare respiratory capacity		1.38	1.86	0.98	1.11	1.94	4.02	0.26	0.68	0.0002 ***

5.3. Desarrollar nuevas herramientas enfocadas en el estudio de la función mitocondrial y la producción de ROS para mejorar el diagnóstico del hombre infértil

Artículo 1: Mitochondrial metabolism determines the functional status of human sperm and correlates with semen parameters.

Pilar Irigoyen, Paula Pintos-Polasky, Lucia Rosa-Villagran, Maria Fernanda Skowronek, Adriana Cassina* y Rossana Sapiro*.
*Ambas autoras comparten la última autoría.
Frontiers in Cell and Developmental Biology 10.926684. DOI: 10.3389/fcell.2022.926684

El objetivo del trabajo fue investigar cómo el metabolismo mitocondrial afecta la función de los espermatozoides humanos y su correlación con los parámetros del espermograma clásico. Analizamos 339 muestras de semen (NC) de donantes con espermogramas variados, normales y alterados utilizando técnicas no tradicionales. Evaluamos la función mitocondrial mediante HRR donde obtuvimos el RCR y la producción de H_2O_2 extracelular ($[H_2O_2]$) mediante la sonda Amplex Red. Además, medimos la capacidad antioxidante del PS utilizando el ensayo de naranja férrico-xilenol (FOX). En primera instancia, observamos que al inhibir la función mitocondrial los espermatozoides disminuyen su motilidad. Además, aquellos pacientes con un espermograma alterado mostraron anormalidades en la estructura de su mitocondria y la pieza intermedia mediante microscopía electrónica. Por tanto, la motilidad y la morfología se encuentran relacionadas con la función y estructura mitocondrial. La motilidad progresiva se correlacionó positivamente con el RCR, la capacidad antioxidante del PS y negativo con $[H_2O_2]$. La morfología normal se correlacionó positivamente con el RCR y negativamente con $[H_2O_2]$, pero no mostró correlación con la capacidad antioxidante del PS. Determinamos la capacidad diagnóstica de los tres métodos utilizando curvas ROC (Receiver Operating Characteristic). Para identificar entre muestras normozoospérmicas y de espermograma alterado, se definió un valor de corte para el RCR de 3.2 con una sensibilidad del 73% y una especificidad de 61%. Para $[H_2O_2]$ el valor de corte fue de 0.2 $\mu M/10^6$ espermatozoides con una sensibilidad del 65% y especificidad del 60%. Esto no fue posible calcular para la capacidad antioxidante del PS ya que no fue capaz de discriminar. Por tanto, nuestros resultados mostraron que el metabolismo mitocondrial es un determinante clave del estado funcional de los espermatozoides. Las alteraciones en la función mitocondrial y el aumento en la producción de H_2O_2 están estrechamente vinculadas con parámetros alterados del semen, sugiriendo que tratamientos que mejoren la función del organelo tendrían un impacto positivo en la fertilidad masculina. Los métodos establecidos durante el trabajo podrían mejorar el análisis de rutina del semen de aquellos pacientes que presentan una infertilidad hoy diagnosticada como idiopática.

Artículo 2: High-Resolution Respirometry to Assess Mitochondrial Function in Human Sperm.

Pilar Irigoyen, Rossana Sapiro y Adriana Cassina.
Jove Journal (196) e65493. DOI: 10.3791/65493

El objetivo del trabajo fue publicar el método para medir la función mitocondrial utilizando el HRR en espermatozoides humanos. Se trata de un método que nos permite medir con una gran sensibilidad el consumo de oxígeno en tiempo real, antes y después de la adición de

moduladores de la función mitocondrial. Los datos de consumo de oxígeno obtenidos mediante el software asociado a los sensores nos permite calcular índices respiratorios indicadores de la función y disfunción del organelo. Esta técnica puede utilizarse tanto en espermatozoides intactos, donde las mitocondrias están presentes en un entorno fisiológico, como en espermatozoides permeabilizados, permitiendo medir actividad de los complejos individuales de la cadena respiratoria (funciona como un subconjunto de mitocondrias aisladas). Frente a otros oxímetros, presenta la ventaja de que los espermatozoides pueden moverse libremente y que al ser en tiempo real, se puede adaptar el método a la heterogeneidad que presentan las muestras humanas. La importancia de los índices respiratorios resultantes radica en que sirven como indicadores de la calidad e integridad de las mitocondrias espermáticas y por tanto, de la función de la célula.

frontiers | Frontiers in Cell and Developmental Biology

TYPE Original Research
PUBLISHED 30 August 2022
DOI 10.3389/fcell.2022.926684

OPEN ACCESS

EDITED BY
Vanina Gabriela Da Ros,
CONICET Instituto de Biología y Medicina Experimental (IBYME), Argentina

REVIEWED BY
Sandra Amaral,
University of Coimbra, Portugal
Clara Isabel Marin-Briggiler,
CONICET Instituto de Biología y Medicina Experimental (IBYME), Argentina

*CORRESPONDENCE
Rossana Sapiro,
rsapiro@fmed.edu.uy

†These authors share seniorship and last authorship

SPECIALTY SECTION
This article was submitted to Molecular and Cellular Reproduction, a section of the journal Frontiers in Cell and Developmental Biology

RECEIVED 22 April 2022
ACCEPTED 08 July 2022
PUBLISHED 30 August 2022

CITATION
Irigoyen P, Pintos-Polasky P, Rosa-Villagran L, Skowronek MF, Cassina A and Sapiro R (2022), Mitochondrial metabolism determines the functional status of human sperm and correlates with semen parameters. *Front. Cell Dev. Biol.* 10:926684. doi: 10.3389/fcell.2022.926684

Mitochondrial metabolism determines the functional status of human sperm and correlates with semen parameters

Pilar Irigoyen[1], Paula Pintos-Polasky[1], Lucia Rosa-Villagran[1], Maria Fernanda Skowronek[1], Adriana Cassina[2,3†] and Rossana Sapiro[1,3*†]

[1]Departamento de Histología y Embriología, Facultad de Medicina, Universidad de la República, Montevideo, Uruguay, [2]Departamento de Bioquímica, Facultad de Medicina, Universidad de la República, Montevideo, Uruguay, [3]Centro de Investigaciones Biomédicas (CEINBIO), Facultad de Medicina, Universidad de la República, Montevideo, Uruguay

The diagnosis of male infertility is based essentially on the patient's medical history and a standard semen analysis. However, the latter rarely provides information on the causes of a possible infertility, emphasizing the need to extend the analysis of the sperm function. Mitochondrial function has been associated with sperm function and dysfunction, the latter primarily through the production of excessive amounts of reactive oxygen species (ROS). We hypothesized that analysis of sperm mitochondrial metabolism together with sperm ROS production could be an additional tool to improve routine semen analysis, after appropriate validations. To test our hypothesis, we performed several experiments using a non-routine method (high-resolution respirometry, HRR) to access mitochondrial function. First, we investigated whether mitochondrial function is related to human sperm motility and morphology. When mitochondrial metabolism was challenged, sperm motility decreased significantly. Additionally, morphological abnormalities in the sperm mid-piece and mitochondria were associated with global sperm defects evaluated by routine methods. Subsequently, sperm mitochondrial function was assessed by HRR. Respiratory control ratio (RCR) was determined and evaluated in the context of classical sperm analysis. In parallel, sperm hydrogen peroxide (H_2O_2) production and seminal plasma (SP) antioxidant capacity were measured. The percentage of sperm with progressive motility correlated positively with RCR, SP antioxidant capacity, and negatively with the concentration of extracellular H_2O_2 production ([H_2O_2]). The percentage of normal sperm morphology correlated positively with RCR and negatively with [H_2O_2]. Sperm morphology did not correlate with seminal plasma antioxidant capacity. Furthermore, Receiver Operating Characteristic curves were used for the first time to test the diagnostic ability of RCR, [H_2O_2], and SP antioxidant capacity as binary classifiers. An RCR cut off value of 3.2 was established with a sensitivity of 73% and a specificity of 61%, using reference values considered normal or abnormal in routine semen analysis. The cut off value for [H_2O_2] was 0.2 μM/10^6 sperm (sensitivity = 65%, specificity = 60%). There were no reference values for SP

antioxidant capacity that distinguished between abnormal and normal sperm samples. We conclude that sperm mitochondrial function indices in combination with [H_2O_2] may be useful tools to complement the routine semen analysis.

KEYWORDS

mitochondria, sperm metabolism, antioxidant status, respirometry assay, reactive oxygen species, male fertility

Introduction

Infertility is a growing problem worldwide, affecting up to 15% of couples of childbearing age (Vander Borght and Wyns, 2018). Although the male factor is responsible for at least 30–40% of cases, the male contribution to infertility among couples has not traditionally been emphasized (Barratt et al., 2018; De Jonge and Barratt, 2019). Male infertility diagnosis is mainly based on the patient's clinical history, clinical examination, and the analysis of standard semen parameters according to the World Health Organization guidelines, which rarely determines the causes or point to possible treatments (WHO, 2010; WHO, 2021; Barratt et al., 2022; Björndahl and Kirkman Brown, 2022). In some cases of male infertility altered parameters in the spermiogram have been detected during semen analysis, but even when endocrine, genetic, and biochemical laboratory tests are added to the male examination (Kliesch, 2014), no cause associated with male infertility is found. These cases are considered as idiopathic and may account for 30–40% of male infertility (Kliesch, 2014). This situation severely limits treatment strategies to rescue fertility, so the inclusion of laboratory advanced tests to the routine semen analysis may assist in accurately diagnosis of male infertility (Agarwal and Bui, 2017).

There are numerous data showing a correlation between semen parameters and both, mitochondrial morphology and function (Wilton et al., 1992; Gopalkrishnan et al., 1995; Mundy et al., 1995; Courtade et al., 1998; Marchetti et al., 2002; Gallon et al., 2006; Amaral and Ramalho-Santos, 2010; Pelliccione et al., 2011; Cassina et al., 2015; Uribe et al., 2017; Durairajanayagam et al., 2021; Tanga et al., 2021). Furthermore, fertilization rate might be related to the proportion of normal mitochondrial structure (Baccetti et al., 2002) and mitochondrial function has been associated to the ability of spermatozoa to fertilize oocytes in mice (Ferreira et al., 2021; Giaccagli et al., 2021) and in humans (Kasai et al., 2002; Malić Vončina et al., 2016; Boguenet et al., 2021).

Despite the large body of data pointing to the importance of mitochondria in sperm function, the mechanisms by which this organelle operates in the male gamete are not fully understood, mainly in what concerns metabolic aspects. Specifically, in many species, including mice (Miki et al., 2004; Mukai and Okuno 2004; Castellini et al., 2021) and humans (Nascimento et al., 2008), is claimed that glycolysis would be used as a preferential pathway to synthesize ATP for maintaining sperm motility. Yet, we and others have previously shown that mitochondrial function is associated to sperm motility in men (Marchetti et al., 2002; Gallon et al., 2006; Amaral and Ramalho-Santos, 2010; Cassina et al., 2015; Uribe et al., 2017), and that coupling efficiency (that reflects the ability to produce mitochondrial ATP) is associated to the cell's ability to fertilize in mice (Ferreira et al., 2021). All in all, previous result, obtained independently, suggest that ATP produced by mitochondria can make an important contribution to sperm function. When producing ATP, in analogy to somatic cells, sperm mitochondria are the major source of reactive oxygen species (ROS) (Aitken et al., 2012b; Cassina et al., 2015). During cellular respiration, approximately 0.2% of the oxygen consumed is converted to superoxide anions through electron leakage from the mitochondrial electron transport chain (Boveris and Chance, 1973; Nohl et al., 2003; Quijano et al., 2007). In the mitochondrial matrix and intermembrane space, superoxide interacts with the antioxidant enzyme superoxide dismutase, which catalyzes the dismutation of superoxide to hydrogen peroxide (H_2O_2) (Messner and Imlay, 2002; Wang et al., 2018). The H_2O_2 diffuses through biological membranes and can be measured in the extracellular space (Cardoso et al., 2012; Wang et al., 2018). The $O_2^{\bullet-}$ reacts quickly with NO to form peroxynitrite. Low levels of $O_2^{\bullet-}$, H_2O_2 and peroxynitrite, modulate cellular functions, but when they are produced in excess cause nitro-oxidative damage (Quijano et al., 2007). Nitro-oxidative stress is associated with altered semen parameters and abnormalities in the process of fertilization and pregnancy (Twigg et al., 1998; Agarwal et al., 2014a; Walters et al., 2020). In addition, mitochondrial dysfunction is associated with an increase in nitro-oxidative damage in sperm and a decrease in sperm motility (Cassina et al., 2015).

Sperm lose most of their cytoplasm and its organelles during differentiation, including some of the cell's antioxidant defenses. It is postulated that the lack of antioxidant enzymes in spermatozoa is compensated by a high antioxidant capacity of seminal plasma (SP) (Agarwal and Deepinder, 2009). However, in clinical practice, neither ROS nor SP antioxidant capacity are usually tested (Agarwal et al., 2021a; 2021b). This may be because there is no consensus on appropriate tests and their clinically relevant cut off values, as well as an absence of standardization of laboratory techniques (Roychoudhury et al., 2016; Agarwal et al., 2021a, 2021b).

Considering the available information, we hypothesized that the analysis of sperm metabolic status and mitochondrial ROS production could provide additional information to complement routine semen evaluation. To prove our hypothesis, we analyzed sperm mitochondrial function using high-resolution respirometry (HRR) in the context of the routine semen analysis. Also, we standardized an assay to measure sperm H_2O_2 production and the antioxidant capacity of SP. We found some cut off values of mitochondrial function and H_2O_2 production that reflect the reference values of semen parameters established by World Health Organization (WHO). These tests could eventually be integrated into the andrology clinic after proper validation.

Material and methods

Reagents and media

Chemicals (unless otherwise indicated) were purchased from Sigma-Aldrich Chemical Co. (St. Louis, MO, United States).

Selection of subjects and ethical guidelines

For this study, men who presented to the Fertilab andrology clinic (Montevideo, Uruguay) for semen testing were recruited. Recruitment was twice weekly, from August 2018 to December 2021. Unless otherwise stated, samples for the different studies were randomly selected (see below).

Clinical examination of patients and diagnostic semen analysis were performed at the andrology clinic according to the methods of WHO (WHO, 2010). Samples were discarded if they had a white blood cell count >0.5 × 10^6/ml or leukocytospermia (WHO, 2010). Sperm cultures were negative for microorganisms. Men who had presented to the clinic for examination as sperm donors (e.g., semen donors for assisted reproduction procedures), that had genital tract infections, varicocele or control after vasectomy were excluded from the study. Not all men were tested for chromosomal, genetic or hormonal anomalies. None of these criteria constituted exclusion criteria.

A total of 339 men who met the inclusion criteria were finally enrolled in this study and randomly distributed as follows: 17 normozoospermic men were included in motility studies and ATP measurements only, 48 semen samples showing different semen parameters were selected for microscopic morphometric analysis. Between them, 5 normozoospermic healthy men who had conceived at least one child at the time of the study and 7 infertile patients were selected for electron microscopic analysis. Inclusion criteria for classifying a man as infertile were: A clinical history of infertility diagnosed as idiopathic (with abnormal spermiogram) and the absence of a female factor in the couple.

The remaining 274 samples were divided into two fractions to analyze HRR and sperm H_2O_2 production when the number of cells was sufficient. Ninety-five SP (considering a wide range of motility and morphology) of these samples were reserved for measuring their antioxidant capacity. The classification criteria for the samples are shown in Supplementary Figure S1. This categorization of samples was independent of fertility status.

The Ethics Committee of the Facultad de Medicina de la Universidad de la República Montevideo, Uruguay approved the experimental protocol. Before sample collection, all participants signed an informed consent form. The laboratory personnel assured the anonymity of the participants without the involvement of the researchers.

Semen evaluation

Semen samples were obtained after 3 days of sexual abstinence by masturbation in special sterile containers. After liquefaction at room temperature for 30 min, semen volume, viability, pH, and normal morphology were analyzed according to the WHO guidelines.

Two sperm counting chambers CELL -VU® (Millennium Sciences, Inc., New York, United States) were loaded, and ten different fields per chamber were randomly examined using a Nikon microscope at 37°C. Concentration and motility parameters were analyzed using an SCA-Microoptics automated analyzer (CASA) (Barcelona, Spain) with default settings according to WHO criteria (WHO, 2010).

Preparation of the samples

Liquefied samples were centrifuged at 400 g for 10 min at room temperature to separate sperm from SP. If a subsequent washing step was included is described below. The SP was aliquoted and frozen at −80°C. Sperm were suspended in either of the following media: Biggers Whitten Whittingham medium (BWW: 95 mM NaCl, 4.6 mM KCl, 1.7 mM $CaCl_2$, 1.2 mM KH_2PO_4, 1.2 mM $MgSO_4$, 5.6 mM glucose, 0.27 mM sodium pyruvate, 20 mM acid-free HEPES, 25 mM $NaHCO_3$, 44 mM lactic acid and 0.3% BSA, pH 7.4) for motility, morphology and respiratory experiments (Koppers et al., 2008), HAM-F10 medium (126 mM NaCl, 3.8 mM KCl, 1.08 mM NaH_2PO_4, 0.6 mM $MgSO_4.7H_2O$, 0.3 mM $CaCl_2$, 6 mM glucose, 20 mM HEPES and 6 mM NaHCO, pH 7.4) for [H_2O_2] measurement or mitochondrial respiration medium (MRM: 0.1% BSA, 5 mM KH_2PO_4, 1 mM EGTA, 5 mM MOPS and 300 mM sucrose, pH 7.4) for motility studies and ATP analysis.

Motility studies on the modulation of glycolysis and mitochondrial respiration

Sperm cells (35×10^6) were suspended in 1,500 µL MRM and divided into seven aliquots. Aliquots were incubated at 37°C with: 1) 0.5% ethanol (OH), 2) 25 mM sodium oxamate (OXA) 3) 100 mM 2-deoxy-D-glucose (2DG), 4) 2.5 µM of antimycin A (AA), 5) 5 µM carbonil cyanide- p-(tri-flouromethoxy) phenyl-hydrazone (FCCP), 6) 25 mM OXA and 2.5 µM AA, 7) 100 mM 2DG and 2.5 µM AA. After 30 min, motility was analyzed using CASA. Aliquots were then centrifuged at 500 g for 10 min. Pellets were resuspended in 500 µL BWW and incubated at 37°C for 180 min, and sperm motility was measured. This study was performed on 11 normozoospermic men.

ATP detection

ATP content was determined using a commercial kit (Cat #700410; Cayman Chemical, Ann Arbor, MI, United States). Spermatozoa (1×10^6) from 6 normozoospermic males were incubated at 37°C for 30 min in MRM with the same drugs used in the motility studies (OH, OXA, 2DG, AA, FCCP, OXA + AA, and 2DG + AA). The medium was removed by centrifugation (600 g for 10 min), and the sperm pellet was washed twice with PBS at 4°C. Spermatozoa were resuspended in 100 µL of ATP detection sample buffer (1X) at 4°C, homogenized by repeated pipetting, and stored at −20°C until use. On the day of measurement, samples were thawed, diluted 1:10 with ATP detection sample buffer (1X), and stored on ice. ATP detection standards were prepared and the assay was performed according to the manufacturer's instructions. The luminescence signal was recorded using a luminometer plate reader (Lumistar Galaxy, BMG, LabTech). Each measurement was performed twice.

Fluorescence evaluation of sperm mitochondrial morphology

Sperm cells from 36 sperm samples were incubated with 50 nM MitoTracker® Red CMXRos - M7512 - (Invitrogen, Waltham, Massachusetts, United States) for 30 min at 37°C in BWW and then spread on a glass slide. The slides were fixed in a mixed solution of 4% w/v paraformaldehyde in 0.1 M phosphate buffer (PB) for 30 min and washed three times in PBS. Sperm nuclei were counterstained with DAPI (4′,6-diamidine-2′-phenylindole dihydrochloride). Slides were mounted and observed using a Nikon Eclipse E400 epifluorescent microscope with a 100X, 1.4 NA oil objective (excitation: λ = 488 nm and λ = 543 nm). Digital images of 50–80 spermatozoa from each individual were acquired and processed. Manual segmentation of sperm intermediate pieces was performed from the MitoTracker channel images using ImageJ/FIJI (Schindelin et al., 2012). Areas of interest (ROI) were defined semi-automatically. Only isolated and well-defined midsections were included in the analysis (Figure 2A). Width, length, and circumference were automatically calculated for each ROI. The mean ± standard error (SE) was calculated for each sample.

Electron microscopy

Semen from 5 fertile control men and 7 infertile men was analyzed by transmission electron microscopy (TEM). After liquefaction, the semen samples were centrifuged at 400g, the supernatant was discarded, and the pellets were fixed in a mixed solution of 4% w/v paraformaldehyde in 0.1 M PB containing 2.5% v/v glutaraldehyde (pH 7.4). Each preparation was then rinsed in PB (pH 7.4), post-fixed in 1% osmium tetroxide (w/v) for 1 h, dehydrated, and embedded in Araldite resin. After polymerization at 58–60°C for 48 h, sections were made on an RMC MT -X ultramicrotome using a DIATOME diamond knife. Semi-thin sections were prepared, stained with toluidine blue 1% w/v and examined under a Nikon ECLIPSE E200 light microscope. Adjacent ultrathin sections (50–70 nm) were stained with uranyl acetate followed by lead citrate and examined using a JEOL JEM-1010 transmission electron microscope at 80 kV accelerating voltage. Images were captured with a Hamamatsu C-4742-95 digital camera and processed with Photoimpact® (Skowronek et al., 2012).

Evaluation of sperm respiration control ratio by high-resolution respirometry

We analyzed mitochondrial function of spermatozoa from 171 men as previously described (Cassina et al., 2015). Oxygen consumption rate (OCR) of 30×10^6 sperm resuspended in BWW was measured by high-resolution respirometry. HRR integrates highly sensitive oxygraphs (Oxygraph-2 K; Oroboros Instruments GmbH, Innsbruck, Austria) with software (DatLab, version 4.2; Oroboros Instruments GmbH) that displays respiration in terms of oxygen flux (pmol $O_2/1 \times 10^6$ cells/sec). For all experiments, the stirrer speed was set to 750 rpm and the temperature was set to 37°C. Basal respiration was measured for 5–10 min before adding 2 µg/ml oligomycin, an ATP synthetase inhibitor. Maximal respiration was achieved by subsequent stepwise addition of the uncoupling agent 0.1–1 µM FCCP. Finally, a complex III inhibitor, 2.5 µM AA, was added to distinguish mitochondrial from residual oxygen consumption (non-mitochondrial respiration). Three indices are described by HRR: Coupling efficiency, spare respiratory capacity, and respiratory control ratio (RCR). We calculated: coupling efficiency (ratio between respiration associated with ATP synthesis and basal respiration), spare

respiratory capacity (ratio between maximal and basal respiration rates), and finally respiratory control ratio (RCR, the ratio between maximal and oligomycin-resistant respiration rates) (Brand and Nicholls, 2011; Ferreira et al., 2021).

Evaluation of sperm of hydrogen peroxide production

Hydrogen peroxide was measured using 10-acetyl-3,7-dihydroxyphenoxazine (Amplex Red). Amplex Red reacts in the presence horseradish peroxidase (HRP) with H_2O_2 in a 1:1 (v:v) stoichiometry to produce a highly red-fluorescent oxidation product, resorufin (Zhou et al., 1997; Messner and Imlay, 2002; González-Perilli et al., 2013). Amplex Red was dissolved in dimethyl sulfoxide (DMSO) to give a concentration of 1.25 mg/ml. This stock was frozen in aliquots and stored at −70°C for several months. A 0.8 ml aliquot of the stock was mixed with 18 ml of 50 mM potassium phosphate, pH 7.4, and kept shielded from light; this preparation is good for several hours (Messner and Imlay, 2002).

During standardization of the method a time-lapse analysis with and without 2.5 µM AA was done during 50 min (Figure 3A). Preliminary experiments were performed to determine the proper amount of human sperm cells and incubation time for H_2O_2 determination (data not shown). Sperm from samples of 136 males were washed with PBS by centrifugation at 400 g and re-suspended in HAM-F10. Between 2 and 6 × 10^6 spermatozoa in HAM-F10 were placed in 96-well Nunc F plates in a final volume of 100 µL and exposed to HRP 8 µg/ml and Amplex Red (Invitrogen, Waltham, Massachusetts, United States) 50 µM. The H_2O_2 present in the sample was compared to a calibration curve of H_2O_2 (final concentration 0.03–8 µM). The measurements were performed for 30 min at 37°C in a Flash Spectral Scanning Multimode Reader (Varioskan, Thermo Fisher Scientific, MA United States) at $\lambda ex = 530\ nm$ and $\lambda em = 590\ nm$. Duplicates were performed in samples and triplicates to perform the standard curve.

Evaluation of the antioxidant status of SP

The antioxidant capacity of SP from 95 men was determined by ferric-xylenol orange assay (FOX: 100 µM xylenol orange, 250 µM Fe^{2+}, 4 mM BHT, 25 mM H_2SO_4, and 90% (v/v) methanol) (Jiang et al., 1990; Reyes et al., 2011) following the H_2O_2 consumption after 30 min (Gay and Gebicki, 2002). H_2O_2 oxidizes ferrous ions to ferric ions. To measure the ferric ions formed, we mixed 35 µL of plasma in a final volume of 1 ml of 50 mM phosphate-sodium buffer, pH 7.4, containing 100 µM H_2O_2. Aliquots of 100 µL were taken from the reaction tube and mixed with 900 µL of FOX at time points 0 and 30 min. All tubes were centrifuged at 2000 g for 5 min to remove all residual precipitate. H_2O_2 consumption was monitored by tracking the changes in absorbance at 560 nm at 25°C using a UV-Visible spectrophotometer UV-2450, Shimadzu. The H_2O_2 extinction coefficient was determined as 53.900 $M^{-1}cm^{-1}$. To determine the final concentration of H_2O_2, a standard curve of [H_2O_2] (concentration 5–200 µM) was included in the assay. At least three independent measurements were performed for each sample. Proteins in SP were quantified using the Bradford method (Bradford, 1976). Note that the less residual hydrogen peroxide measured, the more antioxidant capacity SP has.

Statistics

Statistical analysis was performed based on the GraphPad Prism statistical package version 8.0.1 for Windows, GraphPad Software, San Diego, California United States, www.graphpad.com, and the statistical software JASP Team (2020), JASP (version 0.140). Data were expressed by arithmetic means, the corresponding standard errors, medians, and the 25th and 75th percentiles. Normal distribution of the data was tested using the Shapiro-Wilk normality test, which revealed that most sperm parameter values were not normally distributed. The Pearson test or Spearman correlation test was used to determine the relationship between the parameters and mitochondrial measurements. Comparisons between means were made using either the ANOVA test (multiple groups) or Student's t test or Mann-Whitney test as a function of the normal distribution of the data (two groups). Receiver operating characteristic curves (ROC) were used to show the ability of mitochondrial function, [H_2O_2] and/or antioxidants to discriminate between samples with progressive motility ≥ vs. < 32%, normal sperm morphology ≥ vs. < 4% or normal vs. abnormal spermiogram. Finally, cut off values were chosen to maximize the sum of sensitivity and specificity. Hypotheses were contrasted with two tails, and a p-value of less than 0.05 was considered statistically significant. For the experiments to determine the cut offs, the sample size was calculated with a confidence interval (CI) of 95%, a margin error of 5 and 10% of the population.

Results

Studied population

A total of 339 men aged 18–63 years were included in the study. The mean, standard deviation (SD), median, maximum and minimum values of the six main semen analysis parameters are listed in Table 1. These include sperm concentration, ejaculate volume, sperm viability, round cell concentration, percentage of normal morphology, and progressive motility. Experiments were performed in a total of 206 normozoospermic men and 133 men with abnormal

TABLE 1 Descriptive characteristics of participants' sperm parameters. Data were obtained by analyzing the first spermiogram of 339 individuals who attended the andrology clinic. Max = maximum value. Min = minimum value *lower reference values (WHO, 2010).

Parameter	Mean	SD	Median	Max	Min	*Lower reference limit
Patient age (yr)	34.9	7.3	35.0	63.0	18.0	—
Volume (ml)	3.6	1.5	3.5	10.0	0.5	1.5
Sperm concentration (million/mL)	47.7	38.0	40.6	214.0	0.04	15
Sperm viability (%)	86.5	11.7	89.0	99.0	3.0	58
Normal sperm morphology (%)	7.7	4.3	7.0	28.0	0.0	4
Progressive motility (a+b) (%)	54.4	17.2	58.0	90.0	3.0	32
Round cells (million/ml)	0.7	2.0	0.2	3.0	0.001	1

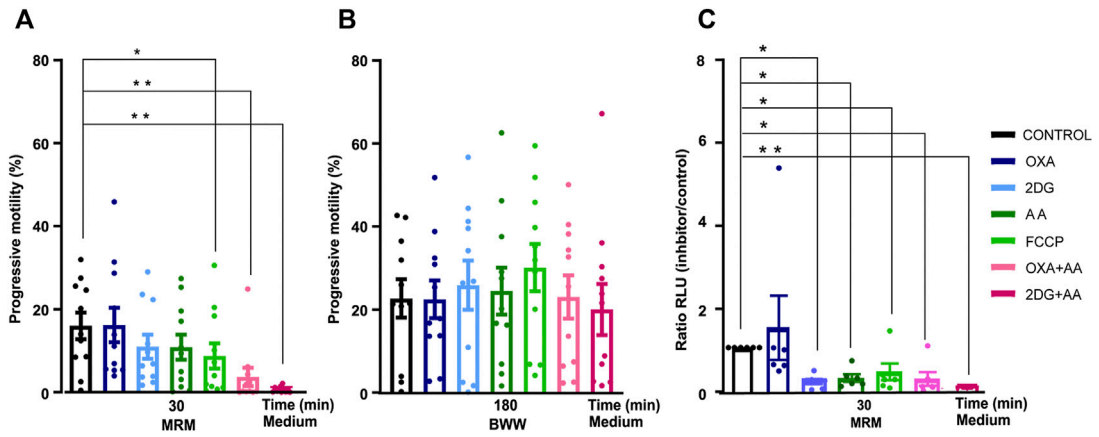

FIGURE 1
Changes in sperm motility and ATP production of human sperm incubated with metabolic inhibitors. Evaluation of the effects of glycolysis inhibitors and mitochondrial agents. **(A)** Progressive motility in presence of inhibitor and control at time = 30 min in MRM ($N = 11$) **(B)** time = 180 min in BWW ($N = 11$); **(C)** ATP production at 30 min in MRM medium ($N = 6$). Bars represent means ± SEM. Statistical significance between the control and the different groups was assessed with a ANOVA, Dunnett's multiple comparison paired test *$p < 0.05$ **$p < 0.01$. OXA (oxamate) 2DG (2-deoxy-glucose), AA (antimycin A), FCCP (carbonil cyanide- p-(tri-flouromethoxy) phenyl-hydrazone), MRM (Mitochondrial Respiration Medium) and BWW (Biggers Whitten Whittingham).

semen parameters (17 asthenozoospermic, 19 teratozoospermic, 30 oligozoospermic, 10 oligo-asthenozoospermic, 8 terato-asthenozoospermic, 17 oligo-terato-asthenozoospermic, and 32 oligo-teratozoospermic males) (Kruger et al., 1988; WHO, 2010) (Supplementary Figure S1).

Changes in mitochondrial function are related to human sperm motility and morphology

Since the role of mitochondria in human sperm function has not been fully elucidated (Ruiz-Pesini and Eperez 2000; Marchetti et al., 2002; Miki et al., 2004; Gallon et al., 2006; Ruiz-Pesini et al., 2007; Ferramosca et al., 2008; Koppers et al., 2008; Nascimento et al., 2008; Ferramosca et al., 2012; Sousa et al., 2011; Goodson et al., 2012; Piomboni et al., 2012; Marques et al., 2014; Moscatelli et al., 2017; Ammar et al., 2020; reviewed in: Amaral et al., 2013; Boguenet et al., 2021; Castellini et al., 2021), we first analyzed the role of the glycolytic and oxidative phosphorylation system (OXPHOS) in sperm motility and ATP production, as well as mitochondrial morphology of sperm.

First, we incubated spermatozoa from normozoospermic men in medium without nutrients (MRM) and added either glycolytic or mitochondrial function inhibitors. We used drugs that act at different levels of cellular metabolism: 2DG inhibits glycolysis by competing with endogenous glucose, OXA is an analog of pyruvate and inhibits the production of lactate, whereas FCCP is a respiratory chain uncoupler from the OXPHOS, and AA inhibits the mitochondrial complex III. Neither OXA nor

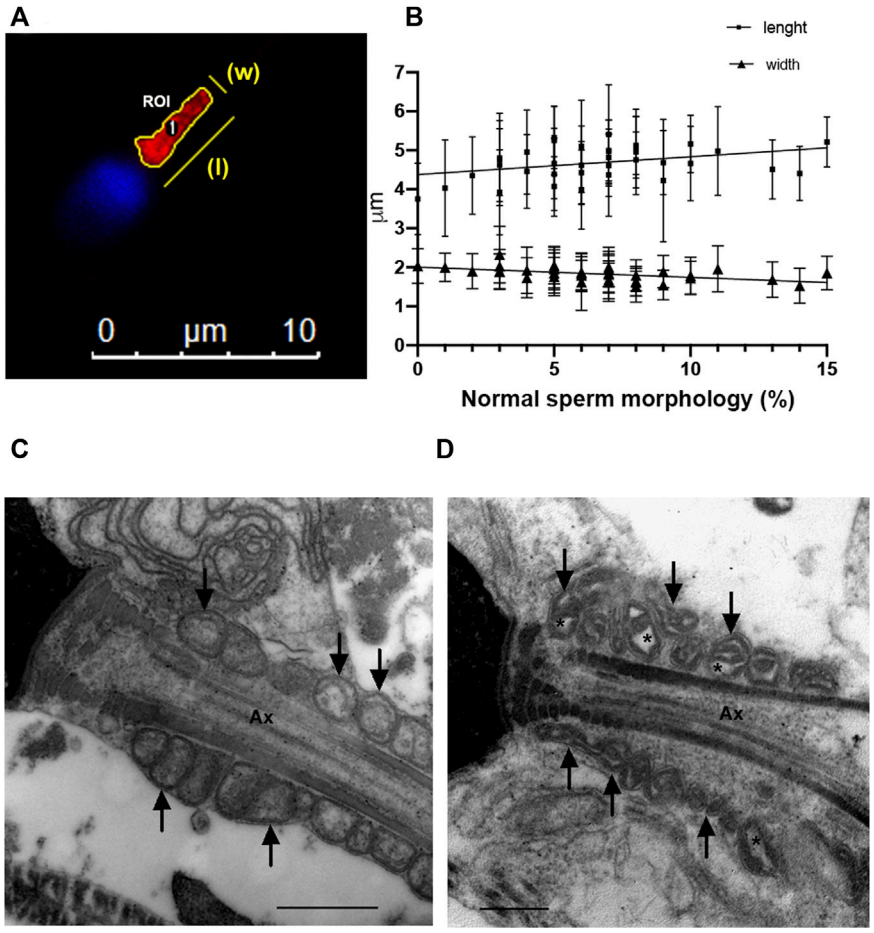

FIGURE 2
Sperm morphology analysis **(A)** Epifluorescence microscopy of the mid-piece of a human sperm cell. Manual segmentation of sperm mid-pieces using ImageJ/FIJI; **(B)** Correlation between mid-piece length and width and normal sperm morphology (N = 36). **(C)** Electron microscopy of sperm from a normozoospermic fertile man. **(D)** Electron microscopy of sperm from an infertile man with abnormal semen parameters. Defects on mitochondria are shown with arrows and asterisks indicate alterations in mitochondrial membranes. Ax = axoneme. Bars: 500 nm.

2DG nor AA significantly modified sperm motility. The sperm motility decreased significantly when the mitochondrial function was challenged by FCCP (Figure 1A). The combination of AA (mitochondrial inhibitor) and OXA or 2DG (glycolytic inhibitors) were required to completely decrease sperm motility. To test sperm viability, we washed sperm and incubated them in medium containing substrates (glucose, lactate, and pyruvate) for 3 h. Under these conditions, recovery of sperm motility was complete in all groups studied. (Figure 1B).

Second, we examined sperm ATP production under the same conditions as in the motility experiments. Sperm ATP production decreased under all the different conditions except when we added OXA (Figure 1C).

Finally, sperm mid-piece and mitochondrial morphology were analyzed (Figure 2). The sperm mid-piece was labeled with a red fluorescent dye that stains mitochondria (Figure 2A). Mid-piece length was positively correlated (Pearson correlation) with the percentage of normal morphology sperm in the semen samples (r = 0.37, p = 0.02), while mid-piece width had a negative correlation with normal progressive motility (graph not shown) and morphology parameters (Figure 2B) (r = −0.56 p = 0.0004 and r = −0.57 p = 0.0013, respectively).

In addition, we examined sperm mitochondria using electron microscopy (Figures 2C,D). We observed that in spermatozoa from samples with a percentage of normal spermatozoa <4%, the sperm mitochondria had abnormal shapes with dilatation of the inner mitochondrial matrix (asterisks in a representative image in Figure 2D).

Overall, these results indicate that sperm motility in normozoospermic males depends on mitochondrial function and that spermatozoa can maintain motility through the mitochondrial pathway. On the other hand, in men with

TABLE 2 Correlation between sperm parameters and mitochondrial indices. Coupling efficiency = ATP turnover/basal respiration. Spare respiratory capacity = maximal respiration rate/basal respiration. RCR = maximal respiration in the presence of FCCP/respiration in the presence of oligomicyn, *N* = number of donors. Statistical analysis was evaluated using Spearman's test *$p < 0.05$, **$p < 0.01$, ***$p < 0.001$.

	Correlations					
	Progressive motility (%)			Normal sperm morphology (%)		
Parameter	*N*	Spearmans' r	*p*-value	*N*	Spearmans' r	*p*-value
Coupling efficiency	166	0.239	0.002**	144	0.146	0.08
Spare respiratory capacity	166	0.174	0.025*	144	0.050	0.540
RCR	171	0.303	<0.001***	147	0.276	<0.001***

altered seminal quality, the mid-piece and the mitochondria also showed abnormalities.

The mitochondrial function of spermatozoa correlates with the sperm parameters of the classical spermiogram

Next, we decided to investigate whether mitochondrial function could be used as an index of sperm health. We measured the OCR of intact spermatozoa in real time, before and after the addition of inhibitors and FCCP.

We examined 171 sperm samples with HRR and analyzed the results in the context of the classical spermiogram (Tables 2, 3). We obtained three indices representing mitochondrial function and dysfunction (Cassina et al., 2015; Ferreira et al., 2021). Respiratory indices are ratios of oxygen consumption. They represent proportions of two rates so they are internally normalized to cell number or protein mass (Brand and Nicholls, 2011). RCR correlated positively with progressive motility and the percentage of normal sperm morphology in semen samples (Table 2). Similarly, the coupling efficiency and the spare respiratory capacity correlated positively with the percentage of sperm that exhibited progressive motility. Coupling efficiency and spare respiratory capacity did not correlate with the percentage of normal sperm morphology. We also divided the three main indices into two groups according to the sperm parameters (WHO's reference values) (Table 3). Only RCR showed statistically significant differences between samples in which both the percentage of motility and morphology were below or above the reference values. Mean ± S.D of RCR of samples with progressive sperm motility ≥32% were statistically higher than those with less than 32% (5.7 ± 6.8, $n = 155$, vs. 2.4 ± 0.9, $N = 16$, $p < 0.001$). Sperm from males with a percentage of normal morphology ≥4% have a higher RCR than those with abnormal sperm morphology <4% (5.4 ± 5.3, $N = 150$ vs. 3.7 ± 4.2 $N = 11$, mean ± SD, $p = 0.03$). Unexpectedly, and although viability correlated to RCR ($r = 0.1754$, $p = 0.0266$, Spearman correlation, graph not shown), we did not see statistically significant differences between samples in which the percentage of viable cells were below or above 58% (WHO's reference value). Also, there were no differences when the indices were analyzed using the reference values for the other semen parameters analyzed (volume or concentration) (data not shown).

These results show that mitochondrial function is correlated with semen parameters. Moreover, RCR is the best index to discriminate between samples with normal and abnormal semen parameters.

The percentage of sperm with progressive motility and normal sperm morphology correlates negatively with hydrogen peroxide production

First, we detected extracellular [H_2O_2] produced by sperm. For this purpose, we measured the reaction between Amplex red and H_2O_2 in the presence of HRP (Richer and Ford, 2001; Baumber et al., 2002; Yánez-Ortiz et al., 2021).

Upon addition of AA, an increase in H_2O_2 production is observed compared with baseline, suggesting that mitochondria may be a source of H_2O_2 in sperm cells as previously shown (Figure 3A) (Koppers et al., 2008; Storey, 2008; Aitken et al., 2012b; Escada-Rebelo et al., 2020).

Subsequently, 136 sperm samples with different sperm parameters were analyzed. The H_2O_2 production per million spermatozoa correlated negatively with sperm concentration ($r = 0.32$, $p < 0.001$, Spearman correlation), percentage of spermatozoa with progressive motility, and percentage of normal sperm morphology (Table 4).

There were no statistical differences between the [H_2O_2] produced by samples with progressive motility ≥ or <32% (0.75 ± 0.19 μM/10^6 spermatozoa and 1.53 ± 0.92 μM/10^6 spermatozoa, respectively, mean ± SEM, Figure 3B). The [H_2O_2] value was significantly higher in the samples with percentage of normal sperm morphology less than 4% (Figure 3C). The mean ± SEM of samples with more than

TABLE 3 Main respiratory indices classified by sperm parameters. RCR = respiratory control ratio SD = standard deviation. Max = maximum. Min = minimum. Statistic analysis, Man Whitney test. *$p < 0.05$, ***$p < 0.001$.

Progressive motility

Indices	Mean		*p*-value	SD		Median		Max		Min	
	≥32%	<32%		≥32%	<32%	≥32%	<32%	≥32%	<32%	≥32%	<32%
Coupling efficiency	0.510	0.442	0.684	0.187	0.161	0.504	0.412	0.955	0.800	0.045	0.200
Spare respiratory capacity	1.982	1.695	0.126	0.807	0.6866	1.788	1.610	6.570	3.267	0.521	0.635
RCR	5.658	2.400	<0.001***	6.796	0.914	3.550	2.124	57.231	4.19	0.744	0.857

Normal sperm morphology

Indices	Mean		*p*-value	SD		Median		Max		Min	
	≥ 4%	<4%		≥ 4%	<4%	≥ 4%	<4%	≥ 4%	<4%	≥ 4%	<4%
Coupling efficiency	0.503	0.497	0.710	0.186	0.170	0.498	0.451	0.955	0.800	0.045	0.288
Spare respiratory capacity	1.992	1.694	0.350	0.826	0.552	1.814	1.726	6.570	2.413	0.521	0.635
RCR	5.434	3.746	0.032*	5.354	4.208	3.610	2.529	31.825	16.132	0.744	1.108

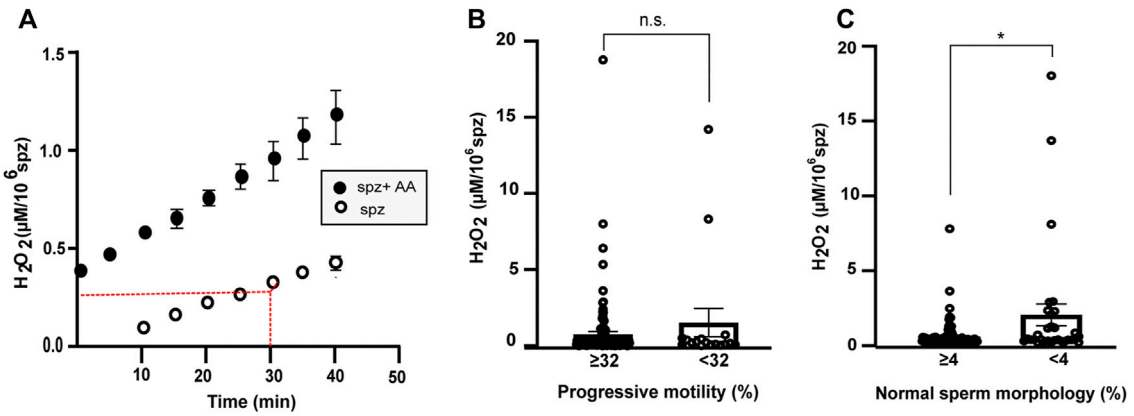

FIGURE 3
Production of extracellular H_2O_2 in s perm cells. **(A)** Production of peroxide by 10^6 sperm cells (spz) from normozoospermic samples as a function of time using detection of resorufin fluorescence emission by Amplex Red assay. Comparison between sperm samples under control conditions (white) and in the presence of antimycin A (AA) (black). **(B,C)** Graphs show H_2O_2 concentration after 30 min in sperm samples classified by progressive motility cut off (≥32% *N* = 119; <32% *N* = 17) **(B)** or percentage of normal and abnormal sperm morphology (*N* = 104 and *N* = 31, respectively, cut off = 4) **(C)**. Error bars represent SEM. A Mann-Witney test was used to evaluate statistical significance. n.s. P > 0.05, *$p < 0.05$.

4% normal morphology was 0.42 ± 0.10 μM/10^6 spermatozoa and 1.96 ± 0.76 μM/10^6 spermatozoa in samples with morphology <4% (Figure 3C). There were no statistical differences in the other parameters analyzed.

Thus, measuring extracellular [H_2O_2] correlates with main semen parameters. The method discriminates between men with percentage of normal sperm morphology ≥4% and <4% in their spermiogram using strict criteria (Kruger et al., 1988).

Seminal plasma antioxidant status correlates with sperm motility

To analyze whether the negative correlation of the production of [H_2O_2] with sperm parameters could be a consequence of variations in the antioxidant capacity of SP, we examined the percentage of residual H_2O_2 after addition of SP.

TABLE 4 Correlation between semen parameters and [H_2O_2] or percentage of residual hydrogen peroxide (antioxidant capacity). Spearman's test was used. *p < 0.05, **p < 0.01 ***p < 0.001. N = number of samples. #percentage of sperm normal morphology.

	[H_2O_2] per million sperm (μM/10^6 sperm)			Residual hydrogen peroxide (%)		
	N	Spearmans' r	*p*-value	*N*	Spearmans' r	*p*-value
Progressive motility (%)	136	−0.175	0.042*	95	−0.342	<0.001***
Sperm morphology#	128	−0.261	0.003**	95	0.014	0.890
[H_2O_2] per million sperm(μM)	—	—	—	45	0.080	0.500

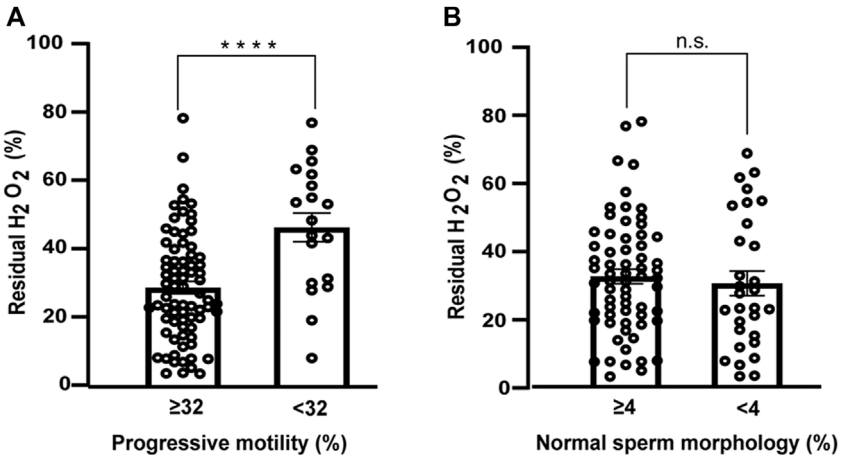

FIGURE 4
Antioxidant capacity of seminal plasma as a function of sperm parameters. **(A)** Progressive motility (≥32% *N* = 76; <32% *N* = 19) **(B)** normal sperm morphology (≥4% *N* = 65; <4% *N* = 30). Bars represent the percentage of residual H_2O_2 after 30min ±SEM. Mann-Whitney test was used to determine statistical significance n.s. P > 0.05, ****p < 0.0001.

The antioxidant capacity of SP correlated with sperm motility and was higher in samples with progressive motility ≥32% (Table 4 and Figure 4A). The mean ± SEM of the antioxidant capacity of SP was 28.6 ± 1.8% in men with progressive sperm motility ≥32% and 46.2 ± 4.2% in men presenting <32% p < 0.00001 (Mann Whitney test). The antioxidant status of SP did not correlate with the percentage of normal sperm morphology of the samples (Table 4 and Figure 4B). The means ± SEM were 32.7 ± 2.1% and 30.7 ± 3.6% when we analyzed SP of samples with normal sperm morphology of more and less than 4%, respectively (p = 0.4, t-test). The [H_2O_2] produced by the same sample did not correlate with the percentage of residual peroxide (Table 4). There were no differences when the indices were analyzed against the reference values for the other sperm parameters (data not shown).

These results suggest that the antioxidant capacity of SP has a strong correlation with progressive sperm motility. Samples with higher motility have higher antioxidant capacity, which is reflected in a lower percentage of residual peroxide. FOX method can distinguish between normal and abnormal sperm motility.

RCR is a good indicator of the functional status of human sperm

The diagnostic ability of the previous indices as binary classifiers was determined using the ROC curves. The results were classified into two groups (using reference values of 32 and 4% for sperm motility and morphology, respectively) (Figures 5A,B; Table 3). The ROC curve showed good specificity and sensitivity in the case of RCR (Figures 5C,D). As for motility, the area under the curve (AUC) corresponded to 0.773 (95% CI between 0.672–0.873, p < 0.001). An RCR cut off point of 2.93 was established with a sensitivity of 75% and a specificity of 69% (Figures 5A,C). In the case of morphology, the AUC corresponded to 0.692

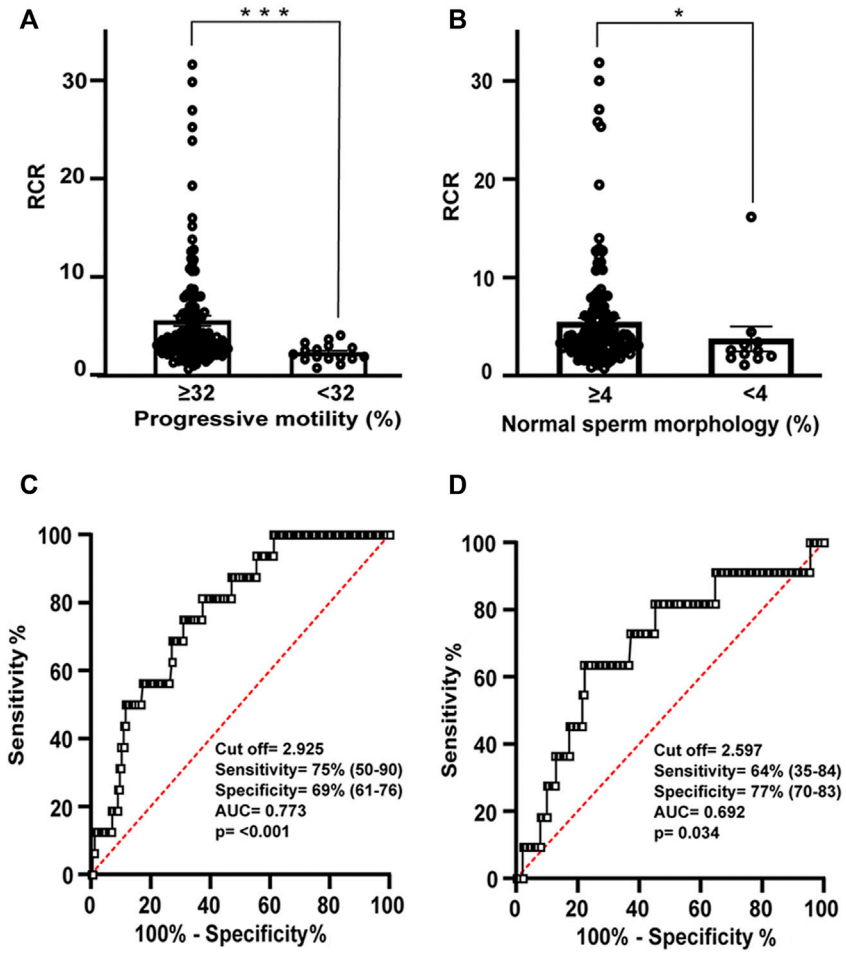

FIGURE 5
Relation between RCR, motility and morphology spermogram parameters. Bars represent means ± SEM of **(A)** progressive motility (≥32% *N* = 155; <32% *N* = 16) and **(B)** normal sperm morphology (≥4% *N* = 150; <4% *N* = 11). Mann-Whitney test was used to determine statistical significance; **p* < 0.05, ****p* < 0.001. **(C)** Receiver operating characteristic (ROC) curve showing RCR cut off value, sensitivity (%), specificity (%), and area under the curve for samples with normal or abnormal percentage of progressive motility and **(D)** ROC curve showing RCR cut off value, sensitivity (%), specificity (%), and area under the curve for samples with normal or abnormal percentage of spermatozoa with normal morphology.

(95% CI between 0.524–0.860, $p = 0.034$) (Figures 5B,D). A cut off point of RCR of 2.60 was set with a sensitivity of 64% and a specificity of 77%.

A ROC curve (AUC = 0.651, 95% CI between 0.530–0.772, $p = 0.012$) determined 0.197 μM $[H_2O_2]/10^6$ spermatozoa as the cut off value with 71% sensitivity and 61% specificity when samples were classified using references values of normal sperm ≥4% in their spermiogram (Figure 3C; Supplementary Figure S2). However, it was not possible to establish a cut off value of the $[H_2O_2]$ when the reference value of the spermiogram was ≥32% of progressive motile sperm (Figure 3B).

In the case of residual hydrogen peroxide, a cut off value of 41% was set only when references value for motility were applied. The ROC curve has an AUC = 0.765 (95% CI between 0.539–0.892, $p < 0.001$) with 68% specificity and 79% sensitivity (Figure 4A; Supplementary Figure S3).

Thus, we were able to establish cut offs for the three different assays with respect to the classic spermiogram.

RCR and H_2O_2 production can distinguish between normal and abnormal samples

Finally, to establish reference values encompassing all sperm parameters, we divided the male population into normozoospermic males and those with at least one abnormal sperm parameter (include: teratozoospermic, asthenozoospermic, oligozoospermic, terato-asthenozoospermic, and oligoasthenoteratozoospermic men).

The cut off value for RCR determined from the ROC curve (AUC = 0.695, 95% CI: 0.5792–0.810, p = 0.003) was 3.15 (sensitivity and specificity 73 and 61%, respectively) (Figures 6A,C).

The ROC curve (AUC = 0.610, 95% CI between 0.512–0.719, p = 0.044) determined a cut off value of $[H_2O_2]$ = 0.198 μM/10^6 spermatozooa (sensitivity of 65% and specificity of 60%) between both groups (Figures 6B,D).

When the population was divided into normozoospermic and abnormal spermiograms, no cut off value was determined for the percentage of residual hydrogen peroxide.

Therefore, RCR and $[H_2O_2]$ are good methods for classifying semen samples with normal or abnormal spermiograms.

Discussion

The source of ATP production for mammalian sperm motility has been widely studied (Miki et al., 2004; Mukai and Okuno, 2004; Miki, 2007; Ruiz-Pesini et al., 2007; Ferramosca et al., 2008, 2012; Goodson et al., 2012; Mukai and Travis, 2012; Piomboni et al., 2012; Moscatelli et al., 2017). The question of whether glycolysis or OXPHOS is the main source of ATP for sperm motility is controversial and considered species-specific (Storey, 2008; Amaral et al., 2013; Castellini et al., 2021; Kumar, 2022). By inhibiting the glycolytic pathway and mitochondrial function, we were able to confirm that energy supply (ATP) formed at the mitochondrial level is important for sperm motility in semen samples with normal parameters. Furthermore, we

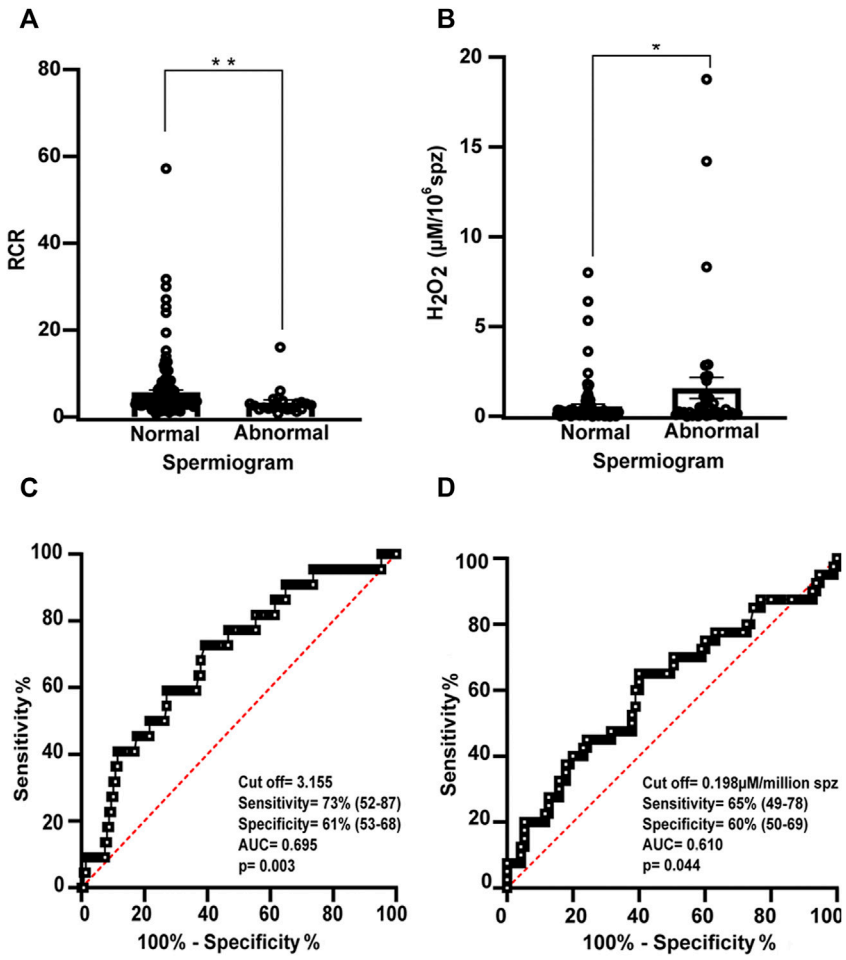

FIGURE 6
Relation between RCR and hydrogen peroxide concentration and spermogram parameters. Bars represent the mean values of **(A)** RCR (normal N = 148; abnormal N = 23) and **(B)** extracellular H_2O_2 concentration (normal N = 95; abnormal N = 40) ± SEM. A Mann-Witney test was used to evaluate statistical significance. *$p < 0.05$, **$p < 0.01$ **(C)** Receiver operating characteristic (ROC) curve showing RCR cut off value, sensitivity (%), specificity (%), and area under the curve for normal and abnormal spermiogram and **(D)** (ROC) curve showing $[H_2O_2]$ cut off value (μM/million sperm), sensitivity (%), specificity (%), and area under the curve for abnormal and normal spermiogram.

observed that motility and morphological alterations detected in routine semen analysis correlated with morphological changes in the mid-piece (Figure 2). Both observations make it reasonable to study mitochondrial sperm function in men with altered sperm parameters.

Our findings are consistent with some previous data emphasizing the role of OXPHOS as an essential ATP source for sperm function in humans and mice (Ruiz-Pesini et al., 1998; Ferramosca et al., 2008; Stendardi et al., 2011; Ferramosca et al., 2012; Piomboni et al., 2012; Ferramosca and Zara, 2014; Cassina et al., 2015; Moscatelli et al., 2017; Marín-Briggiler et al., 2021). Overall, it is now conceivable that both glycolysis and OXPHOS contribute to ATP production and depend on each other in controlling sperm functions reliant on the differential availability of energetic substrates in the environment (Castellini et al., 2021). There are also data from proteomic studies highlighting the contribution of lipid ß-oxidation as a sperm metabolic pathway (Amaral et al., 2013), suggesting that sperm metabolism is complex and needs further analysis.

We have previously shown that markers of mitochondrial function and dysfunction (such as RCR) reflect sperm activity (Cassina et al., 2015) and that they are associated with the cell's ability to fertilize (Ferreira et al., 2021). The data presented here highlight the differences in mitochondrial function in men with different sperm parameters. We propose that assessment of mitochondrial function is useful to provide information on sperm metabolic status in men.

Several analyzes have associated semen parameters with mitochondrial function (Marchetti et al., 2002; Gallon et al., 2006; Amaral and Ramalho-Santos, 2010; Uribe et al., 2017; Durairajanayagam et al., 2021; Tanga et al., 2021). However, the evaluation of sperm mitochondrial activity is not usually part of human sperm testing studies. Oximetry and HRR in particular, have the advantage over other mitochondrial analyzes in that they can examine motile (live) and intact (non-permeabilized) spermatozoa (Cassina et al., 2015; Ferreira et al., 2021). In particular, RCR has high sensitivity to all points of mitochondrial function, so most of them can be analyzed in the same experiment, e.g., respiratory chain, mitochondrial membrane potential, and respiratory reserve capacity. It has the disadvantage of requiring expensive equipment and specialized personnel. Although the sensitivity of the equipment is very high, our team has determined that at least 12 million/ml of sperm are required to detect variations in oxygen consumption. We are aware that this low limit is not only a drawback of the method, but also a limitation of this study because we could not measure sperm from some oligozoospermic males. Other authors have used HRR to analyze sperm metabolism, looking for either changes in mitochondrial function under different experimental conditions (Cedikova et al., 2014; Hereng et al., 2014; Le Foll et al., 2021) or differences between sperm from normozoospermic and asthenozoospermic men (Cedikova et al., 2014; Cedíková et al., 2014) suggesting that this tool has potential applications.

Sperm oxygen consumption has been successfully measured using similar sensitive methods (e.g., Seahorse flux analyzer) (Tourmente et al., 2015; Balbach et al., 2020a, 2020b). These studies have demonstrated the importance of mitochondrial oxygen consumption in sperm capacitation in mice (Balbach et al., 2020b) and the differences between mitochondrial metabolism in several strains of mice (Tourmente et al., 2015). This last method has the advantage of analyzing extracellular acidification (ECAR) and oxygen consumption rates simultaneously. It can eventually be applied to a smaller number of cells. The disadvantage of Seahorse XF is that ECAR is based on measurements of extracellular pH near the plasma membrane, so these experiments exclude the use of HCO_3^-, which is required in some of the sperm media (Traba et al., 2016; Hidalgo et al., 2020). In the Seahorse flux analyzer, cells must adhere to the plates, potentially affecting metabolic functions. HRR has the property that cells can move freely, which is *a priori* an advantage in the case of sperm. Defects in sperm parameters are often directly related to high levels of ROS in the male reproductive tract and semen (Kumar et al., 2009; Agarwal et al., 2014b; Bonanno et al., 2016; Nowicka-Bauer and Nixon, 2020). Consistent with previous reports (Aitken et al., 2012b; Ammar et al., 2020), our data show an association between abnormal mitochondrial sperm morphology and altered sperm motility and morphology in subjects exhibiting multiple alterations in the spermiogram. In other cell types, mitochondrial structural changes have been reported as part of mitochondrial dynamics in response to ROS (Galloway et al., 2012; Martínez et al., 2019, 2020). In mature spermatozoa, mitochondria are arranged around flagella and form a thick mitochondrial sheath stabilized by di-sulfide bonds (Otani et al., 1988). This capsule-like structure provides mechanical stability, protection, and resistance to hypo-osmotic stress (Amaral et al., 2013). Therefore, sperm mitochondria are unlikely to undergo the same dynamic changes observed in other cell types. However, human sperm mitochondria exhibit a looser morphology during capacitation, likely due to an increase in mitochondrial volume (Vorup-Jensen et al., 1999). Capacitation is a functional change in sperm that prepares cells for fertilization (Austin, 1952) and requires small amounts (considered physiological) of ROS (de Lamirande et al., 1997). Whether increased ROS production can alter sperm mitochondrial morphology remains to be investigated.

All in all, these results argue in favor of studying mitochondrial analysis in parallel with the redox status of sperm and semen. Moreover, these results were also consistent with those of respirometry studies; when sperm parameters were abnormal, an increase in H_2O_2 was measured. In this study, we used a previously published assay (Richer and Ford, 2001; Baumber et al., 2002; Yánez-Ortiz et al., 2021) to detect H_2O_2 production in sperm.

We observed a negative correlation between sperm parameters and H_2O_2 production. These results are consistent with those obtained by other methods, such as a correlation between ROS production and oligozoospermia (Agarwal et al., 2014a), asthenozoospermia (Bonanno et al., 2016), and teratozoospermia (Agarwal et al., 2014b). It has already been reported that defective spermatozoa produce higher amounts of ROS than normal ones (Aitken et al., 2012b), but an effect of H_2O_2 upstream on spermatogenesis that interferes with the final sperm production and reduces sperm concentration and/or sperm motility and morphology cannot be excluded.

Although the sensitivity and specificity of various tests measuring ROS have been published, they remain variable, are not standardized, and generally cannot provide diagnostic recommendations (Aitken et al., 2012a; Benjamin et al., 2012; Sharma et al., 2017; Agarwal et al., 2021a). In addition, many tests for ROS are expensive, time-consuming, often require specialized training, and are therefore not readily available in clinical and diagnostic laboratories (Alahmar, 2019; Agarwal et al., 2021a; 2021b). Extracellular hydrogen peroxide measurement by amplex red has the limitation of being an indirect assay. However, this approach has several advantages over other ROS assays. As $O_2^{\bullet-}$ does not cross membranes at physiological pH, measurement of hydrogen peroxide, which is the product of $O_2^{\bullet-}$ dismutation and diffuses through membranes, can then be used as an indicator of mitochondrial $O_2^{\bullet-}$ levels. Furthermore, peroxide is much more stable than $O_2^{\bullet-}$ and can accumulate in easily detectable amounts (Messner and Imlay, 2002; Wang et al., 2018). Our results showed an increase in the formation of hydrogen peroxide when AA (inhibitor of the III complex of the respiratory chain) was added, confirming that mitochondria are a source of ROS formation. An advantage of measuring hydrogen peroxide by this method is that it does not require specialized technicians or sophisticated equipment. It also represents mitochondrial superoxide production in sperm (Wang et al., 2018).

SP contains many enzymatic and non-enzymatic antioxidants, which are a source of sperm protection against oxidative stress (Khosrowbeygi and Zarghami, 2007; du Plessis et al., 2008). Therefore, it is clinically relevant to establish the reference values for measuring ROS in combination with antioxidant capacity in SP (Agarwal et al., 2015). Using a sensitive method that quantifies the amount of residual hydrogen peroxide, we were able to determine the antioxidant capacity of several SP samples. There are already several essays available for measuring antioxidant capacity (Zini et al., 2000; Agarwal and Prabakaran, 2005; Baker and Aitken, 2005; Agarwal et al., 2006; Khosrowbeygi and Zarghami, 2007; Agarwal et al., 2015; Sharma et al., 2017; Robert et al., 2020). The reason for including this particular method in our analysis is that we can directly relate the production of ROS (H_2O_2) to the antioxidant assay chosen (the percentage of decay of H_2O_2 when de SP is added). In our study, seminal antioxidant capacity correlated positively with sperm motility. This is consistent with previous studies indicating that antioxidant capacity is reduced in asthenozoospermic men (Pahune et al., 2013; Madej et al., 2021). However, antioxidant capacity did not correlate with the percentage of normal sperm morphology. It is known that antioxidant capacity in SP is related to age, environmental pollution, lifestyle, chronic or genital (varicocele) diseases (Eroglu et al., 2014; Roychoudhury et al., 2016; Madej et al., 2021). The analysis of these factors was beyond the scope of our study, but some of them could explain the lack of correlation between the antioxidant capacity of SP and sperm morphological alterations in the spermiogram.

The measurement of oxidants in combination with the antioxidant capacity of a sample could be important to integrate the redox status of semen (Agarwal and Bui, 2017; Agarwal and Wang, 2017). Unexpectedly, in this work, the production of H_2O_2 and the antioxidant capacity of SP were analyzed in 45 samples, but no correlation between [H_2O_2] extracellular and the percentage of residual peroxide in SP of the same samples was found. We can speculate that either sperm ROS production is not related to the antioxidant capacity measured by this method, or that other factors may influence semen composition. Since environmental factors affect the antioxidant capacity of SP as suggested above, some of them may be studied in the future to test the latter hypothesis. Using a device that measures the relative proportions of oxidants to reductants (antioxidants) called Male Infertility Oxidative System (MiOXSYS) (Agarwal and Bui, 2017; Agarwal et al., 2021b), the oxidation-reduction potential (ORP) was determined. ORP correlated with sperm parameters and male fertility status (Agarwal et al., 2017), including data from a multicentric study (Agarwal et al., 2019). The technique is promising for the evaluation of sperm oxidative stress. The device is not yet available worldwide, but it will be an alternative for analysis of sperm samples in relation to sperm metabolism.

The present study was performed on samples that are not pure oligozoospermic, asthenozoospermic, or terathozoospermic. This is a limitation of the analysis, however, the main objective of this study was to establish cut off of mitochondrial function in parallel with spermiogram results. In particular, measurement of sperm RCR and their production of ROS by quantification of [H_2O_2] extracellular resulted in good indicators of sperm function and correlated with main semen parameters. Therefore, some reference values were determined. The data presented here show that RCR and [H_2O_2] are good binary classifiers; a RCR cut off point of 3.2 was established with a sensitivity of 73% and a specificity of 61% using reference values of 32 and 4% for sperm motility and morphology, respectively. The cut off value for [H_2O_2] was set at 0.2 μM per million sperm (sensitivity = 65%, specificity = 60%). In contrast, semen antioxidant capacity had not been demonstrated to be a good indicator for classifying semen samples with normal or abnormal spermiograms.

In this work, we established the cut off based on sperm parameters independently of the cause of the fertility status; e.g., we did not include the presence of chromosomal, genetic, hormonal abnormalities or other previously known conditions related to male fertility in the analysis. It will be interesting to test whether the reference values described can distinguish between these conditions.

Men who attend fertility clinics seek fertility advice, but not all men with abnormal sperm parameters are infertile and vice versa (Guzick et al., 2001; Cairo Consensus Workshop Group, 2020; Pandruvada et al., 2021). Infertility with normal semen parameters is one of the new challenges in this field. As a result, fertility clinics are looking for new indices to determine the true fertility potential of sperm. In our study, ROC curves were generated to determine the cut off values, sensitivity, and specificity of the assays using the previous reference parameters. We are aware that a weakness of the study is that the categorization is not between fertile and infertile men. Further studies are planned to apply the indices in the IVF clinic, where the true fertility potential of sperm can be assessed. In addition, multicentric validation of the results must be performed before these tools can be used in clinical practice. Nevertheless, the application of the mitochondrial and H_2O_2 sperm production indices may contribute to the understanding of sperm biology and may be helpful in explaining some cases of infertility.

Conclusion

Semen evaluation is considered one of the most important laboratory tests for assessing male fertility. Although it is the gold standard method for studying infertile men, it still lacks functional analysis of sperm status. We propose that determination of RCR in combination with other analyzes (such as measurement of extracellular [H_2O_2] sperm production and antioxidant capacity of SP) provides results on sperm functional status focusing on energy metabolism, involvement of mitochondrial function, and formation of ROS.

Data availability statement

The raw data supporting the conclusion of this article will be made available by the authors, without undue reservation.

Ethics statement

The studies involving human participants were reviewed and approved by the Ethics Committee of the Facultad de Medicina de la Universidad de la República Montevideo, Uruguay. The patients/participants provided their written informed consent to participate in this study.

Author contributions

PI, LR-V, and PP-P performed the experiments including standardization of protocols, respiratory analysis, and CASA evaluation. MFS performed the morphological studies. PI, AC, and RS designed the experiments, analyzed the results, and wrote the manuscript. All authors read, corrected, and approved the final manuscript.

Funding

AC is supported by grants from Universidad de la República (CSIC_2018, Espacio Interdisciplinario_2021). Additional funding was obtained from the Programa de Desarrollo de Ciencias Básicas (PEDECIBA, Uruguay). PI, MFS, and RS are supported from Universidad de la República (I+D, CSIC 2014; I+D, CSIC 2016, Iniciación a la Investigación, CSIC 2019 and FMV_1_2017_1_136490 ANII- Uruguay). PI is supported by POS_FMV_2018_1_1007814.

Acknowledgments

We thank Gabriela Casanova Facultad de Ciencias—UdelaR, Uruguay for her assistance with the MET experiments. Also, we are very grateful to Andres Trotchansky and Marcelo Reyes for their assistance in the FOX method (Facultad Medicina-Udelar, Uruguay). Finally, we would like to thank the Fertilab Andrology clinic, especially José María Montes and Andrea Torrents, for allowing us access to donors.

Conflict of interest

The authors declare that the research was conducted in the absence of any commercial or financial relationships that could be construed as a potential conflict of interest.

Publisher's note

Supplementary material

The Supplementary Material for this article can be found online at: https://www.frontiersin.org/articles/10.3389/fcell.2022.926684/full#supplementary-material

References

Agarwal, A., Ahmad, G., and Sharma, R. (2015). Reference values of reactive oxygen species in seminal ejaculates using chemiluminescence assay. *J. Assist. Reprod. Genet.* 32, 1721–1729. doi:10.1007/s10815-015-0584-1

Agarwal, A., and Bui, A. D. (2017). Oxidation-reduction potential as a new marker for oxidative stress: Correlation to male infertility. *Investig. Clin. Urol.* 58, 385–399. doi:10.4111/icu.2017.58.6.385

Agarwal, A., and Deepinder, F. (2009). "Determination of seminal oxidants (reactive oxygen species)," in *Infertility in the male*." in Editors C. S. Niederberger, L. I. Lipshultz, and S. S. Howards (Cambridge: Cambridge University Press), 618–632. doi:10.1017/CBO9780511635656.040

Agarwal, A., Finelli, R., Selvam, M. K. P., Leisegang, K., Majzoub, A., Tadros, N., et al. (2021a). A global survey of reproductive specialists to determine the clinical utility of oxidative stress testing and antioxidant use in male infertility. *World J. Mens. Health* 39, 470–488. doi:10.5534/wjmh.210025

Agarwal, A., Leisegang, K., Majzoub, A., Henkel, R., Finelli, R., Panner Selvam, M. K., et al. (2021b). Utility of antioxidants in the treatment of male infertility: clinical guidelines based on a systematic review and analysis of evidence. *World J. Mens. Health* 39, 233–290. doi:10.5534/wjmh.200196

Agarwal, A., Mulgund, A., Sharma, R., and Sabanegh, E. (2014a). Mechanisms of oligozoospermia: an oxidative stress perspective. *Syst. Biol. Reprod. Med.* 60 (4), 206–216. doi:10.3109/19396368.2014.918675

Agarwal, A., Panner Selvam, M., Arafa, M., Okada, H., Homa, S., Killeen, A., et al. (2019). Multi-center evaluation of oxidation-reduction potential by the MiOXSYS in males with abnormal semen. *Asian J. Androl.* 21, 565–569. doi:10.4103/aja.aja_5_19

Agarwal, A., Prabakaran, S., and Allamaneni, S. S. S. R. (2006). Relationship between oxidative stress, varicocele and infertility: a meta-analysis. *Reprod. Biomed. Online* 12, 630–633. doi:10.1016/S1472-6483(10)61190-X

Agarwal, A., and Prabakaran, S. A. (2005). Mechanism, measurement, and prevention of oxidative stress in male reproductive physiology. *Indian J. Exp. Biol.* 43, 963–974.

Agarwal, A., Roychoudhury, S., Sharma, R., Gupta, S., Majzoub, A., Sabanegh, E., et al. (2017). Diagnostic application of oxidation-reduction potential assay for measurement of oxidative stress:clinical utility in male factor infertility. *Reprod. Biomed. Online* 34, 48–57. doi:10.1016/j.rbmo.2016.10.008

Agarwal, A., Tvrda, E., and Sharma, R. (2014b). Relationship amongst teratozoospermia, seminal oxidative stress and male infertility. *Reprod. Biol. Endocrinol.* 12, 45. doi:10.1186/1477-7827-12-45

Agarwal, A., and Wang, S. M. (2017). Clinical relevance of oxidation-reduction potential in the evaluation of male infertility. *Urology* 104, 84–89. doi:10.1016/j.urology.2017.02.016

Aitken, R. J., De Iuliis, G. N., and Baker, M. A. (2012a). "Direct methods for the detection of reactive oxygen species in human semen samples," in *Studies on men's Health and fertility*. Editors A. Agarwal, R. J. Aitken, and J. G. Alvarez (Totowa, NJ: Humana Press), 275–299. doi:10.1007/978-1-61779-776-7_14

Aitken, R. J., Jones, K. T., and Robertson, S. A. (2012b). Reactive oxygen species and sperm function-in sickness and in health. *J. Androl.* 33, 1096–1106. doi:10.2164/jandrol.112.016535

Alahmar, A. T. (2019). Role of oxidative stress in male infertility: an updated review. *J. Hum. Reprod. Sci.* 12, 4–18. doi:10.4103/jhrs.JHRS_150_18

Amaral, A., Lourenço, B., Marques, M., and Ramalho-Santos, J. (2013). Mitochondria functionality and sperm quality. *Reproduction* 146, R163–R174. doi:10.1530/REP-13-0178

Amaral, A., and Ramalho-Santos, J. (2010). Assessment of mitochondrial potential: implications for the correct monitoring of human sperm function. *Int. J. Androl.* 33, e180–e186. doi:10.1111/j.1365-2605.2009.00987.x

Ammar, O., Mehdi, M., and Muratori, M. (2020). Teratozoospermia: its association with sperm DNA defects, apoptotic alterations, and oxidative stress. *Andrology* 8, 1095–1106. doi:10.1111/andr.12778

Austin, C. R. (1952). The capacitation of the mammalian sperm. *Nature* 170, 326. doi:10.1038/170326a0

Baccetti, B., Capitani, S., Collodel, G., Strehler, E., and Piomboni, P. (2002). Recent advances in human sperm pathology. *Contraception* 65, 283–287. doi:10.1016/s0010-7824(02)00290-1

Baker, M. A., and Aitken, R. J. (2005). Reactive oxygen species in spermatozoa: methods for monitoring and significance for the origins of genetic disease and infertility. *Reprod. Biol. Endocrinol.* 3, 67. doi:10.1186/1477-7827-3-67

Balbach, M., Buck, J., and Levin, L. R. (2020a). Using an extracellular flux analyzer to measure changes in glycolysis and oxidative phosphorylation during mouse sperm capacitation. *JoVE*. doi:10.3791/60815

Balbach, M., Gervasi, M. G., Hidalgo, D. M., Visconti, P. E., Levin, L. R., Buck, J., et al. (2020b). Metabolic changes in mouse sperm during capacitation. *Biol. Reprod.* 103, 791–801. doi:10.1093/biolre/ioaa114

Barratt, C. L. R., De Jonge, C. J., and Sharpe, R. M. (2018). 'Man up': the importance and strategy for placing male reproductive health centre stage in the political and research agenda. *Hum. Reprod.* 33, 541–545. doi:10.1093/humrep/dey020

Barratt, C. L. R., Wang, C., Baldi, E., Toskin, I., Kiarie, J., and Lamb, D. J. (2022). What advances may the future bring to the diagnosis, treatment, and care of male sexual and reproductive health? *Fertil. Steril.* 117, 258–267. doi:10.1016/j.fertnstert.2021.12.013

Baumber, J., Vo, A., Sabeur, K., and Ball, B. A. (2002). Generation of reactive oxygen species by equine neutrophils and their effect on motility of equine spermatozoa. *Theriogenology* 57, 1025–1033. doi:10.1016/s0093-691x(01)00710-5

Benjamin, D., Sharma, R. K., Moazzam, A., and Agarwal, A. (2012). *Methods for the detection of ROS in human sperm samples BT - studies on men's health and fertility*." in.Editors A. Agarwal, R. J. Aitken, and J. G. Alvarez (Totowa, NJ: Humana Press), 257–273. doi:10.1007/978-1-61779-776-7_13

Björndahl, L., and Kirkman Brown, J.other Editorial Board Members of the WHO Laboratory Manual for the Examination and Processing of Human Semen (2022). The sixth edition of the WHO laboratory manual for the examination and processing of human semen: ensuring quality and standardization in basic examination of human ejaculates. *Fertil. Steril.* 117, 246–251. doi:10.1016/j.fertnstert.2021.12.012

Boguenet, M., Bouet, P.-E., Spiers, A., Reynier, P., and May-Panloup, P. (2021). Mitochondria: their role in spermatozoa and in male infertility. *Hum. Reprod. Update* 27, 697–719. doi:10.1093/humupd/dmab001

Bonanno, O., Romeo, G., Asero, P., Pezzino, F. M., Castiglione, R., Burrello, N., et al. (2016). Sperm of patients with severe asthenozoospermia show biochemical, molecular and genomic alterations. *Reproduction* 152, 695–704. doi:10.1530/REP-16-0342

Boveris, A., and Chance, B. (1973). The mitochondrial generation of hydrogen peroxide. General properties and effect of hyperbaric oxygen. *Biochem. J.* 134, 707–716. doi:10.1042/bj1340707

Bradford, M. M. (1976). A rapid and sensitive method for the quantitation of microgram quantities of protein utilizing the principle of protein-dye binding. *Anal. Biochem.* 72, 248–254. doi:10.1006/abio.1976.9999

Brand, M. D., and Nicholls, D. G. (2011). Assessing mitochondrial dysfunction in cells. *Biochem. J.* 435, 297–312. doi:10.1042/BJ20110162

Cairo workshop group (2020). The current status and future of andrology: a consensus report from the Cairo workshop group. *Andrology* 8, 27–52. doi:10.1111/andr.12720

Cardoso, A. R., Chausse, B., da Cunha, F. M., Luévano-Martínez, L. A., Marazzi, T. B. M., Pessoa, P. S., et al. (2012). mitochondrial compartmentalization of redox processes. *Free Radic. Biol. Med.* 52, 2201–2208. doi:10.1016/j.freeradbiomed.2012.03.008

Cassina, A., Silveira, P., Cantu, L., Montes, J., Radi, R., Sapiro, R., et al. (2015). Defective human sperm cells are associated with mitochondrial dysfunction and oxidant production. *Biol. Reprod.* 93, 119. doi:10.1095/biolreprod.115.130989

Castellini, C., D'Andrea, S., Cordeschi, G., Totaro, M., Parisi, A., Di Emidio, G., et al. (2021). Pathophysiology of mitochondrial dysfunction in human spermatozoa: focus on energetic metabolism, oxidative stress and apoptosis. *Antioxidants* 10, 695. doi:10.3390/antiox10050695

Cedíková, M., Miklíková, M., Grundmanová, M., Zech, N. H., Králíčková, M., Kuncová, J., et al. (2014). Sperm mitochondrial function in men with normozoospermia and asthenozoospermia. *Ceska Gynekol.* 79, 22–28.

Cedikova, M., Miklikova, M., Stachova, L., Grundmanova, M., Tuma, Z., Vetvicka, V., et al. (2014). Effects of the Czech propolis on sperm mitochondrial function. *Evid. Based. Complement. Altern. Med.*, 248768. doi:10.1155/2014/248768

Courtade, M., Lagorce, C., Bujan, L., Caratero, C., and Mieusset, R. (1998). Clinical characteristics and light and transmission electron microscopic sperm defects of infertile men with persistent unexplained asthenozoospermia. *Fertil. Steril.* 70, 297–304. doi:10.1016/s0015-0282(98)00152-6

De Jonge, C., and Barratt, C. L. R. (2019). The present crisis in male reproductive health: an urgent need for a political, social, and research roadmap. *Andrology* 7, 762–768. doi:10.1111/andr.12673

de Lamirande, E., Jiang, H., Zini, a., Kodama, H., and Gagnon, C. (1997). Reactive oxygen species and sperm physiology. *Rev. Reprod.* 2, 48–54. doi:10.1530/ror.0.0020048

du Plessis, S. S., Makker, K., Desai, N. R., and Agarwal, A. (2008). Impact of oxidative stress on IVF. *Expert Rev. Obstet. Gynecol.* 3, 539–554. doi:10.1586/17474108.3.4.539

Durairajanayagam, D., Singh, D., Agarwal, A., and Henkel, R. (2021). Causes and consequences of sperm mitochondrial dysfunction. *Andrologia* 53, e13666. doi:10.1111/and.13666

Eroglu, M., Sahin, S., Durukan, B., Ozakpinar, O. B., Erdinc, N., Turkgeldi, L., et al. (2014). Blood serum and seminal plasma selenium, total antioxidant capacity and coenzyme q10 levels in relation to semen parameters in men with idiopathic infertility. *Biol. Trace Elem. Res.* 159, 46–51. doi:10.1007/s12011-014-9978-7

Escada-Rebelo, S., Mora, F. G., Sousa, A. P., Almeida-Santos, T., Paiva, A., Ramalho-Santos, J., et al. (2020). Fluorescent probes for the detection of reactive oxygen species in human spermatozoa. *Asian J. Androl.* 22(5):465. doi:10.4103/aja.aja_132_19

Ferramosca, A., Focarelli, R., Piomboni, P., Coppola, L., Zara, V., Coppola, L., et al. (2008). Oxygen uptake by mitochondria in demembranated human spermatozoa: a reliable tool for the evaluation of sperm respiratory efficiency. *Int. J. Androl.* 31, 337–345. doi:10.1111/j.1365-2605.2007.00775.x

Ferramosca, A., Provenzano, S. P., Coppola, L., and Zara, V. (2012). Mitochondrial respiratory efficiency is positively correlated with human sperm motility. *Urology* 79, 809–814. doi:10.1016/j.urology.2011.12.042

Ferramosca, A., and Zara, V. (2014). Bioenergetics of mammalian sperm capacitation. *Biomed. Res. Int.*, 902953. doi:10.1155/2014/902953

Ferreira, J. J., Cassina, A., Irigoyen, P., Ford, M., Pietroroia, S., Peramsetty, N., et al. (2021). Increased mitochondrial activity upon CatSper channel activation is required for mouse sperm capacitation. *Redox Biol.* 48, 102176. doi:10.1016/j.redox.2021.102176

Gallon, F., Marchetti, C., Jouy, N., and Marchetti, P. (2006). The functionality of mitochondria differentiates human spermatozoa with high and low fertilizing capability. *Fertil. Steril.* 86, 1526–1530. doi:10.1016/j.fertnstert.2006.03.055

Galloway, C. A., Lee, H., and Yoon, Y. (2012). Mitochondrial morphology—emerging role in bioenergetics. *Free Radic. Biol. Med.* 53, 2218–2228. doi:10.1016/j.freeradbiomed.2012.09.035

Gay, C. A., and Gebicki, J. M. (2002). Perchloric acid enhances sensitivity and reproducibility of the ferric-xylenol orange peroxide assay. *Anal. Biochem.* 304, 42–46. doi:10.1006/abio.2001.5566

Giaccagli, M. M., Gómez-Elías, M. D., Herzfeld, J. D., Marín-Briggiler, C. I., Cuasnicú, P. S., Cohen, D. J., et al. (2021). capacitation-induced mitochondrial activity is required for sperm fertilizing ability in mice by modulating hyperactivation. *Front. Cell. Dev. Biol.* 9, 767161. doi:10.3389/fcell.2021.767161

González-Perilli, L., Álvarez, M. N., Prolo, C., Radi, R., Rubbo, H., Trostchansky, A., et al. (2013). Nitroarachidonic acid prevents NADPH oxidase assembly and superoxide radical production in activated macrophages. *Free Radic. Biol. Med.* 58, 126–133. doi:10.1016/j.freeradbiomed.2012.12.020

Goodson, S. G., Qiu, Y., Sutton, K. A., Xie, G., Jia, W., O'Brien, D. A., et al. (2012). Metabolic substrates exhibit differential effects on functional parameters of mouse sperm capacitation. *Biol. Reprod.* 87, 175. doi:10.1095/biolreprod.112.102673

Gopalkrishnan, K., Padwal, V., D'Souza, S., and Shah, R. (1995). Severe asthenozoospermia: a structural and functional study. *Int. J. Androl.* 18, 67–74. doi:10.1111/j.1365-2605.1995.tb00642.x

Guzick, D. S., Overstreet, J. W., Factor-Litvak, P., Brazil, C. K., Nakajima, S. T., Coutifaris, C., et al. (2001). Sperm morphology, motility, and concentration in fertile and infertile men. *N. Engl. J. Med.* 345, 1388–1393. doi:10.1056/NEJMoa003005

Hereng, T. H., Elgstøen, K. B. P., Eide, L., Rosendal, K. R., and Skålhegg, B. S. (2014). Serum albumin and HCO3- regulate separate pools of ATP in human spermatozoa. *Hum. Reprod.* 29, 918–930. doi:10.1093/humrep/deu028

Hidalgo, D. M., Romarowski, A., Gervasi, M. G., Navarrete, F., Balbach, M., Salicioni, A. M., et al. (2020). Capacitation increases glucose consumption in murine sperm. *Mol. Reprod. Dev.* 87, 1037–1047. doi:10.1002/mrd.23421

Jiang, Z. Y., Woollard, A. C., and Wolff, S. P. (1990). Hydrogen peroxide production during experimental protein glycation. *FEBS Lett.* 268, 69–71. doi:10.1016/0014-5793(90)80974-n

Kasai, T., Ogawa, K., Mizuno, K., Nagai, S., Uchida, Y., Ohta, S., et al. (2002). Relationship between sperm mitochondrial membrane potential, sperm motility, and fertility potential. *Asian J. Androl.* 4, 97–103.

Khosrowbeygi, A., and Zarghami, N. (2007). Levels of oxidative stress biomarkers in seminal plasma and their relationship with seminal parameters. *BMC Clin. Pathol.* 7, 6. doi:10.1186/1472-6890-7-6

Kliesch, S. (2014). Diagnosis of male infertility: diagnostic work-up of the infertile man. *Eur. Urol. Suppl.* 13, 73–82. doi:10.1016/j.eursup.2014.08.002

Koppers, A. J., De Iuliis, G. N., Finnie, J. M., McLaughlin, E. a., and Aitken, R. J. (2008). Significance of mitochondrial reactive oxygen species in the generation of oxidative stress in spermatozoa. *J. Clin. Endocrinol. Metab.* 93, 3199–3207. doi:10.1210/jc.2007-2616

Kruger, T. F., Acosta, A. A., Simmons, K. F., Swanson, R. J., Matta, J. F., Oehninger, S., et al. (1988). Predictive value of abnormal sperm morphology in *in vitro* fertilization. *Fertil. Steril.* 49, 112–117. doi:10.1016/S0015-0282(16)59660-5

Kumar, N. (2022). Sperm mitochondria, the driving force behind human spermatozoa activities: its functions and dysfunctions - a narrative review. *Curr. Mol. Med.* 22. doi:10.2174/1566524022666220408104047

Kumar, R., Venkatesh, S., Kumar, M., Tanwar, M., Shasmsi, M. B., Kumar, R., et al. (2009). Oxidative stress and sperm mitochondrial DNA mutation in idiopathic oligoasthenozoospermic men. *Indian J. biochem. Biophys.* 46, 172–177.

Le Foll, N., Pont, J.-C., L'Hostis, A., Guilbert, T., Bouillaud, F., Wolf, J.-P., et al. (2021). Cyclic FEE peptide improves human sperm movement parameters without modification of their energy metabolism. *Int. J. Mol. Sci.* 22, 11263. doi:10.3390/ijms222011263

Madej, D., Granda, D., Sicinska, E., and Kaluza, J. (2021). Influence of fruit and vegetable consumption on antioxidant status and semen quality: a cross-sectional study in adult men. *Front. Nutr.* 8, 753843. doi:10.3389/fnut.2021.753843

Malić Vončina, S., Golob, B., Ihan, A., Kopitar, A. N., Kolbezen, M., Zorn, B., et al. (2016). Sperm DNA fragmentation and mitochondrial membrane potential combined are better for predicting natural conception than standard sperm parameters. *Fertil. Steril.* 105, 637–644. doi:10.1016/j.fertnstert.2015.11.037

Marchetti, C., Obert, G., Deffosez, A., Formstecher, P., and Marchetti, P. (2002). Study of mitochondrial membrane potential, reactive oxygen species, DNA fragmentation and cell viability by flow cytometry in human sperm. *Hum. Reprod.* 17, 1257–1265. doi:10.1093/humrep/17.5.1257

Marín-Briggiler, C. I., Luque, G. M., Gervasi, M. G., Oscoz-Susino, N., Sierra, J. M., Mondillo, C., et al. (2021). Human sperm remain motile after a temporary energy restriction but do not undergo capacitation-related events. *Front. Cell. Dev. Biol.* 9, 777086. doi:10.3389/fcell.2021.777086

Marques, M., Sousa, A. P., Paiva, A., Almeida-Santos, T., and Ramalho-Santos, J. (2014). Low amounts of mitochondrial reactive oxygen species define human sperm quality. *Reproduction* 147, 817–824. doi:10.1530/REP-13-0644

Martínez, J., Marmisolle, I., Tarallo, D., and Quijano, C. (2020). Mitochondrial bioenergetics and dynamics in secretion processes. *Front. Endocrinol.* 11, 319. doi:10.3389/fendo.2020.00319

Martínez, J., Tarallo, D., Martínez-Palma, L., Victoria, S., Bresque, M., Rodríguez-Bottero, S., et al. (2019). Mitofusins modulate the increase in mitochondrial length, bioenergetics and secretory phenotype in therapy-induced senescent melanoma cells. *Biochem. J.* 476, 2463–2486. doi:10.1042/BCJ20190405

Messner, K. R., and Imlay, J. A. (2002). *In vitro* quantitation of biological superoxide and hydrogen peroxide generation. *Methods Enzymol.* 349, 354–361. doi:10.1016/s0076-6879(02)49351-2

Miki, K. (2007). Energy metabolism and sperm function. *Soc. Reprod. Fertil. Suppl.* 65, 309–325.

Miki, K., Qu, W., Goulding, E. H., Willis, W. D., Bunch, D. O., Strader, L. F., et al. (2004). Glyceraldehyde 3-phosphate dehydrogenase-S, a sperm-specific glycolytic enzyme, is required for sperm motility and male fertility. *Proc. Natl. Acad. Sci. U. S. A.* 101, 16501–16506. doi:10.1073/pnas.0407708101

Moscatelli, N., Spagnolo, B., Pisanello, M., Lemma, E. D., De Vittorio, M., Zara, V., et al. (2017). Single-cell-based evaluation of sperm progressive motility via fluorescent assessment of mitochondria membrane potential. *Sci. Rep.* 7, 17931. doi:10.1038/s41598-017-18123-1

Mukai, C., and Okuno, M. (2004). Glycolysis plays a major role for adenosine triphosphate supplementation in mouse sperm flagellar movement. *Biol. Reprod.* 71, 540–547. doi:10.1095/biolreprod.103.026054

Mukai, C., and Travis, A. J. (2012). What sperm can teach us about energy production. *Reprod. Domest. Anim.* 47, 164–169. doi:10.1111/j.1439-0531.2012.02071.x

Mundy, A. J., Ryder, T. A., and Edmonds, D. K. (1995). Asthenozoospermia and the human sperm mid-piece. *Hum. Reprod.* 10, 116–119. doi:10.1093/humrep/10.1.116

Nascimento, J. M., Shi, L. Z., Tam, J., Chandsawangbhuwana, C., Durrant, B., Botvinick, E. L., et al. (2008). Comparison of glycolysis and oxidative phosphorylation as energy sources for mammalian sperm motility, using the combination of fluorescence imaging, laser tweezers, and real-time automated tracking and trapping. *J. Cell. Physiol.* 217, 745–751. doi:10.1002/jcp.21549

Nohl, H., Gille, L., Kozlov, A., and Staniek, K. (2003). Are mitochondria a spontaneous and permanent source of reactive oxygen species? *Redox Rep.* 8, 135–141. doi:10.1179/135100003225001502

Nowicka-Bauer, K., and Nixon, B. (2020). Molecular changes induced by oxidative stress that impair human sperm motility. *Antioxidants* 9, E134. doi:10.3390/antiox9020134

Otani, H., Tanaka, O., Kasai, K., and Yoshioka, T. (1988). Development of mitochondrial helical sheath in the middle piece of the mouse spermatid tail: regular dispositions and synchronized changes. *Anat. Rec.* 222, 26–33. doi:10.1002/ar.1092220106

Pahune, P. P., Choudhari, A. R., and Muley, P. A. (2013). The total antioxidant power of semen and its correlation with the fertility potential of human male subjects. *J. Clin. Diagn. Res.* 7, 991–995. doi:10.7860/JCDR/2013/4974.3040

Pandruvada, S., Royfman, R., Shah, T. A., Sindhwani, P., Dupree, J. M., Schon, S., et al. (2021). Lack of trusted diagnostic tools for undetermined male infertility. *J. Assist. Reprod. Genet.* 38, 265–276. doi:10.1007/s10815-020-02037-5

Pelliccione, F., Micillo, A., Cordeschi, G., D'Angeli, A., Necozione, S., Gandini, L., et al. (2011). Altered ultrastructure of mitochondrial membranes is strongly associated with unexplained asthenozoospermia. *Fertil. Steril.* 95, 641–646. doi:10.1016/j.fertnstert.2010.07.1086

Piomboni, P., Focarelli, R., Stendardi, A., Ferramosca, A., and Zara, V. (2012). The role of mitochondria in energy production for human sperm motility. *Int. J. Androl.* 35, 109–124. doi:10.1111/j.1365-2605.2011.01218.x

Quijano, C., Castro, L., Peluffo, G., Valez, V., and Radi, R. (2007). Enhanced mitochondrial superoxide in hyperglycemic endothelial cells: direct measurements and formation of hydrogen peroxide and peroxynitrite. *Am. J. Physiol. Heart Circ. Physiol.* 293, H3404–H3414. doi:10.1152/ajpheart.00761.2007

Reyes, A. M., Hugo, M., Trostchansky, A., Capece, L., Radi, R., Trujillo, M., et al. (2011). Oxidizing substrate specificity of *Mycobacterium tuberculosis* alkyl hydroperoxide reductase E: Kinetics and mechanisms of oxidation and overoxidation. *Free Radic. Biol. Med.* 51, 464–473. doi:10.1016/j.freeradbiomed.2011.04.023

Richer, S. C., and Ford, W. C. (2001). A critical investigation of NADPH oxidase activity in human spermatozoa. *Mol. Hum. Reprod.* 7, 237–244. doi:10.1093/molehr/7.3.237

Robert, K. A., Sharma, R., Henkel, R., and Agarwal, A. (2020). An update on the techniques used to measure oxidative stress in seminal plasma. *Andrologia* 53, e13726. doi:10.1111/and.13726

Roychoudhury, S., Sharma, R., Sikka, S., and Agarwal, A. (2016). Diagnostic application of total antioxidant capacity in seminal plasma to assess oxidative stress in male factor infertility. *J. Assist. Reprod. Genet.* 33, 627–635. doi:10.1007/s10815-016-0677-5

Ruiz-Pesini, E., Diez, C., Lapena, A. C., Perez-Martos, A., Montoya, J., Alvarez, E., et al. (1998). Correlation of sperm motility with mitochondrial enzymatic activities. *Clin. Chem.* 44, 1616–1620. doi:10.1093/clinchem/44.8.1616

Ruiz-Pesini, E., Díez-Sánchez, C., López-Pérez, M. J., and Enríquez, J. A. (2007). The role of the mitochondrion in sperm function: is there a place for oxidative phosphorylation or is this a purely glycolytic process? *Curr. Top. Dev. Biol.* 77, 3–19. doi:10.1016/S0070-2153(06)77001-6

Ruiz-PesiniEPérez, M. J., Diez, C., AlvarEz, E., Enriquez, J. A., and Lopez-Perez, M. J. (2000). Seminal quality correlates with mitochondrial functionality. *Clin. Chim. Acta.* 300, 97–105. doi:10.1016/S0009-8981(00)00305-3

Schindelin, J., Arganda-Carreras, I., Frise, E., Kaynig, V., Longair, M., Pietzsch, T., et al. (2012). Fiji: an open-source platform for biological-image analysis. *Nat. Methods* 9, 676–682. doi:10.1038/nmeth.2019

Sharma, R., Roychoudhury, S., Singh, N., and Sarda, Y. (2017). "Methods to measure reactive oxygen species (ROS) and total antioxidant capacity (TAC) in the reproductive system BT oxidative stress." in *Human reproduction: Shedding light on a complicated phenomenon*. Editors. A. Agarwal, R. Sharma, S. Gupta, A. Harlev, G. Ahmad, S. S. du Plessis, et al. (Cham: Springer International Publishing), 17–46. doi:10.1007/978-3-319-48427-3_2

Skowronek, F., Casanova, G., Alciaturi, J., Capurro, A., Cantu, L., Montes, J. M., et al. (2012). DNA sperm damage correlates with nuclear ultrastructural sperm defects in teratozoospermic men. *Andrologia* 44, 59–65. doi:10.1111/j.1439-0272.2010.01106.x

Sousa, A. P., Amaral, A., Baptista, M., Tavares, R., Caballero Campo, P., Caballero Peregrín, P., et al. (2011). Not all sperm are equal: Functional mitochondria characterize a subpopulation of human sperm with better fertilization potential. *PLoS One* 6, e18112. doi:10.1371/journal.pone.0018112

Stendardi, A., Focarelli, R., Piomboni, P., Palumberi, D., Serafini, F., Ferramosca, A., et al. (2011). Evaluation of mitochondrial respiratory efficiency during *in vitro* capacitation of human spermatozoa. *Int. J. Androl.* 34, 247–255. doi:10.1111/j.1365-2605.2010.01078.x

Storey, B. T. (2008). Mammalian sperm metabolism: oxygen and sugar, friend and foe. *Int. J. Dev. Biol.* 52, 427–437. doi:10.1387/ijdb.072522bs

Tanga, B. M., Qamar, A. Y., Raza, S., Bang, S., Fang, X., Yoon, K., et al. (2021). Semen evaluation: Methodological advancements in sperm quality-specific fertility assessment - a review. *Anim. Biosci.* 34, 1253–1270. doi:10.5713/ab.21.0072

Tourmente, M., Villar-Moya, P., Rial, E., and Roldan, E. R. S. (2015). Differences in ATP generation via glycolysis and oxidative phosphorylation and relationships with sperm motility in mouse species. *J. Biol. Chem.* 290, 20613–20626. doi:10.1074/jbc.M115.664813

Traba, J., Miozzo, P., Akkaya, B., Pierce, S. K., and Akkaya, M. (2016). An optimized protocol to analyze glycolysis and mitochondrial respiration in lymphocytes. *J. Vis. Exp.* doi:10.3791/54918

Twigg, J., Fulton, N., Gomez, E., Irvine, D. S., and Aitken, R. J. (1998). Analysis of the impact of intracellular reactive oxygen species generation on the structural and functional integrity of human spermatozoa: lipid peroxidation, DNA fragmentation and effectiveness of antioxidants. *Hum. Reprod.* 13, 1429–1436. doi:10.1093/humrep/13.6.1429

Uribe, P., Villegas, J. V., Boguen, R., Treulen, F., Sánchez, R., Mallmann, P., et al. (2017). Use of the fluorescent dye tetramethylrhodamine methyl ester perchlorate for mitochondrial membrane potential assessment in human spermatozoa. *Andrologia* 49, e12753. doi:10.1111/and.12753

Vander Borght, M., and Wyns, C. (2018). Fertility and infertility: definition and epidemiology. *Clin. Biochem.* 62, 2–10. doi:10.1016/j.clinbiochem.2018.03.012

Vorup-Jensen, T., Hjort, T., Joanna, V. A. P., Guttmann, P., Jens, C. J., Uggerhøj, E., et al. (1999). X-ray microscopy of human spermatozoa shows change of mitochondrial morphology after capacitation. *Hum. Reprod.* 14, 880–884. doi:10.1093/humrep/14.4.880

Walters, J. L. H., Anderson, A. L., Martins da Silva, S. J., Aitken, R. J., De Iuliis, G. N., Sutherland, J. M., et al. (2020). Mechanistic insight into the regulation of lipoxygenase-Driven lipid peroxidation events in human spermatozoa and their impact on male fertility. *Antioxidants (Basel, Switz.* 10, 10043. doi:10.3390/antiox10010043

Wang, Y., Branicky, R., Noë, A., and Hekimi, S. (2018). Superoxide dismutases: dual roles in controlling ROS damage and regulating ROS signaling. *J. Cell. Biol.* 217, 1915–1928. doi:10.1083/jcb.201708007

Who (2010). WHO Laboratory manual for the examination and processing of human semen. *World Health* 5, 286. doi:10.1038/aja.2008.57

Who (2021). WHO Laboratory manual for the examination and processing of human semen. *World Health* 6, 117. doi:10.1016/j.fertnstert.2021.12.012

Wilton, L. J., Temple-Smith, P. D., and de Kretser, D. M. (1992). Quantitative ultrastructural analysis of sperm tails reveals flagellar defects associated with persistent asthenozoospermia. *Hum. Reprod.* 7, 510–516. doi:10.1093/oxfordjournals.humrep.a137681

Yánez-Ortiz, I., Catalán, J., Mateo-Otero, Y., Dordas-Perpinyà, M., Gacem, S., Yeste, N., et al. (2021). Extracellular reactive oxygen species (ROS) production in fresh donkey sperm exposed to reductive stress,oxidative stress and NETosis. *Antioxidants (Basel, Switz.*, 10. doi:10.3390/antiox10091367

Zhou, M., Diwu, Z., Panchuk-Voloshina, N., and Haugland, R. P. (1997). A stable nonfluorescent derivative of resorufin for the fluorometric determination of trace hydrogen peroxide: applications in detecting the activity of phagocyte NADPH oxidase and other oxidases. *Anal. Biochem.* 253, 162–168. doi:10.1006/abio.1997.2391

Zini, A., Garrels, K., and Phang, D. (2000). Antioxidant activity in the semen of fertile and infertile men. *Urology* 55, 922–926. doi:10.1016/S0090-4295(00)00453-2

Supplementary Material.

Supplementary Figure 1. Semen sample classification for the different experiments. Semen diagnosis from 339 samples was made according to WHO references values (WHO, 2010; WHO 2021).

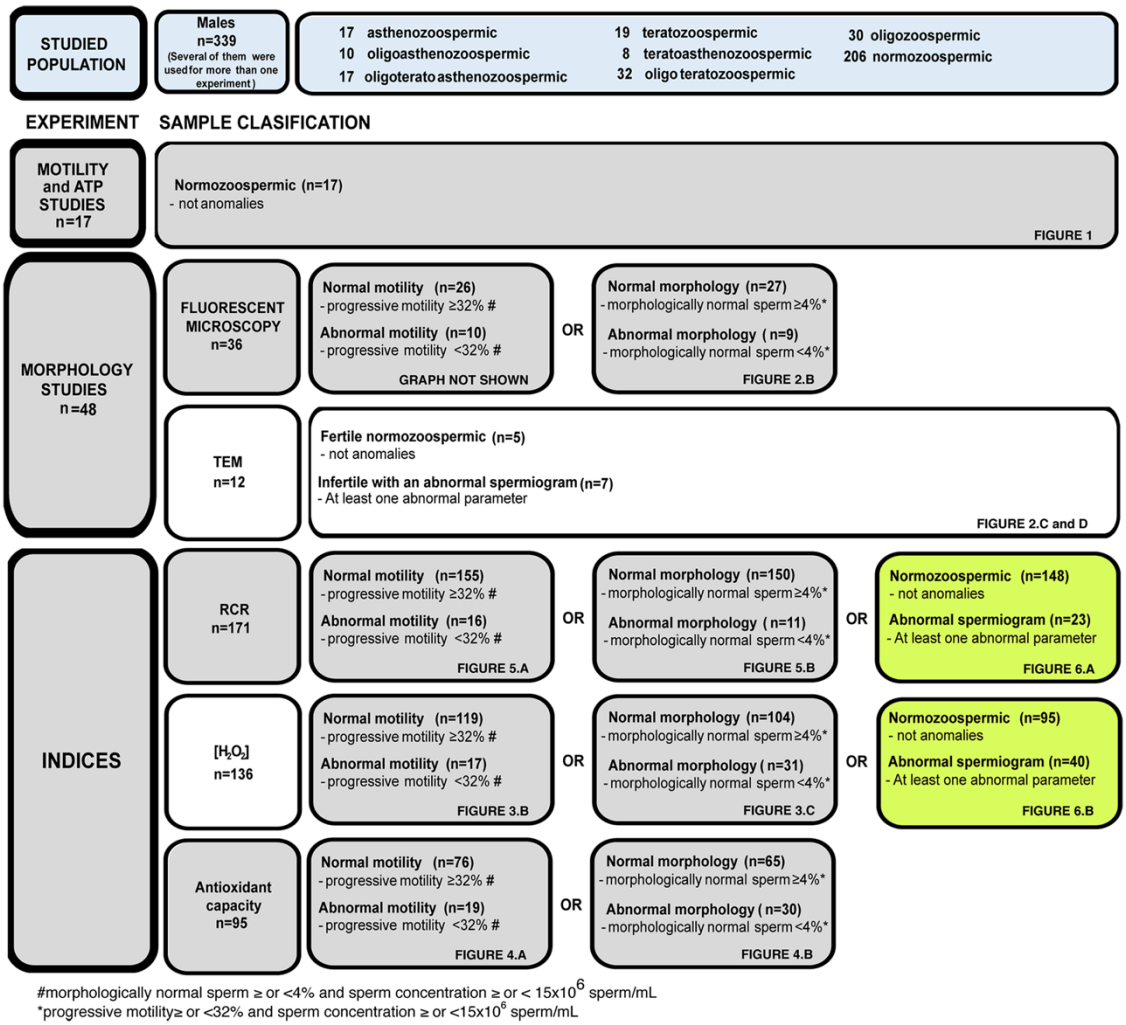

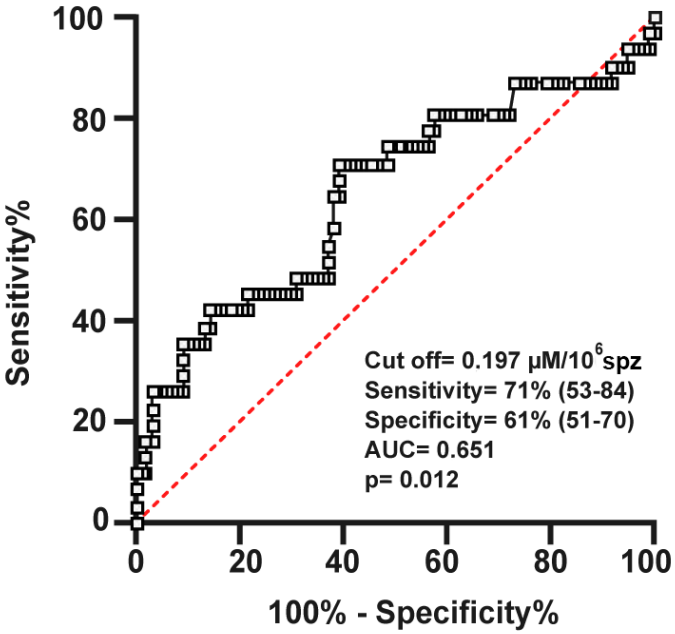

Supplementary Figure 2. Receiver operating characteristic curve (ROC), extracellular [H_2O_2] for samples with normal or abnormal percentage of sperm morphology (reference value ≥ 4%). Area under curve (AUC), sensitivity (%) and specificity (%), cut off are shown.

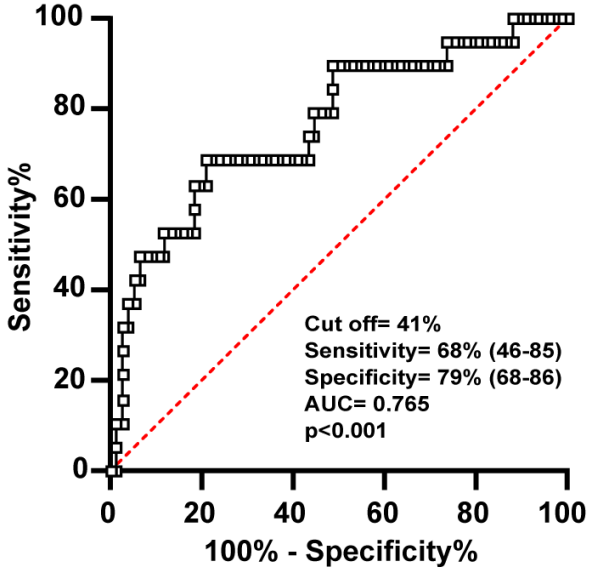

Supplementary Figure 3. Receiver operating characteristic curve (ROC), antioxidant capacity of seminal plasma for samples with normal or abnormal percentage of progressive motility (reference value ≥ 32%). Area under curve (AUC), sensitivity (%) and specificity (%), cut off are shown.

jove

High-Resolution Respirometry to Assess Mitochondrial Function in Human Spermatozoa

Pilar Irigoyen[1], **Rossana Sapiro**[1,3], **Adriana Cassina**[2,3]

[1] Departamento de Histología y Embriología, Facultad de Medicina, Universidad de la República [2] Departamento de Bioquímica, Facultad de Medicina, Universidad de la República [3] Centro de Investigaciones Biomédicas (CEINBIO), Facultad de Medicina, Universidad de la República

Corresponding Authors

Rossana Sapiro
rossanasapiro@gmail.com
Adriana Cassina
adrianamariacassina@gmail.com

Citation

Irigoyen, P., Sapiro, R., Cassina, A. High-Resolution Respirometry to Assess Mitochondrial Function in Human Spermatozoa. *J. Vis. Exp.* (), e65493, doi:10.3791/65493 (2023).

Date Published

June 6, 2023

DOI

10.3791/65493

URL

jove.com/t/65493

Abstract

Semen quality is often studied by routine semen analysis, which is descriptive and often inconclusive. Male infertility is associated with altered sperm mitochondrial activity, so the measurement of sperm mitochondrial function is an indicator of sperm quality. High-resolution respirometry is a method of measuring the oxygen consumption of cells or tissues in a closed-chamber system. This technique can be implemented to measure respiration in human sperm and provides information about the quality and integrity of the sperm mitochondria. High-resolution respirometry allows the cells to move freely, which is an *a priori* advantage in the case of sperm. This technique can be applied with intact or permeabilized spermatozoa and allows for the study of intact sperm mitochondrial function and the activity of individual respiratory chain complexes. The high-resolution oxygraph instrument uses sensors to measure the oxygen concentration coupled with sensitive software to calculate the oxygen consumption. The data are used to calculate respiratory indices based on the oxygen consumption ratios. Consequently, the indices are the proportions of two oxygen consumption rates and are internally normalized to the cell number or protein mass. The respiratory indices are an indicator of sperm mitochondrial function and dysfunction.

Introduction

Male infertility is estimated to account for 40%-50% of all cases of infertility in couples[1]. Conventional semen analysis plays a crucial part in determining male fertility; however, approximately 15% of infertile men have normal sperm parameters[2]. In addition, routine semen analysis provides limited information about sperm function and does not reflect subtle sperm defects[3].

Sperm mitochondria have a special structure, as they are arranged as a helical sheath around the flagella. The mitochondrial sheath contains a variable number of mitochondria connected by intermitochondrial linkers

and anchored to the cytoskeleton by ordered protein arrangements on the outer mitochondrial membrane[4,5]. This structure makes it particularly difficult to isolate sperm mitochondria. Therefore, most studies of sperm mitochondrial function use *in situ* analyses or demembranated sperm[6].

Sperm mitochondrial structure and function have been consistently linked to male infertility[7,8,9,10,11], suggesting that analysis of the structure and function of these organelles may be a good candidate for inclusion in sperm analysis.

Mitochondria play an important role in cellular energy metabolism, particularly by using oxygen to produce adenosine triphosphate (ATP) through oxidative phosphorylation (OXPHOS). In spermatozoa, in particular, the source of ATP (glycolysis vs. OXPHOS) is disputed, and much of the data remains controversial and depends on different experimental approaches[4,12,13]. Measurements of respiration by oximetry offer significant insights into the mitochondrial respiratory capacity, mitochondrial integrity, and energy metabolism of the cell[14,15,16]. Traditionally, this technique has been performed using the Clark oxygen electrode-an instrument that has been used to measure mitochondrial respiration for more than 50 years[17,18]. In addition, sperm mitochondrial oxygen consumption has been analyzed using the classic Clark oxygen electrode[19,20,21]. High-resolution respirometry (HRR) using oxygraphs (Oroboros) provides higher sensitivity than using classical respirometry devices[22]. The oxygraphs are composed of two chambers with injection ports, and each chamber has a polarographic oxygen sensor. With this technique, it is possible to analyze tissue slides, cells, and isolated mitochondrial suspensions. The specimen is continuously stirred in the chamber, and during the experiment, the oxygen consumption is measured, and the oxygen rates are calculated using specific software. The chambers show reduced oxygen leakage, which is an advantage over the conventional oxygen electrode devices[14,23].

As with other cells, in the case of spermatozoa, the sensitivity of HRR equipment is higher than for conventional respirometry, meaning that HRR equipment can be used for the analysis of a limited number of intact or permeabilized sperm cells. There are two main strategies for assessing sperm mitochondrial function: (a) measuring the oxygen consumption in intact cells, which involves reproducing the respiratory function in a medium containing substrates such as glucose, or (b) measuring the oxygen consumption in permeabilized cells using one of the OXPHOS complexes, with the addition of specific substrates to monitor each function separately.

In the present study, we describe the use of high-resolution respirometry (HRR) to determine mitochondrial respiration in human sperm cells.

Protocol

The experiments were approved by the Ethics Committee of the Facultad de Medicina de la Universidad de la República, Montevideo, Uruguay.

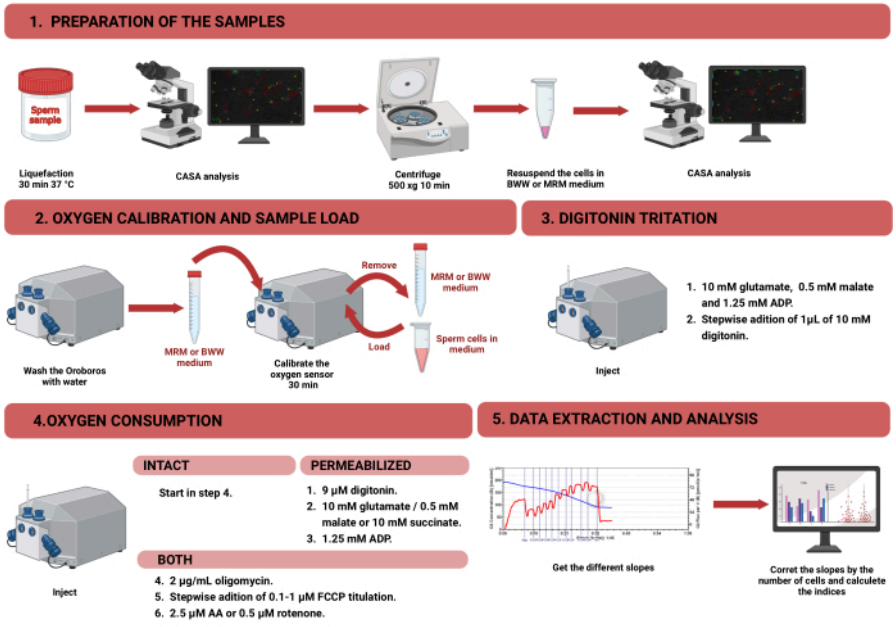

Figure 1: Workflow for high-resolution respirometry to assess mitochondrial function in intact and permeabilized human sperm. The protocol was divided into four different steps: 1) preparation of the sample, 2) oxygen calibration in the Oroboros instrument, 3) oxygen consumption measurement for intact and permeabilized cells, and 4) data extraction from the equipment and analysis. Abbreviations: CASA = computer-assisted sperm analysis; BWW = Biggers Whitten Whittingham medium; MRM = mitochondrial respiration medium; ADP = adenosine diphosphate; FCCP = carbonyl cyanide -p- trifluoromethoxyphenylhydrazone; AA = antimycin A. Please click here to view a larger version of this figure.

NOTE: The workflow for measuring the oxygen consumption in sperm cells using HRR is shown in **Figure 1**. Information on the materials, equipment, and reagents used in the protocol is presented in the **Table of Materials**.

1. Sample preparation

1. Sample collection
    1. Collect freshly ejaculated human semen by masturbation after a recommended 3 day abstinence in a sterile plastic container. Transport the samples immediately to the laboratory.
    2. Incubate the samples for 30-60 min at room temperature (RT) to liquefy completely[24].
    3. After liquefaction, store the samples at 37 °C until the experiment begins.
2. Sperm evaluation with computer-aided sperm analysis (CASA)
    1. Mix the sample, and load 7 µL into a pre-warmed sperm counting chamber.
    2. Place the chamber on the pre-warmed (37 °C) stage of a direct light microscope.

3. Open the computerized sperm analysis software and, enter the motility and concentration module (click on **Mot**).

4. Select the configuration that corresponds to human sperm conditions.

   NOTE: The configuration must be adapted to the type and depth of the chamber as well as to the sample species and the system CASA.

5. Randomly analyze 10 different fields per chamber by clicking on the **Analyze** button.

6. Click on **Results** to obtain the sample concentration and motility.

3. Cell preparation

   NOTE: If the HRR is not calibrated, start with steps 2.1-2.2 before preparing the cells (step 1.3). It is important to measure the oxygen consumption immediately when the sperm cells are resuspended in the medium.

   1. Centrifuge the samples at 400 x *g* for 10 min at RT.

   2. Remove the seminal plasma, and resuspend the spermatozoa in 2 mL of Biggers Whitten Whittingham (BWW) for experiments with intact cells or mitochondrial respiration medium (MRM) for studies with permeabilized cells. The compositions of the media are shown in **Table 1**.

   3. Repeat the steps described in step 1.2 for sperm concentration studies.

2. High-resolution respirometry: OXPHOS analysis

NOTE: HRR integrates highly sensitive oxygraphs (Oxygraph-2 K; Oroboros Instruments GmbH, Innsbruck, Austria) with software (DatLab, version 4.2; Oroboros Instruments GmbH). The experimental data are displayed as the oxygen concentration versus time (as pmol of $O_2/10^6$ cells·min^{-1}) and as real-time transformations of these data, allowing the experimenter to track the respiration (oxygen consumption, oxygen flux) of biological and biochemical samples while the experiment is still running. The HRR can be used to follow the respiration of living and motile cells, which is particularly useful for sperm, whose motility is associated with the sperm quality and fertility potential. The laboratory uses an HRR Oroboros Oxygraph2-k, Oroboros Instruments, with two chambers. The steps described in this protocol must be performed independently for both 2 mL chambers.

1. Equipment preparation

   1. Turn on the high-resolution respirometer, and connect it to the respirometry software (DatLab) for data acquisition and analysis.

   2. Replace the 70% ethanol in the oxygraph chamber with ddH_2O. Stir it continuously with the magnetic stir bar in the chamber at 750 rpm. Let it stand for 10 min, and aspirate the double-distilled (dd) H_2O afterward.

   3. Wash the chamber three times with ddH_2O for 5 min each time.

      NOTE: This step is necessary to remove the remaining ethanol from the chambers. Sperm cells are very sensitive to ethanol. The recording could be compromised if this step is omitted.

2. Calibration of the oxygen sensors

   NOTE: The calibration procedure varies slightly depending on the instrument. Perform an air calibration of the polarographic oxygen sensor as described by the manufacturer[25]. In this section, the calibration protocol is explained briefly.

1. Remove the ddH_2O, and pipette 2 mL of the same medium used for the cell preparation into the chamber. Place the stoppers, leaving an air exchange bubble.
   NOTE: It is important to know the volume of the chamber to determine the exact volume of medium needed.
2. Record the oxygen calibration values (click on **Layout > 01 Calibration Exp. Gr3-Temp**) to monitor the performance of the sensor membrane by stirring the medium with the stir bar at 750 rpm for at least 30 min at 37 °C. Use the other settings as mentioned: gain for sensor: 2; polarization voltage: 800 mV; data recording interval: 2.0 s.
   NOTE: It is expected to obtain an O_2 slope uncorrected (red line) within ±2 $pmol \cdot s^{-1} \cdot mL^{-1}$ with a stable signal from the polarographic sensor.
3. Drag the mouse while holding down the left mouse button and the shift key to select an area where the change in oxygen concentration (Y1 O2 Concentration, blue line) is stable.
4. Open the **O_2 Calibration** window (click on **Oxygraph** > **O2 Calibration**). In **Air Calibration**, change the selected mark to the region selected in step 2.2.3. Finish by clicking on **Calibrate and Copy to Clipboard**.
5. Stop the recording, and save by clicking on **Oxygraph > Ok Control > Save and Disconnect**.
   NOTE: This dataset must be saved so that it can be used in all of the day's experiments. The calibration is only performed once per day for each medium.

3. Digitonin-permeabilization titration

1. Open the chamber, and aspirate the medium inside.
2. Load in the chamber at least 24 x 10^6 and no more than 70 x 10^6 sperm cells in a final volume of 2 mL of MRM.
   NOTE: It is important to measure the number of cells in the chamber in order to adjust the oxygen consumption at the end of the experiment. A lower number of cells than recommended cannot be measured.
3. Close the chamber by pushing the stoppers all the way in, and aspirate the remaining liquid at the top. Start the experiment with the same settings as for the calibration: stirring speed: 750 rpm; temperature: 37 °C; gain for sensor: 2; polarization voltage: 800 mV; and data recording interval: 2.0 s.
4. To load the calibration, double-click on the **Pos Calib** box in the bottom corner. Open the calibration performed in step 2.2 (click on **Oxygraph > O2 Calibration > Copy from File**), and click on **Calibrate and Copy to Clipboard**.
   NOTE: The **POS Calib** box will change from yellow to green. The data are displayed in oxygen flow corrected per volume charts (Layout 05 Flux per Volume uncorrected). Different layouts are available in **Oxygraph > Layout**.
5. Add 5 µL of 0.5 M adenosine diphosphate (ADP), 10 µL of 2 M glutamate, and 2.5 µL of 0.4 M malate (final concentrations: 1.25 mM, 10 mM, and 0.5 mM). Measure the oxygen consumption until the signal stabilizes.
   NOTE: Precision Hamilton micro-syringes are used for injection through the loading port in the stopper. Use one syringe per drug to avoid cross-

contamination. Click on **F4** to register, and mark in the oxygen register when a treatment is added.

NOTE: The substrates are prepared in ultrapure water and stored at −20 °C for 3 months.

6. Tritate by adding 1 µL of 10 mM digitonin in successive steps until the oxygen consumption reaches a maximal level.

NOTE: Thorough washing with water, 70% ethanol, and 100% ethanol is essential if the same chamber is used for two experiments on the same day.

NOTE: Digitonin is prepared in ultrapure water and stored at −20 °C for 3 months.

4. Routine respiratory assessment protocol for intact and permeabilized sperm cells (complex I or complex II)

1. Open the chamber, and aspirate the medium inside.
2. Load in the chamber at least 24 x 10^6 and no more than 70 x 10^6 sperm cells in a final volume of 2 mL of BWW (intact cell analysis) or MRM (permeabilized cell analysis).
3. Start the experiment with the same settings as for the calibration (this is described in step 2.3.3).
4. Load the calibration performed in step 2.2 as described in step 2.3.4.
5. Record the respiration of the cells for at least 5 min until a stable signal is obtained. This measurement corresponds to basal respiration in intact cells.
6. If the experiment is with intact cells, proceed to step 2.4.9. For permeabilized cells, inject 4.5 µL of 10 mM digitonin (final concentration: 22.5 µM). Permeabilize the cells for 5 min.
7. Add the substrates: 10 µL of 2 M glutamate and 2.5 µL of 0.4 M malate (final concentrations: 10 mM and 0.5 mM, respectively) for complex I or 20 µL of 1 M succinate (final concentration: 10 mM) for complex II. Measure the oxygen consumption until the signal increases and stabilizes. This is state 4, which means basal complex I or basal complex II supported respiration in the absence of ADP.

NOTE: The substrates are prepared in milli-Q water and stored at −20 °C for 3 months.

8. Inject 5 µL of 0.5 M ADP (final concentration: 1.25 mM). Measure the oxygen consumption until the signal increases and stabilizes. The addition of ADP increases the signal corresponding to the maximum oxygen consumption through complex I or complex II (state 3, in permeabilized cells).
9. Add 1 µL of 4 mg/mL oligomycin (final concentration: 2 µg/mL), an ATP synthetase inhibitor. Measure the oxygen consumption until the signal decreases and stabilizes.

NOTE: Oligomycin is prepared in ethanol and stored at −20 °C for 3 months.

10. Titrate by adding 1 µL of 0.1 mM to 1 mM carbonyl cyanide-P- trifluoromethoxy-phenylhydrazone (FCCP) in successive steps until a maximum uncoupled respiration rate is reached. Measure the oxygen consumption until the signal increases and stabilizes.

NOTE: FCCP is prepared in ethanol and stored at −20 °C for 3 months.

11. The final concentration of FCCP is sample-dependent. Stop injecting the drug when oxygen consumption begins to decrease.
12. Finally, inject 1 µL of 5 mM antimycin A (2.5 µM final concentration). This is a complex II inhibitor

to discriminate between the mitochondrial and residual oxygen consumption (non-mitochondrial respiration). For the analysis of complex I, add 1 µL of 1 mM rotenone (0.5 µM final concentration), an inhibitor of this complex, instead of AA. Measure the oxygen consumption until the signal decreases and stabilizes.

NOTE: The drugs are prepared in ethanol and stored at −20 °C for 3 months.

3. Data extraction and analysis

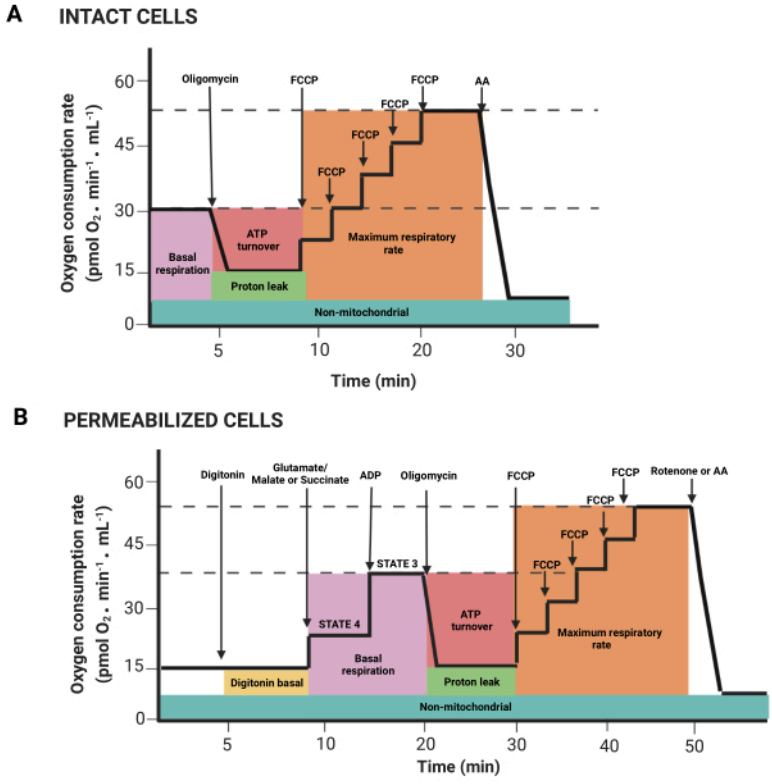

Figure 2: Acquisition of respiratory parameters from a high-resolution respirometry experiment. (**A**,**B**) Schematic representations of graphs obtained, as described in **Figure 1**, for intact and permeabilized cells, respectively. These parameters have been previously described[15]. Please click here to view a larger version of this figure.

1. Drag the mouse by pressing the left mouse button and the shift key to select regions where the oxygen flux per volume correlated (Y2 O2 slope uncorr., red line) is stable after the injection of a substrate or inhibitor. **Figure 2** shows the different parameters obtained from the register previously described[15].

NOTE: The parameters depend on the experiment; all of them are as follows: basal respiration in intact cells and respiration in the presence of glutamate/malate or succinate (state 4), ADP (state 3), oligomycin (proton leak), FCCP (maximum respiration rate), rotenone/AA (non-mitochondrial respiration). In permeabilized cells, basal respiration corresponds to state 3.

2. Click on the **Marks > Statistics** windows, and export the data.
3. Normalize the data obtained per 1 million sperm cells. The units of the slopes are $pmolO_2 \cdot s^{-1} \cdot mL^{-1} \cdot 10^{-6}$ cells.
4. Subtract the non-mitochondrial oxygen consumption from all the values before calculating the indices.
5. Calculate the indices using the various equations previously described[15]:

$$Coupling\ efficiency = \frac{ATP\ turnover}{Basal\ respiration} = \frac{Basal\ respiration - proton\ leak}{Basal\ respiration}$$

$$Spare\ respiratory\ capacity = \frac{Maximum\ respiratory\ rate}{Basal\ respiration}$$

$$Respiration\ control\ ratio\ (RCR) = \frac{Maximum\ respiratory\ rate}{Proton\ leak}$$

$$For\ permeabilized\ cells \mid Respiration\ control\ ratio\ (RCR) = \frac{State\ 3\ (after\ addition\ of\ ADP)}{State\ 4\ (after\ addition\ of\ substrate)}$$

Representative Results

Determination of the optimal concentration of digitonin in sperm cells

In this protocol, we present the use of HRR to monitor real-time changes in OXPHOS in human sperm cells. Since the method can be used to analyze intact or digitonin-permeabilized sperm, we first present the standardization of digitonin concentration required to permeabilize sperm cells (**Figure 3**).

Digitonin is used for chemical permeabilization, which allows substrates to enter cells, and for measuring mitochondrial activity. This compound must be titrated in intact cells to obtain the optimal concentration required to ensure cell membrane permeabilization without compromising mitochondrial membrane integrity. We performed a titration in the presence of ADP, glutamate, and malate. Respiration rates were measured at baseline and after the gradual addition of digitonin (**Figure 3A**). Oxygen consumption rises with increasing detergent concentration and reaches a point where the integrity of the outer mitochondrial membrane starts to be compromised (red arrow in **Figure 3A**). **Figure 3B** shows the mean ± standard error of 4 representative experiments. The result shows that permeabilization is optimal at a digitonin concentration of 22.5 µM (**Figure 3A**,**B**). Mitochondrial activity decreases when too high amounts of digitonin are used.

Representation of successful and suboptimal register of sperm respiration by HRR

During monitoring sperm mitochondrial respiration, the register can be visualized as O_2 concentration (blue line) and O_2 flow per volume correlated (red line) calculated with the DatLab 4 analysis software in both permeabilized and non-permeabilized cells (**Figure 4**). **Figure 4** shows representative curves of intact (**Figure 4A**,**B**) and digitonin-permeabilized (**Figure 4C**,**D**) sperm cells from a semen sample. **Figure 4A** represents a successful recording of intact sperm cells from a semen sample, where the effects of drugs modulating oxygen consumption are observed, and it is possible to extract the parameters for calculating the indices. Basal respiration is recorded in intact cells by oxygen consumption in the presence of exogenous substrates. Then, the non-phosphorylating respiration rate was measured by adding an ATP synthase inhibitor (oligomycin). Subsequently, the protonophore FCCP was injected at different concentrations and the maximal mitochondrial uncoupled respiration rate was determined. This drug leads to an increase in proton permeability of the inner membrane, which allows the passive movement of protons to dissipate the chemiosmotic gradient that causes

an increase in oxygen consumption. Finally, AA was added to inhibit mitochondrial respiration.

The quality of the data obtained is closely related to the cell number. It is important to have a high basal oxygen consumption to obtain a good record. The subsequent analysis depends on subtle changes in O_2 consumption that may not be detected if the basal line is not high enough. Cell counts lower than recommended could lead to a result like **Figure 4B**.

Representative curves obtained using the protocol for complex I or II specific substrates are shown in **Figure 4C** and **Figure 4D**, respectively. To study oxygen consumption through the mitochondrial complex I or complex II, the substrates malate and glutamate or succinate were added after permeabilization of the cells. Then, ADP is added for conversion to ATP (state 3, active complex I or II dependent respiration). Finally, rotenone or AA is administered to inhibit complex I or II, respectively.

For interpretation of the results, it is important to consider that cellular respiration inhibited by oligomycin is a direct measurement of proton leakage rate across the mitochondrial membrane in intact cells, which is comparable to the state 4 of permeabilized cells (without ADP) (**Figure 2B**). In the case of intact cells (non-permeabilized), this amount indicates the fraction of basal mitochondrial oxygen consumption that is independent of ATP synthesis. The maximum respiration rate is reached after the addition of several doses of FCCP. In intact cells depends on two factors; the activity of the electron transport complexes and the number of mitochondria in each cell. State 3 of permeabilized cells after the addition of ADP resembles basal respiration of the intact cell at saturating concentrations of exogenous substrates (**Figure 2B**)[7]. **Table 2** shows an example of the indices calculated from the records in **Figure 4**.

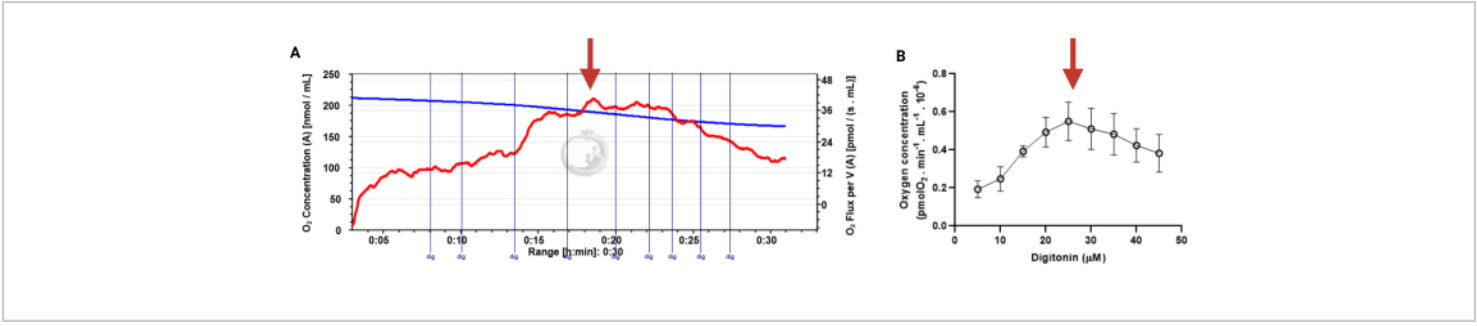

Figure 3: Determination of the optimal concentration of digitonin for the permeabilization of human sperm cells. The respiration rates were measured at 37 °C in MRM medium with glutamate, malate, and adenosine diphosphate. (**A**) Representative respiratory trace. The blue line is the O_2 concentration, and the red line represents the O_2 flow per volume correlated. (**B**) Mitochondria respiration rate means ± standard error, n = 4. The red arrow represents the optimal concentration. Abbreviation: dig = digitonin. Please click here to view a larger version of this figure.

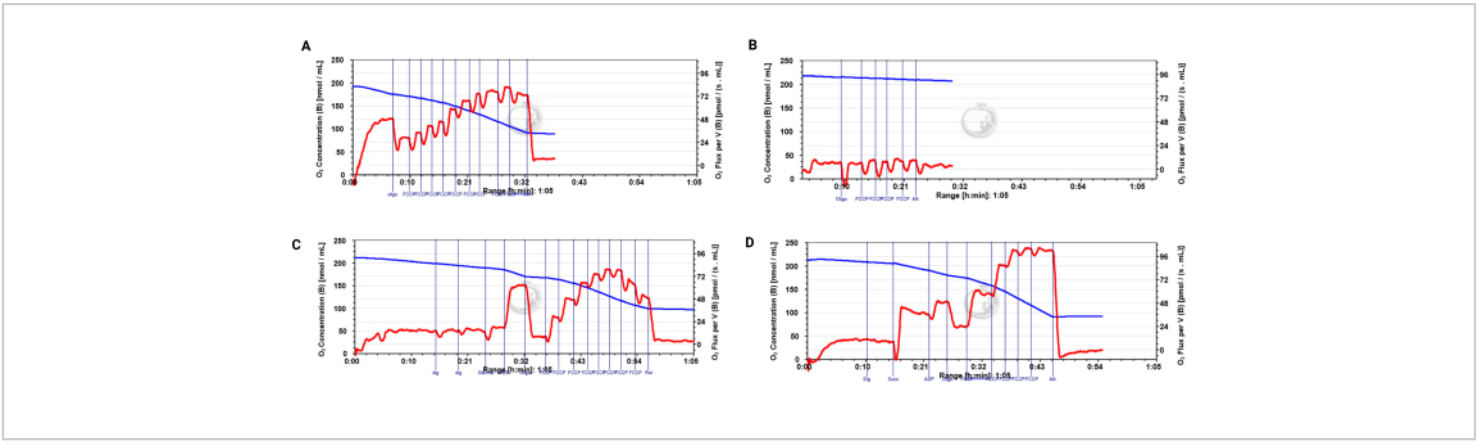

Figure 4: Representative respiratory traces for the oxygen consumption rate obtained using the Oroboros instrument. The respiration rates were measured at 37 °C in (**A**,**B**) intact and (**C**,**D**) permeabilized cells. The blue line is the O_2 concentration, and the red line represents the O_2 flow per volume correlated. The rates in **A**, **C**, and **D** were measured with more than 30 x 10^6 sperm cells, while the rate in **B** was measured with 14 x 10^6 sperm cells. Abbreviations: Oligo = oligomycin; FCCP = carbonyl cyanide -p- trifluoromethoxyphenylhydrazone; Glu/Mal = glutamate/malate; ADP = adenosine diphosphate; AA = antimycin A; Rot = rotenone. Please click here to view a larger version of this figure.

Table 1: Composition of BWW and MRM media for experiments with intact or permeabilized cells, respectively. Please click here to download this Table.

Table 2: Representative examples of HRR indices. Data were obtained from the traces shown in **Figure 4**. The indices were calculated according to **Figure 2** and protocol section 3. Please click here to download this Table.

Discussion

HRR critically depends on several steps: (a) the equipment maintenance, (b) accurate calibration of the oxygen sensors, (c) the uncoupler titration[26], and finally, (d) the adequate use of indices representing the mitochondrial function. The equipment maintenance is crucial. It is recommended to replace the membranes of the polarographic oxygen sensor regularly and to correct the instrumental background. Extensive washing after the collection of spermatozoa from the chambers is essential to obtain good replicates, especially in laboratories in which the instruments are frequently used to analyze various tissues or cells. Spermatozoa are sensitive to even small amounts of rotenone, AA, oligomycin, and FCCP, so the washing step must be performed carefully (at least three times with ethanol and another three times with distilled water). Calibration is a crucial step; it must be performed every day and for each of the media used (see protocol step 2.2). The uncoupler titrations must be performed carefully, as the optimal uncoupler concentrations must be used to achieve the maximum stimulation of flux and avoid over-titration, which paradoxically inhibits respiration[27]. The optimal uncoupler concentration depends on the cell type, cell concentration, and medium and is different for permeabilized cells compared to intact cells[14]. Thus, in the case of sperm samples, in which the sperm cells may be heterogeneous, the uncoupler must be adapted to each sample[28,29,30]. After respirometry, several parameters are obtained that

must be corrected for the number of cells before analysis. Three indices are calculated that allow for the interpretation of mitochondrial function, and these have the advantage of being independent of the number of mitochondria and cells. We highlight the use of respiratory control ratio (RCR), which indicates the efficiency of mitochondrial coupling and is sensitive to multiple potential sites of dysfunction[7]. However, other parameters and indices may be used depending on the experiment[31].

The limitations of HRR are as follows: (a) the device is not automated, so it requires the constant presence of an operator and is time-consuming; (b) the HRR device has only two chambers, and only two assays can be performed simultaneously; (c) the chambers are not single-use and can be contaminated with inhibitors or another type of tissue; (d) although the sensitivity of the instrument is very high, our team found that at least 12 million/mL of sperm are required to detect variations in oxygen consumption, so we could not measure sperm from oligozoospermic males; and (e) the operator must be aware that the measurements are for all the cells present in the samples. Semen samples are heterogeneous and contain other cell types (e.g., leukocytes). To avoid contamination, it is necessary to use samples with low concentrations of leukocytes[7]. Alternatively, an additional sperm purification step can be performed prior to the oximeter experiments (e.g., swim-up or swim-down)[24].

An alternative to HRR is the use of the extracellular flux analyzer. The advantages of the extracellular flux analyzer over the high-resolution oxygraph for measuring sperm metabolism are as follows: (a) the extracellular flux analyzer is a largely automated instrument; (b) it can measure the oxygen consumption in 24-well and 96-well plates for high-throughput screening, meaning it requires smaller amounts of biological samples; and (c) it permits the additional measurement of sperm glycolytic flux. Some advantages of HRR over the extracellular flux analyzer are as follows: (a) with HRR, the cost of the instrument and consumables is lower; (b) with HRR, three to four replicates of each measurement are not required as in the extracellular flux analyzer, for which these replicates are needed to address the high fluorescence variability; (c) the feasibility of the substrate uncoupler inhibitor titration protocols with HRR is high; and (c) the cells are monitored in motion and not attached. Oximetry can analyze the oxygen consumption of motile (live) and intact (non-permeabilized) spermatozoa[7,31,32]. This is an advantage in the case of spermatozoa since sperm adhesion to the plastic surface may potentially alter their movement patterns and function.

HRR is more sensitive than conventional respirometry and is suitable for medical use in human spermatozoa, for which the number of cells from each semen sample cannot be increased (such as cultured cells). This technique can be used to monitor sperm respiration from most semen samples, both from normal and infertile men. RCR can be used as a good indicator of human sperm functional status, and a cut-off value of 3.15 (sensitivity and specificity of 73% and 61%, respectively) distinguishes between sperm samples with normal and abnormal conventional semen analysis[32]. HRR could be used to understand sperm mitochondrial metabolism, which may be responsible for male infertility, and be a complement to standard semen analysis.

The latest new generation of Oroboro instruments allows the analysis of oxygen consumption in conjunction with other sperm functions, such as the production of H_2O_2, and could help to understand sperm function.

Disclosures

The authors have nothing to disclose.

Acknowledgments

We would like to thank the Fertilab Andrology clinic, especially José María Montes and Andrea Torrents, for allowing us access to donors. Funding: A.C. is supported by grants from Universidad de la República (CSIC_2018, Espacio Interdisciplinario_2021). Additional funding was obtained from the Programa de Desarrollo de Ciencias Básicas (PEDECIBA, Uruguay). P.I. and R.S. are supported by Universidad de la República (I+D, CSIC 2014; I+D, CSIC 2016, Iniciación a la Investigación, CSIC 2019 and FMV_1_2017_1_136490 ANII- Uruguay). P.I. is supported by POS_FMV_2018_1_1007814 and CAP-UDELAR 2020. The figures were illustrated using Biorender.com.

References

1. Agarwal, A., Mulgund, A., Hamada, A., Chyatte, M. R. A unique view on male infertility around the globe. *Reproductive Biology and Endocrinology.* **13**, 37 (2015).
2. Guzick, D. S. et al. Sperm morphology, motility, and concentration in fertile and infertile men. *The New England Journal of Medicine.* **345** (19), 1388-1393 (2001).
3. Wang, C., Swerdloff, R. S. Limitations of semen analysis as a test of male fertility and anticipated needs from newer tests. *Fertility and Sterility.* **102** (6), 1502-1507 (2014).
4. Amaral, A. Energy metabolism in mammalian sperm motility. *WIREs Mechanisms of Disease.* **14** (5), e1569 (2022).
5. Leung, M. R. et al. In-cell structures of conserved supramolecular protein arrays at the mitochondria-cytoskeleton interface in mammalian sperm. *Proceedings of the National Academy of Sciences of the United States of America.* **118** (45), e2110996118 (2021).
6. Moraes, C. R., Meyers, S. The sperm mitochondrion: Organelle of many functions. *Animal Reproduction Science.* **194**, 71-80 (2018).
7. Cassina, A. et al. Defective human sperm cells are associated with mitochondrial dysfunction and oxidant production. *Biology of Reproduction.* **93** (5), 119 (2015).
8. Marchetti, C., Obert, G., Deffosez, A., Formstecher, P., Marchetti, P. Study of mitochondrial membrane potential, reactive oxygen species, DNA fragmentation and cell viability by flow cytometry in human sperm. *Human Reproduction.* **17** (5), 1257-1265 (2002).
9. Amaral, A., Lourenço, B., Marques, M., Ramalho-Santos, J. Mitochondria functionality and sperm quality. *Reproduction.* **146** (5), R163-R174 (2013).
10. Durairajanayagam, D., Singh, D., Agarwal, A., Henkel, R. Causes and consequences of sperm mitochondrial dysfunction. *Andrologia.* **53** (1), e13666 (2021).
11. Uribe, P. et al. Use of the fluorescent dye tetramethylrhodamine methyl ester perchlorate for mitochondrial membrane potential assessment in human spermatozoa. *Andrologia.* **49** (9), e12753 (2017).
12. Storey, B. T. Mammalian sperm metabolism: Oxygen and sugar, friend and foe. *The International Journal of Developmental Biology.* **52** (5-6), 427-437 (2008).
13. Tourmente, M., Sansegundo, E., Rial, E., Roldan, E. R. S. Capacitation promotes a shift in energy metabolism

in murine sperm. *Frontiers in Cell and Developmental Biology.* **10**, 950979 (2022).

14. Gnaiger, E. Chapter 12 - Polarographic oxygen sensors, the oxygraph, and high-resolution respirometry to assess mitochondrial function. In *Drug-Induced Mitochondrial Dysfunction.*, edited by Dykens, J. A., Will, Y., 325-352.John Wiley & Sons, Inc. Hoboken, NJ (2008).
15. Brand, M. D., Nicholls, D. G. Assessing mitochondrial dysfunction in cells. *Biochemical Journal.* **435** (2), 297-312 (2011).
16. Awadhpersad, R., Jackson, C. B. High-resolution respirometry to assess bioenergetics in cells and tissues using chamber- and plate-based respirometers. *Journal of Visualized Experiments: JoVE.* (176), e63000 (2021).
17. Chance, B., Williams, G. R. A simple and rapid assay of oxidative phosphorylation. *Nature.* **175** (4469), 1120-1121 (1955).
18. Li, Z., Graham, B. H. Measurement of mitochondrial oxygen consumption using a Clark electrode. *Methods in Molecular Biology.* **837**, 63-72 (2012).
19. Stendardi, A. et al. Evaluation of mitochondrial respiratory efficiency during in vitro capacitation of human spermatozoa. *International Journal of Andrology.* **34** (3), 247-255 (2011).
20. Ferramosca, A., Focarelli, R., Piomboni, P., Coppola, L., Zara, V. Oxygen uptake by mitochondria in demembranated human spermatozoa: A reliable tool for the evaluation of sperm respiratory efficiency. *International Journal of Andrology.* **31** (3), 337-345 (2008).
21. Ferramosca, A. et al. Modulation of human sperm mitochondrial respiration efficiency by plant polyphenols. *Antioxidants.* **10** (2), 217 (2021).
22. Gnaiger, E., Steinlechner-Maran, R., Méndez, G., Eberl, T., Margreiter, R. Control of mitochondrial and cellular respiration by oxygen. *Journal of Bioenergetics and Biomembranes.* **27** (6), 583-596 (1995).
23. Gnaiger, E. O2k Quality Control 1: Polarographic oxygen sensors and accuracy of calibration. At <https://www.bioblast.at/images/archive/7/77/20210819114548%21MiPNet06.03_POS-Calibration-SOP.pdf> (2020).
24. World Health Organization. WHO Laboratory Manual for the Examination and Processing of Human Semen. At <https://www.who.int/publications/i/item/9789240030787> (2010).
25. Gnaiger, E. O2k-protocols SOP: O2k quality control 1. At <https://www.bioblast.at/images/9/9c/MiPNet06.03_POS-Calibration-SOP_DatLab8.pdf> (2021).
26. Gnaiger, E. *Mitochondrial Pathways and Respiratory Control.* OROBOROS MiPNet Publications. Innsbruck, Austria (2012)
27. Steinlechner-Maran, R., Eberl, T., Kunc, M., Margreiter, R., Gnaiger, E. Oxygen dependence of respiration in coupled and uncoupled endothelial cells. *The American Journal of Physiology.* **271** (6 Pt 1), C2053-C2061 (1996).
28. Holt, W. V., Van Look, K. J. W. Concepts in sperm heterogeneity, sperm selection and sperm competition as biological foundations for laboratory tests of semen quality. *Reproduction.* **127** (5), 527-535 (2004).

29. Sousa, A. P. et al. Not all sperm are equal: Functional mitochondria characterize a subpopulation of human sperm with better fertilization potential. *PloS One.* **6** (3), e18112 (2011).

30. Moscatelli, N. et al. Single-cell-based evaluation of sperm progressive motility via fluorescent assessment of mitochondria membrane potential. *Scientific Reports.* **7**, 17931 (2017).

31. Ferreira, J. J. et al. Increased mitochondrial activity upon CatSper channel activation is required for mouse sperm capacitation. *Redox Biology.* **48**, 102176 (2021).

32. Irigoyen, P. et al. Mitochondrial metabolism determines the functional status of human sperm and correlates with semen parameters. *Frontiers in Cell and Developmental Biology.* **10**, 926684 (2022).

Table 1. Composition of BWW and MRM media for experiments with intact or permeabilized cells, respectivetly.

Reagent	Final concentration (mM)
BWW medium (1L)	
NaCl	95
$NaC_3H_5O_3$	44
HEPES	20
D-Glucose	5.6
KCl	4.6
$CaCl_2\ 2H_2O$	1.7
KH_2PO_4	1.2
$MgSO_4\ 7H_2O$	1.2
Pyruvate	0.27
BSA	0.30 %
$NaHCO_3$	25
MRM medium (1L)	
EGTA	1
MOPS	5
Saccharose	300
KH_2PO_4	5
BSA	0,10%

Table 2.Representative examples of HRR indices. Data were obtained from the traces shown in Figure 4. The indices were calculated according to Figure 2 and protocol section 3.

		Basal	Oligo	FCCP	AA or ROT	**RCR**	**Coupling efficiency**	**Spare respratory capacity**
Intact cells (Figure 4.A)		47.59	28.99	81.23	6.32	3.30	0.45	1.82
Substract AA		41.27	22.66	74.91	0.00			
	Glu/Mal or Succ	ADP	Oligo	FCCP	AA or ROT	**RCR**	**Coupling efficiency**	**Spare respratory capacity**
Complex I (Figure 4.C)	17.67	62.62	8.07	79.23	3.30	4.13	0.92	1.28
Substract Rot	14.37	59.32	4.77	75.93	0.00			
Complex II (Figure 4.D)	38.73	48.75	23.66	102.21	0.00	1.26	0.51	2.10
Substract AA	38.73	48.75	23.66	102.21	0.00			

Table of Materials		
Name of Material	**Company**	**Catalog Number**
Sperm Counting Chamber DRM-600	Millennium Sciences CELL-VU	
Sodium pyruvate	Sigma Aldrich	P2256
Sodium lactate	Sigma Aldrich	L7022
HEPES	Sigma Aldrich	H3375
D-glucose	Sigma Aldrich	G7021
Potassium chloride	Sigma Aldrich	P3911
Calcium chloride	Sigma Aldrich	C4901
Magnesium sulphate	Sigma Aldrich	M7506
Acid free- Bovine serum albumine	Sigma Aldrich	A8806
Sodium bicarbonate	Sigma Aldrich	S5761
Saccharose	Sigma Aldrich	S0389
MOPS	Sigma Aldrich	M1254
EGTA	Sigma Aldrich	E4378
Monopotassium phosphate	Sigma Aldrich	P5655
Digitonin	Sigma Aldrich	D141
Succinate disodium salt	Sigma Aldrich	W327700
L malic acid	Sigma Aldrich	M1000
L glutamic acid	Sigma Aldrich	G1251
Oligomycin A	Sigma Aldrich	75351
carbonyl cyanide-P- trifluoromethoxy-phenylhydrazone	Sigma Aldrich	C2920
Animycin A from streptomyces sp.	Sigma Aldrich	A8674
Rotenone	Sigma Aldrich	R8875
Adenosine 5'-diphosphate monopotassium salt dihydrate	Sigma Aldrich	A5285
Name of Equipment		
Oxygraph-2 K	Oroboros Instruments GmbH	
DatLab sofware version 4,2	Oroboros Instruments GmbH	
Microscope Eclipse E200 with phase contrast 10X Ph+	Nikon	
Microscope camera	Basler	acA780-75gc
Power O2k-Respirometer	Oroboros Intruments	10033-01

Sperm class analyzer 6.3.0.59 Evolution-SCA Research	Microptic	
Microliter Syringes	Hamilton	87900 or 80400

6. Discusión general

El factor masculino puede ser causa de la infertilidad de pareja en hasta un 50% de los casos. A pesar de la multiplicidad de estudios existentes, hay consenso de que la comprensión de la fisiología del espermatozoide humano maduro es limitada y que esto representa un obstáculo significativo para el desarrollo de herramientas diagnósticas y terapéuticas imprescindibles para mejorar las condiciones de fertilidad de las parejas[10,167–170]. La tesis se centra en comprender el rol de la mitocondria en la fisiología del espermatozoide, analizando su función en hombres normozoospérmicos, específicamente en la capacitación espermática. Se trabajó también con un modelo de ratón KO que carece del canal Catsper, principal responsable de la entrada del Ca^{2+} y modulador de la capacitación. En este modelo se analizó el papel de la mitocondria en la fecundación, lo cual no es posible realizar por razones éticas y legales en los espermatozoides humanos. Los datos obtenidos fueron aplicados para obtener índices de función mitocondrial en muestras de semen humanas con potencialidad en andrología.

La fuente de energía para la función de los espermatozoides es motivo de controversia. Existe consenso en que la capacitación espermática requiere energía para los procesos como la RA y la hiperactivación, sin embargo, el papel de la mitocondria en la capacitación continúa siendo debatido. Para algunos autores, la glucólisis es suficiente para mantener tanto la motilidad progresiva como los parámetros de capacitación[122,123,127,136,171–174]. Intentando esclarecer estos mecanismos y buscando comprender las causas de los resultados aparentemente contradictorios en la literatura, utilizamos HRR para medir la actividad mitocondrial en espermatozoides en condiciones NC y CAP (artículos 1,2 y 3). En particular, el HRR, además de su alta sensibilidad, para nuestro modelo tiene dos grandes ventajas. Primero, es que los espermatozoides no deben ser adheridos en placa, la medición se realiza en células vivas y móviles[116,175,176]. Segundo, el protocolo puede ajustarse en tiempo real en cada experimento, lo cual es importante debido a la heterogeneidad de las muestras de semen[177,178].

Mediante HRR demostramos que la función mitocondrial aumenta durante la capacitación espermática en ratón y humano (artículos 1,2 y 3). Observamos en ambos modelos, un aumento en el RCR en los espermatozoides CAP. El RCR refleja aspectos clave de la función mitocondrial, como la eficiencia de la cadena respiratoria, el PMM y la cantidad de O_2 consumido destinado a la producción de ATP, lo que sugiere un aumento general en la actividad mitocondrial durante la capacitación espermática[76,116]. Confirmamos los datos midiendo el PMM (artículos 1 y 2), utilizando la sonda sensible al voltaje TMRM (tetramethyl rhodamine methyl ester perchlorate) a nivel poblacional por citometría de flujo y en células individuales mediante microscopía óptica (en ratones, artículo 1)[179]. En conjunto, estos resultados refuerzan el papel fundamental de la función mitocondrial en el proceso de capacitación[49,53,115].

Nuestros datos mostraron que el aumento de la actividad mitocondrial espermática se relaciona con la hiperactivación y la fecundación, pero no es necesaria para la RA ni la fosforilación de tirosina (artículos 1 y 2). Hallazgos similares fueron reportados por otros autores en ratones KO para CatSper, donde los espermatozoides no logran hiperactivarse ni fertilizar, pero la RA y la fosforilación de tirosina permanecen intactas[180]. Consistentemente, observamos que los espermatozoides de los ratones KO para CatSper, no muestran aumento en su función mitocondrial (ni RCR, ni PMM) en condiciones capacitantes. Esto condujo a hipotetizar que la entrada de Ca^{2+} por Catsper puede estar asociada al aumento del RCR observado en espermatozoides CAP. Aunque los blancos *downstream* del aumento de Ca^{2+} citoplasmático mediado por CatSper no se han caracterizado completamente[37,180], otros trabajos han mostrado que los espermatozoides KO para CatSper presentan un déficit en la producción de ATP. Es posible que la propagación de Ca^{2+} desde la cola hasta la cabeza, iniciada por la activación de

CatSper, desencadene un aumento en [NADH] y regule la homeostasis de ATP[181].

Planteamos la hipótesis de que el Ca^{2+} que ingresa durante la capacitación podría entrar en la mitocondria y regular su función, desencadenando el aumento en la actividad mitocondrial observado. Los espermatozoides capacitados de ratón y humano, mostraron un aumento del Ca^{2+} mitocondrial (artículos 1 y 2). Consistente con lo reportado en células somáticas este incremento se produce a través del MCU[182,183], ya que la inhibición de este canal redujo, tanto los niveles de Ca^{2+} mitocondrial en espermatozoides de ratón durante la capacitación, como la hiperactivación. Nuestros resultados no descartan que existan otros reservorios de Ca^{2+} que sean fuente del Ca^{2+} intramitocondrial. Se sabe que el MCU tiene una baja afinidad para captar Ca^{2+}[183,184], y pueden existir otros sitios de ingreso del ion a las mitocondrias, por ejemplo en regiones especializadas de contacto cercano entre ellas y los residuos de RE presentes en los espermatozoides[183,185]. Es importante destacar que nuestros hallazgos sugieren que el papel del Ca^{2+} en la homeostasis mitocondrial durante la CAP es un mecanismo común en ambas especies estudiadas (humano y ratón). Tanto la actividad mitocondrial como la concentración de Ca^{2+} mitocondrial están aumentados en espermatozoides CAP humanos.

La regulación de la función mitocondrial mediada por Ca^{2+} podría no solamente estar orientada hacia la producción de ATP sino también de ROS necesarias para la capacitación. El papel de ROS en la capacitación ha sido estudiado pero nuevamente, los mecanismos *downstream* no se conocían hasta el momento[106,155,186]. El aumento de la función mitocondrial, resulta en un incremento en el suministro de NADH y FADH que podría contribuir a mantener un pool reducido de formas de mononucleótidos de flavina o ubiquinona, facilitando la transferencia de un electrón al oxígeno para formar $O_2^{\bullet-}$ [90,187]. Esta hipótesis se basa en el hecho de que, paralelamente al aumento de la función mitocondrial observado mediante HRR, los espermatozoides humanos CAP mostraron una mayor respiración mitocondrial en presencia de AA, en comparación con los espermatozoides NC (artículo 3). En presencia de sustratos mitocondriales, la AA inhibe el complejo III de la cadena respiratoria, lo que lleva a un aumento en la formación de semiquinonas y, por ende se favorece la reducción parcial del oxígeno favoreciendo la producción de $O_2^{\bullet-}$ por el complejo II[90]. Esto se vio reflejado en un aumento de ROS en los espermatozoides, lo cual fue respaldado por un aumento en la formación de H_2O_2 extracelular en los espermatozoides CAP. Debido a la selectividad de la reactividad del $O_2^{\bullet-}$ hacia el grupo Fe-S de la ACO2, su actividad se ha convertido en un ensayo sensible para medir la variación de los niveles de $O_2^{\bullet-}$ dentro de las células y las mitocondrias en una amplia variedad de tipos de células y condiciones[188]. Comprobamos que la mayoría del H_2O_2 podría tener un origen mitocondrial midiendo la actividad de la ACO2 en los espermatozoides y cuantificando la producción relativa de $O_2^{\bullet-}$ por los mismos. Los espermatozoides CAP producen aproximadamente un 60% más de $O_2^{\bullet-}$ en comparación con los NC (artículo 3).

La producción de ROS en los espermatozoides juega un papel dual en la función o disfunción celular, dependiendo de la tasa de formación y los niveles de equilibrio[157]. Nosotros mostramos un aumento de ROS durante la capacitación que no produce daño espermático (no hay cambios ni en la peroxidación lipídica ni en la actividad del complejo II, artículo 3), lo que sugiere que la producción de ROS durante la capacitación tienen un rol en la señalización del proceso, concentraciones superiores de estas especies podrían llevar al daño celular.

A partir de los datos obtenidos de las dos primeras secciones proponemos el siguiente modelo (Figura 9): durante la capacitación espermática, la activación del canal CatSper induce un influjo de Ca^{2+} que produce un aumento en la concentración citoplasmática del ión. Este aumento de Ca^{2+} intracelular comienza en la pieza principal y se propaga a través de la pieza media llegando a la cabeza. El canal MCU transporta Ca^{2+} a las mitocondrias, que activa enzimas intra-mitocondriales resultando en un aumento en la función mitocondrial. La mayor actividad de la

cadena de transportes de electrones produce un incremento en la producción de ATP y la formación de $O_2^{\bullet-}$ mitocondrial. El $O_2^{\bullet-}$ interacciona con otras moléculas generando otras ROS, como el H_2O_2, que poseen un rol en la señalización durante el proceso no generando daño por estrés oxidativo. El mecanismo descrito es esencial para que se den cambios fisiológicos que implican la capacitación, entre estos, la hiperactivación necesaria para fertilizar el ovocito.

Finalmente, buscamos aplicar los resultados obtenidos en la práctica clínica. Existen diversos estudios que han asociado los parámetros del semen con la función mitocondrial[116,120,189–193]. Sin embargo, la evaluación de la actividad mitocondrial de los espermatozoides no suele incluirse en los estudios de análisis de semen en humanos. Apoyando la importancia de incluir mediciones de actividad mitocondrial en los estudios del hombre infértil, es la correlación positiva observada entre el RCR con la morfología y la motilidad espermática en muestras de donantes con múltiples alteraciones en el espermograma (artículo 4). El análisis detallado (describiendo los pasos y controles necesarios para obtener resultados confiables con este método) se puede encontrar en Irigoyen et al (artículo 5). Aunque aún son pocos los reportes usando HRR, otros investigadores han empleado esta técnica para analizar el metabolismo espermático, evaluando cambios en la función mitocondrial bajo diferentes condiciones experimentales[194–196] o diferencias entre espermatozoides de hombres normozoospérmicos y astenozoospérmicos[194,197], lo que apoya su potencial aplicación.

Las pruebas de función espermática, como la generación de ROS y la evaluación del daño subsecuente a la célula, tienen un valor clínico significativo (ver revisiones [198,199]). Sin embargo, estos ensayos aún no se han traducido en pruebas robustas que se utilicen de manera rutinaria en el ámbito clínico probablemente por las complejidades de la generación de ROS y la evaluación/impacto del daño por ROS. En consecuencia, desarrollar un ensayo que pueda reflejar fácilmente la generación patológica de ROS y el daño con valores de corte y rangos de referencia claros que pueda ser incluido práctica diaria andrológica no ha sido posible[198,200].

En este trabajo, optimizamos el uso de la sonda Amplex Red para la cuantificación de H_2O_2 extracelular en 339 muestras de semen (artículo 4). Encontramos una correlación negativa entre los parámetros espermáticos y la producción de H_2O_2, lo cual concuerda con otros estudios que han demostrado asociaciones entre la producción de ROS y condiciones como oligozoospermia[201], astenozoospermia[202], y teratozoospermia[203]. Aunque se han publicado estudios sobre la sensibilidad y especificidad de diversas pruebas para medir ROS, estas varían considerablemente, no están estandarizadas y, en general, no ofrecen recomendaciones claras para su uso diagnóstico[204–206]. Frente a muchas de estas pruebas, nuestro método es económico, rápido y no requiere de personal con formación especializada, lo que facilita su aplicación en laboratorios clínicos y de diagnóstico. La medición de H_2O_2 puede utilizarse como un indicador indirecto de los niveles mitocondriales de $O_2^{\bullet-}$.

Proponemos que parte del fracaso en el valor predictivo de los tests existentes hasta el momento es no incluir estudios que valoren especies oxidantes y antioxidantes en la misma muestra. Dado que el PS contiene numerosos antioxidantes que protegen a los espermatozoides contra el estrés oxidativo[38,163,207], resulta racional la medición de ROS en combinación con la capacidad antioxidante total del PS[208]. Utilizando un método sensible que cuantifica la cantidad de H_2O_2 residual, determinamos la TAC en varias muestras de PS. Hay varios ensayos disponibles para medir la capacidad antioxidante total[205,207–212], pero el método utilizado en este trabajo posee la ventaja de que nos permite relacionar directamente la producción de ROS (H_2O_2) con la capacidad antioxidante total (el porcentaje de reducción de H_2O_2 al añadir PS). Observamos una correlación positiva entre la capacidad antioxidante total del PS y la motilidad espermática, lo cual coincide con estudios previos que indican que la capacidad antioxidante total disminuye en hombres con astenozoospermia[213,214] pero no con la morfología espermática. Se sabe que la

capacidad antioxidante total en el PS se relaciona con factores como la edad, contaminación ambiental, estilo de vida, y enfermedades crónicas o genitales (como el varicocele)[165,213,215]. Aunque el análisis de estos factores estaba fuera del alcance de nuestro estudio, algunos de ellos podrían explicar la falta de correlación con la morfología.

Actualmente se comercializan herramientas como el Sistema de Oxidación Masculina para la Infertilidad (MiOXSYS®, ttps://mioxsys.com/mioxsys-system/) y el OxiSperm® (Halotech©)[166,216] que determinan el potencial de óxido-reducción de la muestra. Si bien, se encuentra reportado que los indicadores medidos por ambos métodos tienen una correlación con los parámetros espermáticos y el estado de fertilidad masculina[217,218], no parecían tener un importante valor clínico[219] por lo que los índices y valores de corte de este trabajo, podrían eventualmente traducirse en nuevos métodos o kits diagnósticos.

Resaltamos que estas herramientas diagnósticas son también necesarias para desarrollar tratamientos de reproducción racionales. Por ejemplo, para utilizar con éxito antioxidantes en el tratamiento de la disfunción espermática, es necesario demostrar primero que el estrés oxidativo es la causa de la infertilidad. El continuo uso fallido de antioxidantes para la infertilidad masculina es un testimonio del hecho de que aún no hemos resuelto este problema[200].

En conclusión, los espermatozoides (provenientes de muestras normozoospérmicas) durante la capacitación experimentan un incremento en la función mitocondrial acompañado por un aumento del Ca^{2+} intramitocondrial dependiente de la activación del canal CatSper. Este incremento se encuentra vinculado a una mayor producción de ATP y $O_2^{\bullet -}$ mitocondrial. Nuestros datos sugieren un papel del Ca^{2+} y las ROS en la regulación del proceso.

Planteamos que el análisis mitocondrial en espermatozoides tiene el potencial de mejorar la evaluación de la calidad del semen en hombres con infertilidad y permitirá guiar la aplicación de terapias innovadoras en TRA.

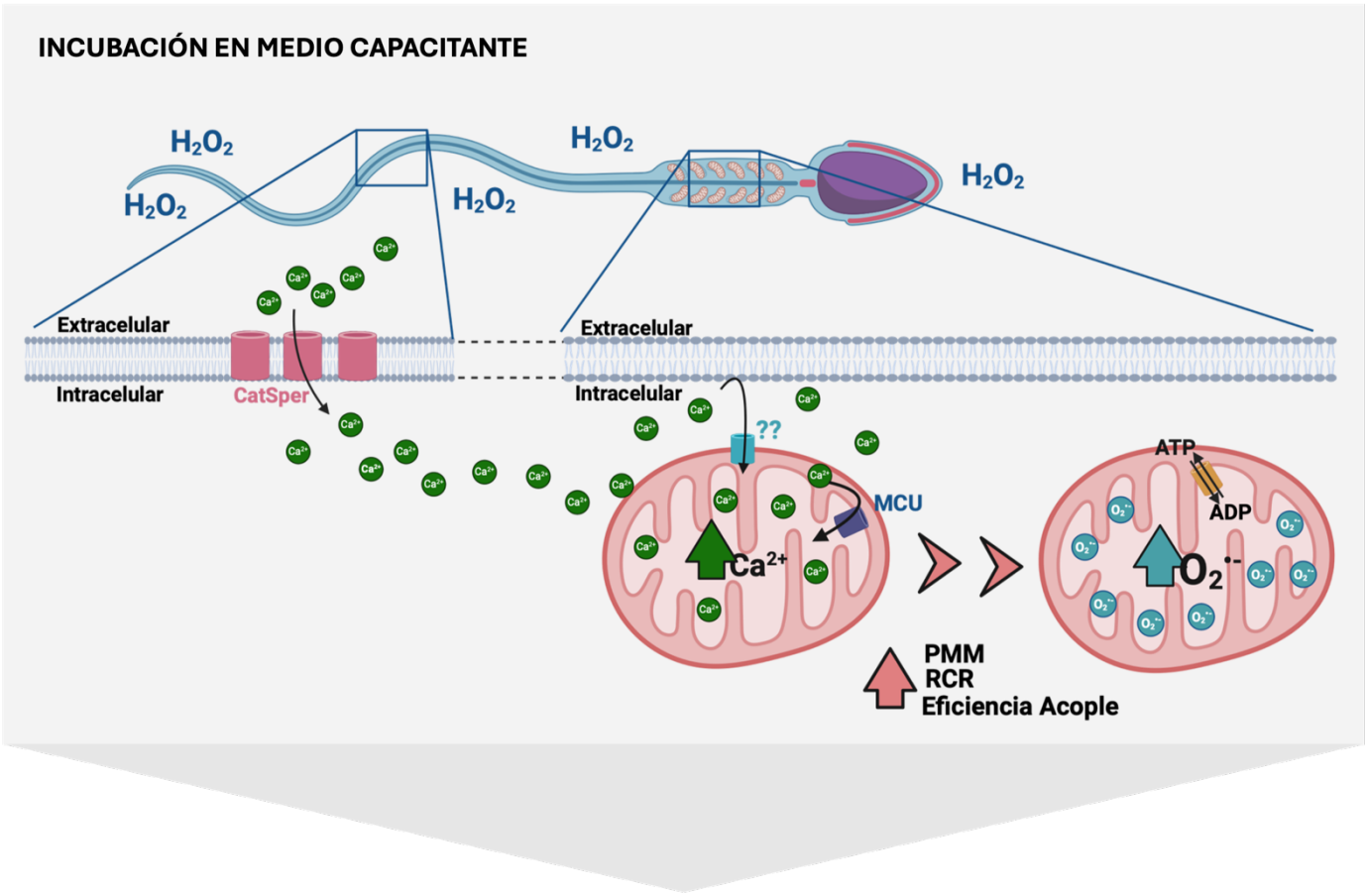

FIGURA 9: **Modelo propuesto para el rol de la mitocondria en la capacitación/hiperactivación de los espermatozoides humanos. La incubación de espermatozoides en medio capacitantes produce la activación de CatSper que determina la entrada de Ca^{2+} y el aumento de [Ca^{2+}] citoplasmático, que comienza en la pieza principal del espermatozoide, se propaga a través de la pieza intermedia y llega a la cabeza en unos pocos segundos. Nuestros datos muestran que la propagación de Ca^{2+} a través de la pieza intermedia conduce a un aumento del Ca^{2+} mitocondrial mediado por MCU. El aumento del Ca^{2+} intramitocondrial activa enzimas del organelo produciendo un aumento de la función mitocondrial. Esta modificación resulta en un incremento en el superóxido mitocondrial (que produce peróxido de hidrógeno extracelular) y de la producción de ATP, sin presencia de daño por estrés oxidativo. El mecanismo descrito contribuiría a la modulación de la capacitación espermática, en particular a la hiperactivación.**

7. Perspectivas futuras

Planteamos:

- Confirmar que los canales CatSper y MCU están involucrados en el incremento del Ca^{2+} intramitocondrial en espermatozoides humanos, para asegurar que se trata de un mecanismo conservado entre los dos modelos. Esto implicaría analizar la concentración de Ca^{2+} intramitocondrial en espermatozoides humanos utilizando inhibidores específicos de ambos canales.

- Conocer los cursos temporales de las modificaciones descritas dentro de las 4 horas de incubación en medio capacitante. En una siguiente etapa, utilizaremos la última generación de instrumentos Oroboro que nos permite el análisis del consumo de oxígeno en conjunto con la medición de sondas fluorescentes, permitiéndonos medir la producción de H_2O_2 y concentración de Ca^{2+} en la célula en tiempo real.

- Determinar cuáles enzimas mitocondriales son las que se activan mediante el aumento de Ca^{2+} intramitocondrial durante la capacitación espermática. Para ello, sería necesario medir la actividad de diferentes enzimas en espermatozoides NC y CAP así como a concentraciones variables de Ca^{2+}.

- Estudiar el rol de otras ROS y RNS productos de la interacción del $O_2^{\bullet-}$ con otras moléculas, así como determinar cuál es la contribución de la mitocondria en su producción. Sería clave utilizar sondas fluorescentes específicas para las diferentes especies reactivas que sean dirigidas a la mitocondria.

- Identificar los principales objetivos de señalización de las ROS mitocondriales y el Ca^{2+} que median los eventos de capacitación.

- Estudiar si las modificaciones observadas durante la capacitación se mantienen en muestras patológicas en donde la disregulación de estos mecanismos podría explicar parte de la infertilidad masculina.

8. Bibliografía

1. WHO laboratory manual for the Examination and processing of human semen. (2021).
2. WHO laboratory manual for the Examination and processing of human semen. (2010).
3. Dey, S. K. Review series: introduction How we are born. *J Clin Invest* **120**, 952–955 (2010).
4. Douglas T. Carrell, Peter N. Schlegel, Catherine Racowsky, L. G. *Biennial Review of Infertility Volume 4*. vol. D (2015).

5. Murray, C. J. L. *et al.* Population and fertility by age and sex for 195 countries and territories, 1950–2017: a systematic analysis for the Global Burden of Disease Study 2017. *The Lancet* **392**, 1995–2051 (2018).
6. Wang, H. *et al.* Global age-sex-specific fertility, mortality, healthy life expectancy (HALE), and population estimates in 204 countries and territories, 1950–2019: a comprehensive demographic analysis for the Global Burden of Disease Study 2019. *The Lancet* **396**, 1160–1203 (2020).
7. Skakkebaek, N. E. *et al.* Populations, decreasing fertility, and reproductive health. *The Lancet* vol. 393 1500–1501 Preprint at https://doi.org/10.1016/S0140-6736(19)30690-7 (2019).
8. Vander Borght, M. & Wyns, C. Fertility and infertility: Definition and epidemiology. *Clin Biochem* **62**, 2–10 (2018).
9. A.J., H., B., M. & A., A. Male infertility: A critical review of pharmacologic management. *Expert Opin Pharmacother* **13**, 2511–2531 (2012).
10. De Jonge, C. & Barratt, C. L. R. The present crisis in male reproductive health: an urgent need for a political, social, and research roadmap. *Andrology* **7**, 762–768 (2019).
11. Irvine, D. Stewart. Epidemiology and aetiology of male infertility. *Human Reproduction* **13**, 33–44 (1998).
12. Sullivan, R. & Mieusset, R. The human epididymis: its function in sperm maturation. *Human Reproduction* **22**, 1–14 (2016).
13. Rosa-Villagrán, L., Barrera, N., Montes, J., Riso, C. & Sapiro, R. Decline of semen quality over the last 30 years in Uruguay. *Basic Clin Androl* **31**, (2021).
14. Muroňová, J. *et al.* Lack of CCDC146, a ubiquitous centriole and microtubule-associated protein, leads to non-syndromic male infertility in human and mouse. (2024) doi:10.7554/eLife.86845.2.
15. Ferlin, A. *et al.* Male infertility: Role of genetic background. *Reproductive BioMedicine Online* vol. 14 734–745 Preprint at https://doi.org/10.1016/S1472-6483(10)60677-3 (2007).
16. Poongothai J, Gopenath TS & Manonayaki S. *Genetics of Human Male Infertility*. *Review Article Singapore Med J* vol. 50 (2009).
17. Meinhardt, A. Andrology 3rd edition—E. Nieschlag, H.M. Behre, S. Nieschlag (eds). *Asian J Androl* **12**, 458–458 (2010).
18. Dohle, G. R. *et al.* EAU guidelines on male infertility. *Eur Urol* **48**, 703–711 (2005).
19. Esteves, S. C., Miyaoka, R. & Agarwal, A. An update on the clinical assessment of the infertile male. *Clinics* vol. 66 691–700 Preprint at https://doi.org/10.1590/S1807-59322011000400026 (2011).
20. Sloter, E. *et al.* Quantitative effects of male age on sperm motion. *Human Reproduction* **21**, 2868–2875 (2006).
21. Marín-Briggiler, C. I. *et al.* Human Sperm Remain Motile After a Temporary Energy Restriction but do Not Undergo Capacitation-Related Events. *Front Cell Dev Biol* **9**, (2021).
22. Samplaski, M. K., Agarwal, A., Sharma, R. & Sabanegh, E. New generation of diagnostic tests for infertility: Review of specialized semen tests. *International Journal of Urology* vol. 17 839–847 Preprint at https://doi.org/10.1111/j.1442-2042.2010.02619.x (2010).
23. Hull, M. G. R. *et al.* MEDICAL-PRACTICE Contemporary Themes Population study of causes, treatment, and outcome of infertility. *Br Med J* **291**, 1693–1697 (1985).

24. Barratt CLR, W. C. B. E. T. I. K. J. L. D. other E. B. M. of the W. L. M. for the E. and P. of H. Semen. What advances may the future bring to the diagnosis, treatment, and care of male sexual and reproductive health? *Fertil Steril.* (2022).
25. Aitken, R. J. , Koopman, P. , & Lewis, S. E. M. Seeds of concern. *Nature Fertility* (2004).
26. Wojciech pawlina. Histología texto y Atlas. Correlación con Biología molecular y celular. (2020).
27. Welsch. Ulrich. *Sobotta. Histologìa.* (2014).
28. Hess, R. A. & Luiz Renato de Franca. Spermatogenesis and cycle of the seminiferous epithelium. *Adv Exp Med Biol* **636**, (2008).
29. Costa, J., Braga, P. C., Rebelo, I., Oliveira, P. F. & Alves, M. G. Mitochondria Quality Control and Male Fertility. *Biology* vol. 12 Preprint at https://doi.org/10.3390/biology12060827 (2023).
30. Nozawa, Y. I., Yao, E., Gacayan, R., Xu, S. M. & Chuang, P. T. Mammalian Fused is essential for sperm head shaping and periaxonemal structure formation during spermatogenesis. *Dev Biol* **388**, 170–180 (2014).
31. C Brucker & G B Lipford. The human sperm acrosome reaction: physiology and regulatory mechanisms. An update. *Hum Reprod Update* (1995).
32. Eddy, E. M., Toshimori, K. & O'Brien, D. A. Fibrous sheath of mammalian spermatozoa. *Microsc Res Tech* **61**, 103–115 (2003).
33. Linck, R. W., Chemes, H. & Albertini, D. F. The axoneme: the propulsive engine of spermatozoa and cilia and associated ciliopathies leading to infertility. *Journal of Assisted Reproduction and Genetics* vol. 33 141–156 Preprint at https://doi.org/10.1007/s10815-016-0652-1 (2016).
34. Fainberg, J. & Kashanian, J. A. Recent advances in understanding and managing male infertility. *F1000Res* **8**, (2019).
35. Zamboni, L. Sperm structure and its relevance to infertility. An electron microscopic study. . *Arch Pathol Lab Med* (1992).
36. Sironen, A., Shoemark, A., Patel, M., Loebinger, M. R. & Mitchison, H. M. Sperm defects in primary ciliary dyskinesia and related causes of male infertility. *Cellular and Molecular Life Sciences* vol. 77 2029–2048 Preprint at https://doi.org/10.1007/s00018-019-03389-7 (2020).
37. Molina, L. C. P. *et al.* Molecular basis of human sperm capacitation. *Frontiers in Cell and Developmental Biology* vol. 6 Preprint at https://doi.org/10.3389/fcell.2018.00072 (2018).
38. Juyena, N. S. & Stelletta, C. Seminal plasma: An essential attribute to spermatozoa. *J Androl* **33**, 536–551 (2012).
39. Druart, X. & de Graaf, S. Seminal plasma proteomes and sperm fertility. *Anim Reprod Sci* **194**, 33–40 (2018).
40. Ahmadi, H. *et al.* Composition and effects of seminal plasma in the female reproductive tracts on implantation of human embryos. *Biomedicine and Pharmacotherapy* vol. 151 Preprint at https://doi.org/10.1016/j.biopha.2022.113065 (2022).
41. Pirie, N. Biochemistry of semen and of the male reproductive tract. (1964).
42. Guidobaldi, H. A., Teves, M. E., Uñates, D. R., Anastasía, A. & Giojalas, L. C. Progesterone from the cumulus cells is the sperm chemoattractant secreted by the rabbit oocyte cumulus complex. *PLoS One* **3**, (2008).
43. Teves, M. E. *et al.* Molecular mechanism for human sperm chemotaxis mediated by progesterone. *PLoS One* **4**, (2009).

44. Uñates, D. R. *et al.* Versatile action of picomolar gradients of progesterone on different sperm subpopulations. *PLoS One* **9**, (2014).
45. Visconti, P. E. *et al.* Capacitation of mouse spermatozoa. *Development* **121**, 1129–1137 (1995).
46. Aitken, R. J. & Nixon, B. Sperm capacitation: a distant landscape glimpsed but unexplored. *Mol Hum Reprod* **19**, 785–793 (2013).
47. Battistone, M. A. *et al.* Functional human sperm capacitation requires both bicarbonate-dependent PKA activation and down-regulation of Ser/Thr phosphatases by Src family kinases. *Mol Hum Reprod* **19**, 570–580 (2013).
48. Gervasi, M. G. & Visconti, P. E. Chang's meaning of capacitation: A molecular perspective. *Molecular Reproduction and Development* vol. 83 860–874 Preprint at https://doi.org/10.1002/mrd.22663 (2016).
49. Balbach, M. *et al.* Metabolic changes in mouse sperm during capacitation. *Biol Reprod* **103**, 791–801 (2020).
50. Hicks, J. J., Martínez-Manautou, J., Pedron, N. & Rosado, A. Metabolic Changes in Human Spermatozoa Related to Capacitation*†*Supported in part by a Grant from the Ford Foundation (66-334).†Presented in part at the 27th Annual Meeting of The American Fertility Society, New Orleans, Louisiana, March 24-27, 1971. *Fertil Steril* **23**, 172–179 (1972).
51. Zaferani, M., Suarez, S. S. & Abbaspourrad, A. Mammalian sperm hyperactivation regulates navigation via physical boundaries and promotes pseudo-chemotaxis. *PNAS* **118**, 2107500118 (2021).
52. Burkman, L. J. Characterization of hyperactivated motility by human spermatozoa during capacitation: Comparison of fertile and oligozoospermic sperm populations. *Syst Biol Reprod Med* **13**, 153–165 (1984).
53. Giaccagli, M. M. *et al.* Capacitation-Induced Mitochondrial Activity Is Required for Sperm Fertilizing Ability in Mice by Modulating Hyperactivation. *Front Cell Dev Biol* **9**, (2021).
54. Fraser, L. R. The 'switching on' of mammalian spermatozoa: molecular events involved in promotion and regulation of capacitation. *Molecular Reproduction and Development* vol. 77 197–208 Preprint at https://doi.org/10.1002/mrd.21124 (2010).
55. Breitbart, H. Intracellular calcium regulation in sperm capacitation and acrosomal reaction. *Mol Cell Endocrinol* **187**, 139–144 (2002).
56. La Spina, F. A. *et al.* Mouse sperm begin to undergo acrosomal exocytosis in the upper isthmus of the oviduct. *Dev Biol* **411**, 172–182 (2016).
57. Simons, J. & Fauci, L. A Model for the Acrosome Reaction in Mammalian Sperm. *Bull Math Biol* (2018).
58. Florman, H. M. Sequential Focal and Global Elevations of Sperm Intracellular Ca2+ Are Initiated by the Zona Pellucida during Acrosomal Exocytosis. *DevelopmentalBiology* **65**, 152–164 (1994).
59. Darszon, A., Nishigaki, T., Beltran, C. & Treviño, C. L. CALCIUM CHANNELS IN THE DEVELOPMENT, MATURATION, AND FUNCTION OF SPERMATOZOA. *Physiol Rev* **91**, 1305–1355 (2011).
60. Travis, A. J. *et al.* Functional Relationships between Capacitation-dependent Cell Signaling and Compartmentalized Metabolic Pathways in Murine Spermatozoa. *Journal of Biological Chemistry* **276**, 7630–7636 (2001).
61. Visconti, P. E., Krapf, D., De La Vega-Beltrán, J. L., Acevedo, J. J. & Darszon, A. Ion channels, phosphorylation and mammalian sperm capacitation. *Asian*

Journal of Andrology vol. 13 395–405 Preprint at https://doi.org/10.1038/aja.2010.69 (2011).
62. Hernández-González, E. O. *et al.* Sodium and epithelial sodium channels participate in the regulation of the capacitation-associated hyperpolarization in mouse sperm. *Journal of Biological Chemistry* **281**, 5623–5633 (2006).
63. Visconti, P. E. & Kopf, G. S. Regulation of Protein Phosphorylation during Sperm Capacitation1. Biology of Reproduction,. *Biol Reprod* **59**, 1–6 (1998).
64. Lyon, M. D. *et al.* SLO3: A Conserved Regulator of Sperm Membrane Potential. *International Journal of Molecular Sciences* vol. 24 Preprint at https://doi.org/10.3390/ijms241311205 (2023).
65. Chávez, J. C. *et al.* SLO3 K+ channels control calcium entry through CATSPER channels in sperm. *Journal of Biological Chemistry* **289**, 32266–32275 (2014).
66. Santi, C. M. *et al.* The SLO3 sperm-specific potassium channel plays a vital role in male fertility. *FEBS Lett* **584**, 1041–1046 (2010).
67. Vicente-Carrillo, A., Álvarez-Rodríguez, M. & Rodriguez-Martinez, H. The Cation/Calcium Channel of Sperm (CatSper): A Common Role Played Despite Inter-Species Variation? *International Journal of Molecular Sciences* vol. 24 Preprint at https://doi.org/10.3390/ijms241813750 (2023).
68. Baro Graf, C. *et al.* Everything you ever wanted to know about PKA regulation and its involvement in mammalian sperm capacitation. *Mol Cell Endocrinol* **518**, (2020).
69. Hidalgo, D. M. *et al.* Capacitation increases glucose consumption in murine sperm. *Mol Reprod Dev* **87**, 1037–1047 (2020).
70. Sansegundo, E., Tourmente, M. & Roldan, E. R. S. Energy Metabolism and Hyperactivation of Spermatozoa from Three Mouse Species under Capacitating Conditions. *Cells* **11**, (2022).
71. O'Flaherty, C. Redox regulation of mammalian sperm capacitation. *Asian J Androl* **17**, 583–590 (2015).
72. Kudryavtseva, A. V *et al. Mitochondrial Dysfunction and Oxidative Stress in Aging and Cancer*. vol. 7 www.impactjournals.com/oncotarget (2016).
73. Kühlbrandt, W. Structure and function of mitochondrial membrane protein complexes. *BMC Biology* vol. 13 Preprint at https://doi.org/10.1186/s12915-015-0201-x (2015).
74. Nelson, D. L. & Cox, M. M. *Lehninger. Principios de Bioquímica*. (2018).
75. Schapira, A. Mitochondrial disease. *Lancet* **368**, 70–82 (2006).
76. Brand, M. D. & Nicholls, D. G. Assessing mitochondrial dysfunction in cells. *Biochemical Journal* **435**, 297–312 (2011).
77. Contreras, L., Drago, I., Zampese, E. & Pozzan, T. Mitochondria: The calcium connection. *Biochimica et Biophysica Acta - Bioenergetics* vol. 1797 607–618 Preprint at https://doi.org/10.1016/j.bbabio.2010.05.005 (2010).
78. Parikh, S. *et al.* Diagnosis and management of mitochondrial disease: A consensus statement from the Mitochondrial Medicine Society. *Genetics in Medicine* vol. 17 689–701 Preprint at https://doi.org/10.1038/gim.2014.177 (2015).
79. Berridge, M., Bootman, M. D. & Roderick, H. L. Calcium signalling dynamics, homeostasis and remodelling. *Nat Rev Mol Cell Biol* 517–529 (2003).
80. Matuz-Mares, D., González-Andrade, M., Araiza-Villanueva, M. G., Vilchis-Landeros, M. M. & Vázquez-Meza, H. Mitochondrial Calcium: Effects of Its Imbalance in Disease. *Antioxidants* vol. 11 Preprint at https://doi.org/10.3390/antiox11050801 (2022).

81. Rossi, A., Pizzo, P. & Filadi, R. Calcium, mitochondria and cell metabolism: A functional triangle in bioenergetics. *Biochimica et Biophysica Acta - Molecular Cell Research* vol. 1866 1068–1078 Preprint at https://doi.org/10.1016/j.bbamcr.2018.10.016 (2019).
82. Elustondo, P. A., Nichols, M., Robertson, G. S. & Pavlov, E. V. Mitochondrial Ca2+ uptake pathways. *J Bioenerg Biomembr* **49**, 113–119 (2017).
83. Denton, R. M. Regulation of mitochondrial dehydrogenases by calcium ions. *Biochimica et Biophysica Acta - Bioenergetics* vol. 1787 1309–1316 Preprint at https://doi.org/10.1016/j.bbabio.2009.01.005 (2009).
84. Nohl, H., Gille, L., Kozlov, A. & Staniek, K. Are mitochondria a spontaneous and permanent source of reactive oxygen species? *Redox Report* vol. 8 135–141 Preprint at https://doi.org/10.1179/135100003225001502 (2003).
85. Drogue, W. Free Radicals in the Physiological Control of Cell Function. *The American Physiological Society* **82**, 47–95 (2002).
86. Kowalczyk, P. *et al.* Mitochondrial oxidative stress—a causative factor and therapeutic target in many diseases. *International Journal of Molecular Sciences* vol. 22 Preprint at https://doi.org/10.3390/ijms222413384 (2021).
87. Boveris, A. & Chance, B. *The Mitochondrial Generation of Hydrogen Peroxide GENERAL PROPERTIES AND EFFECT OF HYPERBARIC OXYGEN*. *Biochem. J* vol. 134 (1973).
88. Chance, B. *Hydroperoxide Metabolism in Mammalian Organs*. *PHYSIOLOGICAL REVIEWS* vol. 59 (1979).
89. Kowaltowski, A. J., de Souza-Pinto, N. C., Castilho, R. F. & Vercesi, A. E. Mitochondria and reactive oxygen species. *Free Radical Biology and Medicine* vol. 47 333–343 Preprint at https://doi.org/10.1016/j.freeradbiomed.2009.05.004 (2009).
90. Murphy, M. P. How mitochondria produce reactive oxygen species. *Biochemical Journal* vol. 417 1–13 Preprint at https://doi.org/10.1042/BJ20081386 (2009).
91. Valeria Valez, Adrán Aicardo, Adriana Cassina, C. Q. and R. R. Oxidative Stress in Mitochondria. **I**, 423–444 (2005).
92. Castro, L. & Freeman, B. A. Reactive oxygen species in human health and disease. *Nutrition Metabolism Classic with Perspective Overview* (1954).
93. Cardoso, A. R. *et al.* Mitochondrial compartmentalization of redox processes. *Free Radical Biology and Medicine* vol. 52 2201–2208 Preprint at https://doi.org/10.1016/j.freeradbiomed.2012.03.008 (2012).
94. Wang, Y., Branicky, R., Noë, A. & Hekimi, S. Superoxide dismutases: Dual roles in controlling ROS damage and regulating ROS signaling. *Journal of Cell Biology* vol. 217 1915–1928 Preprint at https://doi.org/10.1083/jcb.201708007 (2018).
95. Aitken, R. J. Reactive oxygen species as mediators of sperm capacitation and pathological damage. *Molecular Reproduction and Development* vol. 84 1039–1052 Preprint at https://doi.org/10.1002/mrd.22871 (2017).
96. Serial Review: Nitric Oxide in Mitochondria Guest Editors: Christoph Richter and Matthias Schweizer INTRODUCTION TO SERIAL REVIEWS ON NITRIC OXIDE IN. **33**, 5849 (2002).
97. Radi, R. Peroxynitrite, a stealthy biological oxidant. *Journal of Biological Chemistry* vol. 288 26464–26472 Preprint at https://doi.org/10.1074/jbc.R113.472936 (2013).
98. Radi, R., Cassina, A., Hodara, R., Quijano, C. & Castro, L. Peroxynitrite reactions and formation in mitochondria. *Free Radic Biol Med* (2002).

99. Yang, S. & Lian, G. ROS and diseases: role in metabolism and energy supply. *Molecular and Cellular Biochemistry* vol. 467 Preprint at https://doi.org/10.1007/s11010-019-03667-9 (2020).
100. Gohil, V. M. *et al.* Discovery and therapeutic potential of drugs that shift energy metabolism from mitochondrial respiration to glycolysis. *Nat Biotechnol* **28**, 249–255 (2011).
101. Nunnari, Jodi (Department of Molecular and Cellular Biology, University of California, Davis, Davis, CA 95616, U. & Suomalainen, Anu (Research Programs Unit, Molecular Neurology, Biomedicum-Helsinki, University of Helsinki, 00290 Helsinki, Finland; Department of Neurology, Helsinki University Central Hospital, 00290 Helsinki, F. Mitochondria: In Sickness and in Health. *Cell* **148**, 1145–1159 (2012).
102. O'Flaherty. *Oxidative Stress in Applied Basic Research and Clinical Practice: Studies on Men's Health and Fertility*. (2012). doi:10.1007/978-1-61779-776-7.
103. Sies, H., Berndt, C. & Jones, D. P. Oxidative Stress. **50**, 11 (2024).
104. Chirino, Y., Orozco Ibarra, M. & Pedraza Chaverrí, J. Evidencias de la participación del peroxinitrito en diversas enfermedades. *Revista de Investigación Clínica* **58**, 350–358 (2006).
105. Sanocka, D. & Kurpisz, M. *Reactive Oxygen Species and Sperm Cells*. http://www.rbej.com/content/2/1/12 (2004).
106. Aitken, R. J. & Jones, K. T. Reactive Oxygen Species and Sperm Function--In Sickness and In Health. *J Androl* **33**, 1096–1106 (2012).
107. Castro, J. P., Jung, T., Grune, T. & Siems, W. 4-Hydroxynonenal (HNE) modified proteins in metabolic diseases. *Free Radical Biology and Medicine* vol. 111 309–315 Preprint at https://doi.org/10.1016/j.freeradbiomed.2016.10.497 (2017).
108. Aitken, R. J., Smith, T. B., Jobling, M. S., Baker, M. A. & De Iuliis, G. N. Oxidative stress and male reproductive health. *Asian Journal of Andrology* vol. 16 31–38 Preprint at https://doi.org/10.4103/1008-682X.122203 (2014).
109. Moraes, C. R. & Meyers, S. The sperm mitochondrion: Organelle of many functions. *Anim Reprod Sci* **194**, 71–80 (2018).
110. Amaral, A., Lourenço, B., Marques, M. & Ramalho-Santos, J. Mitochondria functionality and sperm quality. *Reproduction* vol. 146 Preprint at https://doi.org/10.1530/REP-13-0178 (2013).
111. Costa, J., Braga, P. C., Rebelo, I., Oliveira, P. F. & Alves, M. G. Mitochondria Quality Control and Male Fertility. *Biology* vol. 12 Preprint at https://doi.org/10.3390/biology12060827 (2023).
112. Otani, H., Tanaka, O., Kasai, K.-I. & Yoshioka, T. Development of mitochondrial helical sheath in the middle piece of the mouse spermatid tail:Regular Dispositions and Synchronized Changes. *Anat Rec* **222**, 26–33 (1998).
113. Designed Research; M, -B.-M R L & Performed Research; P, -B.-M M. In-cell structures of conserved supramolecular protein arrays at the mitochondria-cytoskeleton interface in mammalian sperm. **118**, (2021).
114. Ye, Z. W., Zhang, J., Townsend, D. M. & Tew, K. D. Oxidative stress, redox regulation and diseases of cellular differentiation. *Biochimica et Biophysica Acta - General Subjects* vol. 1850 1607–1621 Preprint at https://doi.org/10.1016/j.bbagen.2014.11.010 (2015).
115. Shivaji, S., Kota, V. & Silva, A. B. The role of mitochondrial proteins in sperm capacitation. *J Reprod Immunol* **83**, 14–18 (2009).

116. Cassina, A. *et al.* Defective Human Sperm Cells Are Associated with Mitochondrial Dysfunction and Oxidant Production. *Biol Reprod* **93**, 119 (2015).
117. Mundy, A. J., Ryder, T. A. & Edmonds, D. K. Asthenozoospermia and the human sperm mid-piece. *Human Reproduction* **10**, 116–119 (1995).
118. GOPALKRISHNAN, K., PADWAL, V., D'SOUZA, S. & SHAH, R. Severe asthenozoospermia: a structural and functional study. *Int J Androl* **18**, 67–74 (1995).
119. Pelliccione, F. *et al.* Altered ultrastructure of mitochondrial membranes is strongly associated with unexplained asthenozoospermia. *Fertil Steril* **95**, 641–646 (2011).
120. Gallon, F., Marchetti, C., Jouy, N. & Marchetti, P. The functionality of mitochondria differentiates human spermatozoa with high and low fertilizing capability. *Fertil Steril* **86**, 1526–1530 (2006).
121. Marchetti, P., Ballot, C., Jouy, N., Thomas, P. & Marchetti, C. Influence of mitochondrial membrane potential of spermatozoa on in vitro fertilisation outcome. **44**, 136–141 (2011).
122. Zhu, Z. *et al.* Gene expression and protein synthesis in mitochondria enhance the duration of high-speed linear motility in boar sperm. *Front Physiol* **10**, 1–13 (2019).
123. Ford, W. C. L. Glycolysis and sperm motility: Does a spoonful of sugar help the flagellum go round? *Hum Reprod Update* **12**, 269–274 (2006).
124. Piomboni, P., Focarelli, R., Stendardi, A., Ferramosca, A. & Zara, V. The role of mitochondria in energy production for human sperm motility. *Int J Androl* **35**, 109–124 (2012).
125. Williams, A. C. & Ford, W. C. L. The role of glucose in supporting motility and capacitation in human spermatozoa. *J Androl* **22**, 680–695 (2001).
126. Cardullo, R. A. & Baltz, J. M. Metabolic regulation in mammalian sperm: Mitochondrial volume determines sperm length and flagellar beat frequency. *CellMotilityandtheCytoskeleton* **19**, 180–188 (1991).
127. Storey, B. T. Mammalian sperm metabolism: Oxygen and sugar, friend and foe. *International Journal of Developmental Biology* **52**, 427–437 (2008).
128. Nevo, A. C. & Rikmenspoel, R. Diffusion of ATP in sperm flagella. *J Theor Biol* **26**, 11–18 (1970).
129. Takao, D. & Kamimura, S. FRAP analysis of molecular diffusion inside sea-urchin spermatozoa. *Journal of Experimental Biology* **211**, 3594–3600 (2008).
130. Williams, A. C. & Ford, W. C. L. The role of glucose in supporting motility and capacitation in human spermatozoa. *J Androl* **22**, 680–695 (2001).
131. Mukai, C. & Okuno, M. Glycolysis Plays a Major Role for Adenosine Triphosphate Supplementation in Mouse Sperm Flagellar Movement. *Biol Reprod* **71**, 540–547 (2004).
132. Miki, K. *et al.* Glyceraldehyde 3-phosphate dehydrogenase-Sa Sperm-Specific Glycolytic Enzyme, Is Required for Sperm Motility and Male Fertility. *Sciences-New York* **101**, (2004).
133. Danshina, P. V. *et al.* Phosphoglycerate kinase 2 (PGK2) is essential for sperm function and male fertility in mice. *Biol Reprod* **82**, 136–145 (2010).
134. Narisawa, S. *et al.* Testis-Specific Cytochrome c -Null Mice Produce Functional Sperm but Undergo Early Testicular Atrophy . *Mol Cell Biol* **22**, 5554–5562 (2002).
135. Tourmente, M., Villar-Moya, P., Rial, E. & Roldan, E. R. S. Differences in ATP generation via glycolysis and oxidative phosphorylation and relationships with

sperm motility in mouse species. *Journal of Biological Chemistry* **290**, 20613–20626 (2015).
136. Odet, F., Gabel, S., London, R. E., Goldberg, E. & Eddy, E. M. Glycolysis and mitochondrial respiration in mouse LDHC-Null sperm. *Biol Reprod* **88**, (2013).
137. Storey, B. T. Mammalian sperm metabolism: Oxygen and sugar, friend and foe. *International Journal of Developmental Biology* **52**, 427–437 (2008).
138. Carrageta, D. F. *et al.* Mitochondrial activation and reactive oxygen-species overproduction during sperm capacitation are independent of glucose stimuli. *Antioxidants* **9**, 1–17 (2020).
139. Wennemuth, G., Babcock, D. F. & Hille, B. Calcium clearance mechanisms of mouse sperm. *Journal of General Physiology* **122**, 115–128 (2003).
140. Lishko, P. V. & Mannowetz, N. CatSper: a unique calcium channel of the sperm flagellum. *Curr Opin Physiol* **2**, 109–113 (2018).
141. Xia, J., Reigada, D., Mitchell, C. H. & Ren, D. CATSPER channel-mediated Ca2+ entry into mouse sperm triggers a tail-to-head propagation. *Biol Reprod* **77**, 551–559 (2007).
142. McCormack, J. G., Halestrap, A. P. & Denton, R. M. Role of calcium ions in regulation of mammalian intramitochondrial metabolism. *Physiol Rev* **70**, (1990).
143. Glancy, B. & Balaban, R. S. Role of mitochondrial Ca 2+ in the regulation of cellular energetics. *Biochemistry* **51**, 2959–2973 (2012).
144. Simpson, P. B. & Russell, J. T. *Interactive Report Role of Mitochondrial Ca 2q Regulation in Neuronal and Glial Cell Signalling 1. Brain Research Reviews* vol. 26 (1998).
145. Costello, S. *et al.* Ca2+-stores in sperm: their identities and functions. *Reproduction* **138**, 425–437 (2009).
146. Delamirande, E. & Cagnon, C. Human sperm hyperactivation and capacitation as parts of an oxidative process. *Free Radical Biologyand Medicine* **14**, 157–166 (1993).
147. Herrero, M. B. & Gagnon, C. Nitric oxide: A novel mediator of sperm function. *Journal of Andrology* vol. 22 349–356 Preprint at https://doi.org/10.1002/j.1939-4640.2001.tb02188.x (2001).
148. Rodriguez, P. C. & Beconi, M. T. Peroxynitrite participates in mechanisms involved in capacitation of cryopreserved cattle. *Anim Reprod Sci* **110**, 96–107 (2009).
149. Machado-Oliveira, G. *et al.* Mobilisation of Ca2+ stores and flagellar regulation in human sperm by S-nitrosylation: A role for NO synthesised in the female reproductive tract. *Development* **135**, 3677–3686 (2008).
150. Lamirande, E. De & Gagnon, C. A positive role for the superoxide anion in triggering hyperactivation and capacitation of human spermatozoa. *Int J Androl* **16**, 21–25 (1993).
151. Ferramosca, A. & Zara, V. Bioenergetics of mammalian sperm capacitation. *BioMed Research International* vol. 2014 Preprint at https://doi.org/10.1155/2014/902953 (2014).
152. Boell, E. J. Oxygen consumption of mouse sperm and its relationship to capacitation. *JournalofExperimentalZoology* **234**, 105–116 (1985).
153. Leemans, B. *et al.* REPRODUCTION REVIEW Update on mammalian sperm capacitation: how much does the horse differ from other species? (2019) doi:10.1530/REP.
154. Bánfi, B. *et al.* A Ca2+-activated NADPH Oxidase in Testis, Spleen, and Lymph Nodes. *Journal of Biological Chemistry* **276**, 37594–37601 (2001).

155. Miguel-Jiménez, S. *et al.* NADPH Oxidase 5 and Melatonin: Involvement in Ram Sperm Capacitation. *Front Cell Dev Biol* **9**, (2021).
156. Musset, B. *et al.* NOX5 in human spermatozoa: Expression, function, and regulation. *Journal of Biological Chemistry* **287**, 9376–9388 (2012).
157. Aitken, R. J., Drevet, J. R., Moazamian, A. & Gharagozloo, P. Male Infertility and Oxidative Stress: A Focus on the Underlying Mechanisms. *Antioxidants* vol. 11 Preprint at https://doi.org/10.3390/antiox11020306 (2022).
158. Ahmed T. Alahmar. Role of Oxidative Stress in Male Infertility: An Updated Review. *J Hum Reprod Sci* **11**, 247–253 (2018).
159. Wagner, H., Cheng, J. W. & Ko, E. Y. Role of reactive oxygen species in male infertility: An updated review of literature. *Arab J Urol* **16**, 35–43 (2018).
160. Janiszewska, E. *et al.* Are There Associations between Seminal Plasma Advanced Oxidation Protein Products and Selected Redox-Associated Biochemical Parameters in Infertile Male Patients? A Preliminary Report. *Cells* **11**, (2022).
161. Tremellen, K. Oxidative stress and male infertility: A clinical perspective. *Studies on Men's Health and Fertility* **14**, 325–353 (2012).
162. Aitken, R. J., Gibb, Z., Baker, M. A., Drevet, J. & Gharagozloo, P. Causes and consequences of oxidative stress in Spermatozoa. *Reprod Fertil Dev* **28**, 1–10 (2016).
163. Agarwal, A. & Deepinder, F. Determination of seminal oxidants. *Anim Reprod Sci* **110**, 96–107 (2009).
164. Rodriguez-Martinez, H., Martinez, E. A., Calvete, J. J., Peña Vega, F. J. & Roca, J. Seminal plasma: Relevant for fertility? *International Journal of Molecular Sciences* vol. 22 Preprint at https://doi.org/10.3390/ijms22094368 (2021).
165. Roychoudhury, S., Sharma, R., Sikka, S. & Agarwal, A. Diagnostic application of total antioxidant capacity in seminal plasma to assess oxidative stress in male factor infertility. *J Assist Reprod Genet* **33**, 627–635 (2016).
166. Agarwal, A. *et al.* Utility of antioxidants in the treatment of male infertility: Clinical guidelines based on a systematic review and analysis of evidence. *World Journal of Men's Health* vol. 39 1–58 Preprint at https://doi.org/10.5534/WJMH.200196 (2021).
167. Barratt, C. L. R. *et al.* The diagnosis of male infertility: An analysis of the evidence to support the development of global WHO guidance-challenges and future research opportunities. *Hum Reprod Update* **23**, 660–680 (2017).
168. Barratt, C. L. R. *et al.* A global approach to addressing the policy, research and social challenges of male reproductive health. *Human Reproduction Open* vol. 2021 Preprint at https://doi.org/10.1093/hropen/hoab009 (2021).
169. Schlegel, P. N. *et al.* Diagnosis and treatment of infertility in men: AUA/ASRM guideline part I. *Fertil Steril* **115**, 54–61 (2021).
170. Johnston, Z. C. *et al.* High-throughput phenotypic screening of the human spermatozoon. (2022) doi:10.1530/REP.
171. Ruiz-Pesini, E. *et al.* Correlation of sperm motility with mitochondrial enzymatic activities. *Clin Chem* **44**, 1616–1620 (1998).
172. Meyers, S., Bulkeley, E. & Foutouhi, A. Sperm mitochondrial regulation in motility and fertility in horses. *Reproduction in Domestic Animals* **54**, 22–28 (2019).
173. Ferramosca, A., Pinto Provenzano, S., Coppola, L. & Zara, V. Mitochondrial Respiratory Efficiency is Positively Correlated With Human Sperm Motility. *Uruology* **79**, 809 (2012).

174. Barbagallo, F. *et al.* Evaluation of sperm mitochondrial function: A key organelle for sperm motility. *J Clin Med* **9**, (2020).
175. Greiner, E. O2k Quality Control 1: Polarographic oxygen sensors and accuracy of calibration. *<https://www.bioblast.at/images/ archive/7/77/20210819114548%21MiPNet06. 03_POS- Calibration-SOP.pdf>* (2020).
176. Gnaiger, E. Chapter 12 - Polarographic oxygen sensors, the oxygraph, and high-resolution respirometry to assess mitochondrial function. In Drug-Induced Mitochondrial Dysfunction. 325–352 (2008).
177. Holt, W. V. & Van Look, K. J. W. Concepts in sperm heterogeneity, sperm selection and sperm competition as biological foundations for laboratory test of semen quality. *Reproduction* vol. 127 527–535 Preprint at https://doi.org/10.1530/rep.1.00134 (2004).
178. Sousa, A. P. *et al.* Not all sperm are equal: Functional mitochondria characterize a subpopulation of human sperm with better fertilization potential. *PLoS One* **6**, (2011).
179. Moscatelli, N. *et al.* Single-cell-based evaluation of sperm progressive motility via fluorescent assessment of mitochondria membrane potential. *Sci Rep* **7**, (2017).
180. Quill, T. A. *et al. Hyperactivated Sperm Motility Driven by CatSper2 Is Required for Fertilization CELL BIOLOGY*. *PNAS December* vol. 9 www.pnas.orgcgidoi10.1073pnas.2136654100 (2003).
181. Xia, J., Reigada, D., Mitchell, C. H. & Ren, D. CATSPER channel-mediated Ca2+ entry into mouse sperm triggers a tail-to-head propagation. *Biol Reprod* **77**, 551–559 (2007).
182. Patron, M. *et al.* The mitochondrial calcium uniporter (MCU): Molecular identity and physiological roles. *Journal of Biological Chemistry* vol. 288 10750–10758 Preprint at https://doi.org/10.1074/jbc.R112.420752 (2013).
183. Rizzuto, R., De Stefani, D., Raffaello, A. & Mammucari, C. Mitochondria as sensors and regulators of calcium signalling. *Nat Rev Mol Cell Biol* **13**, 566–578 (2012).
184. Wang, P., Fernandez-Sanz, C., Wang, W. & Sheu, S. S. Why don't mice lacking the mitochondrial Ca2+ uniporter experience an energy crisis? *Journal of Physiology* vol. 598 1307–1326 Preprint at https://doi.org/10.1113/JP276636 (2020).
185. Ho, H.-C. & Suarez, S. S. Characterization of the Intracellular Calcium Sotre at the Base of the Sperm Flagellum That Regulates Hyperactivated Motility. *Biol Reprod* **68**, 1590–1596 (2003).
186. Aitken, R. J. Reactive oxygen species as mediators of sperm capacitation and pathological damage. *Mol Reprod Dev* **84**, 1039–1052 (2017).
187. Wong, H. S., Dighe, P. A., Mezera, V., Monternier, P. A. & Brand, M. D. Production of superoxide and hydrogen peroxide from specific mitochondrial sites under different bioenergetic conditions. *Journal of Biological Chemistry* vol. 292 16804–16809 Preprint at https://doi.org/10.1074/jbc.R117.789271 (2017).
188. Tórtora, V., Quijano, C., Freeman, B., Radi, R. & Castro, L. Mitochondrial aconitase reaction with nitric oxide, S-nitrosoglutathione, and peroxynitrite:Mechanism and relative contributions to aconitase inactivation. *Free Radic Biol Med* **42**, 1075–1088 (2007).

189. Marchetti, C., Obert, G., Deffosez, A., Formstecher, P. & Marchetti, P. *Study of Mitochondrial Membrane Potential, Reactive Oxygen Species, DNA Fragmentation and Cell Viability by Flow Cytometry in Human Sperm*. *Human Reproduction* vol. 17 (2002).
190. Uribe, P. *et al.* Use of the fluorescent dye tetramethylrhodamine methyl ester perchlorate for mitochondrial membrane potential assessment in human spermatozoa. *Andrologia* **49**, (2017).
191. Amaral, A. & Ramalho-Santos, J. Assessment of mitochondrial potential: Implications for the correct monitoring of human sperm function. *Int J Androl* **33**, (2010).
192. Tanga, B. M. *et al.* Semen evaluation: Methodological advancements in sperm quality-specific fertility assessment - A review. *Anim Biosci* **34**, 1253–1270 (2021).
193. Durairajanayagam, D., Singh, D., Agarwal, A. & Henkel, R. Causes and consequences of sperm mitochondrial dysfunction. *Andrologia* (2020).
194. Cedikova, M. *et al.* Sperm mitochondrial function in men with normozoospermia and asthenozoospermia. *Ceská gynekologie / Ceská lékarská spolecnost J. Ev. Purkyne* **79**, 22–28 (2014).
195. Hereng, T. H., Elgstøen, K. B. P., Eide, L., Rosendal, K. R. & Skålhegg, B. S. Serum albumin and HCO3- regulate separate pools of ATP in human spermatozoa. *Human Reproduction* **29**, 918–930 (2014).
196. Le Foll, N. *et al.* Cyclic FEE peptide improves human sperm movement parameters without modification of their energy metabolism. *Int J Mol Sci* **22**, (2021).
197. Cedikova, M. *et al.* Effects of the Czech propolis on sperm mitochondrial function. *Evidence-based Complementary and Alternative Medicine* **2014**, (2014).
198. John Aitken, R. & Bakos, H. W. Should we be measuring DNA damage in human spermatozoa? New light on an old question. *Human Reproduction* **36**, 1175–1185 (2021).
199. Oehninger, S. & Ombelet, W. Limits of current male fertility testing. *Fertility and Sterility* vol. 111 835–841 Preprint at https://doi.org/10.1016/j.fertnstert.2019.03.005 (2019).
200. Aitken, R. J. Antioxidant trials—the need to . test for stress. *F and S Reports* vol. 1 176 Preprint at https://doi.org/10.1016/j.xfre.2020.09.013 (2020).
201. Agarwal, A., Mulgund, A., Sharma, R. & Sabanegh, E. Mechanisms of oligozoospermia: An oxidative stress perspective. *Systems Biology in Reproductive Medicine* vol. 60 206–216 Preprint at https://doi.org/10.3109/19396368.2014.918675 (2014).
202. Bonanno, O. *et al.* Sperm of patients with severe asthenozoospermia show biochemical, molecular and genomic alterations. *Reproduction* **152**, 695–704 (2016).
203. Agarwal, A., Tvrda, E. & Sharma, R. Relationship amongst teratozoospermia, seminal oxidative stress and male infertility. *Reproductive Biology and Endocrinology* **12**, (2014).
204. Aiken, R. J., De Iuliis, G. N. & Baker, M. A. Direct Methods for the Detection of Reactive Oxygen Species in Human Semen Samples. *Studies on Men´s Health and Fertility* 275–299 (2012).
205. Sharma, R., Roychoudhury, S., Singh, N. & Sarda, Y. Methods to measure reactive oxygen species (ROS) and total antioxidant capacity (TAC) in the

reproductive system. in *Oxidative Stress in Human Reproduction: Shedding Light on a Complicated Phenomenon* 17–46 (Springer International Publishing, 2017). doi:10.1007/978-3-319-48427-3_2.
206. Agarwal, A. *et al.* A global survey of reproductive specialists to determine the clinical utility of oxidative stress testing and antioxidant use in male infertility. *World Journal of Men's Health* **39**, (2021).
207. Khosrowbeygi, A. & Zarghami, N. Levels of oxidative stress biomarkers in seminal plasma and their relationship with seminal parameters. *BMC Clin Pathol* **7**, (2007).
208. Agarwal, A., Ahmad, G. & Sharma, R. Reference values of reactive oxygen species in seminal ejaculates using chemiluminescence assay. *J Assist Reprod Genet* **32**, 1721–1729 (2015).
209. Baker, M. A. & Aitken, R. J. Reactive oxygen species in spermatozoa: Methods for monitoring and significance for the origins of genetic disease and infertility. *Reproductive Biology and Endocrinology* vol. 3 Preprint at https://doi.org/10.1186/1477-7827-3-67 (2005).
210. Zini, A., Garrels, K. & Phang, D. Antioxidant activity in the semen of fertile and infertile men. *Urology* **55**, (2000).
211. Agarwal, A., Prabakaran, S. & Allamaneni, S. S. Relationship between oxidative stress, varicocele and infertility: a meta-analysis. *Reprod Biomed Online* **12**, (2006).
212. Robert, K. A., Sharma, R., Henkel, R. & Agarwal, A. An update on the techniques used to measure oxidative stress in seminal plasma. *Andrologia* **53**, (2020).
213. Madej, D., Granda, D., Sicinska, E. & Kaluza, J. Influence of Fruit and Vegetable Consumption on Antioxidant Status and Semen Quality: A Cross-Sectional Study in Adult Men. *Front Nutr* **8**, (2021).
214. Pahune, P. P., Choudhari, A. R. & Muley, P. A. The total antioxidant power of semen and its correlation with the fertility potential of human male subjects. *Journal of Clinical and Diagnostic Research* **7**, 991–995 (2013).
215. Eroglu, M. *et al.* Blood Serum and Seminal Plasma Selenium, Total Antioxidant Capacity and Coenzyme Q10 Level in Relation to Semen Parameters in Men with Idiopathic Infertility. *Biol Trace Elem Res* **159**, (2014).
216. Agarwal, A. & Bui, A. D. Oxidation-reduction potential as a new marker for oxidative stress: Correlation to male infertility. *Investigative and Clinical Urology* vol. 58 385–399 Preprint at https://doi.org/10.4111/icu.2017.58.6.385 (2017).
217. Agarwal, A., Makker, K. & Sharma, R. Clinical relevance of oxidative stress in male factor infertility: An update. *American Journal of Reproductive Immunology* **59**, 2–11 (2008).
218. Agarwal, A. *et al.* Multi-center evaluation of oxidation-reduction potential by the MiOXSYS in males with abnormal semen. *Asian J Androl* **21**, 565–569 (2019).
219. Castleton, P. *et al.* MiOXSYS® and OxiSperm® II assays appear to provide no clinical utility for determining oxidative stress in human sperm—results from repeated semen collections. *Andrology* **11**, 1566–1578 (2023).